

Design and Study of Hybrid DNA Nanostructures and Complex 3D DNA Materials

by

Raghu Narayanan Pradeep

A Dissertation Presented in Partial Fulfillment
of the Requirements for the Degree
Doctor of Philosophy

Approved April 2021 by the
Graduate Supervisory Committee:

Hao Yan, Co-Chair
Nicholas Stephanopoulos, Co-Chair
Yan Liu
Jeremy Mills

ARIZONA STATE UNIVERSITY

May 2021

ABSTRACT

Over the past four decades, DNA nanotechnology has grown exponentially from a field focused on simple structures to one capable of synthesizing complex nano-machines capable of drug delivery, nano-robotics, digital data storage, logic gated circuitry, nano-photonics, and other applications. The construction of these nanostructures is possible because of the predictable and programmable Watson-Crick base pairing of DNA. However, there is an increasing need for the incorporation of chemical diversity and functionality into these nanostructures. To overcome this challenge, this work explored creating hybrid DNA nanostructures by making self-assembling small molecule/protein-DNA conjugates.

In one direction, well studied host-guest interactions (i.e. cucurbituril[7]-adamantane) were used as the choice of self-assembling species. Binding studies using these small molecule-DNA conjugates were performed and thereafter they were used to assemble larger DNA origami nanostructures. Finally, a stimulus responsive DNA nano-box that opens and closes based on these interactions was also demonstrated. In another direction, a trimeric KDPG aldolase protein-DNA conjugate was probed as a structural building block by assembling it into a DNA origami tetrahedron with four cavities. This hybrid building block was thereafter characterized by single particle cryo-EM and the resulting electron density map was best fit by simulating origami cages with varying number of proteins (ranging from 0 to 4).

Next, to increase access and for larger democratization of the field, an automation designer software tool capable of making DNA nanostructures was made. In this work, the focus was on making curved 3D DNA nanostructures. The last direction probed in this

work was to make optical metamaterials based on complex 3D DNA architectures. Realization of a self-assembled 3D tetrastack geometry is still an unachieved dream in the field of DNA self-assembly. Thus, this direction was probed using DNA origami icosahedrons. Finally, the work covered in my thesis probes multiple directions for advancing DNA nanotechnology, both fundamentally and for potential applications.

ACKNOWLEDGEMENTS

As I look back over the 6 years of my Ph.D. life, I must admit that it has been an incredible journey to finally arrive at this point. This would not have been possible without the support and guidance of all the people who have supported me scientifically and emotionally. But first and foremost, I must thank my advisors Professors Hao Yan and Nicholas Stephanopoulos, without whom none of this would have been possible. When I met Professor Hao Yan for the first time, I was in awe with his personality, calm demeanor, and to the point scientific thinking. I immediately knew that I wanted to work under his guidance. I met Professor Nicholas Stephanopoulos through a course I was taking. His in-depth knowledge on self-assembly, his excitement about the science and his sense of humor were the first things that made me want to work with him. I am highly indebted to both my PIs for mentoring me, making me think critically on science, guiding me through my highs and lows. They helped me keep my focus when I faltered, allowed me to explore scientific thoughts on my own, scolding me when I became too over-confident or carried away in my own thoughts and above all, they were always there when I needed them (sometimes just to listen to my problems).

Towards the end of my second year, I took a course with Professor Po-Lin Chiu on cryo-EM and I immediately developed a fondness for both the technique and the instructor, which made me pursue a project in that direction. My advisors were benevolent enough to allow me to explore the avenue. Little did I know that this project would consume most of my Ph.D. period and ultimately direct me to pursue the technique into my post-doctoral training. I am also highly indebted to Dr. Dewight Williams without whom none of my learning in cryo-EM would have been possible. He was extremely nice in helping me learn

the skillsets required to prepare and run samples on the microscope. Both of them are some of the most kindhearted scientists I have known and have always been there to discuss scientific problems, life in general as well as my future. I also want to thank Professor Petr Šulc who introduced me to the world of simulations and oxDNA. I eventually ended up taking a herculean task of assembling higher ordered DNA origami structures under his guidance. Coming to think of it, he would be a co-author on all the projects that I would be publishing from my Ph.D. work at ASU. I am much grateful for his mentorship, suggestions and help throughout my time here. I also want to thank Professors Yan Liu and Jeremy Mills for their critical suggestions on my experiments which helped me improve my work.

I would like to thank all the Yan lab and Stephanopoulos lab members for making my Ph.D. journey a wonderful experience. I especially want to thank one of our ex-lab member Dr. Fei Zhang for believing in me, supporting me when I needed it most and for just being an amazing mentor. I also want to thank Alex Buchberger and Tara MacCulloch for not only being the best lab mates but, for also being the best friends here. Thank you for just being there for me, helping me get accustomed to the culture and for always willing to grab a drink when I needed it. I also want to thank Swarup Dey for being an amazing friend and for just being there discuss any lab issues, life in general. I also want to thank Dr. Minghui Liu for teaching me the basic experimental techniques and for always being there to discuss and troubleshoot my experiments in lab. I also want to thank Dr. Xiaodong and Dr. Yang for being there to discuss anything and everything in the protein world. I also want to thank Jonah and Erik for all the help with simulations, cryo fitting and for being there to solve any software/simulation problem that I have bothered them with. I want to

specially thank Dr. Michael Matthies, for his experimental insights and inputs in the DNA origami assembly work. I want to thank my collaborators Purbasha Nandi for helping me process the cryo-EM data and in putting together the cryo-EM paper. I also want to thank Professor Matthew Webber at University of Notre Dame for sending us the small molecules without which the host-guest project would not have been possible. I also thank Daniel Fu at Duke University who has now become more of a good friend through the collaborative effort on the automated design project.

Finally, I would also like to thank my friends here Zachary Dobson, Tim Baxter, Pritha Bisarad, Leeza Abraham, Srivatsan Mohana Rangan, Shatabdi Roy Chowdhury, Sree Ganesh, Skanda Vishnu, Soma Choudhary, Akanksha Singh, Joydeep Banerjee, Bharat Sampath Kumar, Sohini, Jayaprakash, Karthik, Pon Arasu and Sanchari for helping me cope with life and survive through the grad school. I want to thank my buddies Chandrasekhar, Srinath, Karteek, Harsha, Elvis, Sasidhar, Pallavi and Faiza for being there for me always when I needed them.

At last, I would like to thank my family for supporting me, believing in me and just being my rock that I can fall onto, without which this endeavor could never have been possible and to take my Ph.D. to the finish line. Particularly my dad, Professor Pradeep for being my hero, who I have always looked up to, for being so inspirational, for discussing science with me, for aiding me shape my future and for always helping me pick myself up when I am down. I want to thank my mom, Subha, for being the backbone of our family, for keeping us all together (without you, we will not be here). Finally, would like to thank my sister Laya for just being you. Although we are 8 years apart, we might both become doctors at the same time, you being the doctor who actually saves lives.

TABLE OF CONTENTS

| | Page | |
|--|------|----|
| LIST OF FIGURES | x | |
| CHAPTER | | |
| 1 INTRODUCTION..... | 1 | |
| 1.1 Self Assembly and Biomimetics..... | 1 | |
| 1.2 DNA Nanotechnology..... | 1 | |
| 1.3 Complex 3D DNA lattices..... | 7 | |
| 1.4 Hybrid DNA nanostructures..... | 11 | |
| 1.5 Cryo-EM for structural insights..... | 14 | |
| 1.6 Need for automation..... | 16 | |
| 1.7 Dissertation overview..... | 19 | |
| 1.8 References..... | 20 | |
| 2 STIMULUS-RESPONSIVE DNA NANOSTRUCTURES VIA HIGH-AFFINITY HOST-GUEST INTERACTIONS..... | | 25 |
| 2.1 Introduction..... | 25 | |
| 2.2 Ad/CB[7]-DNA conjugate assembly..... | 27 | |
| 2.3 One pot assembly of cuboidal origami fibers..... | 29 | |
| 2.4 Hierarchical assembly of fibers..... | 32 | |
| 2.5 Stimulus responsive nano-system..... | 34 | |
| 2.6 Conclusions and Future directions..... | 37 | |
| 2.7 References..... | 38 | |

| CHAPTER | Page |
|--|------|
| 3 CHARACTERIZATION OF PROTEIN-DNA HYBRID NANOSTRUCTURES THROUGH EXPERIMENT AND SIMULATION..... | 42 |
| 3.1 Introduction..... | 42 |
| 3.2 Results and discussion..... | 45 |
| 3.2.1 Synthesis of KDPG aldolase protein-DNA building blocks..... | 45 |
| 3.2.2 Design and synthesis of DNA tetrahedral origami cage..... | 45 |
| 3.2.3 Incorporation of Protein into the origami cage..... | 46 |
| 3.2.4 Simulation development for Protein-DNA hybrid system..... | 46 |
| 3.2.5 Simulation Preparation of Tetrahedral Origami..... | 47 |
| 3.2.6 Simulation results of the tetrahedral protein origami cage..... | 49 |
| 3.2.7 Fluorophore Assay..... | 53 |
| 3.3 Conclusions and future directions..... | 54 |
| 3.4 References..... | 55 |
| 4 AUTONOMOUS DESIGN OF BIOMIMETIC 3D DNA ORIGAMI CAPSULES..... | 58 |
| 4.1 Introduction..... | 58 |
| 4.2 Design inspiration and DNA pottery..... | 59 |
| 4.3 Software details..... | 60 |
| 4.4 Variable Reinforcement..... | 65 |
| 4.5 Experimental Demonstrations..... | 65 |
| 4.6 Asymmetric structures..... | 68 |

| CHAPTER | Page |
|--|------|
| 4.7 Conclusions and future directions..... | 70 |
| 4.8 References..... | 71 |
| 5 ASSEMBLING AN ORDERED 3D DNA TETRASTACK FROM MODELING TO EXPERIMENTS..... | 74 |
| 5.1 Introduction..... | 74 |
| 5.2 Motivation and design of the monomer..... | 76 |
| 5.3 Formation of the monomer..... | 77 |
| 5.4 Formation of Chains..... | 80 |
| 5.5 Formation of Lattices..... | 81 |
| 5.6 Testing New Designs..... | 83 |
| 5.7 Conclusions and Future directions..... | 85 |
| 5.8 References..... | 85 |
| 6 CONCLUSIONS AND FUTURE DIRECTIONSEXPERIMENTS..... | 88 |
| 6.1 Conclusions..... | 88 |
| 6.2 Future directions..... | 90 |
| 6.2.1 Functional biomimicry..... | 90 |
| 6.2.2 Improvements in protein-DNA nanotechnology..... | 91 |
| 6.2.3 Automation of DNA nanotechnology..... | 92 |
| 6.2.4 Structural DNA nanotechnology..... | 92 |
| 6.3 References..... | 93 |
| REFERENCES..... | 96 |

| APPENDIX | Page |
|---|------|
| A SUPPLEMENTAL MATERIAL FOR CHAPTER 2..... | 114 |
| B SUPPLEMENTAL MATERIAL FOR CHAPTER 3..... | 155 |
| C SUPPLEMENTAL MATERIAL FOR CHAPTER 4..... | 177 |
| D SUPPLEMENTAL MATERIAL FOR CHAPTER 5..... | 190 |
| E PERMISSIONS TO USE COPYRIGHTED MATERIALS..... | 200 |

LIST OF FIGURES

| Figure | Page |
|--|------|
| 1.1. Structure of DNA | 2 |
| 1.2. 1D and 2D Motifs used in DNA nanotechnology | 3 |
| 1.3. DNA origami | 4 |
| 1.4. Scale up of DNA nanotechnology | 7 |
| 1.5. DNA lattices | 10 |
| 1.6. Hybrid nanostructures | 13 |
| 1.7. Cryo-EM characterization for DNA nanostructures | 15 |
| 1.8. Example Software Packages | 18 |
| 2.1. Self-assembly of DNA nanostructures using host–guest interactions | 25 |
| 2.2. Characterization of host–guest complexation | 29 |
| 2.3. One-pot assembly of DNA origami nanofibers..... | 31 |
| 2.4. Hierarchical assembly of nanofibers | 32 |
| 2.5. Peptide based lock and key mechanism | 35 |
| 3.1. Schematic of the project..... | 44 |
| 3.2. Reconstruction of Tetrahedral Origami Cages | 47 |
| 3.3. Simulated Models of Tetrahedral Origami Cages | 49 |
| 3.4. Comparison of Simulated Models | 50 |
| 3.5. Comparison between Models with and without Protein | 51 |
| 3.6. Fitting of Experimental Data with Simulations..... | 52 |
| 3.7. Fluorophore assay | 54 |

| Figure | Page |
|--|------|
| 4.1. The design process of CADAxisDNA | 64 |
| 4.2. Reinforcement Strategy..... | 66 |
| 4.3. Tomograms of Example Nanostructures | 68 |
| 4.4. Simulation of Asymmetric Structures | 70 |
| 5.1. Examples of 3D DNA lattices achieved..... | 76 |
| 5.2. Monomer Formation | 79 |
| 5.3. Formation of Icosahedral chains..... | 81 |
| 5.4. Lattice structures | 84 |

CHAPTER 1

INTRODUCTION

1.1 Self-assembly and Biomimetics

Self-assembly is a process where molecules/macromolecules/polymers/cells self-organize themselves into different architectures. Nature is filled with such examples of self-assembling functional entities, starting from the fundamental building block of life: the cell. As inquisitive beings as humans are, this fundamental building block has been, and continues to be, investigated in detail for its organization and function. This marvel of a living entity, just a few micrometers in size, still manages to inspire and excite a wide a range of scientists across the world. In the pursuit of better understanding of these self-assembled systems, there has been a large interest in biomimicry. Taking inspiration from these naturally occurring examples, programmable self-assembling systems are one key direction that has inspired scientists in the past 50 years. Deoxyribonucleic acid (DNA) is one such example of a programmable self-assembling building block.

1.2 DNA Nanotechnology

DNA is a macromolecule polymer that forms a double helix composed of two antiparallel strands held together by hydrogen bonds ². These hydrogen bonds are highly specific, and take place between the constituent purines and pyrimidines, a phenomenon known as Watson-Crick base pairing ² (Figure 1.1). The specific nature of these hydrogen bonds makes them programmable, and this property is of key interest to scientists interested in biomimetics. Using these predictable and programmable interactions of DNA, the field of DNA nanotechnology was born in 1982 ⁵.

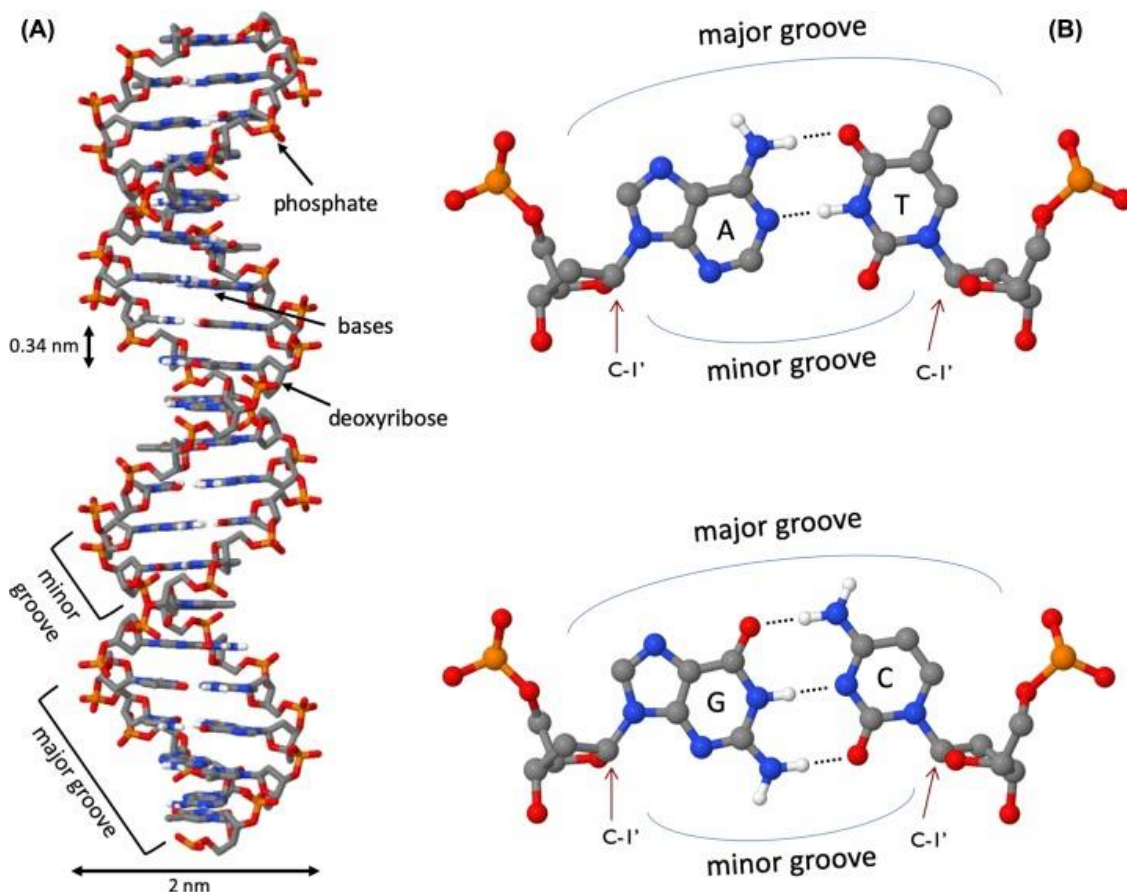


Figure 1.1: Structure of DNA: Illustration of B-form DNA⁷ showing two antiparallel strands and the programmable Watson-Crick base pairing.

Roughly 40 years ago, Nadrian Seeman envisioned building programmable 3D crystals by making a repeating DNA structural lattice via a bottom-up approach. Thus, he started looking at various fundamental DNA building blocks that could achieve this goal. The first direction was to look at immovable Holliday junctions that could be used for constructing rigid 3D lattices⁵ (Figure 1.2 A (ii)). Later, he considered individual DNA building blocks that could grow into repeating lattices, also popularly known as the DNA tile approach. This method is essentially the formation of individual bricks that could grow and make large repeating lattices. The earliest example in this direction was the

invention of double crossover tiles also known as DX (double crossover antiparallel) and PX (paranemic crossover) tiles ⁹ (Figure 1.2 A). These tiles and other 2D tiles like TX (triple crossover) ¹⁰, were envisioned as building blocks of large 2D structures with a repeating building block. The first such demonstration in this direction was done by Winfree and Seeman in the year 1998 when they demonstrated the growth of 2D lattices using these DX tiles (Figure 1.2 B) ¹². Later on Seeman and other scientists went on to make branched 2D tiles, which have also demonstrated the capability of growing into large 2D lattices or even quasicrystals ¹⁴.

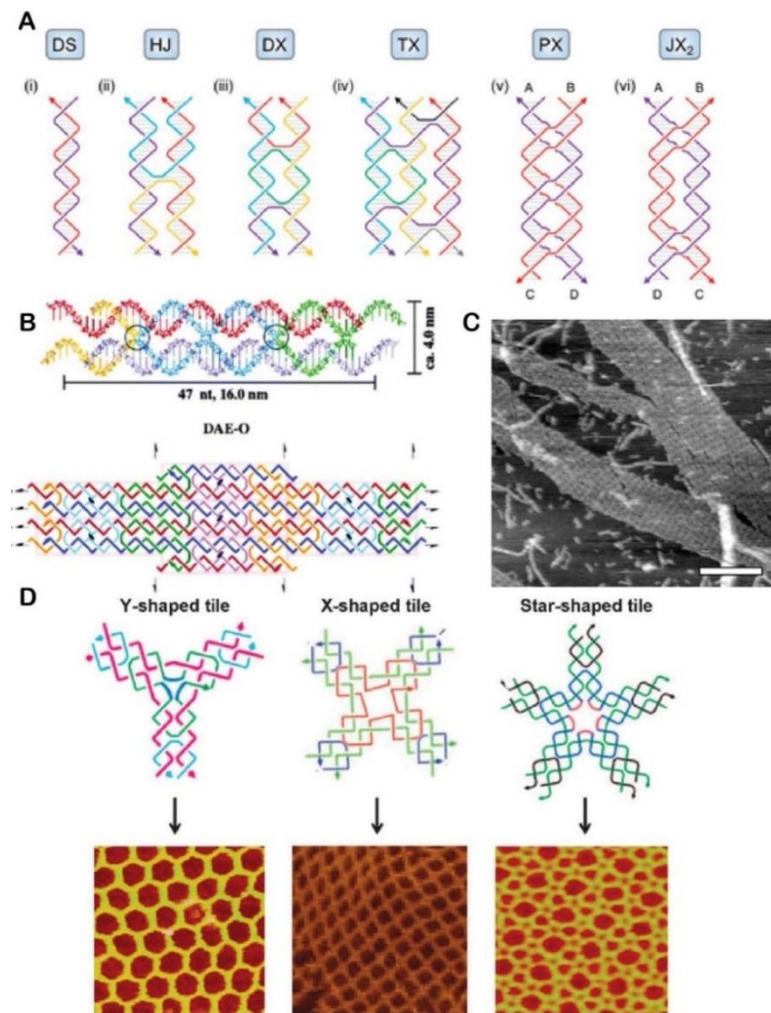


Figure 1.2: 1D and 2D Motifs used in DNA nanotechnology: A) 1D motifs¹¹ (i) Double-stranded DNA (DS). (ii) Holliday junction (HJ), a four-arm junction that results from a single reciprocal exchange between double helices. (iii) Double-crossover (DX) molecule (iv) Triple-crossover (TX) molecule (v) Paranemic crossover (PX) DNA, (vi) JX₂ molecule, a topoisomer of PX that lacks two crossovers in the middle in contrast to the PX molecule. B) Schematic of DAE tile and its hierarchical assembly¹² C) Experimental validation of (B). D) 2D motifs¹³ used in DNA nanotechnology 3, 4 and 5 junction tiles and their hierarchical assembly shown in AFM images.

In the early days of DNA nanotechnology the field was largely limited to using these materials for positioning proteins, nanoparticles, or other functional entities, e.g. for electronics/photronics or biosensing applications¹⁵. Hao Yan was a pioneer in this area and demonstrated several directions where these materials could be functional¹⁵⁻¹⁶. However, the field continued to think about making 3D lattices, although this goal was not realized until 2009, when the first rigid 3D self-assembled crystals were realized¹⁷.

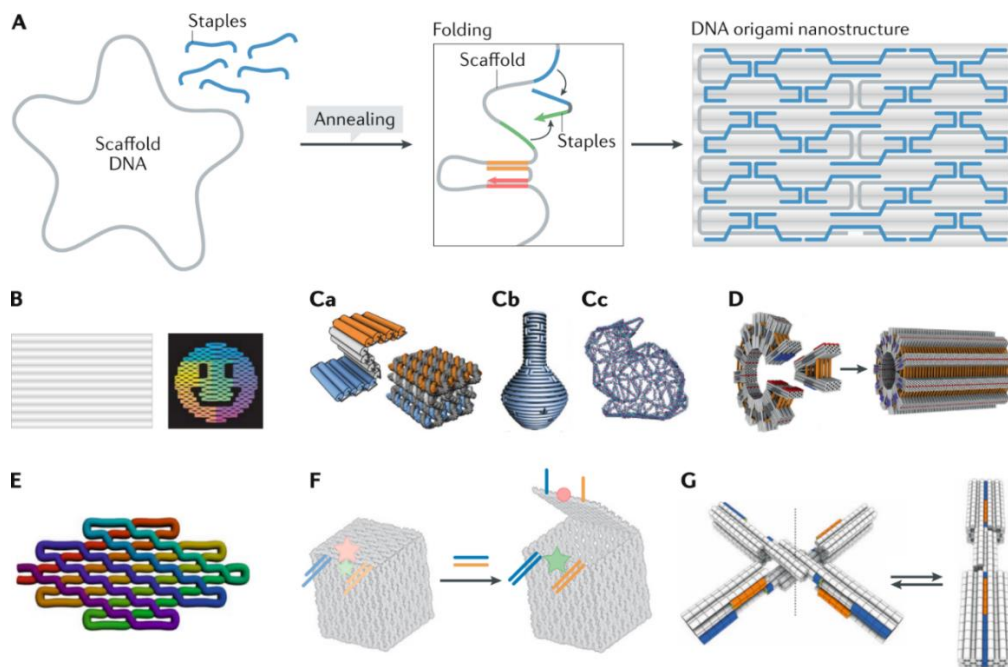


Figure 1.3 DNA origami¹⁸. Principle of DNA origami B-G) Examples of DNA origami shapes assembled: B) 2D planar shapes, C) 3D DNA nanostructures, D) Superstructures assembled from 3D DNA nanostructures, E) single stranded DNA origami, F-G) examples of dynamic DNA nanostructures.

DNA nanotechnology made a significant leap in 2006, when Paul Rothemund invented DNA origami¹⁹ to make complex DNA architectures. This invention changed the outlook of the whole field and suddenly making any kind of target shape became a possibility. As a result, the field rapidly expanded and allowed scientists to explore the fundamentals of designing and constructing extremely complicated DNA-based nanomaterials. DNA origami is a method wherein a circularized long single-stranded viral genome strand is annealed with short oligonucleotides to create desired target shapes (Figure 1.3 A). This technology is to date the most widely used method to make designed DNA nanostructures in the field.

One continuing interest in the field thereafter was to push the limit of self-assembly to assemble hierarchically complex geometries that mimic larger cellular components and even possibly the whole cell itself. Many steps have been taken to this date by different scientists across the field. One example in this direction was the creation of huge three-dimensional gigadalton (GDa) DNA origami structures (Figure 1.3D) by the Dietz lab²⁰. This work demonstrated the use of shape programmability to achieve these architectures ranging from 240 MDa all the way up to 1.2 GDa. The other example in this field was the creation of micrometer scale 2D DNA origami arrays²¹ with arbitrary patterns. The authors used a three-stage hierarchical self-assembly process to generate 8x8 array with unique identifiers on its edges to make patterns like Mona Lisa and a rooster (Figure 1.4A). These examples discussed above utilize a multiple 2D/3D DNA origami units as foundational building blocks for assembling into larger architectures. However, other scientists have

invented other approaches like the use of DNA bricks²², Meta-DNA²³ and ssDNA origami²⁴ (Figure 1.3E) as alternative techniques for nanostructure building.

The technology of DNA bricks utilizes thousands of unique short DNA sequences to build complex 3D DNA architectures. The technology demonstrates the capability of making complex DNA architectures with complex cavities inside the shapes like of a teddy bear, helicoid, and other (Figure 1.4B). Meta-DNA on the other hand, uses a 6-helix DNA origami bundle having a dimension of 420x16nm as a bundle capable of complex 2D and 3D polygons (Figure 1.4C). The researchers further demonstrated the capability of the building block to undergo strand displacement, a technique needed to perform logic-gated operations. The Yan lab further developed ssDNA origami as a technique that used a single long scaffold to fold onto itself using parallel crossovers without the use of short staple strands to form complex 2D shapes.

While these nanostructures were being realized, scientists in the field thought about their applicability in various directions. One such direction was to utilize the material properties of the created architectures²⁵. And the other was to improve the functionality of these materials by combining them with other functional entities. This thesis addresses both these directions.

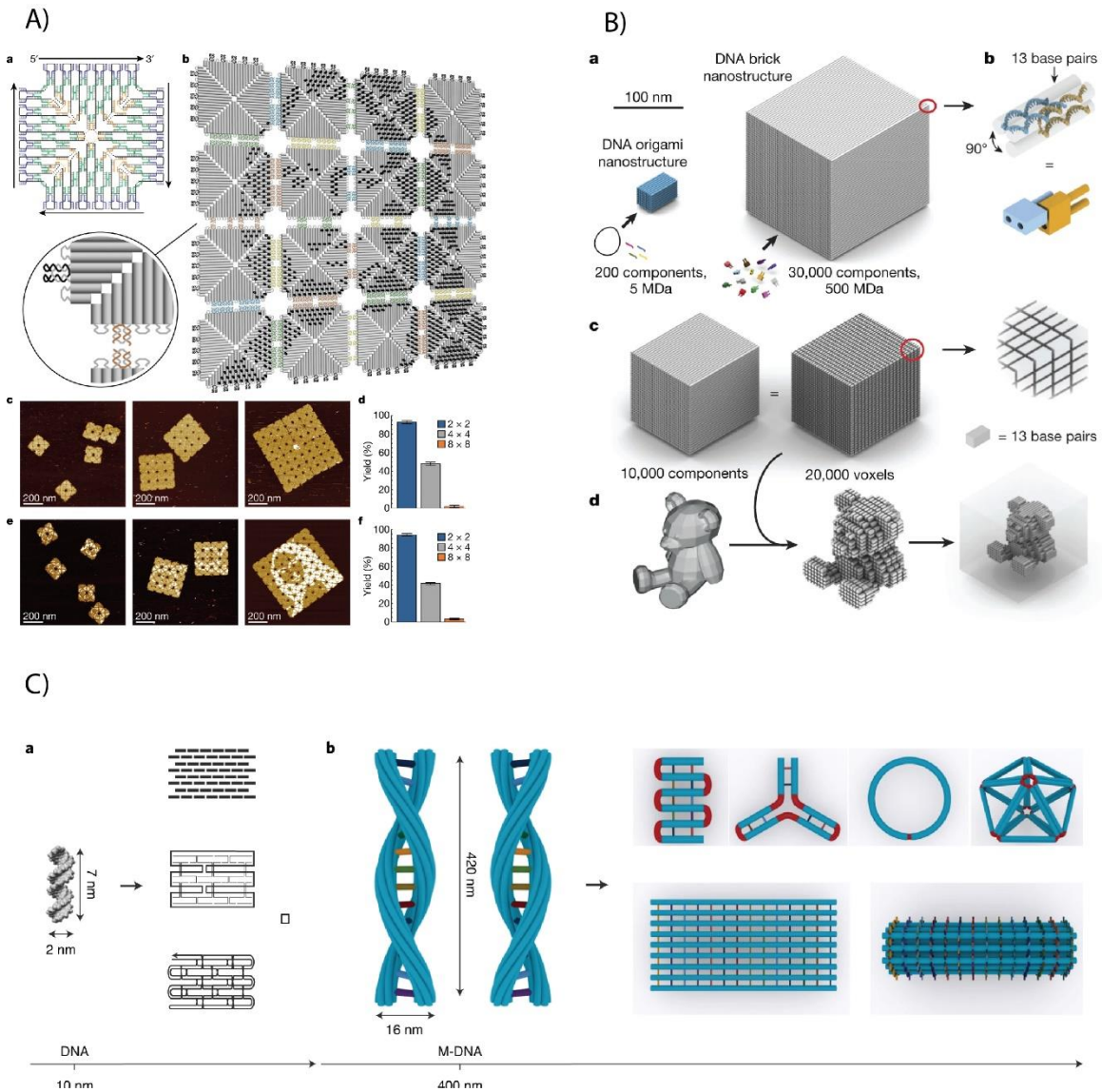


Figure 1.4. Scale up of DNA nanotechnology. A) Fractal assembly of 2D DNA origami Mona Lisa²¹. B) DNA bricks technology showing the formation of a cavity in the shape of a teddy bear²². C) Meta-DNA technology capable of making polygons²³.

1.3 Complex 3D DNA lattices

Creation of these nanostructures of any shape brought much attention to the field from scientists across disciplines, as they finally had a material where programmable architectures could be realized in a robust, easy, and efficient manner. Researchers wondered at the possibilities inherent in making repeating 3D lattice structures could be

made utilizing this technology. 3D repeating DNA lattice architectures have been of foundational importance to the field as it realizes the capability of positioning proteins at precise locations within their cavities, e.g. for structural resolution using X-ray crystallography. To this end, efforts have been made in two different directions, wherein a repeating lattice was created by a monomer made out of a tile comprised of a few strands (Figure 1.5 A-C) or by a DNA origami (Figure 1.5 D-H).

Nadrian Seeman realized the foundational goal of the 3D lattice in 2009 by making a crystal¹⁷ having a tensegrity triangle as its repeating motif. In this work, the group used three strands to form the monomer which propagated itself to a periodic lattice, and the authors solved the crystal structure to 4Å resolution (Figure 1.5 A). Following this work, the Yan lab demonstrated the capability of making another self-assembled crystal by utilizing three strands to make a 3D layered lattice²⁶ (Figure 1.5 C). The motif used in this work employed a five-nucleotide repeating sequence that weaved through a series of two-turn DNA duplexes. The Yan lab further developed a layered crossover tile²⁷ similar to the DX tiles mentioned before, except in three dimensions, capable of making lattices of several hundred micrometers (Figure 1.5 B).

While these developments were being pursued, DNA origami-based lattice structures were being built in parallel. The Liedl lab utilized origami tensegrity triangles²⁸ to build 3D rhombohedral crystals with a cavity size of $1.83 \times 10^5 \text{ nm}^3$ capable of holding 20 nm gold nanoparticles (Figure 1.5 D). The Gang lab on the other hand showed a series of 3D lattice constructions using both gold nanoparticles templated onto DNA origami polyhedral shapes²⁹⁻³⁰ (Figure 1.5 E) to DNA origami frames by themselves as way to

make hierarchically self-assembled lattices³¹. They demonstrated a wide range of lattice structures such a cubic diamond lattice, hexagonal diamond lattice, and others. Recently, they have also utilized these lattice architectures for the controlled placing of quantum dots and enzymes, wherein these 3D crystals showed an increasing enzymatic function³¹ (Figure 1.5 G) proving the increasing potential for these materials. Gang and coworkers recently utilized these architectures to create a superconducting framework by silicising them and thereafter coating it with Niobium³² (Figure 1.5 F). The very same group also demonstrated the capability of controlled silicisation of these 3D lattices and showed that the created material³³ had an increased stability to extreme temperatures ($> 1000^{\circ}\text{C}$) and pressures (8 GPa) (Figure 1.5 H). Chapter 5 in this thesis later explores the capabilities DNA nanotechnology offers in producing photonic crystals.

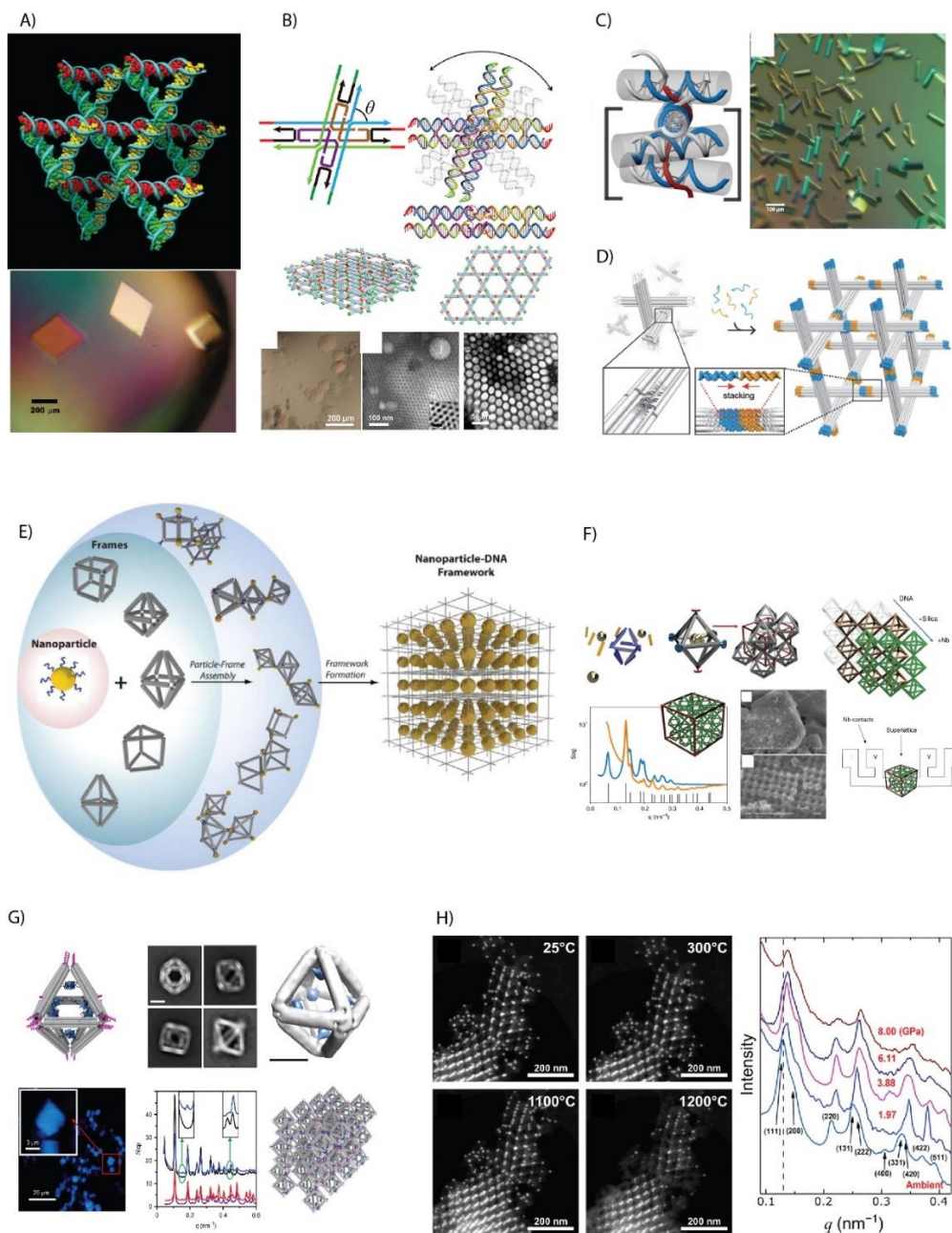


Figure 1.5. DNA lattices. A-C) DNA lattices based off of tiles. A) Self assembled crystal from tensegrity triangle.¹⁷ B) Layered crystal.²⁷ C) Self-assembled 4x5 crystal.²⁶ D-H) DNA origami based 3D lattices. D) DNA origami tensegrity triangle based lattice.²⁸ E) Lattices based off gold nanoparticles on the vertices.³⁰ F-H) Applications of these formed lattice structures. F) Niobium coated crystals showing superconductivity.³² G) crystals encapsulating enzymes showing increased activity.³¹ H) lattices when silicised in a controlled fashion showing increased stability to thermal and pressure changes.³³

1.4 Hybrid DNA nanostructures

While complex DNA-based nanostructures were being synthesized, utilization of the created structures for applications became increasingly important. The lack of chemical diversity and functionality became an increasing hurdle, and spurred efforts to integrate other functional entities into these structures. Nature overcomes this problem by the utilization of lipids/proteins/peptides/ glycans etc. One effective way for doing this is to conjugate³⁴ the molecule of interest to the strands of DNA. Several groups in the field have probed such directions.

The Shih lab used DNA-lipid conjugates to make a virus-inspired DNA nanostructure. This work was a pioneer in this direction wherein the authors made a PEG-ylated unilamellar DNA octahedron (Figure 1.6 A) and tested its efficiency towards nuclease degradation using DNA1 *in vitro*, and thereafter towards immune activation *in vivo* in mouse models³⁵. The Shih, Rotheman, and Lin labs in a collaborative effort thereafter used these conjugates to make controlled sized liposomes using DNA templates³⁶. In this work, they used a bio-inspired templating method to generate highly monodisperse sub-100 nm unilamellar vesicles (Figure 1.6 B). They used DNA frames of varying sizes from 29 nm to 94 nm and also controlled the number of DNA-lipid seed conjugates (2 to 16) within the frame to determine the efficient pathway to synthesize a monodisperse unilamellar liposome. After understanding the parameters from the study for liposome formation, the Lin lab extended this study to thereafter place, shape, and template liposomes with reconfigurable DNA nanocages³⁷⁻³⁸.

Protein-DNA hybrid nanostructures are the other important class of hybrid materials. One of the early examples where protein-DNA hybrid nanostructures were made was by the Mao lab, where they demonstrated the use of biotinylated strands on the DNA to make Streptavidin bound DNA polygons³⁹. Another example, demonstrated by the Dietz lab was to use of DNA-binding proteins to self-assemble and form hybrid DNA nanostructures⁴⁰ (Figure 1.6 C). For this they used transcription activator like (TAL) effector proteins binding to the major groove of the DNA construct complex hybrid architectures. The Stephanopoulos lab on the other hand used site specific conjugation to a KDPG aldolase trimeric protein to assemble a hybrid DNA tetrahedral cage⁴¹. This was the first such demonstration using a protein-DNA conjugate used as a structural building block in the field (Figure 1.6 D).

Peptide-DNA hybrid nanostructures on the other hand have been a relatively new area of investigation within the field. The Woolfson and Turberfield laboratories demonstrated the use of DNA origami structures to determine the effect of multivalency on peptide binding constants⁴². The Stephanopoulos lab used DNA-coiled coil peptide conjugates as a self-assembling motif to build large 1D DNA origami fibers⁴³ (Figure 1.6 E). The Ke lab utilized electrostatic interactions as a way to make these hybrid nanostructures for which they used a collagen mimetic peptide which electrostatically bound to 2D rectangular DNA origami sheets⁴⁴ (Figure 1.6 F).

Although, this section shows multiple examples of several hybrid nanostructures encompassing naturally occurring biomolecules, another class not covered here is the synthetic (artificial) polymer⁴⁵/ nanoparticle³¹ based DNA hybrid materials. The next step

in the field would be to integrate multiple of these hybrid materials together at a time into these nanostructures. However, for this to happen, the design rules of these entities need to be elucidated. For effective and faster realization of such systems, structural insights from cryo-EM and simulation models are required, but currently efforts in this direction are limited to a select few labs. Our work in chapter 3 later is one step in this direction which will try to address this challenge.

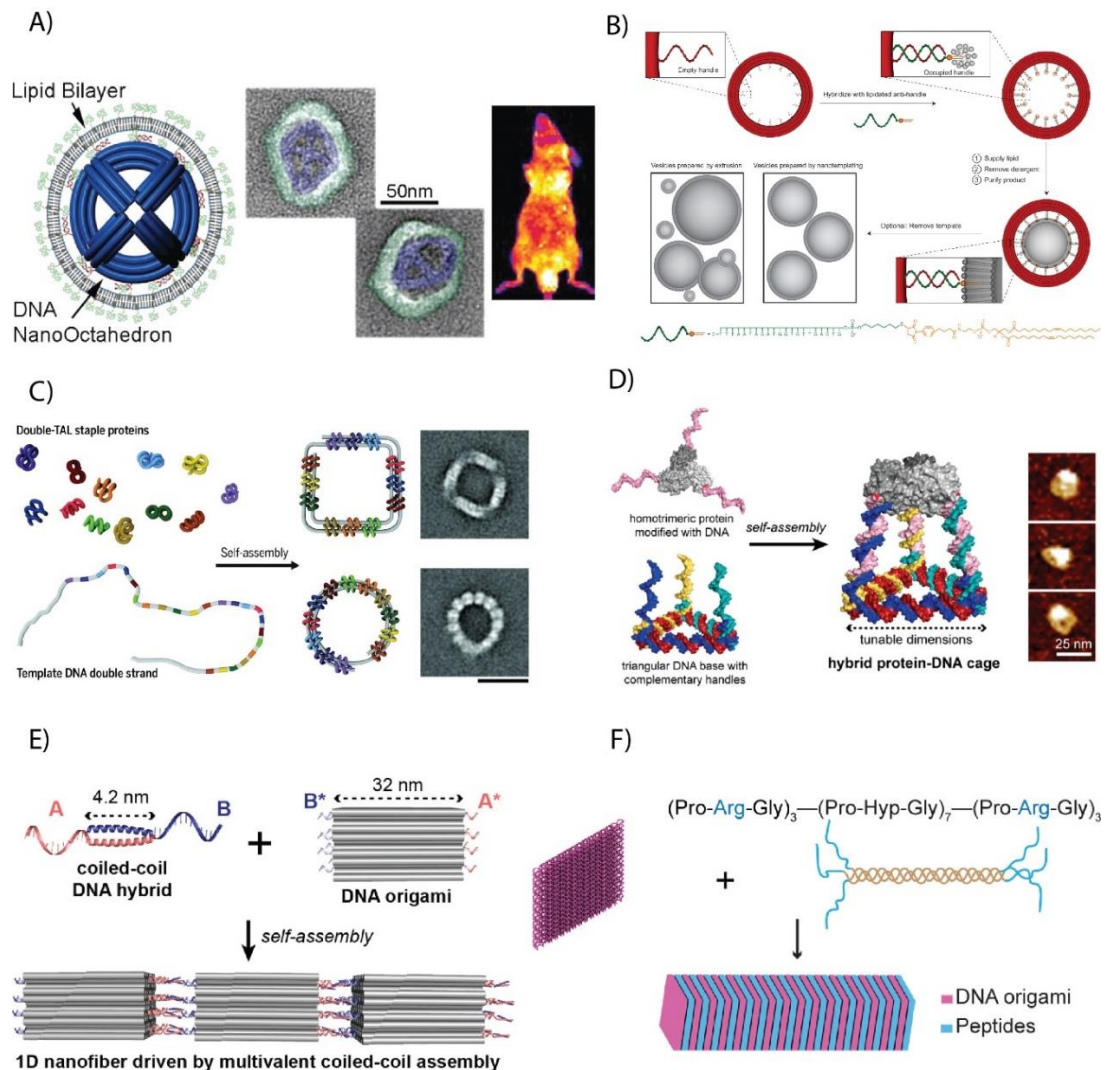


Figure 1.6. Hybrid nanostructures. A-B) Hybrid Lipid-DNA nanostructures³⁵⁻³⁶. C-D) Hybrid Protein-DNA nanostructures⁴⁰⁻⁴¹. E-F) Hybrid peptide-DNA nanostructures⁴³⁻⁴⁴.

1.5 Cryo-EM for structural insights

Since the discovery of the direct electron detector⁴⁶, and thereafter the Nobel Prize for cryo-electron microscopy, various scientists across the world have increasingly utilized this technique to their advantage. The field of DNA nanotechnology is no different.

Although the technique was used by a select few scientists to characterize DNA nanostructures using the CCD camera¹ (Figure 1.7 A), the technique gained increasing prominence when a DNA origami nanostructure was structurally resolved by single-particle reconstruction³(Figure 1.7 B). After this work was published, the technique has made a foothold in the field for characterizing 3D DNA nanostructures.

There have been several reports thereafter, wherein DNA nanostructures were used as molecular supports for solving protein structures. Three examples exist to date where different scientists have approached the problem with unique solutions. The Dietz lab resolved the structure of a p53 transcription factor protein using a DNA origami construct to ~ 15 Å (Figure 1.7 C)⁴. In this study, they first constructed a hollow DNA origami object capable of binding the p53 protein inside it along with a marker on the periphery for distinguishing the different orientations of the object. They further realized that the origami objects preferred to sit in the ice layer in an orientation wherein the hydrophobic groups tried to stick out at the air water interface. They utilized this to their advantage to design a DNA frame protecting the protein from aggregation and used the sequence inside the cavity for orienting it to get information from all angles. Following

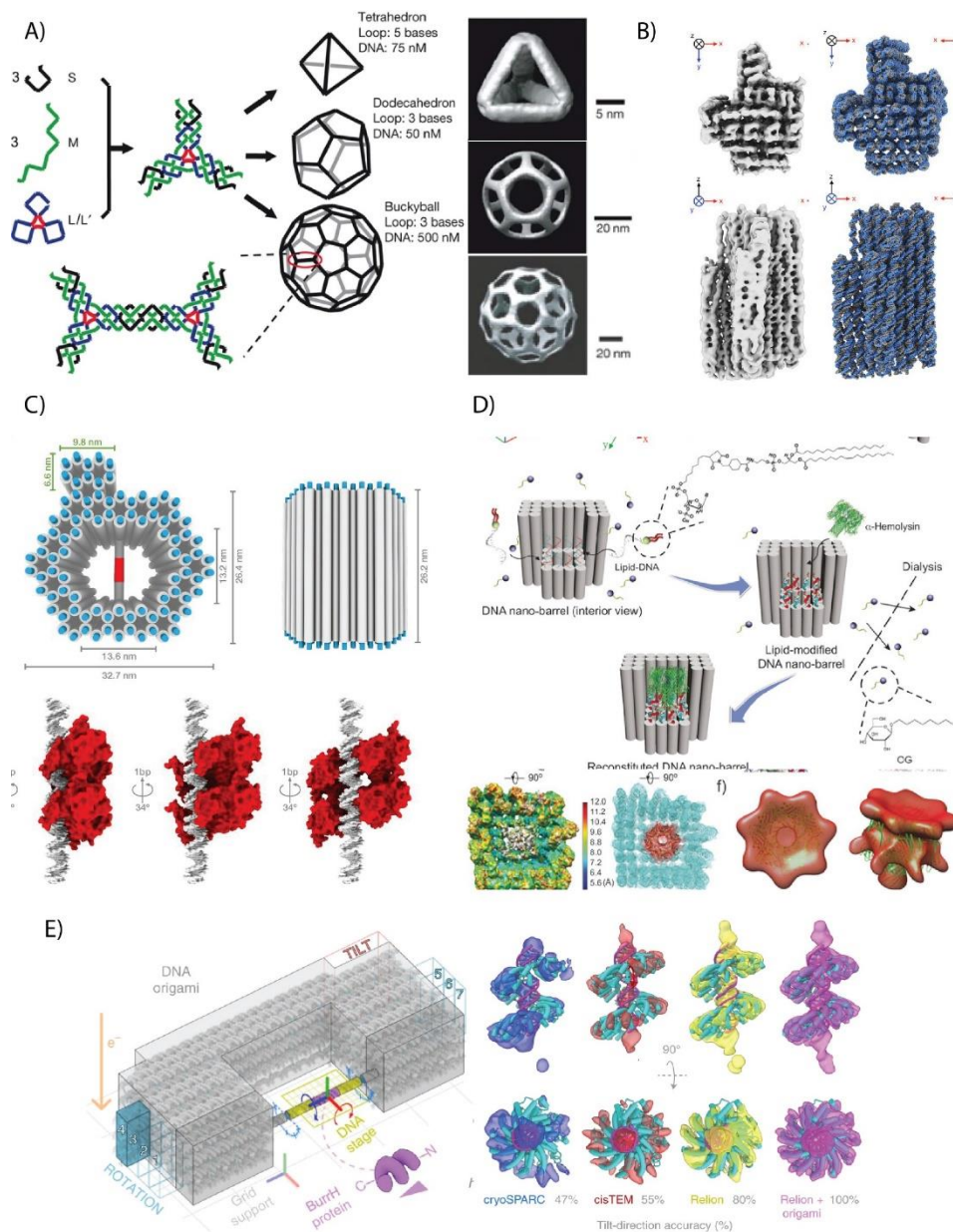


Figure 1.7 Cryo-EM characterization for DNA nanostructures. A) Examples of DNA nanostructures solved by cryo-EM using a CCD camera¹. B) The first DNA origami nanostructure solved by Cryo-EM³. C) DNA nanostructure used for anchoring and solving a DNA-bound protein⁴. D) DNA nanostructure conjugated to lipids for solving a α -hemolysin⁶. E) DNA goniometer used for solving a small protein BurrH to the highest resolution achieved to date (6.5 Å)⁸.

this study, the Mao lab in 2018 utilized a lipid conjugated DNA origami nanobarrel to solve the structure of α -hemolysin to 30Å (Figure 1.7 D) ⁶. Although, the resulting electron density map of the protein was not solved to high resolution, this was the first such method holding potential for the structural elucidation of membrane proteins or GPCRs. In 2021, learning from the above examples, the Douglas lab pushed the resolution of the small protein BurrH using a DNA origami to 6.5Å (Figure 1.7 E)⁸. This work represents the state of the art of technology which was capable of using DNA origami constructs as a goniometer to effectively introduce angular information to solve the structure of the protein. They compared their resultant electron density maps with and without the goniometer technology and realized that with only with the angle information provided from the goniometer the protein electron density fit well with the known crystal structure. These demonstrations are a scarce few among the whole family of proteins available in nature, and much needs to be done in the world of these hybrid DNA nanostructures. These can only be achieved if DNA nanotechnology and its methodologies are available to the larger scientific community.

1.6 Need for automation

DNA nanotechnology and its wide variety of capabilities, ranging from drug-delivery to photonic crystals, is one of the most promising nanotechnology approaches for realizing Richard Feynman's dream of building architectures by controlling atoms one by one. Although the field is growing, it is still largely limited to a small number of expert labs at this point. True realization of the capabilities can only be realized if a process of democratization were to occur. One major obstacle to this goal is the

unavailability of design software for DNA nanotechnology. Although, a few user-friendly programs—like Tiamat⁴⁷ and caDNAno⁴⁸ exist for the construction of tile- and origami-based structures, they are limited in their use because the user requires prior knowledge of designing DNA architectures. Thus, scientists in these past few years have made efforts to develop more general and user-friendly packages. METIS⁴⁹, TALOS⁵⁰, DAEDALUS⁵¹, vHelix⁵², vHelix-BSCOR⁵³ and PERDIX⁵⁴ are some software that meet this need. METIS and TALOS are programs capable of making 2D and 3D DNA nanostructures, respectively; however, their building unit is a six-helix bundle, whereas the others use a wireframe design and DX tile architectures. The field is especially limited and in its infancy with respect to automation. Much needs to be done to fully incorporate all the architectures that can be designed in the DNA nanotechnology world, and an automated software incorporating all of these design principles would greatly benefit scientists across multiple disciplines. Chapter 4 of the work in this thesis is one step in this direction. DAEDALUS⁵¹ are software packages for 3D design (the former uses 6 helix bundles and the later uses wireframe designs).

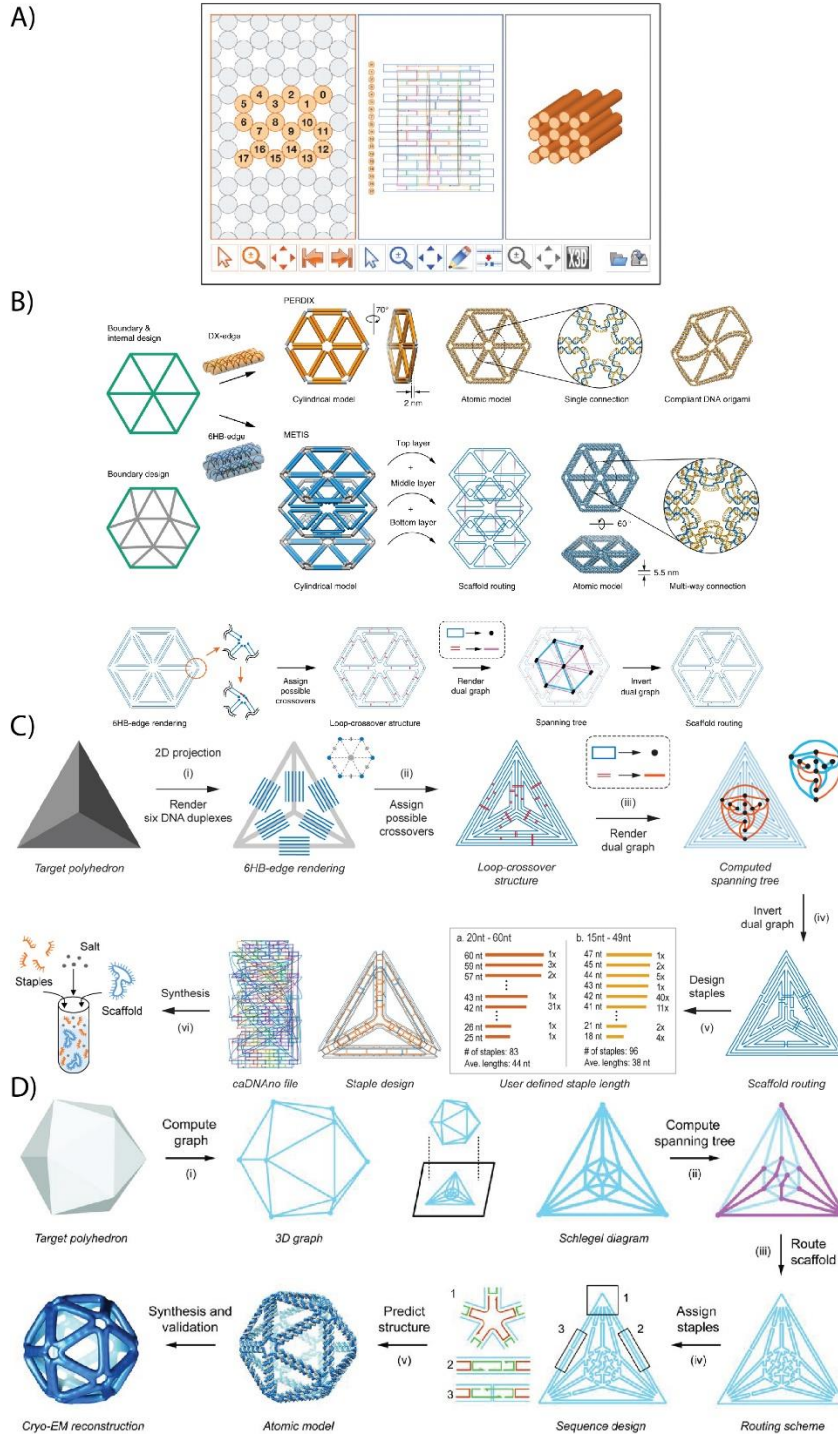


Figure 1.8. Example Software Packages: A) caDNAno, is the first software used for manual design of DNA origami⁴⁸. B-D) Automated design software packages B) PERDIX⁵⁴ and METIS⁴⁹ software packages for 2D origami structures C and D) TALOS⁵⁰ and

1.7 Dissertation overview

This dissertation focuses on advancing DNA nanotechnology in four different directions: 1) Probing alternate self-assembling molecules and integrating them with DNA nanostructures; 2) Characterizing hybrid protein-DNA nanostructures with novel new techniques like Cryo-EM and simulations to elucidate structural information; 3) Using automation to make curved DNA nanostructures; and 4) Assembling complex hierarchical DNA nanostructure assemblies. Chapter 2 demonstrates the use of host-guest interactions as a novel self-assembly tool that can be used in DNA nanotechnology. The chapter includes a brief introduction, the need and use of these novel interactions in DNA nanotechnology, and how this technology could be used for making functional DNA nanostructures. Chapter 3 describes the design and characterization of protein-DNA hybrid nanostructures using simulations and cryo-EM. It encompasses a detailed lead-up to the methods developed for the structural characterization of the hybrid nanostructures using cryo-EM, followed by simulation studies to provide important insights for developing hybrid nanostructures in the future. Chapter 4 delves into the need for democratization of DNA nanotechnology by automated design wherein we demonstrated the capability of making a nanocapsule structures with curvature. Chapter 5 goes on to probe the direction of assembling a DNA tetrastack lattice based on modelling and simulations, wherein we demonstrated the creation of 1D DNA origami icosahedral assemblies and the capability to characterize octahedral lattice structures. Chapter 6 concludes this thesis and provides future directions on where the field of DNA nanotechnology is headed into.

1.8 References

1. He, Y.; Ye, T.; Su, M.; Zhang, C.; Ribbe, A. E.; Jiang, W.; Mao, C., Hierarchical self-assembly of DNA into symmetric supramolecular polyhedra. *Nature* **2008**, *452* (7184), 198-201.
2. Watson, J. D.; Crick, F. H. C., Molecular Structure of Nucleic Acids: A Structure for Deoxyribose Nucleic Acid. *Nature* **1953**, *171* (4356), 737-738.
3. Bai, X.-c.; Martin, T. G.; Scheres, S. H. W.; Dietz, H., Cryo-EM structure of a 3D DNA-origami object. *Proceedings of the National Academy of Sciences* **2012**, *109* (49), 20012-20017.
4. Martin, T. G.; Bharat, T. A. M.; Joerger, A. C.; Bai, X.-c.; Praetorius, F.; Fersht, A. R.; Dietz, H.; Scheres, S. H. W., Design of a molecular support for cryo-EM structure determination. *Proceedings of the National Academy of Sciences* **2016**, *113* (47), E7456-E7463.
5. Seeman, N. C., Nucleic acid junctions and lattices. *Journal of Theoretical Biology* **1982**, *99* (2), 237-247.
6. Dong, Y.; Chen, S.; Zhang, S.; Sodroski, J.; Yang, Z.; Liu, D.; Mao, Y., Folding DNA into a Lipid-Conjugated Nanobarrel for Controlled Reconstitution of Membrane Proteins. *Angewandte Chemie International Edition* **2018**, *57* (8), 2072-2076.
7. Minchin, S.; Lodge, J., Understanding biochemistry: structure and function of nucleic acids. *Essays Biochem* **2019**, *63* (4), 433-456.
8. Aksel, T.; Yu, Z.; Cheng, Y.; Douglas, S. M., Molecular goniometers for single-particle cryo-electron microscopy of DNA-binding proteins. *Nature biotechnology* **2021**, *39* (3), 378-386.
9. Fu, T. J.; Seeman, N. C., DNA double-crossover molecules. *Biochemistry* **1993**, *32* (13), 3211-3220.
10. LaBean, T. H.; Yan, H.; Kopatsch, J.; Liu, F.; Winfree, E.; Reif, J. H.; Seeman, N. C., Construction, Analysis, Ligation, and Self-Assembly of DNA Triple Crossover Complexes. *Journal of the American Chemical Society* **2000**, *122* (9), 1848-1860.
11. Wang, X.; Chandrasekaran, A. R.; Shen, Z.; Ohayon, Y. P.; Wang, T.; Kizer, M. E.; Sha, R.; Mao, C.; Yan, H.; Zhang, X.; Liao, S.; Ding, B.; Chakraborty, B.; Jonoska, N.; Niu, D.; Gu, H.; Chao, J.; Gao, X.; Li, Y.; Ciengshin, T.; Seeman, N. C., Paranemic Crossover DNA: There and Back Again. *Chemical Reviews* **2019**, *119* (10), 6273-6289.

12. Winfree, E.; Liu, F.; Wenzler, L. A.; Seeman, N. C., Design and self-assembly of two-dimensional DNA crystals. *Nature* **1998**, *394* (6693), 539-544.
13. Roh, Y. H.; Ruiz, R. C. H.; Peng, S.; Lee, J. B.; Luo, D., Engineering DNA-based functional materials. *Chemical Society Reviews* **2011**, *40* (12), 5730-5744.
14. Liu, L.; Li, Z.; Li, Y.; Mao, C., Rational Design and Self-Assembly of Two-Dimensional, Dodecagonal DNA Quasicrystals. *Journal of the American Chemical Society* **2019**, *141* (10), 4248-4251.
15. Yan, H.; Park, S. H.; Finkelstein, G.; Reif, J. H.; LaBean, T. H., DNA-Templated Self-Assembly of Protein Arrays and Highly Conductive Nanowires. *Science* **2003**, *301* (5641), 1882-1884.
16. Yan, H.; Zhang, X.; Shen, Z.; Seeman, N. C., A robust DNA mechanical device controlled by hybridization topology. *Nature* **2002**, *415* (6867), 62-65.
17. Zheng, J.; Birktoft, J. J.; Chen, Y.; Wang, T.; Sha, R.; Constantinou, P. E.; Ginell, S. L.; Mao, C.; Seeman, N. C., From molecular to macroscopic via the rational design of a self-assembled 3D DNA crystal. *Nature* **2009**, *461* (7260), 74-77.
18. Dey, S.; Fan, C.; Gothelf, K. V.; Li, J.; Lin, C.; Liu, L.; Liu, N.; Nijenhuis, M. A. D.; Saccà, B.; Simmel, F. C.; Yan, H.; Zhan, P., DNA origami. *Nature Reviews Methods Primers* **2021**, *1* (1), 13.
19. Rothemund, P. W. K., Folding DNA to create nanoscale shapes and patterns. *Nature* **2006**, *440* (7082), 297-302.
20. Wagenbauer, K. F.; Sigl, C.; Dietz, H., Gigadalton-scale shape-programmable DNA assemblies. *Nature* **2017**, *552* (7683), 78-83.
21. Tikhomirov, G.; Petersen, P.; Qian, L., Fractal assembly of micrometre-scale DNA origami arrays with arbitrary patterns. *Nature* **2017**, *552* (7683), 67-71.
22. Ong, L. L.; Hanikel, N.; Yaghi, O. K.; Grun, C.; Strauss, M. T.; Bron, P.; Lai-Kee-Him, J.; Schueder, F.; Wang, B.; Wang, P.; Kishi, J. Y.; Myhrvold, C.; Zhu, A.; Jungmann, R.; Bellot, G.; Ke, Y.; Yin, P., Programmable self-assembly of three-dimensional nanostructures from 10,000 unique components. *Nature* **2017**, *552* (7683), 72-77.
23. Yao, G.; Zhang, F.; Wang, F.; Peng, T.; Liu, H.; Poppleton, E.; Šulc, P.; Jiang, S.; Liu, L.; Gong, C.; Jing, X.; Liu, X.; Wang, L.; Liu, Y.; Fan, C.; Yan, H., Meta-DNA structures. *Nature Chemistry* **2020**, *12* (11), 1067-1075.

24. Han, D.; Qi, X.; Myhrvold, C.; Wang, B.; Dai, M.; Jiang, S.; Bates, M.; Liu, Y.; An, B.; Zhang, F.; Yan, H.; Yin, P., Single-stranded DNA and RNA origami. *Science* **2017**, *358* (6369), eaao2648.
25. Hu, Y.; Niemeyer, C. M., From DNA Nanotechnology to Material Systems Engineering. *Advanced Materials* **2019**, *31* (26), 1806294.
26. Simmons, C. R.; Zhang, F.; Birktoft, J. J.; Qi, X.; Han, D.; Liu, Y.; Sha, R.; Abdallah, H. O.; Hernandez, C.; Ohayon, Y. P.; Seeman, N. C.; Yan, H., Construction and Structure Determination of a Three-Dimensional DNA Crystal. *Journal of the American Chemical Society* **2016**, *138* (31), 10047-10054.
27. Hong, F.; Jiang, S.; Lan, X.; Narayanan, R. P.; Šulc, P.; Zhang, F.; Liu, Y.; Yan, H., Layered-Crossover Tiles with Precisely Tunable Angles for 2D and 3D DNA Crystal Engineering. *Journal of the American Chemical Society* **2018**, *140* (44), 14670-14676.
28. Zhang, T.; Hartl, C.; Frank, K.; Heuer-Jungemann, A.; Fischer, S.; Nickels, P. C.; Nickel, B.; Liedl, T., 3D DNA Origami Crystals. *Advanced Materials* **2018**, *30* (28), 1800273.
29. Tian, Y.; Zhang, Y.; Wang, T.; Xin, H. L.; Li, H.; Gang, O., Lattice engineering through nanoparticle-DNA frameworks. *Nature materials* **2016**, *15* (6), 654-661.
30. Liu, W.; Tagawa, M.; Xin, H. L.; Wang, T.; Emamy, H.; Li, H.; Yager, K. G.; Starr, F. W.; Tkachenko, A. V.; Gang, O., Diamond family of nanoparticle superlattices. *Science (New York, N.Y.)* **2016**, *351* (6273), 582-586.
31. Tian, Y.; Lhermitte, J. R.; Bai, L.; Vo, T.; Xin, H. L.; Li, H.; Li, R.; Fukuto, M.; Yager, K. G.; Kahn, J. S.; Xiong, Y.; Minevich, B.; Kumar, S. K.; Gang, O., Ordered three-dimensional nanomaterials using DNA-prescribed and valence-controlled material voxels. *Nature Materials* **2020**, *19* (7), 789-796.
32. Shani, L.; Michelson, A. N.; Minevich, B.; Fleger, Y.; Stern, M.; Shaulov, A.; Yeshurun, Y.; Gang, O., DNA-assembled superconducting 3D nanoscale architectures. *Nature Communications* **2020**, *11* (1), 5697.
33. Majewski, P. W.; Michelson, A.; Cordeiro, M. A. L.; Tian, C.; Ma, C.; Kisslinger, K.; Tian, Y.; Liu, W.; Stach, E. A.; Yager, K. G.; Gang, O., Resilient three-dimensional ordered architectures assembled from nanoparticles by DNA. *Science Advances* **2021**, *7* (12), eabf0617.
34. Madsen, M.; Gothelf, K. V., Chemistries for DNA Nanotechnology. *Chemical Reviews* **2019**, *119* (10), 6384-6458.

35. Perrault, S. D.; Shih, W. M., Virus-Inspired Membrane Encapsulation of DNA Nanostructures To Achieve In Vivo Stability. *ACS Nano* **2014**, *8* (5), 5132-5140.
36. Yang, Y.; Wang, J.; Shigematsu, H.; Xu, W.; Shih, W. M.; Rothman, J. E.; Lin, C., Self-assembly of size-controlled liposomes on DNA nanotemplates. *Nature chemistry* **2016**, *8* (5), 476-483.
37. Zhang, Z.; Yang, Y.; Pincet, F.; Llaguno, M. C.; Lin, C., Placing and shaping liposomes with reconfigurable DNA nanocages. *Nature Chemistry* **2017**, *9* (7), 653-659.
38. Grome, M. W.; Zhang, Z.; Pincet, F.; Lin, C., Vesicle Tubulation with Self-Assembling DNA Nanosprings. *Angewandte Chemie International Edition* **2018**, *57* (19), 5330-5334.
39. Zhang, C.; Tian, C.; Guo, F.; Liu, Z.; Jiang, W.; Mao, C., DNA-Directed Three-Dimensional Protein Organization. *Angewandte Chemie International Edition* **2012**, *51* (14), 3382-3385.
40. Praetorius, F.; Dietz, H., Self-assembly of genetically encoded DNA-protein hybrid nanoscale shapes. *Science* **2017**, *355* (6331), eaam5488.
41. Xu, Y.; Jiang, S.; Simmons, C. R.; Narayanan, R. P.; Zhang, F.; Aziz, A.-M.; Yan, H.; Stephanopoulos, N., Tunable Nanoscale Cages from Self-Assembling DNA and Protein Building Blocks. *ACS Nano* **2019**, *13* (3), 3545-3554.
42. Jin, J.; Baker, E. G.; Wood, C. W.; Bath, J.; Woolfson, D. N.; Turberfield, A. J., Peptide Assembly Directed and Quantified Using Megadalton DNA Nanostructures. *ACS Nano* **2019**, *13* (9), 9927-9935.
43. Buchberger, A.; Simmons, C. R.; Fahmi, N. E.; Freeman, R.; Stephanopoulos, N., Hierarchical Assembly of Nucleic Acid/Coiled-Coil Peptide Nanostructures. *Journal of the American Chemical Society* **2020**, *142* (3), 1406-1416.
44. Jiang, T.; Meyer, T. A.; Modlin, C.; Zuo, X.; Conticello, V. P.; Ke, Y., Structurally Ordered Nanowire Formation from Co-Assembly of DNA Origami and Collagen-Mimetic Peptides. *Journal of the American Chemical Society* **2017**, *139* (40), 14025-14028.
45. Trinh, T.; Liao, C.; Toader, V.; Barłóg, M.; Bazzi, H. S.; Li, J.; Sleiman, H. F., DNA-imprinted polymer nanoparticles with monodispersity and prescribed DNA-strand patterns. *Nature Chemistry* **2018**, *10* (2), 184-192.
46. Deptuch, G.; Besson, A.; Rehak, P.; Szelezniak, M.; Wall, J.; Winter, M.; Zhu, Y., Direct electron imaging in electron microscopy with monolithic active pixel sensors. *Ultramicroscopy* **2007**, *107* (8), 674-84.

47. Williams, S.; Lund, K.; Lin, C.; Wonka, P.; Lindsay, S.; Yan, H., *Tiamat: A Three-Dimensional Editing Tool for Complex DNA Structures*. 2008; Vol. 5347, p 90-101.
48. Douglas, S. M.; Marblestone, A. H.; Teerapittayanon, S.; Vazquez, A.; Church, G. M.; Shih, W. M., Rapid prototyping of 3D DNA-origami shapes with caDNAno. *Nucleic Acids Research* **2009**, *37* (15), 5001-5006.
49. Jun, H.; Wang, X.; Bricker, W. P.; Bathe, M., Automated sequence design of 2D wireframe DNA origami with honeycomb edges. *Nature Communications* **2019**, *10* (1), 5419.
50. Jun, H.; Shepherd, T. R.; Zhang, K.; Bricker, W. P.; Li, S.; Chiu, W.; Bathe, M., Automated Sequence Design of 3D Polyhedral Wireframe DNA Origami with Honeycomb Edges. *ACS Nano* **2019**, *13* (2), 2083-2093.
51. Veneziano, R.; Ratanalert, S.; Zhang, K.; Zhang, F.; Yan, H.; Chiu, W.; Bathe, M., Designer nanoscale DNA assemblies programmed from the top down. *Science* **2016**, *352* (6293), 1534-1534.
52. Benson, E.; Mohammed, A.; Gardell, J.; Masich, S.; Czeizler, E.; Orponen, P.; Högberg, B., DNA rendering of polyhedral meshes at the nanoscale. *Nature* **2015**, *523* (7561), 441-444.
53. Benson, E.; Mohammed, A.; Bosco, A.; Teixeira, A. I.; Orponen, P.; Högberg, B., Computer-Aided Production of Scaffolded DNA Nanostructures from Flat Sheet Meshes. *Angewandte Chemie International Edition* **2016**, *55* (31), 8869-8872.
54. Jun, H.; Zhang, F.; Shepherd, T.; Ratanalert, S.; Qi, X.; Yan, H.; Bathe, M., Autonomously designed free-form 2D DNA origami. *Science Advances* **2019**, *5* (1), eaav0655.

CHAPTER 2

STIMULUS-RESPONSIVE DNA NANOSTRUCTURES VIA HIGH-AFFINITY HOST-GUEST INTERACTIONS

2.1 Introduction

Self-assembly in nature arises from the combination of multiple different non-covalent intermolecular forces. Inspired by the functional diversity of these systems, nanoscale materials have sought to integrate different and orthogonal interactions. Over the past 30 years, the field of DNA nanotechnology has yielded a suite of programmable structures driven by Watson-Crick pairing.¹⁻⁷ Recently, orthogonal non-covalent interactions have been introduced beyond the canonical forces underlying DNA structural organization, including: self-assembling peptides,⁸⁻¹² proteins,¹³⁻¹⁶ hydrophobic packing,¹⁷⁻¹⁹ and “peg in hole” base stacking.²⁰⁻²¹ These hybrid structures introduce the added control of different assembly “modes” with orthogonal molecular triggers, or leverage interactions beyond DNA hybridization for incorporation of other species.

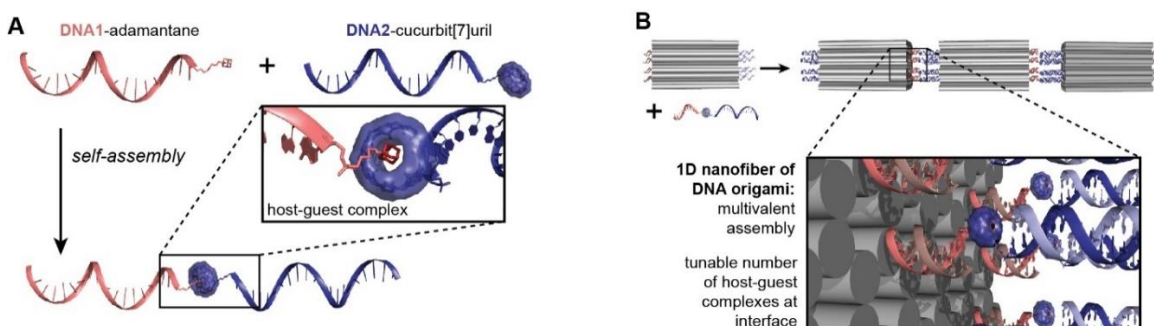


Figure 2.1. Self-assembly of DNA nanostructures using host-guest interactions. A) DNA strands modified with small molecule adamantane or cucurbit[7]uril moieties self-assemble by host-guest interactions. B) DNA origami cuboids bearing complementary handles assemble into long, 1D nanofibers by multiple interfacial host-guest complexes.

The recognition from a macrocycle host binding a small molecule guest has not been extensively explored in DNA nanotechnology. In a recent report, the Walther group demonstrated self-assembly of DNA origami cuboids into 1D fibers through interaction of β -cyclodextrin (β CD) macrocycles with adamantane (Ad) guests; efficient assembly required between 18-36 host-guest complexes per origami.²² Among host-guest motifs, the family of cucurbit[n]uril (CB[n]) macrocycles have particular utility compared to cyclodextrin.²³⁻²⁴ Within this family, CB[7] is especially promising for its solubility in water and exceptionally high binding affinity, with K_{eq} of order 10^{17} M^{-1} for certain guests.²⁵ For comparison, among the best interactions for β CD is its binding to an Ad guest, with K_{eq} of order 10^4 M^{-1} .²⁶ The dimensions and cavity volumes of β CD and CB[7] macrocycles are nearly identical.²⁷ Thus, the significantly enhanced affinity afforded by CB[7] expands the supramolecular design tool set, especially with the demonstration of routes to modify CB[7] with functional handles for inclusion on materials.²⁸⁻²⁹

Building off our work with heterodimeric coiled-coil peptides⁹, we show here the high-affinity CB[7]-Ad complex drives 1D fiber assembly with only 8 interactions per origami. At comparable valency, limited short oligomers were observed with β CD-Ad. The CB[7]-Ad motif thus provides an efficient orthogonal interaction for integration with DNA nanotechnology to enable hierarchical assembly through lightly modified programmable interfaces, or to display prosthetic moieties such as proteins, peptides, or nanoparticles.

Our design modifies two ssDNA handles (termed DNA1 and DNA2) with CB[7] or Ad at their 5' end. At a 1:1 ratio, Ad-DNA1 and CB[7]-DNA2 will form a heterodimer

with the host–guest motif linking the two oligonucleotides (Figure 2.1A). This heterodimer can then assemble DNA origami nanostructures bearing complementary handles to yield extended 1D nanofiber arrays (Figure 2.1B). In this design, the origami faces serve as programmable molecular pegboards, displaying a multivalent pattern of matched host–guest complexes, similar to diverse and cooperative interactions on protein–protein interfaces. Compared with sticky ends, interactions based on CB[7]–guest recognition have the added advantage of small size for a tight interface, as well as tunable interaction affinities spanning ~ 15 order of magnitude.²⁴⁻²⁵ As a model DNA origami nanostructure, we used a cuboid with dimensions 32 x 19.5 x 16 nm,^{9, 30} allowing for precise control of both the number and spatial distribution of complementary handles. For design of the origami cuboids, and handle locations, see Section S6 and Figure S2.5.

2.2 Ad/CB[7]-DNA conjugate assembly

DNA1 (10 nt) and DNA2 (21 nt) bearing a 5'-thiol were linked to adamantane via a maleimide-Ad conjugate. Separately, CB[7]-N₃ was synthesized by reported methods²⁸ and linked to DNA1 or DNA2 to via strain-promoted azide-alkyne cycloaddition (SPAAC) with a 5' dibenzocyclooctyne (DBCO)-functionalized oligonucleotide. For comparison, we conjugated β CD-N₃ to DNA1 via SPAAC. The structure of DNA conjugates used is shown in Figure 2.2A; for synthesis, purification, and characterization see Section S4. Next, we probed hetero-complex formation of the conjugates using native polyacrylamide gel electrophoresis (Figure 2.2B). Compared with the individual DNA conjugates (lanes 2 and 3), a 1:1 mixture of Ad-DNA1 and β CD-DNA1 (1 μ M each) did not show a band shift indicative of complex formation (lane 4); bands corresponding to the individual conjugates

remained, suggesting this concentration was below the effective K_d for the β CD–Ad complex. Comparatively, Ad-DNA1 and CB[7]-DNA1 (lanes 6 and 7) showed almost complete shift to a higher molecular weight species (lane 8, yellow arrow) indicative of stable complex formation resulting from a high-affinity CB[7]–Ad interaction.

To quantify the relative binding affinity between the Ad-DNA1 and CB[7]-DNA1 complex (cmplx), competition studies using 1-hydroxyadamantane (Ad-OH, K_{eq} of $2.3 \times 10^{10} \text{ M}^{-1}$ with CB[7])³¹ were performed. Exposing cmplx to increasing molar equivalents of Ad-OH decreased the intensity of the high-molecular weight band, with a concomitant increase in bands for Ad-DNA1 and CB[7]-DNA1 (Figure 2.2C). The reduction in cmplx as a function of Ad-OH “inhibitor” concentration was fit to a standard 3-parameter least squares regression, and the concentration ratio at the IC50 was multiplied by the known affinity of Ad-OH to yield a relative association constant ($K_{eq,rel}$) of $1.3 \times 10^{10} \text{ M}^{-1}$ for binding of Ad-DNA1 to CB[7]-DNA1 (Figure 2.2D). This value is consistent with those from competition NMR for a similar amide-linked Ad in binding to CB[7],³² suggesting DNA conjugation does not significantly perturb the binding of CB[7] to the Ad guest and validating use of this high-affinity interaction with DNA nanotechnology.

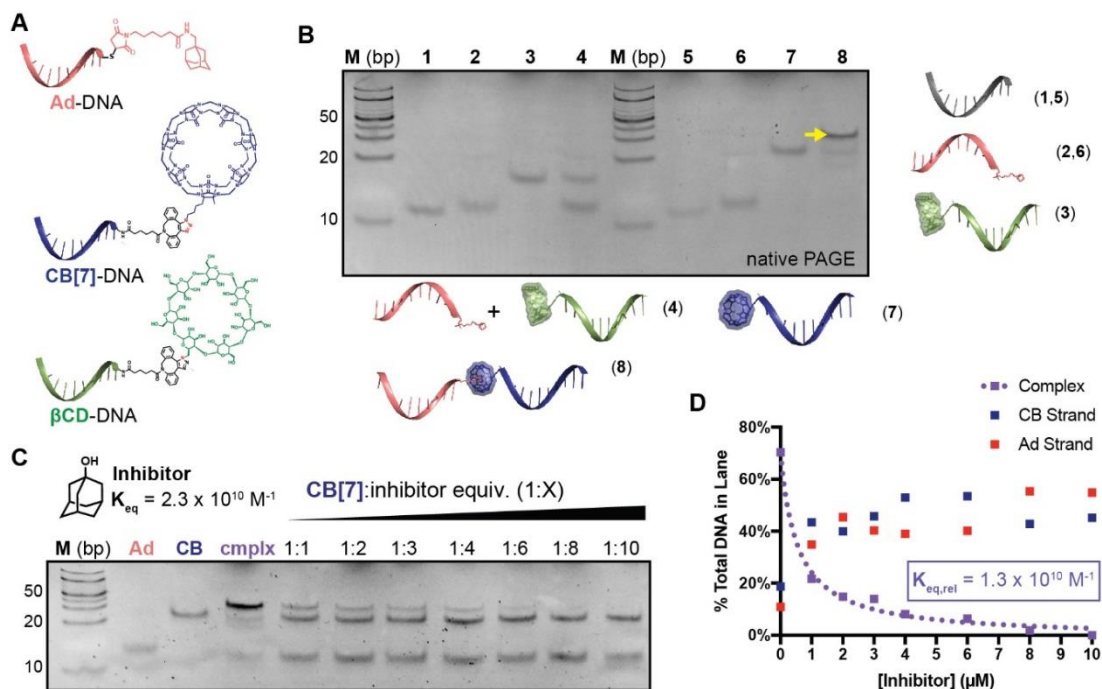


Figure 2.2. Characterization of host–guest complexation. A) Structures of Ad-DNA, CB[7]-DNA, and β CD-DNA. B) Native-PAGE analysis of host–guest complexation. DNA strands are depicted as single-stranded, but had their complement added prior to PAGE to form dsDNA and enhance staining. Lane M: dsDNA ladder (bp); 1,5: DNA1; 2,6: Ad-DNA1; 3: β CD-DNA1; 4: Ad-DNA1 + β CD-DNA1; 7: CB[7]-DNA1; 8: Ad-DNA1 + CB[7]-DNA1. C) Native-PAGE competition experiment between inhibitor (Ad-OH) and the Ad-DNA1 + CB[7]-DNA1 complex (cmplx). Lane M: dsDNA ladder (bp). Ad: Ad-DNA1; CB: CB[7]-DNA1; cmplx: Ad-DNA1 + CB[7]-DNA1; subsequent lanes: cmplx + indicated equivalents of Ad-OH. D) Plot of cmplx remaining as a function of Ad-OH inhibitor added.

2.3 One pot assembly of cuboidal origami fibers

We next turned to assembling the DNA origami cuboids, and attached Ad to DNA2 to avoid scrambling with CB[7]-DNA1. We first investigated a “one pot” annealing protocol, whereby all the components (i.e., the M13 scaffold, staple strands, staples bearing handles, and the small molecule-DNA conjugates) were mixed in a single tube and annealed from 65 to 4 °C over 40 h (Figure 2.3A). Given the high-affinity interaction

between CB[7] and Ad, we presume this recognition is minimally impacted by elevated temperatures. Accordingly, the CB[7]–Ad complex forms first under these conditions, followed by assembly of the core origami structure ($T_m \sim 55 \text{ }^\circ\text{C}$), and finally hybridization to the cuboids of the DNA handles ($T_m \sim 40\text{-}45 \text{ }^\circ\text{C}$).

We monitored cuboid assembly by agarose gel electrophoresis (AGE), as well as by negative stain TEM. By AGE, unmodified cuboids showed a distinct band for the nanostructure, along with a large higher-mobility band for excess staple strands (Figure 2.3B, lane 1). Cuboids bearing only CB[7]-DNA1 or Ad-DNA2 (8 handles) also showed only monomer bands (lanes 2 and 3). However, cuboids with 8 handles on both ends showed an aggregated band in the loading well, indicating formation of large structures (lane 4). By contrast, cuboids with Ad-DNA2 and β CD-DNA1 (8 handles) lacked this aggregate band, and were primarily monomers or very short oligomers (lane 5). Control experiments where the handles on Ad and CB[7] were swapped still yielded aggregates (Figure 2.3B, lane 7), whereas co-assembly with origami bearing mismatched poly(T) handles gave only short oligomers due to blunt-end stacking (Figure 2.3B, lanes 8 and 9). Studies with 1-7 handles per side yielded shorter fibers (Figure S2.5), so all further experiments employed 8 handles. We analyzed the structures prepared with Ad-DNA2 and CB[7]-DNA1 (lane 4) or β CD-DNA1 (lane 5) by TEM, and found that origami assembled with the Ad/CB[7] interaction formed long, 1D assemblies linked at the interfaces bearing host–guest motifs (Figure 2.3C). Fitting the length distribution of these fibers (Figure 2.3E) resulted in an average extent of polymerization (\bar{X}_n) of 7.9 ± 3.3 monomers.

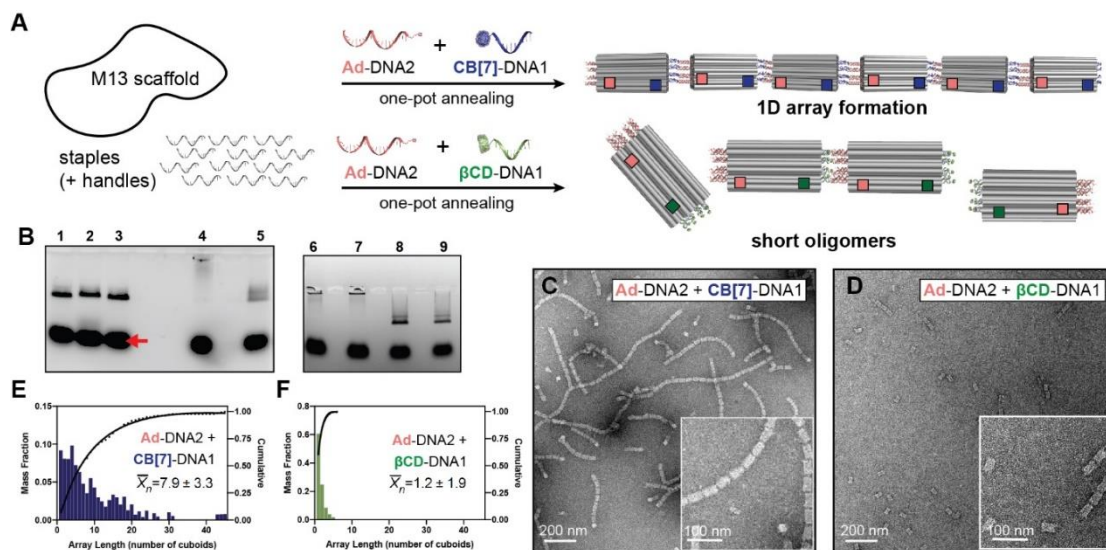


Figure 2.3. One-pot assembly of DNA origami nanofibers. A) Protocol for one-pot annealing; colored squares on origami indicate the location of Ad (pink), CB[7] (blue), or β CD (green). B) Agarose gel electrophoresis (AGE) of cuboid assembly. The red arrow indicates free staples. Lane 1: unmodified cuboids; 2: cuboids + Ad-DNA2; 3: cuboids + CB[7]-DNA1; 4,6: cuboids + Ad-DNA2 + CB[7]-DNA1; 5: cuboids + Ad-DNA2 + β CD-DNA1; 7: cuboids + Ad-DNA1 + CB[7]-DNA2; 8,9: cuboids with poly(T) handles with Ad-DNA2 + CB[7]-DNA1 (lane 8) or Ad-DNA1 + CB[7]-DNA2 (lane 9). C,D) Negative stain TEM images of samples in lanes 4 and 5, respectively. E,F) Histograms of array length by mass fraction (bars) and cumulative fraction (lines) of samples in lanes 4 and 5, respectively.

Some fibers surpassed 20-30 monomers, with the longest observed measuring 45 monomers and $\sim 2 \mu\text{m}$ in length. By contrast, origami assembled with the Ad/ β CD interaction yielded primarily monomers and the rare short oligomer ($\bar{X}_n = 1.2 \pm 1.9$), consistent with prior work which showed minimal 1D assembly when 9 handles were used.²² Taken together, our results demonstrate the advantage of high-affinity Ad/CB[7] motifs as efficient interactions to direct assembly of DNA cuboids, compared with the similarly sized Ad/ β CD recognition motif with affinity ~ 6 orders of magnitude lower.

2.4 Hierarchical assembly of fibers

In our work using coiled-coil peptides⁹, the modularity of disparate supramolecular modes enabled hierarchical assembly, whereby origami formed by a primary annealing step could be subsequently assembled into fibers through a second, lower-temperature incubation.

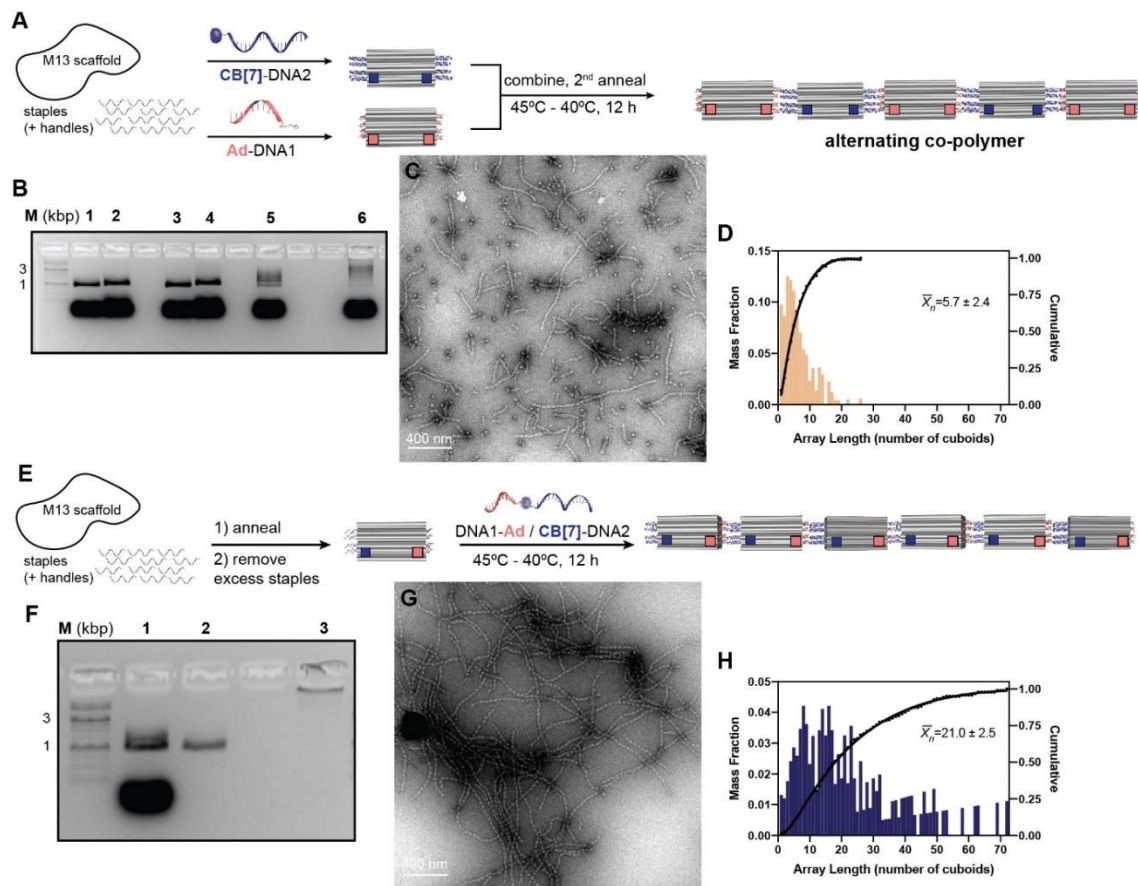


Figure 2.4. Hierarchical assembly of nanofibers. A) Protocol for copolymer formation (Pathway 1); colored squares on origami indicate the location of Ad (pink) or CB[7] (blue). B) AGE of cuboid assembly. Lane M: dsDNA ladder (kbp); 1,2: cuboids with Ad-DNA1 or CB[7]-DNA1 on both sides, respectively; 3,4: cuboids with Ad-DNA2 or CB[7]-DNA2 on both sides, respectively; 5: lane 1 + lane 4, after second anneal; 6: lane 2 + lane 3, after second anneal. C) Negative stain TEM images of lane 6 fibers. D) Histograms of array length by mass fraction (bars) and cumulative fraction (lines) for lane 6 fibers. E) Protocol for assembly of purified origami by pre-formed host-guest complex with DNA handles

(Pathway 2). F) AGE of cuboid assembly. Lane M: dsDNA ladder (kbp); 1: unpurified cuboids; 2: purified cuboids; 3: purified cuboids + DNA2-Ad/CB[7]-DNA1 complex, after second anneal. G) Negative stain TEM images of fibers. H) Histograms of array length by mass fraction (bars) and cumulative fraction (lines) for fibers.

Thus, we next probed two alternate assembly pathways to optimize formation of Ad/CB[7]-directed 1D arrays: (1) separately forming origami cuboids with Ad or CB[7] on both sides, and then co-assembling them into an “alternating copolymer” (Figure 2.4A); and (2) purifying origami cuboids bearing complementary DNA handles, and then assembling them with pre-formed DNA1-Ad/CB[7]-DNA2 complex (Figure 2.4E). For both routes, the second annealing was conducted at 45-40 °C over 12 h, followed by rapid cooling to 4 °C. Analysis of the “copolymer” route (pathway 1) by both AGE (Figure 2.4B) and TEM (Figure 2.4C, D) revealed the formation of 1D nanofibers. The fibers are morphologically similar to those of the one-pot system: long and straight, yet somewhat shorter ($\bar{X}_n = 5.7 \pm 2.4$ monomers). By contrast, purified cuboids combined with pre-formed DNA1-Ad/CB[7]-DNA2 complex (pathway 2) showed dramatically longer fibers by TEM (Figure 2.4G,H), with $\bar{X}_n = 21.0 \pm 2.5$ monomers, and the longest observed fiber reaching 72 cuboids ($\sim 3.3 \mu\text{m}$) in length. Interestingly, these results parallel those obtained from our work with peptide heterodimers,⁹ with the sequential assembly of purified cuboids giving the longest fibers. The similarity in respective length distributions suggests a universality

in DNA cuboid self-assembly arising from disparate motifs—coiled-coil assembly vs. host-guest binding—with each capable of high-affinity (i.e., sub-nanomolar) interactions.

2.5 Stimulus responsive nano-system

Stimulus-responsive host–guest affinity motifs have great potential for external control of DNA assembly³³. Toward this end, we designed a DNA nano-box having CB[7] moieties on its faces as an example nanostructure that could be closed by a trigger Ad-peptide-Ad as the lock (response –Box in its closed state) and further opened back to its original state with an MMP8 protein which would act as the key (Figure 2.5 B). The demonstration using a DNA-nanostructure that can be opened in a tumor microenvironment by the use of MMP-8 protein holds particular promise in the context of cancer therapy because of the overexpression of these MMP enzymes³⁴.

For this we first tested out and optimized the functional components that act as our lock and key. Then, we first selected and synthesized a known peptide with a recognizable sequence³⁵ by the MMP8 protein and modified it with Ad on both its terminal ends (Figure S2.13). After this we carried out a binding study with our CB[7]-DNA2 system and characterized it using Native-PAGE (Figure 2.5A). We first annealed Ad-peptide-Ad with CB[7]-DNA2 (lane3) and ran the annealed mixture on the gel with controls of just CB[7]-DNA2 (lane 2) and unmodified DNA2 (lane1) and probed their assembly by the formation of an upper band. The uppermost band in lane 3 corresponds to two molecules of CB[7]-DNA2 interacting with the Ad-peptide-Ad and the band below corresponds to the peptide binding to a single molecule. We then confirmed that these assemblies were due to

CB[7]/Ad interactions by running a control of unmodified DNA2 along with the Ad-peptide-Ad and saw no formation of any assembled species (lane 4). We then tested the capability of MMP8 protein to recognize the Ad-peptide-Ad when complexed with the

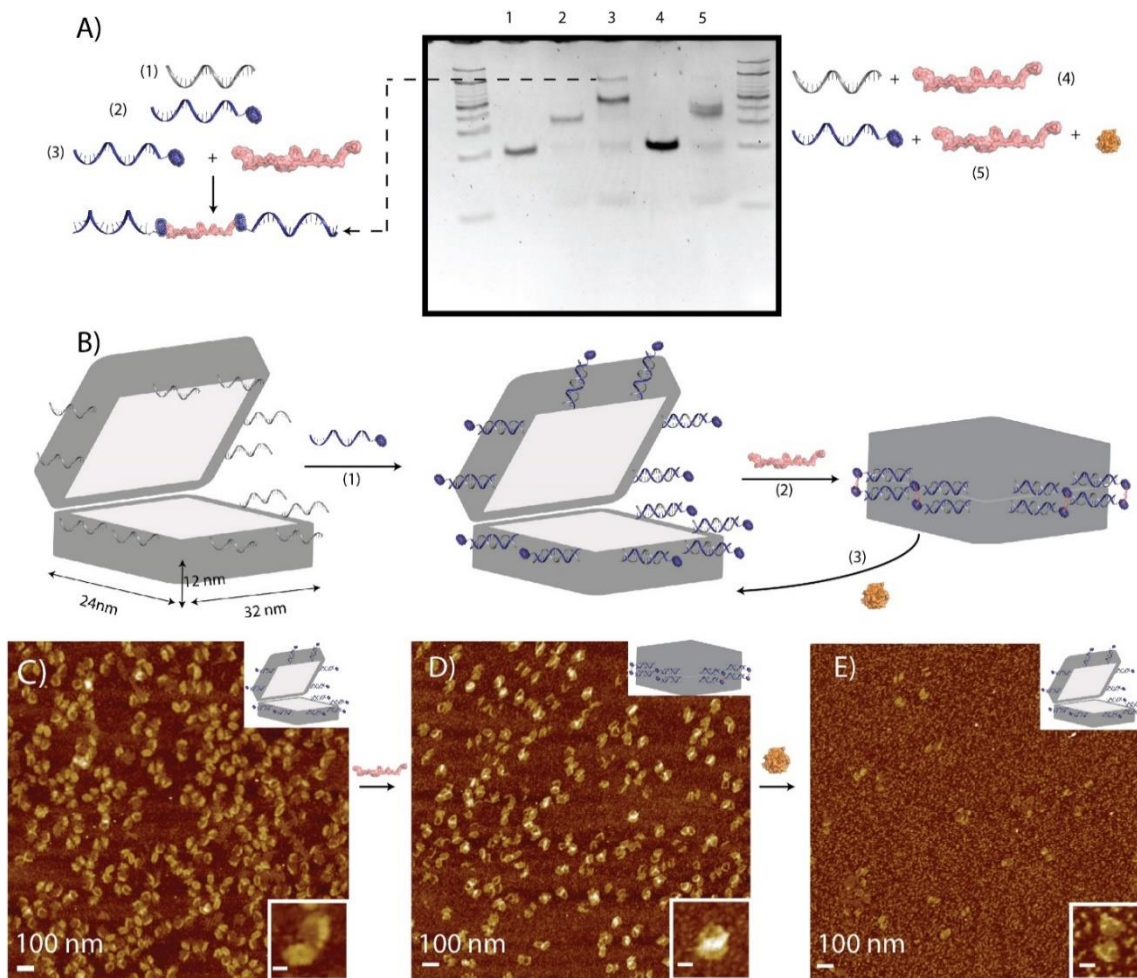


Figure 2.5. Peptide based lock and key mechanism. (A) Characterization of Ad-Peptide-Ad with CB[7]-DNA2. Lane 1: DNA2, lane2: CB[7]-DNA2, Lane3: Ad-peptide-Ad annealed with CB[7]-DNA2, Lane 4: unmodified DNA2 annealed with peptide, Lane5: MMP8 protein added to sample in lane 3. (B) Schematic of lock and key mechanism of DNA-Box with Ad-peptide-Ad and MMP8 protein. (1-3) Addition of (1) CB[7]-DNA2 to the DNA box. (2) Ad-peptide-Ad. (3) MMP8 protein. (C) AFM image with inset of open DNA Box-CB[7] (D) AFM image with inset of closed DNA box-CB[7] with Ad-peptide-Ad. (E) AFM image with inset showing the opening back of DNA box using the MMP8 protein. Inset scale bars are 30nm.

CB[7] system. For this we incubated (Section S6) the MMP8 protein with the assembled species from lane 3 and saw that the protein cleaved the assembled species back into the CB[7]-DNA2 as shown in lane5. After the effective realization of lock and key components, we then proceed to utilize this system on the DNA-nano-box.

We designed the box with two equivalent halves 24 x 32 x 12 nm in size, utilizing the M13p18 scaffold. Thereafter we chose 12 positions on the box (six per half) for placing the complementary handle sequences for their hybridization to CB[7]-DNA2 (Figure S2.12). Each handle per side of the face was spaced at a distance of 42 bases (~14.28 nm). This spacing was chosen to avoid crosstalk between the Ad-peptide-Ad bound to the adjacent CB[7]-DNA2 on the same half. The handle extensions from the frame were also provided flexibility via two thymidines in between to accommodate for possible steric interferences when the Ad-peptide-Ad bound to the two halves (Figure S2.12). The working principle was to close (“lock”) the two halves of the DNA box using the Ad-peptide-Ad and open it back again with a MMP8 protein as the “key”, as illustrated in the schematic of Figure 2.5 B. We first tested out this working hypothesis by AGE. Lane 1 of Figure S2.14 shows the formation of the nano-box in good yield; however, as expected the box moved more slowly in the gel when 12 handle extensions were added to it (lane 2). The nanostructure grew larger still (i.e. showed reduced migration) when CB[7]-DNA2 was added (lane 3). Lane 4 of Figure S2.14, however, showed a downward shift when Ad-peptide-Ad was annealed with the nano-box bearing CB[7]-DNA2. We attribute this faster migration to the conformational change of the nano-box to a closed (and thus more compact) state. Next, these samples were imaged

using AFM, as shown in Figures (2.5C,D). These images illustrate that the nano-box remains in an open confirmation when CB[7]-DNA 2 is added and it closes when the peptide is added to it. We further added MMP8 protein to the closed nano-box, imaged the structure via AFM, and saw that the box was opened back again (Figure 2.5E). We have yet to confirm the efficiency of opening and closing of the nano-box, but intend to perform a Fluorescence Resonance Energy Transfer (FRET) assay to quantify this value.

2.6 Conclusion and future directions

In conclusion, we have demonstrated that the high-affinity Ad/CB[7] recognition motif is an effective orthogonal self-assembling interaction that holds promise for the construction of next-generation DNA nanostructures. Firstly, we effectively demonstrated the capability of these interactions for the hierarchical 1D assembly of DNA nanostructure to form micron-length supramolecular polymers. Relative to prior reports using host-guest recognition of Ad by similarly sized β CD macrocycles, with distributions of 1D arrays \sim 12 cuboids in length when using 36 handles,²² the optimized assembly path here generates significantly longer 1D arrays while requiring only 8 handles on each interface. We then demonstrated the effective use of these interactions via a lock-and-key mechanism on a DNA box nanostructure using a peptide recognizable by a MMP-8 protein. Although, a quantitative yield needs to be calculated for both the closing and opening processes, the results here hold promise for the stimulus-responsive modulation of DNA nanostructures.

A key advantage of the Ad/CB[7] motif is the small footprint needed for recognition, relative to DNA hybridization. Thus, these interactions should be useful for attaching larger functional species such as proteins to DNA scaffolds, or in engineering

tighter interfaces between DNA nanostructures compared with sticky ends. Encoding multiple orthogonal interfaces between DNA nanostructures may also be possible by spatially controlled distribution of CB[7] and Ad moieties, similar to the work using peg-in-hole base-stacked DNA nanostructures.²⁰⁻²¹ Encapsulating hydrophobic drug molecules into these CB[7] moieties and anchoring them into nano-vehicles could also be a direction that holds promise. Thus, in future, Ad/CB[7] interactions hold much promise to be used as orthogonal interactions in parallel with Watson-Crick base pairing for the construction of “smart” DNA nano-vehicles for targeted delivery of drugs.

2.7 References

1. Winfree, E.; Liu, F.; Wenzler, L. A.; Seeman, N. C., Design and self-assembly of two-dimensional DNA crystals. *Nature* **1998**, *394* (6693), 539-544.
2. Yan, H.; Park, S. H.; Finkelstein, G.; Reif, J. H.; LaBean, T. H., DNA-Templated Self-Assembly of Protein Arrays and Highly Conductive Nanowires. *Science* **2003**, *301* (5641), 1882-1884.
3. Rothemund, P. W. K., Folding DNA to create nanoscale shapes and patterns. *Nature* **2006**, *440* (7082), 297-302.
4. Douglas, S. M.; Dietz, H.; Liedl, T.; Högberg, B.; Graf, F.; Shih, W. M., Self-assembly of DNA into nanoscale three-dimensional shapes. *Nature* **2009**, *459* (7245), 414-418.
5. Ke, Y.; Ong, L. L.; Shih, W. M.; Yin, P., Three-Dimensional Structures Self-Assembled from DNA Bricks. *Science* **2012**, *338* (6111), 1177-1183.
6. Hong, F.; Zhang, F.; Liu, Y.; Yan, H., DNA Origami: Scaffolds for Creating Higher Order Structures. *Chemical Reviews* **2017**, *117* (20), 12584-12640.
7. Zheng, J.; Birktoft, J. J.; Chen, Y.; Wang, T.; Sha, R.; Constantinou, P. E.; Ginell, S. L.; Mao, C.; Seeman, N. C., From molecular to macroscopic via the rational design of a self-assembled 3D DNA crystal. *Nature* **2009**, *461* (7260), 74-77.

8. Jin, J.; Baker, E. G.; Wood, C. W.; Bath, J.; Woolfson, D. N.; Turberfield, A. J., Peptide Assembly Directed and Quantified Using Megadalton DNA Nanostructures. *ACS Nano* **2019**, *13* (9), 9927-9935.
9. Buchberger, A.; Simmons, C. R.; Fahmi, N. E.; Freeman, R.; Stephanopoulos, N., Hierarchical Assembly of Nucleic Acid/Coiled-Coil Peptide Nanostructures. *Journal of the American Chemical Society* **2020**, *142* (3), 1406-1416.
10. Freeman, R.; Han, M.; Álvarez, Z.; Lewis, J. A.; Wester, J. R.; Stephanopoulos, N.; McClendon, M. T.; Lynsky, C.; Godbe, J. M.; Sangji, H.; Luijten, E.; Stupp, S. I., Reversible self-assembly of superstructured networks. *Science* **2018**, *362* (6416), 808-813.
11. Daly, M. L.; Gao, Y.; Freeman, R., Encoding Reversible Hierarchical Structures with Supramolecular Peptide–DNA Materials. *Bioconjugate Chemistry* **2019**, *30* (7), 1864-1869.
12. Jiang, T.; Meyer, T. A.; Modlin, C.; Zuo, X.; Conticello, V. P.; Ke, Y., Structurally Ordered Nanowire Formation from Co-Assembly of DNA Origami and Collagen-Mimetic Peptides. *Journal of the American Chemical Society* **2017**, *139* (40), 14025-14028.
13. Xu, Y.; Jiang, S.; Simmons, C. R.; Narayanan, R. P.; Zhang, F.; Aziz, A.-M.; Yan, H.; Stephanopoulos, N., Tunable Nanoscale Cages from Self-Assembling DNA and Protein Building Blocks. *ACS Nano* **2019**, *13* (3), 3545-3554.
14. Praetorius, F.; Dietz, H., Self-assembly of genetically encoded DNA-protein hybrid nanoscale shapes. *Science* **2017**, *355* (6331), eaam5488.
15. Kashiwagi, D.; Sim, S.; Niwa, T.; Taguchi, H.; Aida, T., Protein Nanotube Selectively Cleavable with DNA: Supramolecular Polymerization of “DNA-Appended Molecular Chaperones”. *Journal of the American Chemical Society* **2018**, *140* (1), 26-29.
16. McMillan, J. R.; Mirkin, C. A., DNA-Functionalized, Bivalent Proteins. *Journal of the American Chemical Society* **2018**, *140* (22), 6776-6779.
17. Goetzfried, M. A.; Vogele, K.; Mückl, A.; Kaiser, M.; Holland, N. B.; Simmel, F. C.; Pirzer, T., Periodic Operation of a Dynamic DNA Origami Structure Utilizing the Hydrophilic–Hydrophobic Phase-Transition of Stimulus-Sensitive Polypeptides. *Small* **2019**, *15* (45), 1903541.
18. Wilks, T. R.; Bath, J.; de Vries, J. W.; Raymond, J. E.; Herrmann, A.; Turberfield, A. J.; O’Reilly, R. K., “Giant Surfactants” Created by the Fast and Efficient Functionalization of a DNA Tetrahedron with a Temperature-Responsive Polymer. *ACS Nano* **2013**, *7* (10), 8561-8572.

19. Serpell, C. J.; Edwardson, T. G. W.; Chidchob, P.; Carneiro, K. M. M.; Sleiman, H. F., Precision Polymers and 3D DNA Nanostructures: Emergent Assemblies from New Parameter Space. *Journal of the American Chemical Society* **2014**, *136* (44), 15767-15774.
20. Woo, S.; Rothmund, P. W. K., Programmable molecular recognition based on the geometry of DNA nanostructures. *Nature Chemistry* **2011**, *3* (8), 620-627.
21. Gerling, T.; Wagenbauer, K. F.; Neuner, A. M.; Dietz, H., Dynamic DNA devices and assemblies formed by shape-complementary, non-base pairing 3D components. *Science* **2015**, *347* (6229), 1446-1452.
22. Loescher, S.; Walther, A., Supracolloidal Self-Assembly of Divalent Janus 3D DNA Origami via Programmable Multivalent Host/Guest Interactions. *Angewandte Chemie International Edition* **2020**, *59* (14), 5515-5520.
23. Kim, J.; Jung, I.-S.; Kim, S.-Y.; Lee, E.; Kang, J.-K.; Sakamoto, S.; Yamaguchi, K.; Kim, K., New Cucurbituril Homologues: Syntheses, Isolation, Characterization, and X-ray Crystal Structures of Cucurbit[n]uril (n = 5, 7, and 8). *Journal of the American Chemical Society* **2000**, *122* (3), 540-541.
24. Barrow, S. J.; Kasera, S.; Rowland, M. J.; del Barrio, J.; Scherman, O. A., Cucurbituril-Based Molecular Recognition. *Chemical Reviews* **2015**, *115* (22), 12320-12406.
25. Cao, L.; Šekutor, M.; Zavalij, P. Y.; Mlinarić-Majerski, K.; Glaser, R.; Isaacs, L., Cucurbit[7]uril-Guest Pair with an Attomolar Dissociation Constant. *Angewandte Chemie International Edition* **2014**, *53* (4), 988-993.
26. Eftink, M. R.; Andy, M. L.; Bystrom, K.; Perlmutter, H. D.; Kristol, D. S., Cyclodextrin inclusion complexes: studies of the variation in the size of alicyclic guests. *Journal of the American Chemical Society* **1989**, *111* (17), 6765-6772.
27. Webber, M. J.; Langer, R., Drug delivery by supramolecular design. *Chemical Society Reviews* **2017**, *46* (21), 6600-6620.
28. Vinciguerra, B.; Cao, L.; Cannon, J. R.; Zavalij, P. Y.; Fenselau, C.; Isaacs, L., Synthesis and Self-Assembly Processes of Monofunctionalized Cucurbit[7]uril. *Journal of the American Chemical Society* **2012**, *134* (31), 13133-13140.
29. Ghosh, S. K.; Dhamija, A.; Ko, Y. H.; An, J.; Hur, M. Y.; Boraste, D. R.; Seo, J.; Lee, E.; Park, K. M.; Kim, K., Superacid-Mediated Functionalization of Hydroxylated Cucurbit[n]urils. *Journal of the American Chemical Society* **2019**, *141* (44), 17503-17506.

30. Tigges, T.; Heuser, T.; Tiwari, R.; Walther, A., 3D DNA Origami Cuboids as Monodisperse Patchy Nanoparticles for Switchable Hierarchical Self-Assembly. *Nano Letters* **2016**, *16* (12), 7870-7874.
31. Moghaddam, S.; Yang, C.; Rekharsky, M.; Ko, Y. H.; Kim, K.; Inoue, Y.; Gilson, M. K., New Ultrahigh Affinity Host–Guest Complexes of Cucurbit[7]uril with Bicyclo[2.2.2]octane and Adamantane Guests: Thermodynamic Analysis and Evaluation of M2 Affinity Calculations. *Journal of the American Chemical Society* **2011**, *133* (10), 3570-3581.
32. Zou, L.; Braegelman, A. S.; Webber, M. J., Spatially Defined Drug Targeting by in Situ Host–Guest Chemistry in a Living Animal. *ACS Central Science* **2019**, *5* (6), 1035-1043.
33. Braegelman, A. S.; Webber, M. J., Integrating Stimuli-Responsive Properties in Host-Guest Supramolecular Drug Delivery Systems. *Theranostics* **2019**, *9* (11), 3017-3040.
34. Juurikka, K.; Butler, G. S.; Salo, T.; Nyberg, P.; Åström, P., The Role of MMP8 in Cancer: A Systematic Review. *Int J Mol Sci* **2019**, *20* (18), 4506.
35. Patterson, J.; Hubbell, J. A., Enhanced proteolytic degradation of molecularly engineered PEG hydrogels in response to MMP-1 and MMP-2. *Biomaterials* **2010**, *31* (30), 7836-7845.

CHAPTER 3

CHARACTERIZATION OF PROTEIN-DNA HYBRID NANOSTRUCTURES THROUGH EXPERIMENT AND SIMULATION

3.1 Introduction

The field of Deoxyribonucleic acid (DNA) technology¹⁻² is considered to be one of the frontrunners in realizing Richard Feynman's dreams of building objects at the nanoscale. DNA nanotechnology works by manipulating oligonucleotides using their programmable and predictable Watson-Crick base pairing³ to fold into designed shapes. The nano-objects thus formed have been utilized for a variety of applications, including molecular storage⁴⁻⁵, logic gate circuits⁶⁻⁹, and drug delivery machines¹⁰⁻¹¹. However, using these nanostructures as biocompatible drug delivery vehicles has become increasingly relevant in the context of an ever changing disease prone world¹². But, the field has yet to achieve any substantial jump in this direction (noting a few exceptions)¹²⁻¹³. This has much to do with the limiting chemical functionality of the fundamental building block of these nanostructures, which is DNA. Nature overcomes this problem by making functional proteins using its chemically diverse toolkit of amino acids. However, designing nanostructures using amino acids is not a trivial feat, as their chemistry lacks predictability in comparison to nucleic acids. The most commonly used technique to design protein nanostructures revolves around using the software 'Rosetta'¹⁴, but this technique is limited to a few protein design scientists because of its difficulty. We believe that a true realization of a functional nano-robot can only be realized if there is a way to design and demonstrate

Protein-DNA hybrid nanostructures (PDHNs). This is a difficult problem to achieve for two reasons: first, the design rules have yet to be figured out completely, and second, designer software integrating both these components are rare and typically not scalable to DNA origami system sizes. Our work in this chapter is a step in this direction. Protein-DNA hybrid nanostructures can only be realized if researchers are able to make a designer-friendly protein-DNA fundamental building block. One such direction is to use DNA binding proteins as a building block¹⁵. However, PDHNs can realize its true purpose only if we can use other functional proteins. To do so, there is a need to conjugate these proteins to DNA in a site-specific manner without losing their functionality. Understanding design parameters of such a building block requires us to have insight into various parameters like: 1) proper site of conjugation on the protein, 2) the choice of chemistry to use for conjugation, 3) flexibility of the small molecule linker length between the DNA backbone to the conjugation site on the protein surface. Once such a building block has been made, using it for making a hybrid system is the next challenge. Oftentimes the incorporation efficiency of the conjugate into the nanostructure is low, and there could be multiple reasons on why that is the case, e.g. the unavailability of complementary DNA handle sites, or the resulting steric hindrance the nanostructure experiences after the incorporation of the conjugate. In order to address these challenges and design these PDHNs in a better way, we need to perform experiments and correlate them with simulations. For this purpose, we started working with our previously published building block KDPG aldolase-DNA conjugate¹⁶.

In this work here, we used the same structural building block as before¹⁶ (Figure 3.1B) and incorporated it into a DNA origami nanostructure. We developed this strategy for multiple reasons: 1) to develop a protein-DNA hybrid simulation model with structural insights from experiments; 2) to figure out essential structural insights through simulations on the linker length and incorporation efficiency of the building block into DNA nanostructures; and 3) to demonstrate the applicability of our tool across various DNA nanostructures traditionally made and characterized by cryogenic transmission electron microscopy (cryo-TEM). With these requirements in mind, we first designed a DNA origami tetrahedral cage with four available sites to incorporate our building block into it (Figure 3.1) which was characterized by cryo-TEM and fit with simulations.

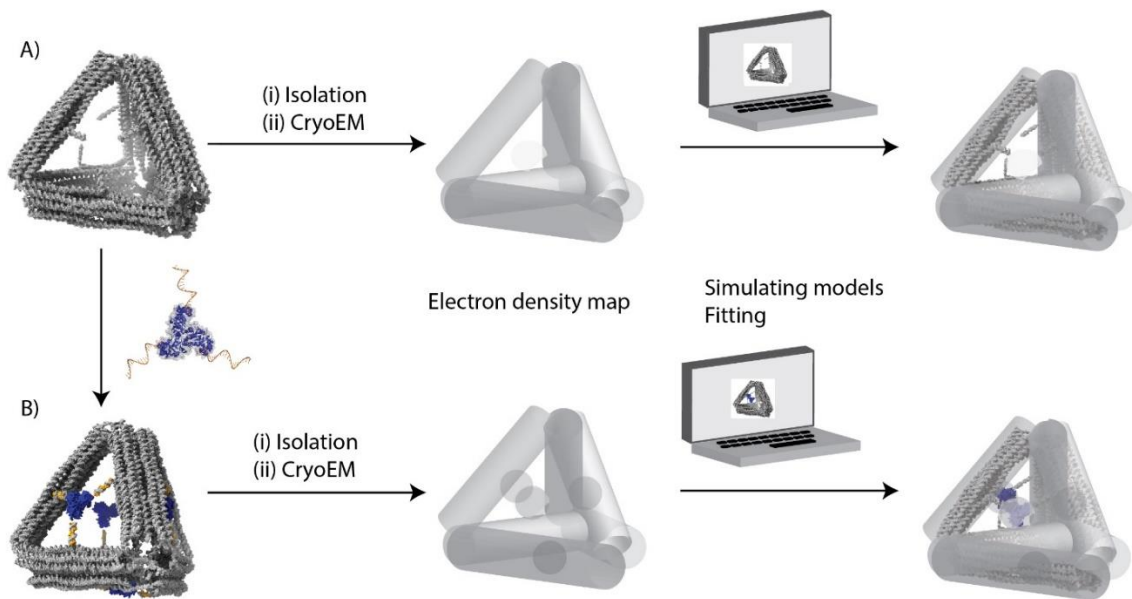


Figure 3.4: Schematic of the project. Elucidating the electron density map of the (A) tetrahedral origami cage and (B) the protein incorporated cage and using the electron density map from Cryo-EM reconstruction to be fit by the simulated models to find the best correlation fit.

3.2 Results and discussion

3.2.1 Synthesis of KDPG aldolase protein-DNA building blocks (PDNA-bbs):

The PDNA-bb was made by first expressing and purifying KDPG aldolase protein having a non-canonical amino acid 4-azidophenylalanine (azF) at site E54 as has been reported in our work before¹⁶. The conjugation to this purified protein was done through strain promoted azide-alkyne click chemistry, using a 21-base single stranded DNA (ssDNA) as has been previously reported¹⁶. This conjugate was then used for incorporation into a DNA origami tetrahedral cage.

3.2.2 Design and synthesis of DNA tetrahedral origami cage:

The origami cage was designed using the software Cadnano¹⁷ with each arm consisting of 10 helices. Design details can be found in Supplementary information Figure S3.1. Each side was designed to have a length of 35 nm. The handles for the incorporation of the PDNA-bb were positioned in such a way that the conjugate would bind onto each of the four faces of the tetrahedron. The design was tested and optimized (Figure S3.1C). The tetrahedral frame was also chosen to avoid the preferred orientation problem¹⁸ often faced in the field of single-particle reconstruction by cryo-EM. The samples were characterized by gel and the desired band was purified and tested by negative stain TEM (Supplementary information Figure S3.2). This purified tetrahedral cage was plunged (Supplementary

information Figure S3.4) and characterized by cryo-TEM (Figure 3.2A). Images were collected, processed, and reconstructed (supplementary information) using RELION 3.0 (Figure 3.2C). Once this was achieved, we moved onto the formation of the PDNAbb incorporated tetrahedral cage.

3.2.3 Incorporation of Protein into the origami cage:

The tetrahedral origami cage was mixed with 40 equivalents of the conjugate before purification and reannealed from 45°C to 4°C to obtain a PDNA-incorporated tetrahedral cage (Figure 3.2B). The sample was also characterized by negative stain TEM and cryo-TEM (Supplementary information Figure S3.4) as before. The resulting reconstruction (Figure 3.2D) shows clear density in the center demonstrating the incorporation of protein into the tetrahedral frame. At this point, we wanted to fit our data into these electron density maps. For this we developed simulation models of five different systems (Figure 3.3A-E) and try to fit our density into the corresponding map.

3.2.4 Simulation development for Protein-DNA hybrid system:

Using our recently developed coarse-grained protein-DNA hybrid simulation¹⁹, we investigated how differences in protein incorporation and spacer length affected the mechanical properties of the DNA nanostructures, and compared our results to those obtained experimentally.

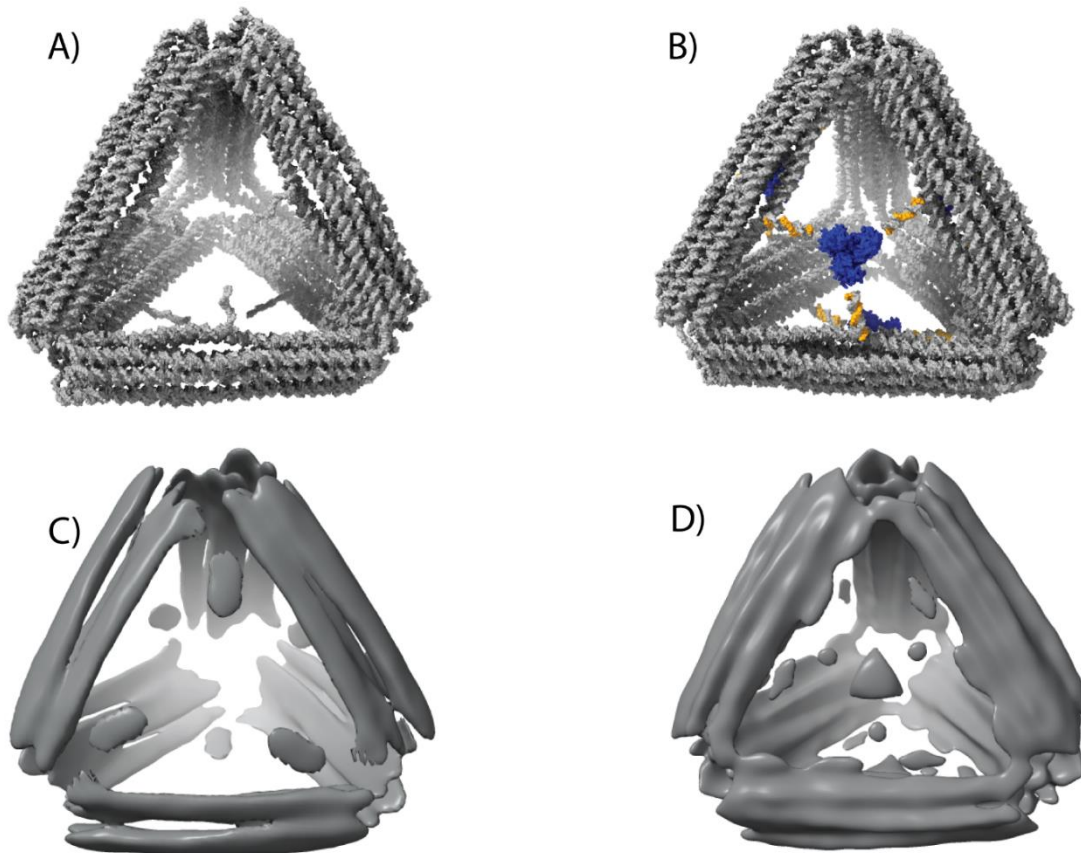


Figure 3.2: Reconstruction of Tetrahedral Origami Cages. (A) Schematic of the tetrahedral cage. (B) Schematic of PDNA-BB incorporated tetrahedral cage. (C) Cryo-EM reconstruction of (A) at 26 Å. (D) Cryo-EM reconstruction of (B) at 28 Å.

3.2.5 Simulation Preparation of Tetrahedral Origami:

The Cadnano design of the origami was first converted into oxDNA using tacoxDNA²⁰ and then relaxed. Subsequent modifications to the structure—including 11T spacers at the origami’s vertices, and handles for incorporation of the PDNA-bb—were performed in oxView²¹. Five fully-formed alternate structures, differing only by the number of PDNA-bb (from 0 – 4) were then generated and relaxed. Each structure was

simulated for 1×10^9 steps ($\sim 3\mu\text{s}$) at two sets of conditions: (1) 300 K with 1 M salt concentration (“high temp”), and (2) 113 K with 0.1 M salt concentration (“low temp”).

To approximately mimic the dynamics of the protein, an Anisotropic Network Model (ANM) was linearly fit to the crystallographic B factors of the trimer KDPG Aldolase PDB file (1WAU) at a cutoff of 13 Å and a spring force constant of 40.815 pN/Å. Comparison between the crystallographic B factors and the calculated B factors of the ANM match closely at 100 K (Section 3.6).

The SPDP linkers employed in experiment to conjugate the KDPG Aldolase to DNA were modeled in previously by the Sulc lab¹⁹, by fitting a fully atomistic simulation of the linker to a spring potential. We used the same linker parameterization between the corresponding azidophenylalanine residues and DNA nucleotides of the PDNA-bb. The DNA tetrahedral cage itself was modeled using the oxDNA2 model²². Figure 3.3B shows the atomic model of the SPDP linker represented by the spring potential. Figure 3.3C-G shows the mean structures for all variants of the tetrahedral cage at the low temp conditions.

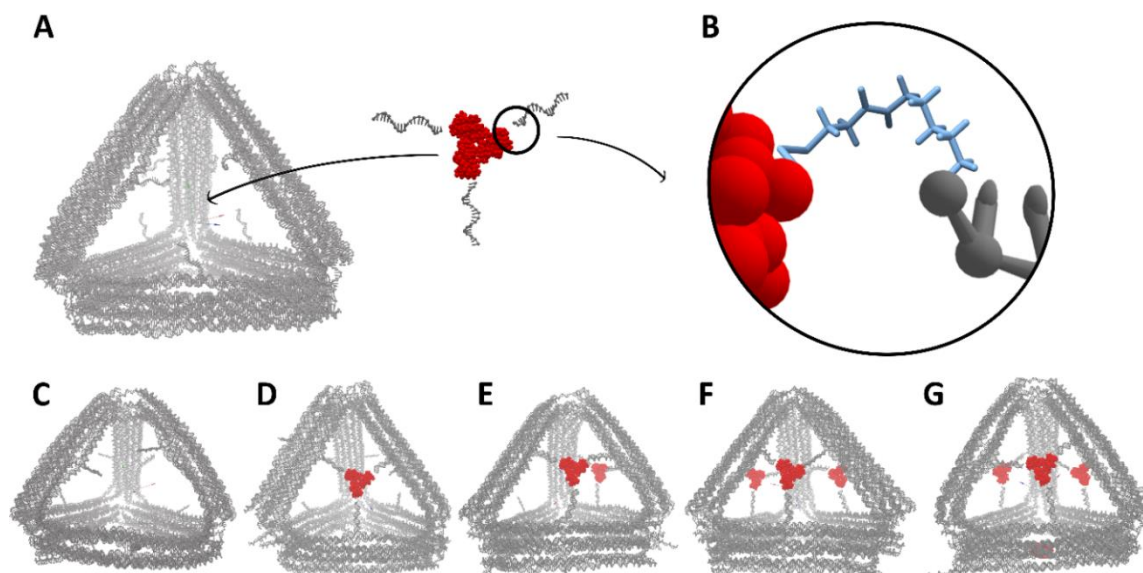


Figure 3.3: Simulated Models of Tetrahedral Origami Cages. A) Schematic of PDNA-bb incorporation in simulation models. B) Atomic model of the SPDP linker represented by a spring potential in simulation. C-G) mean structures of each of the five variants at low temp conditions.

3.2.6 Simulation results of the tetrahedral protein origami cage:

To characterize the differences between each system, we first analyzed the effect that the addition of PDNA-bbs would play on the DNA cage flexibility. By comparing the root mean squared fluctuations (RMSF) of each model's identical DNA cage relative to one another, we can see how the addition of the PDNA-bb to the system affects the flexibility of the tetrahedral cage at the individual nucleotide level.

Figure 3.4 depicts the difference between the RMSF values from the calculated mean structure between each unique pair of models. Both the mean structure and RMSF of each model were averaged over the simulation trajectory using oxDNA analysis tools²¹. Higher (red) values indicate an increase in rigidity in the structure, while lower (blue)

indicate a decrease in rigidity between the models. In both conditions (high temp and low temp) the PDNA-bb caused a clear decrease in the RMSF values of arms with occupied handles. The decrease in RMSF corresponds to a local rise in rigidity from the mechanical pull of the PDNA-bb on the DNA handles attached to the scaffold of the DNA origami. However, the addition of each subsequent PDNA-bb introduces additional pulling forces on adjacent faces, resulting in an increase of flexibility in arms with both DNA handles occupied by the protein. Additional nonlocal effects from the PDNA-bb incorporation are seen from RMSF changes at non-adjacent vertices.

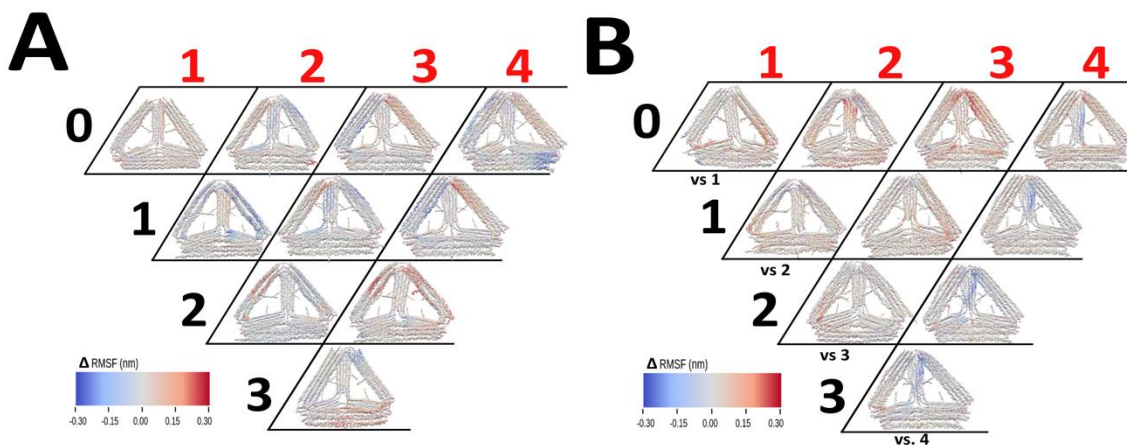


Figure 3.4: Comparison of Simulated Models. Difference in RMSF between horizontal model (black index denoting the model by the number of PDNA-bb incorporated) and vertical model (red index). Differences are displayed on the simulation models of the red index with A) being the relative differences in RMSF between all high temp simulation models and B) being the relative differences in RMSF between all low temp mean simulation models.

Beyond RMSF, differences in the mean structures suggest that the PDNA-bb has a rigidifying effect on the face of the DNA cage to which it is attached. The four PDNA-bb mean structures show a significant change in the origami curvature, as evidenced by its

straighter arms relative to all other mean structures. Figure 3.3 depicts the major changes in curvature between the 0 PDNA-bb and the 4 PDNA-bb mean structures at the low temp conditions.

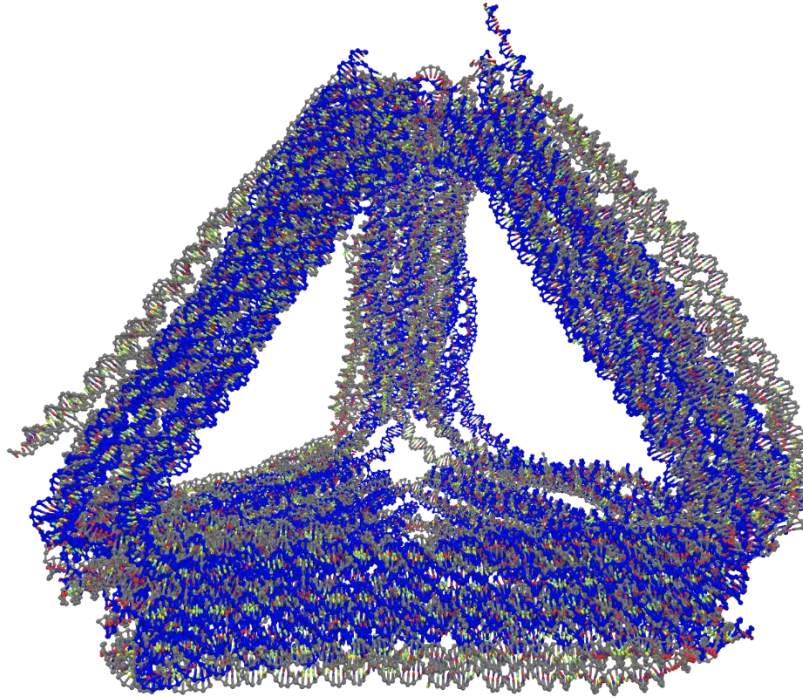


Figure 3.5: Comparison between Models with and without Protein. Aligned comparison of the four protein mean models (blue) and the no protein mean model (grey) at low temp conditions.

Comparison with the symmetrized Cryo-EM maps of both the cage with the protein (P) and the cage without the protein (NP) against the mean models generated from the simulations is shown in Figure 3.5. The mean structure files were stripped of their protein and DNA handles to avoid biasing the fitting, and the structures were converted to PDB format. Using Chimera²³, volume maps of the mean structures were generated from the

atomic coordinates and fit to the experimental cryo-EM maps at matching resolutions (28Å for P and 26Å for NP).

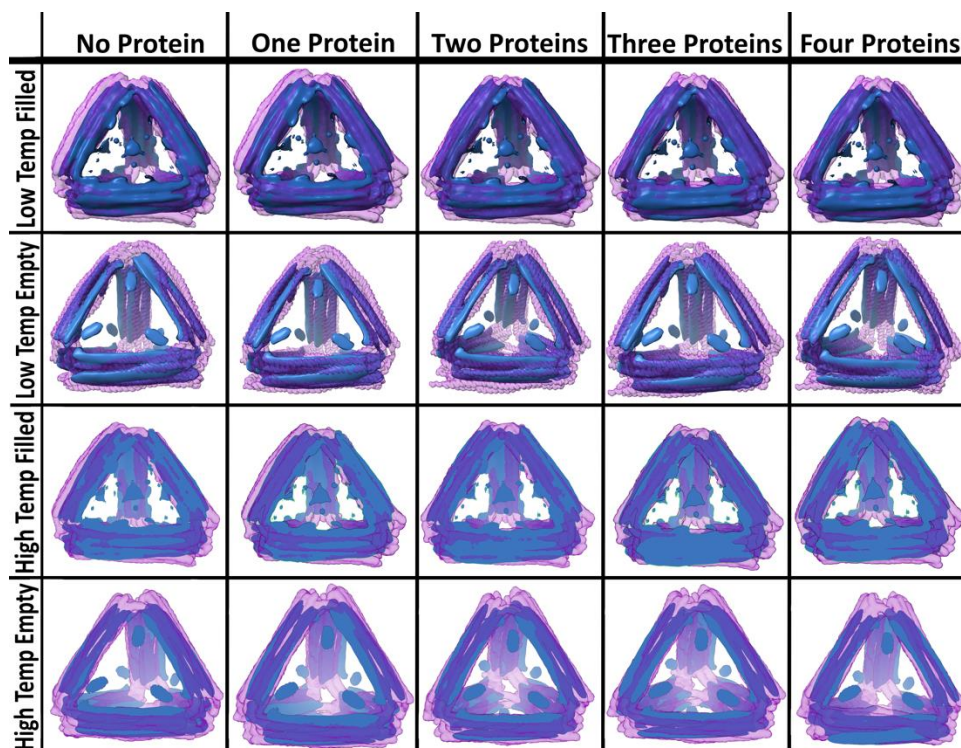


Figure 3.6: Fitting of Experimental Data with Simulations. Images of cryo-EM fitting of the mean structures of both the low temp and high temp mean models. Rows 1 and 3 use the cryo-EM map with protein density and rows 2 and 4 use the cryo-EM map without protein density.

The generated atomic maps (translucent purple in figure 3.6) closely fit the experimental maps (blue in figure 3.6). The density of the protein in P closely matched the position of the protein in simulation, and confirmed some level of PDNA-bb incorporation into the system. We analyzed the fittings to determine whether the slight differences in curvature between the Cryo-EM maps could indicate the preferred level of incorporation of PDNA-bb into the system. Unfortunately, the fittings were unable to distinguish a clear difference

between the models. The bulk assay, and low-resolution nature of the cryo-EM maps combined with the subtle differences between models, made it impossible to determine a clear preference for PDNA-bb incorporation from minor deviations in curvature. Fitting values and images of both the symmetrized and unsymmetrized cryo-EM maps are available in SI S7.

3.2.7 Fluorophore Assay:

Because our reconstruction was performed with a small data set and was reconstructed with a tetrahedral symmetry, we wanted to probe PDNA-bb direction in a cost-effective and more dispositive way than cryo-EM. For this we performed a fluorophore-based assay, wherein we made a fresh PDHN-bb as before but where the DNA had a FAM dye at the 5' end (Figure 3.7A) and the tetrahedral frame had a Cy5 dye on it. Then we proceeded to perform a fluorophore-based assay to elucidate the average number of proteins bound to the tetrahedral origami frame.

Then we elucidated a calibration curve using known concentrations of Cy5 handle strand and a FAM PDHN-bb (SI S5). Care was taken to perform these experiments using a double stranded version in order to better match the protein attached to the cage. After this calibration curve was obtained, we then made our PDHN-bb incorporated tetrahedral cage as before and obtained emission values for this sample at the respective emission wavelengths. We then used the calibration curves to obtain the concentrations of the sample, yielding values of 3.59 nM for the tetrahedral frame, and 11.33nM for PDHN-bb,

corresponding to ~78.9% protein incorporation (assuming four possible proteins), or ~3 proteins per cage.

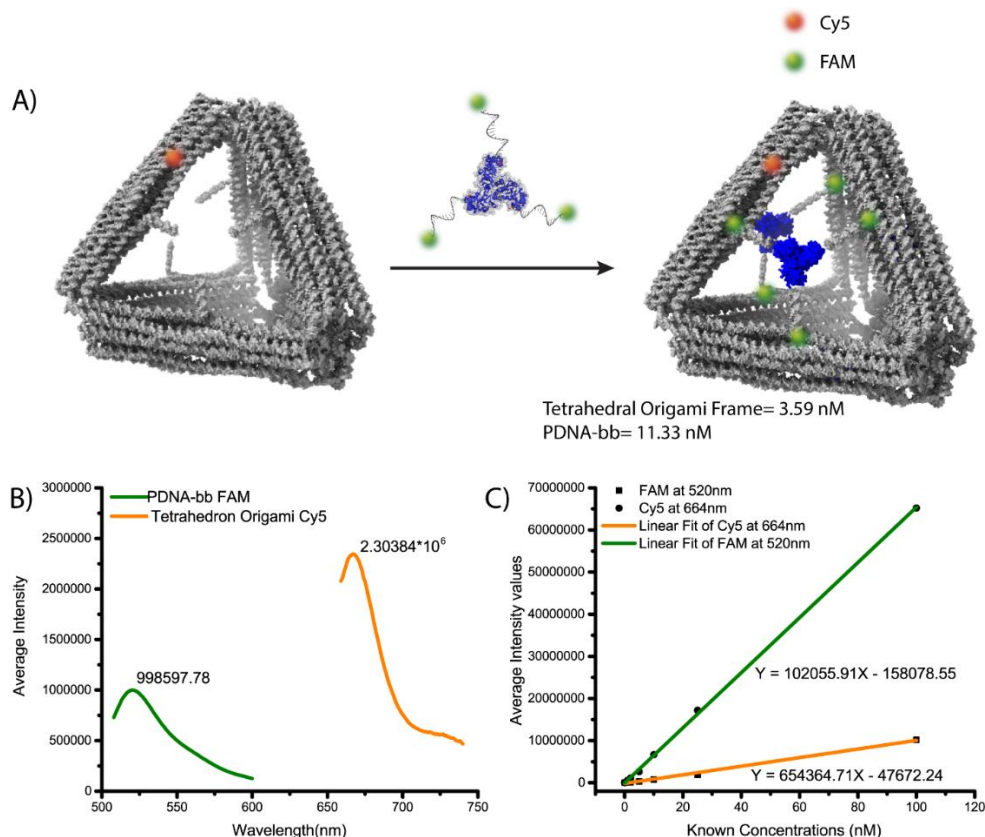


Figure 3.7: Fluorophore assay. (A) Schematic of the fluorophores present on the PDNA-bb incorporated tetrahedral origami frame. (B) Calibration curve obtained from using known concentrations of double stranded Cy5 DNA handle. (C) Calibration curve obtained from using known concentrations of double stranded version of FAM PDNA-bb.

3.3 Conclusions and future directions

We successfully elucidated a low resolution cryo-EM electron density map for the tetrahedral DNA origami cage with and without the PDHN-bb attached to it. This is the first such demonstration for a DNA-protein conjugate as a novel self-assembling building block. We simulated various models ranging from zero to four protein-incorporated

origami cages, and fit our experimental data to this model. Although the correlation factors could not give us an insight into the incorporation efficiency, we could narrow down the average number of proteins per frame using a fluorophore assay.

We further intend to investigate the energy differences in the DNA cage of all simulation models. Energetic penalties from incorporation of a fourth PDNA-bb (e.g. due to unfavorable distortions) would corroborate the fluorophore assay data. We intend to further demonstrate the applicability of this technique on a 4-turn DNA tetrahedron from previous work¹⁶ and elucidate structural insights on this novel building block.

3.4 References:

1. Krishnan, Y.; Seeman, N. C., Introduction: Nucleic Acid Nanotechnology. *Chemical Reviews* **2019**, *119* (10), 6271-6272.
2. Hong, F.; Zhang, F.; Liu, Y.; Yan, H., DNA Origami: Scaffolds for Creating Higher Order Structures. *Chemical Reviews* **2017**, *117* (20), 12584-12640.
3. Watson, J. D.; Crick, F. H. C., Molecular Structure of Nucleic Acids: A Structure for Deoxyribose Nucleic Acid. *Nature* **1953**, *171* (4356), 737-738.
4. Chen, K.; Kong, J.; Zhu, J.; Ermann, N.; Predki, P.; Keyser, U. F., Digital Data Storage Using DNA Nanostructures and Solid-State Nanopores. *Nano Letters* **2019**, *19* (2), 1210-1215.
5. Chen, K.; Zhu, J.; Bošković, F.; Keyser, U. F., Nanopore-Based DNA Hard Drives for Rewritable and Secure Data Storage. *Nano Letters* **2020**, *20* (5), 3754-3760.
6. Song, T.; Eshra, A.; Shah, S.; Bui, H.; Fu, D.; Yang, M.; Mokhtar, R.; Reif, J., Fast and compact DNA logic circuits based on single-stranded gates using strand-displacing polymerase. *Nature Nanotechnology* **2019**, *14* (11), 1075-1081.
7. Qian, L.; Winfree, E., Scaling Up Digital Circuit Computation with DNA Strand Displacement Cascades. *Science* **2011**, *332* (6034), 1196-1201.

8. Seelig, G.; Soloveichik, D.; Zhang, D. Y.; Winfree, E., Enzyme-Free Nucleic Acid Logic Circuits. *Science* **2006**, *314* (5805), 1585-1588.
9. Thubagere, A. J.; Thachuk, C.; Berleant, J.; Johnson, R. F.; Ardelean, D. A.; Cherry, K. M.; Qian, L., Compiler-aided systematic construction of large-scale DNA strand displacement circuits using unpurified components. *Nature Communications* **2017**, *8* (1), 14373.
10. Li, S.; Jiang, Q.; Liu, S.; Zhang, Y.; Tian, Y.; Song, C.; Wang, J.; Zou, Y.; Anderson, G. J.; Han, J.-Y.; Chang, Y.; Liu, Y.; Zhang, C.; Chen, L.; Zhou, G.; Nie, G.; Yan, H.; Ding, B.; Zhao, Y., A DNA nanorobot functions as a cancer therapeutic in response to a molecular trigger in vivo. *Nature Biotechnology* **2018**, *36* (3), 258-264.
11. Jiang, Q.; Song, C.; Nangreave, J.; Liu, X.; Lin, L.; Qiu, D.; Wang, Z.-G.; Zou, G.; Liang, X.; Yan, H.; Ding, B., DNA Origami as a Carrier for Circumvention of Drug Resistance. *Journal of the American Chemical Society* **2012**, *134* (32), 13396-13403.
12. Hu, Q.; Li, H.; Wang, L.; Gu, H.; Fan, C., DNA Nanotechnology-Enabled Drug Delivery Systems. *Chemical Reviews* **2019**, *119* (10), 6459-6506.
13. Douglas, S. M.; Bachelet, I.; Church, G. M., A Logic-Gated Nanorobot for Targeted Transport of Molecular Payloads. *Science* **2012**, *335* (6070), 831-834.
14. Das, R.; Baker, D., Macromolecular Modeling with Rosetta. *Annual Review of Biochemistry* **2008**, *77* (1), 363-382.
15. Praetorius, F.; Dietz, H., Self-assembly of genetically encoded DNA-protein hybrid nanoscale shapes. *Science* **2017**, *355* (6331), eaam5488.
16. Xu, Y.; Jiang, S.; Simmons, C. R.; Narayanan, R. P.; Zhang, F.; Aziz, A.-M.; Yan, H.; Stephanopoulos, N., Tunable Nanoscale Cages from Self-Assembling DNA and Protein Building Blocks. *ACS Nano* **2019**, *13* (3), 3545-3554.
17. Douglas, S. M.; Marblestone, A. H.; Teerapittayanon, S.; Vazquez, A.; Church, G. M.; Shih, W. M., Rapid prototyping of 3D DNA-origami shapes with caDNAno. *Nucleic Acids Research* **2009**, *37* (15), 5001-5006.
18. Lyumkis, D., Challenges and opportunities in cryo-EM single-particle analysis. *J Biol Chem* **2019**, *294* (13), 5181-5197.
19. Procyk, J.; Poppleton, E.; Sulc, P., *Coarse-Grained Nucleic Acid-Protein Model for Hybrid Nanotechnology*. 2020.
20. Suma, A.; Poppleton, E.; Matthies, M.; Šulc, P.; Romano, F.; Louis, A. A.; Doye, J. P. K.; Micheletti, C.; Rovigatti, L., TacoxDNA: A user-friendly web server for

simulations of complex DNA structures, from single strands to origami. *Journal of Computational Chemistry* **2019**, *40* (29), 2586-2595.

21. Poppleton, E.; Bohlin, J.; Matthies, M.; Sharma, S.; Zhang, F.; Šulc, P., Design, optimization and analysis of large DNA and RNA nanostructures through interactive visualization, editing and molecular simulation. *Nucleic Acids Research* **2020**, *48* (12), e72-e72.

22. Snodin, B. E.; Randisi, F.; Mosayebi, M.; Šulc, P.; Schreck, J. S.; Romano, F.; Ouldrige, T. E.; Tsukanov, R.; Nir, E.; Louis, A. A.; Doye, J. P., Introducing improved structural properties and salt dependence into a coarse-grained model of DNA. *The Journal of chemical physics* **2015**, *142* (23), 234901.

23. Pettersen, E. F.; Goddard, T. D.; Huang, C. C.; Couch, G. S.; Greenblatt, D. M.; Meng, E. C.; Ferrin, T. E., UCSF Chimera--a visualization system for exploratory research and analysis. *J Comput Chem* **2004**, *25* (13), 1605-12.

CHAPTER 4

AUTONOMOUS DESIGN OF BIOMIMETIC 3D DNA ORIGAMI CAPSULES

4.1 Introduction

Biomimetic nano-capsules hold huge promise in the area of drug –delivery as they can be used to organize, transport, and protect drug molecules through the cell machinery by specifically tailoring their shape, surface properties, composition, and dynamic processes. The wide variety of COVID-19 vaccines employed today utilize such a strategy to deliver mRNA into our systems. Examples of such capsules include inactive viral capsids,¹⁻² liposomes,³ polymer capsules,⁴ and also several Protein⁵ and DNA nanocages.⁶ Biomimicry of natural capsules and their properties is thus a significant goal for nanoscience, and DNA nanotechnology is well-equipped to satisfy this ambition. Several strategies exist at present to construct these complex 3D DNA nanostructures. The most popular DNA origami technique⁷ is one that has been used to create block-like 3D structures by stacking flat sheets,⁸ polygonal structures,⁹⁻¹³ and rounded structures.¹⁴⁻¹⁵ The other technique is using DNA bricks,¹⁶ which eliminates the scaffold strand by using an even greater number of very short single-stranded DNA strands, here known as bricks that connect to each other and can form gigadalton DNA nanostructures.¹⁷ These strategies are however limited to a select few DNA nanotechnologists who understand the design rules of making these complex DNA architectures using preliminary software tools.¹⁸⁻¹⁹ For the wider accessibility of DNA nanotechnology to any scientist, a need for automation¹¹⁻¹² is very much felt. Efforts in this direction have thus been made by scientists for democratization. However, to this date only 3 automation design softwares exist for

creating 3D DNA architectures¹¹⁻¹³ and none of them are capable of making completely closed 3D DNA nanocapsules which are of utmost need. In this work, we address this unmet need while demonstrating in parallel other design rules that would need to be considered while designing these 3D nanostructures.

4.2 Design inspiration and DNA pottery

As a precursor to the primary focus in this work, Han and co-workers demonstrated an inspiring technique for the general design of hollow-shell DNA origami nanostructures by rolling a single layer of DNA origami upon itself to create a cyclic structure.¹⁵ By controlling the topography and stability of the single layer by careful design of the crossover network, the 3D structure could exhibit complex in-plane and out-of-plane curvature unique from the capabilities of other DNA nanostructure design techniques. The structures are also naturally enclosing, meaning they form an encapsulated cavity. In addition, the globular shape and intrinsic barrier properties lend the structures created by this technique to be suitable to use as capsules. Due to the biomimicry of these attributes, we term structures created in this particular DNA origami design strategy as “DNA capsules”. Enclosing DNA nanostructures have been used in previous work, although not referred to as capsules but serving the same purpose, for the templated growth of metallic nanoparticles²⁰⁻²¹ or liposomes,²² as bioreactors for controlling reactions,²³⁻²⁴ or as drug delivery vehicles.²⁵⁻²⁶ Yet, among these cases, there is no unified design technique, and the shapes and structures are manually designed on a specific-use basis. Many of these are also block-like structures lacking complex geometries.

Here, we have identified design principles and the automation thereof consolidated into a web-based CAD tool named CADAxISDNA (Computer-Aided Design of Axially Symmetric

DNA Origami) for rapidly designing DNA capsules using a CAD file input generated from any traditional shape-drawing CAD software tool. We prefer to call the design process “DNA pottery” due to its geometric similarity to shapes that can be created using a pottery wheel.

Furthermore, we have identified that applications of DNA capsules may have permeability or rigidity requirements that demand the utility and stability of multilayer DNA nanostructures and have extended the previous technique of Han et al. to generate novel multilayer shapes. We also show how the addition of multiple layers to single layer DNA capsules can serve to “reinforce”

High-resolution or structurally weak features and improve their formation.

4.3 Software details

The software automates much of the same design process that was established in previous work, while further providing the ability to design reinforced DNA capsules. There are several primary challenges we seek to resolve that tend to prove challenging or tedious to a human expert who pursues a manual design process. First, the size and spacing of DNA helix rings in order to approximate target shape geometry. Second, due to the curvature and irregular periodicity of nearest-neighbor helices, valid crossover positions may be obscure to a human designer. Third, the size scale of structures is much easier to handle computationally, especially for rapidly generating multiple unique designs. Finally,

a digital representation is more immediately compatible with a growing suite of coarse-grained simulation tools becoming pivotal in DNA nanostructure design.²⁷⁻²⁹

Overall, the design process proceeds as follow. We first position ring-shaped DNA helices to approximate an axially symmetric curved 3D shape, adding additional rings where necessary to create additional layers, then adjust the helical geometries of the rings to optimize synthesis yields plus to define the placement of crossovers and nicks in a simple and balanced manner around the structure, then routing scaffold and staple strands with chosen crossovers and nicks, then finally outputting the generated structure as a sequence of needed staple strands. The process to do so is compartmentalized into two main modules, meshing and routing. In the meshing module, a single layer structure is approximated from a rendered 3D model using latitudinal rings, with nearest distances between adjacent rings spaced to approximately the interhelical distance (2.6 nm), to create a circle-based mesh. Each ring corresponds to a DNA double helix. A scaffold strand will later be routed to fully traverse all rings along one strand of the double helix and spans between adjacent rings via selected crossover points, while staple strands fill remaining crossover points to connect adjacent rings.

Then, the local geometries of each DNA double helix are determined which decide the eventual placement of crossovers and nick points. Each structure is globally described by a base crossover factor (x), typically 3, 4, or 5, which describes how many crossovers span adjacent rings. Each ring is described by four values: circumference, height, crossover factor multiple, and crossover spacing. Due to that simplicity, structures may also be input in a comma-separated values (CSV) format describing each of these values. Circumference

(c) and height (h) serve to describe the ring's position. An integer crossover factor multiple ($k \in \mathbb{Z}$) scales to allow more crossovers to be used for large rings in order to maintain stability such that the number of crossovers on a ring, or the crossover count, is kx . Crossover spacing ($s \in \{2; 3; 4; 5\}c$) describes an integer number of full helical turns in terms of base pairs between adjacent crossovers, and this is bounded for stability. To preserve symmetry and simply crossover placement, the circumference is rounded to the nearest multiple of the crossover count kx . The circumference, crossover number, and crossover spacing tuple (c, kx, s) calculate the base pairs per turn ($\text{bps/turn} = c/kxs$), and as provided by previous work, this value should be kept within 9 bps/turn to 12 bps/turn for best synthesis yield. Thus, the helix geometries are adjusted to fall within this range. If we desire a structure to be multilayer, a scaled ring is placed with respect to the target base ring at the interhelical distance. We term this process "reinforcement" due to its effect of increasing structural rigidity and the formation of high-resolution features in DNA pottery. Previously, Han et al. had set rules for in-plane placement of rings, or 2D reinforcement, which corresponded to scaling the circumference by 48 or 50 bps, depending on the crossover factor, but we have further extended this to be less restrictive. The 3-tuple (c, kx, s) of the new ring is again adjusted to satisfy the bps/turn range between 9 and 12, then the structure is "fully reinforced".

This can be repeated for any number of rings such that the structure is variably multilayer, with the condition that reinforcing rings must be added as adjacent pairs such that any new ring has an outgoing path for the scaffold routing. In addition, if the number of added rings causes the full length of required scaffold to surpass the size of a single

scaffold, we have shown that additional scaffolds may be added to complete the reinforced structure. Following this, the routing module converts rings to DNA helices, with nucleotides spaced and positioned according to the bps/turn, which also decides the rotation per base pair ($\phi/\text{bp}=360 \text{ deg}/[\text{bps}/\text{turn}]$). Crossover points are then aligned based on pairs of nucleotide pairs aligned to the angle of two adjacent rings. While each ring has varying bps/turn that misaligns them on a linear grid, it is still possible to periodically align them on a polar coordinate system if the crossover factor is the same. A number of crossovers equal to the crossover count are then created to join adjacent helices.

It is necessary to note that the crossover density increases in multilayer structures, thus reinforcement is most effective when the crossover spacing is already high such that staple domains remain as long as possible. In order to handle large, multiple layer designs, we introduce several parameters that assist in heuristically searching for appropriate crossover networks. Due to the discretization of angle positions by nucleotides along the ring and the malleability of DNA, alignments do not need to be perfect. An alignment threshold defines how close two crossover positions on adjacent helices can be to be considered a valid position. In addition, multiple layer crossovers sharply increase the crossover density, which reduces the average continuous staple-scaffold binding domain length. If domains are too short, they may transiently disassociate and significantly lower the stability of the resulting DNA origami nanostructure. A spacing parameter controls how close any crossover may be placed within the proximity of another.

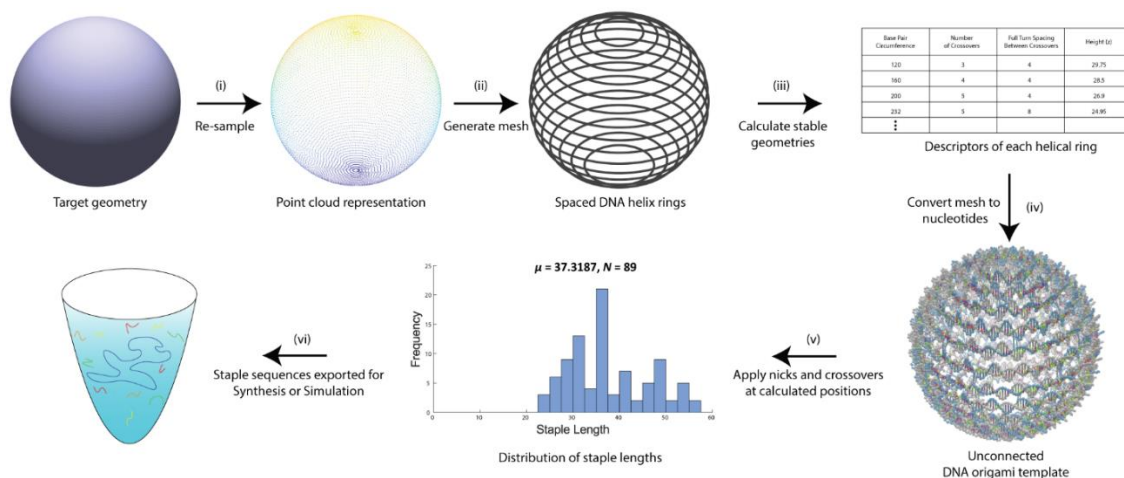


Figure 4.1 The design process of CADAxisDNA. (A) The 3D model is sampled to (B) generate a custom circular mesh. (C) Each mesh line is regarded as a DNA helix and helical geometric properties are applied and adjusted to satisfy a routing performed in (D). A network of crossovers and nicks are systematically applied to (E) produce staples within a certain length range (30-60), which can be (F) used to synthesize the DNA nanostructure.

Staple nicks can also shorten this continuous binding domain, typically when near a crossover, so the distance of nicks to crossover points is also controlled. These parameters can be relaxed to accept looser definitions of valid crossover networks and nicks, up to a point where designs may have reached unacceptable geometries defined by greatly lowered synthesis yields. Provided careful placement of crossovers, staple nicks can also be optionally optimized to ensure each staple has a nucleation site, which has been shown to improve yields. Or, as may be desirable for downstream applications, staple nicks can also be optimized to have outward or inward facing positions more closely conducive to adding surface modifications and functional groups for guest molecules. Upon routing the scaffold and staples using the generated crossovers and nicks, output can be formatted and produced for either simulation or synthesis. (For a more detailed description of each process, refer to the Supplementary Materials.)

4.4 Variable Reinforcement

Provided that reinforcement of at least one layer can offer mechanical improvements in the structure, we also investigate its benefits for the variable reinforcement of selected features. For example, in the cone example provided in Figures 2A, 2B, reinforcement assists in stabilizing features that have been experimentally demonstrated to be difficult to form (Figure 2E). The tip of the cone demonstrates consistent use of much narrower rings than has been demonstrated in previous work and initially does not form. Reinforcement is also able to stabilize this feature to improve yields. Consolidating the simulation results of only the unstable sections also shows a marked increase in rigidity, while the unreinforced sections remain the same (Figure 2C, 2D) insets of cone and reinforced cone respectively, demonstrating complete formation of the reinforced part of the cone.

4.5 Experimental Demonstrations

Several structures are experimentally assembled and characterized by transmission electron microscopy (TEM) (Figure S2). We experimentally demonstrated the effects of reinforcement on the cone design. In non-reinforced cases, the weak part of the structure is not resolvable in images (Figure 4.2E). In comparison, objects with reinforcement have those same sections clearly visible (Figure 4.2F). This reflects the simulated results as described by decreasing RMSD in those sections. Additional structures of varying complexity are also selected to show the experimental validity of the software. Cone, gourd, and bowl shapes further demonstrate design complexity focusing on specific traits

of curvature. Additional shapes were designed to utilize a full scaffold strand for their single layer construction only, then as reinforcing layers were added and the total length of

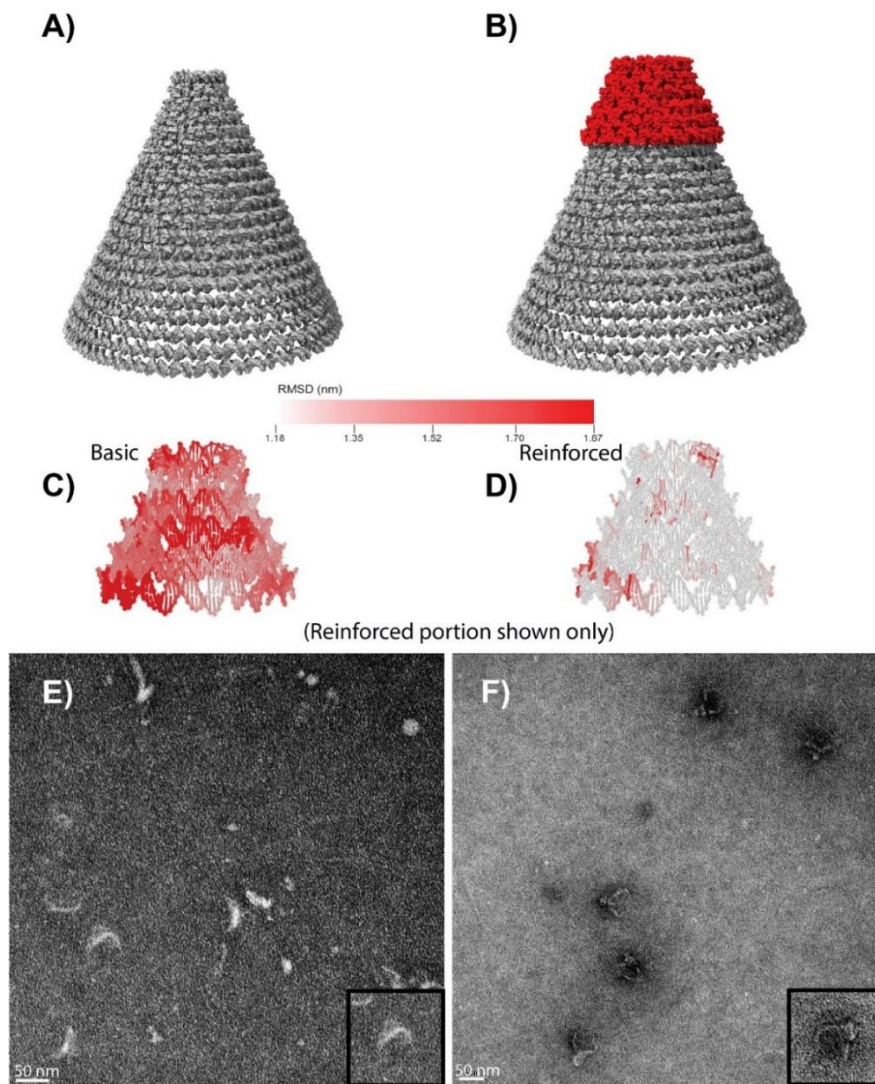


Figure 4.2 Reinforcement Strategy. (A) Schematic of Cone and (B) Reinforced Cone. Reinforced part is shown in red. (C) and (D) Simulated results on the effect of reinforcement. Only the inner layer is shown for comparison. (E) and (F) TEM images with of (A) and (B) with insets.

DNA surpassed a single scaffold strand, another scaffold was added. While this often results in large lengths of an additional scaffold strand being unused, as reinforcement of

only specific sections of the shape may only require 1000 bps to be added to the design, we do not observe any critical errors in assembly.

The following shapes used M13mp18 as their base scaffold, then added phi X 174 when necessary. The vase shape demonstrates a combination of straight and curved elements. The “weight” on each side has nonuniform latitudinal curvature, as opposed to a sphere that has consistent curvature. These are joined by a cylindrical handle. Depending on the length and diameter of the handle, it may not be rigid and cause the two weights to become noncollinear. This is another example where reinforcement may offer the necessary structural integrity. The gourd shape demonstrates nonuniform curvature but with a profile that has both convex and concave sections. Furthermore, the two convex sections are created such that they have different degrees of curvature. In TEM images, the shape of the gourd according to its input 3D model can be clearly discerned inside views. Other particles frequently appearing are most likely top or bottom views of the same structure (Figure S2B). The aspect ratio of the gourd may sometimes bias its imaging cross-section to be viewed from top to bottom. In these profiles, two rings are clearly visible corresponding to the smaller and larger bulbs of the gourd. The cryo-tomogram of the shape in Figure 3 clearly demonstrates the formation of the shape. The bowl shape explores the concept of a part of the structure being depressed into an encapsulating section of itself. The shape demonstrates extreme concave features, a very small cavity space, as well as an acute corner. Similar to the gourd, the bowl shape is biased towards top or bottom views and often appear as circles (Figure S2A), however the Cryo-TEM tomogram in Figure 3 demonstrates their clear formation.

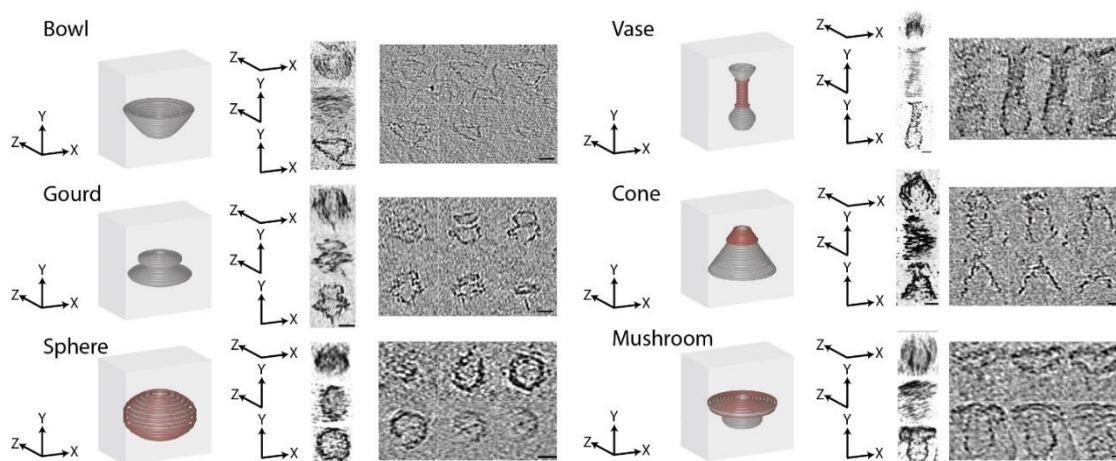


Figure 4.3 Tomograms of Example Nanostructures. Representative images of Cryo-tomogram sections of the various example nanostructures (on the left) and experimental demonstration of the same on the right.

4.6 Asymmetric structures

In the interest to truly realize biomimetic nanocapsules, we intend to test and realize structures featuring asymmetric features along the axis. For this we needed to enable in-plane asymmetry that breaks away from the limitations of a straight, central axis. Bending of helix bundles can be implemented in multiple layer thickness structures by segmenting the wall into helix bundle groups, then applying a varying gradient of insertions and deletions along the helix bundle path. The gradient can be straightforwardly calculated by viewing the helix bundle as a simple beam and applying Euler-Bernoulli beam theory. Lengthwise deformations are converted to base pair values by dividing by the B-form DNA axial rise of 0.332 nm. For a single bend, this method induces closely accurate bending in the helix bundle.

However, we have found that for structures with inflections, that is, shapes such as the clover which are comprised of both concave and convex arcs, strain from the longer

arcs overwhelm their adjacent arcs through the inflection. For example, longer convex sections cause adjacent concave sections to become straight. We further describe an overcompensation strategy that appears to remedy this issue. Overcompensation is applying an insertion-deletion gradient for a larger angle than originally intended. This can range from a 10° up to a 60° increase. Overcompensation in the shorter and weaker arcs was observed to be a successful strategy to be able to add sufficient counter-strain into the structure to form both convex and concave sections within the same helix bundle. The range varies significantly as a steeper insertion-deletion gradient also narrows the shortest segment (with the most deletions) of the arc, which in effect can reduce optimal crossover placement and stability to counteract successful overcompensation. Thus, we see the necessity of automated software here to heuristically search for optimum parameters.

We also intend to demonstrate a departure from a straight, central axis, such as in demonstrated Klein bottle designs. Consecutive rings are designed to be at slightly tilted angles between each other. A gradual progression of this tilt can form a shape along a curved axis. However, the curvature is not enforced in the rings themselves, rather, curved pathways must be anchored at both endpoints. This primarily demonstrates the utility of the elasticity of DNA, where the crossovers bonds will be slightly strained along the outer curvature of any curved path.

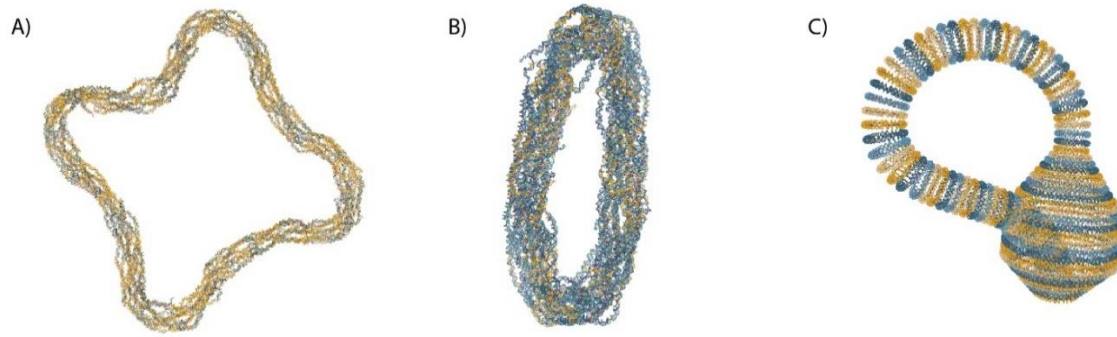


Figure 4.4 Simulation of Asymmetric Structures. Ox-DNA simulation demonstrating the (A) last configuration state of Clover and (B) last configuration state of ellipse (C) initial configuration state of Klein Bottle.

4.7 Conclusions and future directions

Here, we have demonstrated the first system for the design of curved DNA capsules, which features improvements in geometric complexity as well as mechanical rigidity, which will limit permeability, promote stability and assist in achieving increasingly ambitious biomimetic structures and applications. The wide array of structures were all designed by following the same algorithms and testifies to the robustness of the design strategy for rapidly generating globular DNA nanostructures. Designed shapes are consistently observed, despite minimal application of optimization strategies that have since been developed for lattice-based DNA origami. Furthermore, software tools may accelerate the development of new techniques for exploring novel shapes and biomechanical properties of nonlinear DNA nanostructures due to the rate at which a programmable, digital representation can be modified. The methods here have also been demonstrated to scale to sizes consisting of at least two scaffold strands, thus enabling the implementation of stable, complex features.

While current demonstrations are static, new strategies for dynamic actuation of DNA nanostructures will need to be developed and could be integrated in structures demonstrated here via additions to the published software. This type of globular, freeform shape mimicry is a strength of DNA nanotechnology and could accelerate the study and exploitation of micro and nanoscale dynamics to create smart and stable programmable nanodevices. The current work is another step forward in democratizing the capabilities of DNA nanotechnology to the general scientific audience, thereby leading towards more complex and biomimetic molecular machinery.

4.8 References

1. Gao, D.; Lin, X. P.; Zhang, Z. P.; Li, W.; Men, D.; Zhang, X. E.; Cui, Z. Q., Intracellular cargo delivery by virus capsid protein-based vehicles: From nano to micro. *Nanomedicine : nanotechnology, biology, and medicine* **2016**, *12* (2), 365-76.
2. Somiya, M.; Liu, Q.; Kuroda, S. i., Current Progress of Virus-mimicking Nanocarriers for Drug Delivery. *Nanotheranostics* **2017**, *1* (4), 415-429.
3. Sercombe, L.; Veerati, T.; Moheimani, F.; Wu, S. Y.; Sood, A. K.; Hua, S., Advances and Challenges of Liposome Assisted Drug Delivery. *Frontiers in Pharmacology* **2015**, *6* (286).
4. Tanner, P.; Baumann, P.; Enea, R.; Onaca, O.; Palivan, C.; Meier, W., Polymeric Vesicles: From Drug Carriers to Nanoreactors and Artificial Organelles. *Accounts of Chemical Research* **2011**, *44* (10), 1039-1049.
5. Bhaskar, S.; Lim, S., Engineering protein nanocages as carriers for biomedical applications. *NPG Asia Materials* **2017**, *9* (4), e371-e371.
6. Chandrasekaran, A. R.; Levchenko, O., DNA Nanocages. *Chemistry of Materials* **2016**, *28* (16), 5569-5581.
7. Rothemund, P. W. K., Folding DNA to create nanoscale shapes and patterns. *Nature* **2006**, *440* (7082), 297-302.

8. Douglas, S. M.; Dietz, H.; Liedl, T.; Högberg, B.; Graf, F.; Shih, W. M., Self-assembly of DNA into nanoscale three-dimensional shapes. *Nature* **2009**, *459* (7245), 414-418.
9. Zhang, F.; Jiang, S.; Wu, S.; Li, Y.; Mao, C.; Liu, Y.; Yan, H., Complex wireframe DNA origami nanostructures with multi-arm junction vertices. *Nature Nanotechnology* **2015**, *10* (9), 779-784.
10. Jun, H.; Zhang, F.; Shepherd, T.; Ratanalert, S.; Qi, X.; Yan, H.; Bathe, M., Autonomously designed free-form 2D DNA origami. *Science Advances* **2019**, *5* (1), eaav0655.
11. Veneziano, R.; Ratanalert, S.; Zhang, K.; Zhang, F.; Yan, H.; Chiu, W.; Bathe, M., Designer nanoscale DNA assemblies programmed from the top down. *Science* **2016**, *352* (6293), 1534-1534.
12. Jun, H.; Shepherd, T. R.; Zhang, K.; Bricker, W. P.; Li, S.; Chiu, W.; Bathe, M., Automated Sequence Design of 3D Polyhedral Wireframe DNA Origami with Honeycomb Edges. *ACS Nano* **2019**, *13* (2), 2083-2093.
13. Benson, E.; Mohammed, A.; Gardell, J.; Masich, S.; Czeizler, E.; Orponen, P.; Högberg, B., DNA rendering of polyhedral meshes at the nanoscale. *Nature* **2015**, *523* (7561), 441-444.
14. Dietz, H.; Douglas, S. M.; Shih, W. M., Folding DNA into Twisted and Curved Nanoscale Shapes. *Science* **2009**, *325* (5941), 725-730.
15. Han, D.; Pal, S.; Nangreave, J.; Deng, Z.; Liu, Y.; Yan, H., DNA Origami with Complex Curvatures in Three-Dimensional Space. *Science* **2011**, *332* (6027), 342-346.
16. Ke, Y.; Ong, L. L.; Shih, W. M.; Yin, P., Three-Dimensional Structures Self-Assembled from DNA Bricks. *Science* **2012**, *338* (6111), 1177-1183.
17. Ong, L. L.; Hanikel, N.; Yaghi, O. K.; Grun, C.; Strauss, M. T.; Bron, P.; Lai-Kee-Him, J.; Schueder, F.; Wang, B.; Wang, P.; Kishi, J. Y.; Myhrvold, C.; Zhu, A.; Jungmann, R.; Bellot, G.; Ke, Y.; Yin, P., Programmable self-assembly of three-dimensional nanostructures from 10,000 unique components. *Nature* **2017**, *552* (7683), 72-77.
18. Douglas, S. M.; Marblestone, A. H.; Teerapittayanon, S.; Vazquez, A.; Church, G. M.; Shih, W. M., Rapid prototyping of 3D DNA-origami shapes with caDNAno. *Nucleic Acids Research* **2009**, *37* (15), 5001-5006.
19. Williams, S.; Lund, K.; Lin, C.; Wonka, P.; Lindsay, S.; Yan, H. In *Tiamat: A Three-Dimensional Editing Tool for Complex DNA Structures*, Berlin, Heidelberg, Springer Berlin Heidelberg: Berlin, Heidelberg, 2009; pp 90-101.

20. Sun, W.; Boulais, E.; Hakobyan, Y.; Wang, W. L.; Guan, A.; Bathe, M.; Yin, P., Casting inorganic structures with DNA molds. *Science* **2014**, *346* (6210), 1258361.
21. Helmi, S.; Ziegler, C.; Kauert, D. J.; Seidel, R., Shape-Controlled Synthesis of Gold Nanostructures Using DNA Origami Molds. *Nano Letters* **2014**, *14* (11), 6693-6698.
22. Zhang, Z.; Yang, Y.; Pincet, F.; Llaguno, M. C.; Lin, C., Placing and shaping liposomes with reconfigurable DNA nanocages. *Nature Chemistry* **2017**, *9* (7), 653-659.
23. Grossi, G.; Dalgaard Ebbesen Jepsen, M.; Kjems, J.; Andersen, E. S., Control of enzyme reactions by a reconfigurable DNA nanovault. *Nature Communications* **2017**, *8* (1), 992.
24. Linko, V.; Eerikäinen, M.; Kostianen, M. A., A modular DNA origami-based enzyme cascade nanoreactor. *Chemical Communications* **2015**, *51* (25), 5351-5354.
25. Douglas, S. M.; Bachelet, I.; Church, G. M., A Logic-Gated Nanorobot for Targeted Transport of Molecular Payloads. *Science* **2012**, *335* (6070), 831-834.
26. Li, S.; Jiang, Q.; Liu, S.; Zhang, Y.; Tian, Y.; Song, C.; Wang, J.; Zou, Y.; Anderson, G. J.; Han, J.-Y.; Chang, Y.; Liu, Y.; Zhang, C.; Chen, L.; Zhou, G.; Nie, G.; Yan, H.; Ding, B.; Zhao, Y., A DNA nanorobot functions as a cancer therapeutic in response to a molecular trigger in vivo. *Nature Biotechnology* **2018**, *36* (3), 258-264.
27. Snodin, B. E. K.; Romano, F.; Rovigatti, L.; Ouldrige, T. E.; Louis, A. A.; Doye, J. P. K., Direct Simulation of the Self-Assembly of a Small DNA Origami. *ACS Nano* **2016**, *10* (2), 1724-1737.
28. Snodin, B. E.; Randisi, F.; Mosayebi, M.; Šulc, P.; Schreck, J. S.; Romano, F.; Ouldrige, T. E.; Tsukanov, R.; Nir, E.; Louis, A. A.; Doye, J. P., Introducing improved structural properties and salt dependence into a coarse-grained model of DNA. *The Journal of chemical physics* **2015**, *142* (23), 234901.
29. Kim, D.-N.; Kilchherr, F.; Dietz, H.; Bathe, M., Quantitative prediction of 3D solution shape and flexibility of nucleic acid nanostructures. *Nucleic Acids Research* **2011**, *40* (7), 2862-2868.

CHAPTER 5

ASSEMBLING AN ORDERED 3D DNA TETRASTACK FROM MODELING TO EXPERIMENTS

5.1 Introduction

Metamaterials are materials that are engineered to have specific properties. This is accomplished by assembling various components into complex structural assemblies. This ‘structural arrangement’ of the component materials is the source for the interesting properties and is not because of their inherent nature. Optical metamaterials is a class among these materials which have specific properties for photons, thus making them capable for information processing with light.

Optical metamaterials have long been of great interest to the materials community¹⁻³. In analogy to semiconductors, which have an electronic band gap, a metamaterial lattice can be designed to possess an optical band-gap, which prevents the transport of photons of particular wavelengths in the material. If such a lattice could be assembled with cavity sizes comparable to the wavelength of visible or infrared light, it would open new possibilities of manipulating light for information processing. Several 3D nano-lattices that poses band-gaps in the visible light domain have been proposed⁴⁻⁸. Of particular interest is the tetrastack (pyrochlore) lattice (Fig. 5.1G) [1, 3], which has been identified as having an omnidirectional photonic band gap that is robust with respect to defects in the lattice and which allows multiple materials for the crystal lattice to possess the band gap.

The traditional way of creating such metamaterials is the top-down approach for nanoscale patterning like electron beam lithography⁹. These require large facilities, clean rooms and are limited to successive iterations of 2D patterning. A self-assembling strategy of assembling these architectures would solve this problem in a huge way and thus is of much interest to scientists. DNA being a programmable material because of its Watson and Crick base pairing is an immediate choice for such an application. DNA coated colloids for nanocrystal assembly is a direction that scientists have probed¹⁰⁻¹¹. However, DNA nanotechnology is the more promising approach to be considered, as literature demonstrates the capability of making a wide range of architectures from complex origami shapes¹², cages¹³⁻¹⁵ and all the way to complex self-assembled 3D architectures (Figure 5.1 E,F)¹⁶.

This chapter only outlines the experimental side of the project and does not dwell into the modelling side upon which the project was developed. The modeling side of this project has already been published¹⁷, and resulted into a suggested set of DNA nanostructures that have been predicted, in simulation, to assemble into the pyrochlore (tetrastack) lattice. The paper describes a modeling solution to self-assemble a tetrastack from homogeneous components. The simulations and models in the paper were based on the 3D DNA nanostructures well characterized in literature. These nanostructures having the right size when self-assembled into a pyrochlore lattice are capable of having metamaterial properties when silicised. Since, the process of silicisation of DNA nanostructural assemblies has already been demonstrated¹⁸, the practical realization of this project hold much promise.

5.2 Motivation and design of the monomer

Although many 3D DNA lattices (Figure 5.1 A-F) have been achieved, a tetrastack

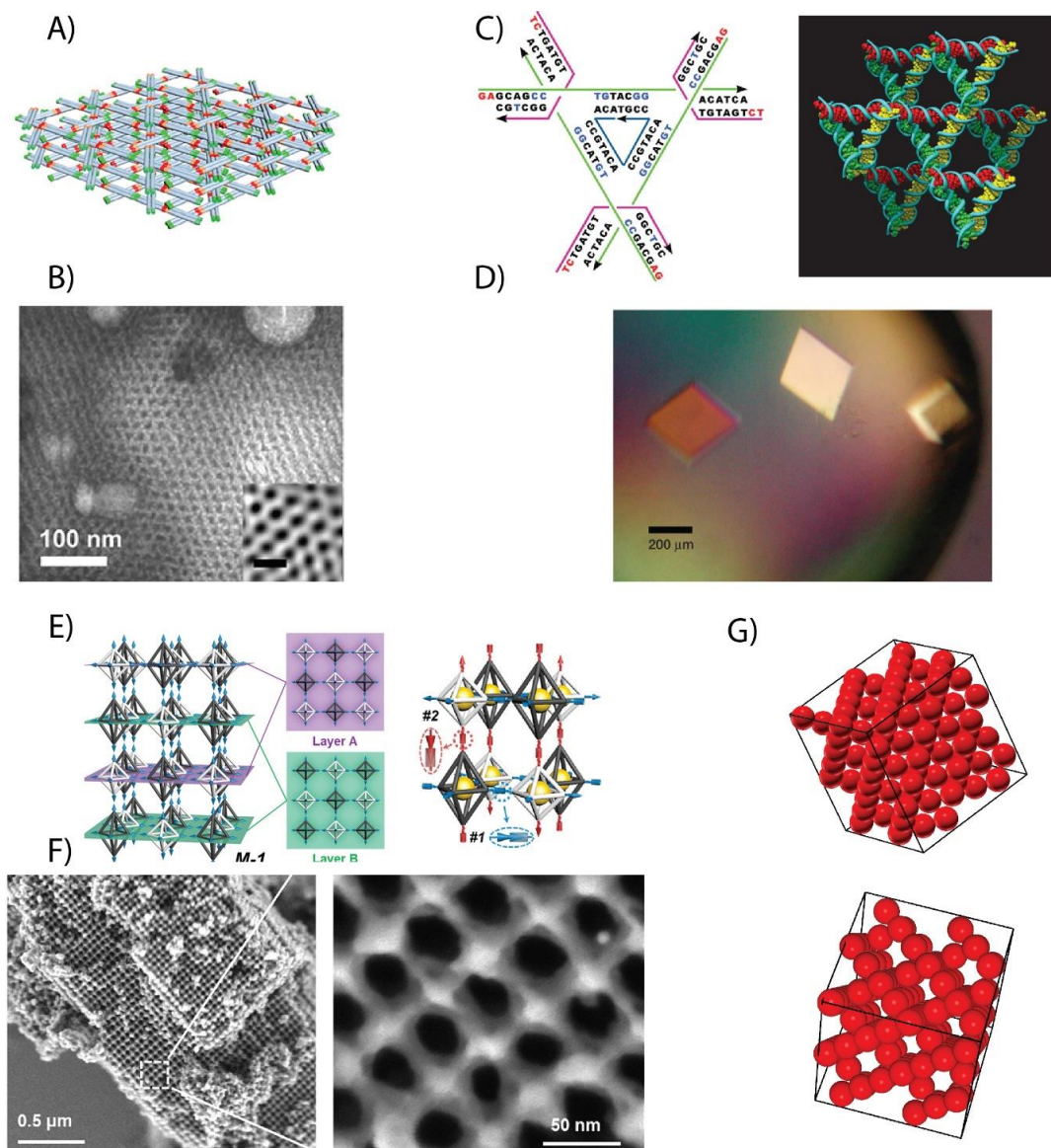


Figure 5.5 Examples of 3D DNA lattices achieved. A) Schematic of tile based layered DNA lattice¹⁹ B) TEM image demonstrating (A). C) Ned Seeman's tensegrity triangle crystal²⁰. D) Experimental demonstration of (C) wherein single crystals were achieved. E) Self-assembled lattices made of 3D DNA origami octahedrons with AuNP incorporated into them²¹. F) HR-SEM demonstration of the silica coated lattices of (E). G) Expected tetrastack lattice.

(pyrochlore) lattice (Figure 5.1 G) is something that has not been achieved and is a lattice that is utmost desired by scientists aspiring to create optical metamaterials. In order to achieve this we need a spherical DNA nanostructure with possible dimensions ranging from 25nm to 50nm. For this purpose we designed a DNA icosahedral origami structure.

This structure designed was a wireframe structure²² owing to the rationale that they form in high yields (>70 %). This structure was designed to use a single stranded scaffold p3120 (Figure 5.2A). We also did choose the positions on the structure for the purposes of attaching to other fellow icosahedrons using complimentary handles and also for the incorporation of Au Nanoparticles (AuNPs) into this structure (Figure 5.3 A). These handles for the incorporation of AuNPs into these nanostructures are necessary for two reasons. One, as Small angle X-ray Scattering (SAXS) experiments yield better signals when AuNPs are present in the formed periodic lattice. Second, these formed lattice structures are better visualized in cryo-Scanning tunneling electron microscopy experimental micrographs when they have AuNPs incorporated into them.

5.3 Formation of the monomer

We started by the production of p3120 scaffold by the amplification method²³ as described in this paper. Figure S1A shows an agarose gel at different concentrations (200nM to 5nM) of the home made scaffold. The single band in the gel demonstrates the high yield and purity of the scaffold made. Now that the scaffold was made, we proceeded to form the monomer. For this we made the origami solution at 20nM concentration wherein 20nM of the scaffold was added in a PCR tube along with 5X (100nM) excess of staples and 10X (200nM) excess of handles were added into the tube

wherein the buffer contained was 1X TAE-500mM NaCl. Care was taken to employ this buffer condition as the modeling end of this project was done using NaCl as the salt instead of the traditionally used Magnesium in the DNA nanotechnology world. This mixture was annealed using the 12 hour annealing protocol (Supplementary Information S2). The mixture was thereafter characterized by Agarose gel electrophoresis (AGE) (Figure 5.2B) and then visualized by TEM as shown in (Figure 5.2C). The TEM images indicated the formation of the icosahedron and the AG indicated the formation of a single monomer species in high yield.

Following this, we also chose handles locations for the incorporation of AuNPs onto the Icosahedron (Figure 5.3A marked in yellow). After this, we synthesized and incorporated the AuNPs as has been described in (Supplementary Information S2). Care was taken to purify the AuNP incorporated Icosahedron (Figure 5.2D) by AGE shown by the yellow arrow in lane1 (Figure 5.2 E) and validate their formation by negative stain TEM (Figure 5.2F). Lane 2 of the gel shows mobility of AuNPS as it has DNA attached to it when compared the same with Lane3 of the gel. A point to further note is that AuNPs always appeared a strong red band in white light and as a strong white band when imaged in the gel scanner. Lane 5 is a control sample showing that when handles for the icosahedron were not present and annealed in the same way as before with AuNPs they did not show the occurrence of a red band as in Lane 1(ii).

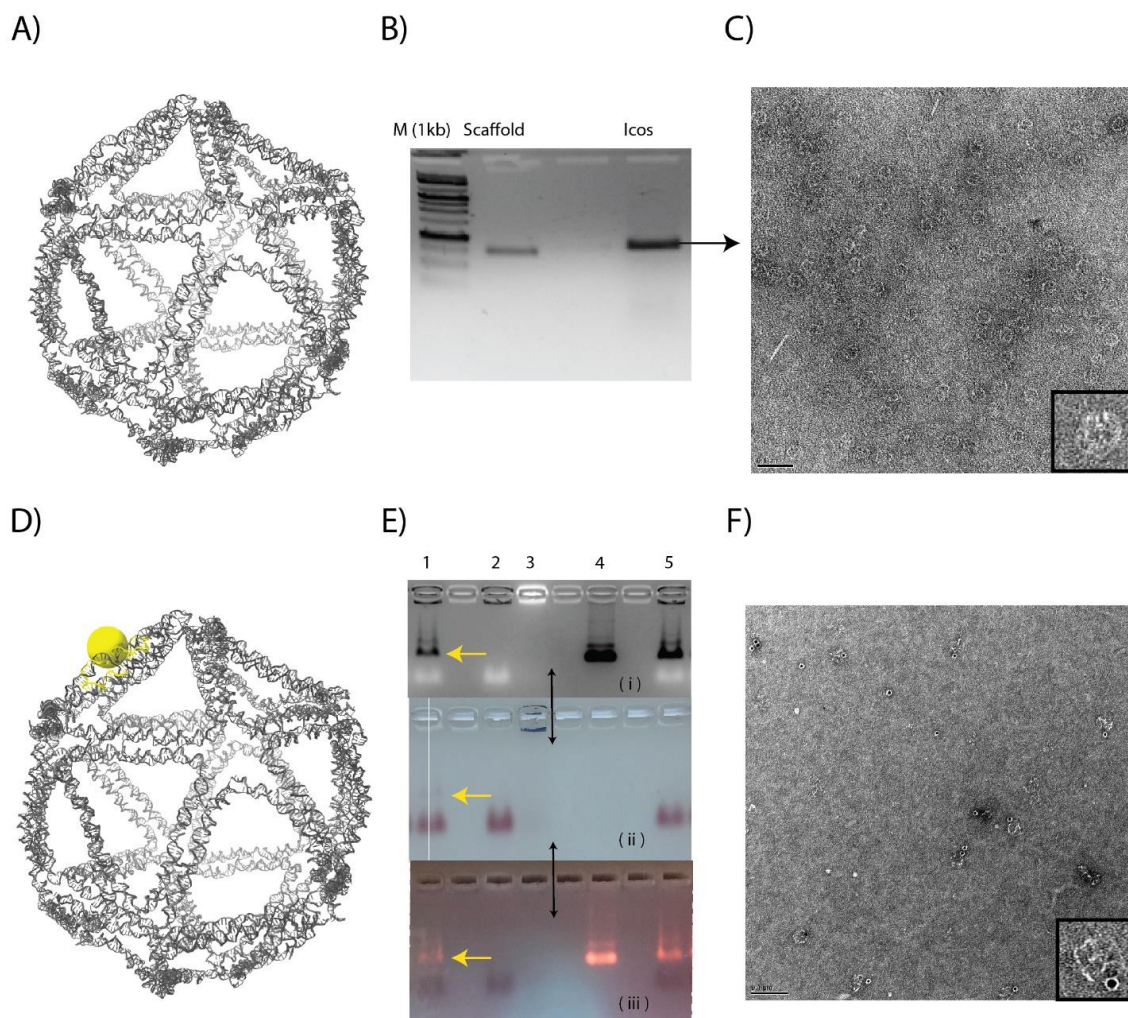


Figure 5.2 Monomer Formation. A) Schematic illustration of monomer. B) Agarose gel showing the formation of the monomer, M(1kb) refers to marker lane of 1kilo basepairs, Scaffold refers to the p3120 scaffold, Icos refers to the formation of the icosahedron monomer which was imaged in C) Negative stained TEM image having an inset demonstrating the formation of the monomer in high yield. D) Schematic illustration of AuNP bound to Icosahedron. E) AGE characterization of (D). Lane 1 is annealed Icosahedron monomers with 5nm AuNPs, Lane 2 is 5nm AuNP-with DNA, Lane 3 is nm AuNP without any DNA attached to it, Lane 4 is Icosahedrons alone (control), Lane 5 is Icosahedrons without handles for the incorporation of AuNPs mixed with AuNP-with DNA (control). (i), (ii) and (iii) are the same gels imaged in three different conditions, (i) imaged using a gel scanner at the EtBr emission wavelength (ii) imaged in white light (iii) imaged under a handheld UV lamp.

5.4 Formation of Chains

After the formation of the monomer, we chose handle locations to be used for the connection to other icosahedron monomers (marked in red in the figure). The handles were chosen such that three handles were on the vertices of a triangular face on the top and the other three on a triangular face on the bottom (Figure 5.3 A). Upon deciding on the position of the handles, we then tested various handle lengths. A handle oligonucleotide (Figure 5.3 B) has three regions, a) the staple part that incorporates into the icosahedron, b) the poly thymidine (polyT) linker region which gives the monomer flexibility to accommodate any steric hindrance and torsional strain and c) the complementary region that binds to the other icosahedron. We tested various designs like 9-10, 10-5 and 12-10 (wherein the first number refers to the complimentary region and the second number refers to the linker polyT region). We saw chain formations in both the 9-10 and 12-10 cases and not in the 10-5 case proving that a linker length of 10 served best for the formation of chains. We further realized from modelling and our experiments that 9-10 was the sweet spot to choose such that, the binding was not too strong and yet sufficient enough to proceed to the formation of ordered lattice structures.

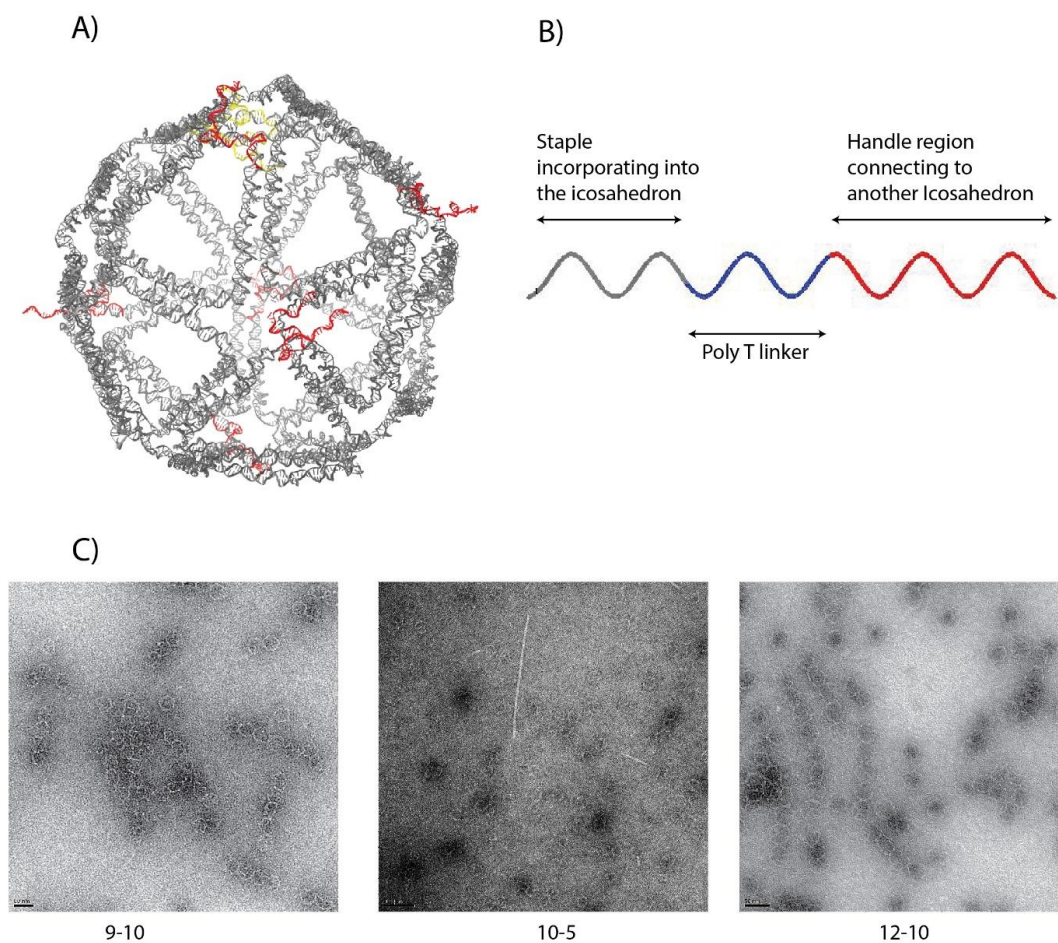


Figure 5.3. Formation of Icosahedral chains. A) Schematic representation of Icosahedron showing the position of handles, where red represents the handles for connecting to other icosahedrons and yellow represents the handles chosen for the anchoring of AuNP on the icosahedron. B) Schematic of a handle sequence C) TEM images illustrating the formation of Chains formed by using various handle lengths.

5.5 Formation of Lattices

After the formation of chains, we used the design parameters learnt from our previous experiment to form the desired tetrastack lattice (Figure 5.4A). Before we tested out the formation of a lattice, we first optimized the formation of a dimer. For this we first tested out the amount of staples required for assembly by AGE and realized that 5X staples was more than enough for the formation a dimer instead of 8X or 10X (Fig. Supplementary

S1B). After this we went onto optimize the annealing protocol (thermal ramp) required for the assembly of the dimers. We performed this by using the 9-10 system and tested the time required for formation of dimer in high efficiency by AGE. Upon AGE characterization we realized that if the thermal ramp was extended from 12 hours to 6 days, the dimer formation efficiency improved (Figure Supplementary information S1C). After this we proceeded to check the formation of the lattices by employing the newly optimized conditions (6 days anneal and 5X staples). For this the first experiment that we carried out was to check the temperature range at which assembly starts. We probed this by both AGE and TEM. The samples were taken immediately from the PCR machine at the corresponding temperatures and thereafter applied onto the grid and imaged. Upon analysis of the result from AGE (Figure Supplementary information S1D), we realized that the smearing of bands started around 33°C and became prominent after into a gradual disappearance well in consistent with our previous results indicating the formation of large assemblies (being not able to travel into the gel). We confirmed these results by TEM too, where we realized the temperature range of assembly was somewhere in between 36°C-26°C (Figure Supplementary figure S2).

We then proceeded onto forming assemblies to test out two different designs a two particle system AB with the 9-10 design and also the 4 particle design (Figure Supplementary information S1E) wherein 2 and 4 individual monomers were put together to form assemblies. We further characterized this by negative stain TEM (Figure 5.4 B). Upon characterization, we realized that the formed aggregates do not have an ordered arrangement as expected, but are more towards liquid like assembly structures. This was

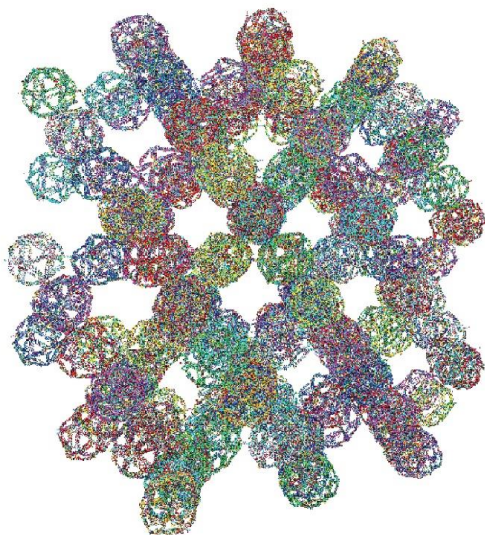
hypothesized to be because of multiple reasons. One possible reason could be the connections between the icosahedrons are too flexible and not enough to form an ordered assembly. The other reason could be the inherent flexibility of the structural arms (as each arm is made of just 2 DNA duplexes). To test out this hypothesis, we wanted to use published designs having higher structural rigidity (6 helix arms) as described in the next section.

5.6 Testing New Designs

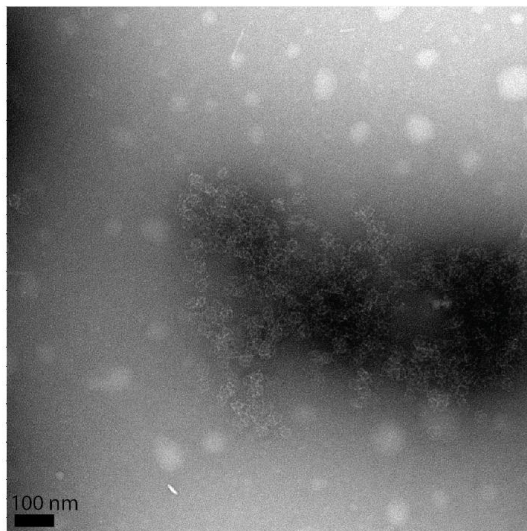
Since the formation of a tetrastack lattice was realized to be more challenging than envisioned, we proceeded to test whether we could replicate the simple cubic lattice formed by octahedrons in literature²⁴ (Figure 5.4 C,D). Since we realized we could, we have decided to trouble shoot a few parameters like, 1) the number of handle oligonucleotides required for assembling a tetrahedron from an icosahedron, 2) temperature of formation of the assemblies and arrive at the exact crystallization temperature needed for assembly.

For the first case, we intend to test out a design having 3 handles per vertex, meaning 9 per face (instead of 3 per face as before). For the second case, we intend to use dynamic light scattering as a tool to probe the temperature at which the formation of assemblies takes place.

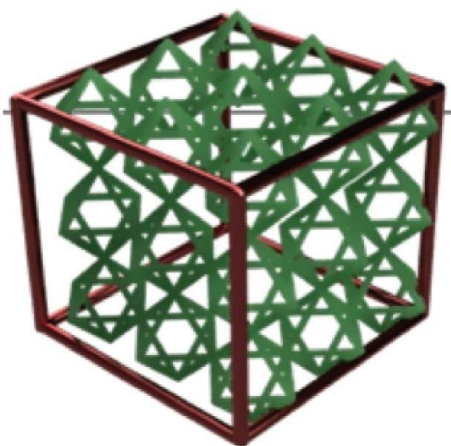
A)



B)



C)



D)

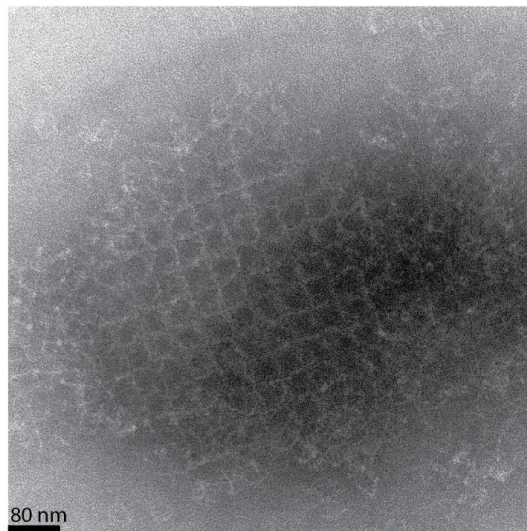


Figure 5.4. Lattice structures. A) Schematic of a tetrastack lattice made from icosahedrons. B) Possible formation of a lattice. C) Square lattice formed from octahedron monomer demonstrated by a previously published report.²⁴ D) Experimental demonstration of the same in our lab.

5.7. Conclusions and Future directions

We have successfully shown the formation of an Icosahedron monomer, conjugation to AuNPs and the formation of 1D chains using the data predicted from the modelling end. Although, we are yet to demonstrate the formation of an assembled tetra stack, the assemblies formed till now hold promise in this direction. We have also demonstrated our capability of replicating and forming a simple cubic super-lattice from existing literature. The newer designs show promise in this direction as the monomers used are made of 6 helix bundle arms instead of a flexible wireframe structure. The skills learnt through the process of characterizing these assembled structures gives us much confidence that the system can be debugged efficiently to realize a tetrastack lattice.

5.8 References

1. Ducrot, É.; Gales, J.; Yi, G.-R.; Pine, D. J., Pyrochlore lattice, self-assembly and photonic band gap optimizations. *Opt. Express* **2018**, *26* (23), 30052-30060.
2. Hynninen, A.-P.; Thijssen, J. H. J.; Vermolen, E. C. M.; Dijkstra, M.; van Blaaderen, A., Self-assembly route for photonic crystals with a bandgap in the visible region. *Nature Materials* **2007**, *6* (3), 202-205.
3. Ngo, T. T.; Liddell, C. M.; Ghebrebrhan, M.; Joannopoulos, J. D., Tetrastack: Colloidal diamond-inspired structure with omnidirectional photonic band gap for low refractive index contrast. *Applied Physics Letters* **2006**, *88* (24), 241920.
4. Edagawa, K.; Kanoko, S.; Notomi, M., Photonic amorphous diamond structure with a 3D photonic band gap. *Phys Rev Lett* **2008**, *100* (1), 013901.
5. Garcia-Adeva, A., Band gap atlas for photonic crystals having the symmetry of the kagomé and pyrochlore lattices. *New Journal of Physics* **2006**, *8* (6), 86-86.
6. Holland, B. T.; Blanford, C. F.; Stein, A., Synthesis of Macroporous Minerals with Highly Ordered Three-Dimensional Arrays of Spheroidal Voids. *Science* **1998**, *281* (5376), 538-540.

7. Maldovan, M.; Thomas, E. L., Diamond-structured photonic crystals. *Nature Materials* **2004**, *3* (9), 593-600.
8. Zhang, J.; Sun, Z.; Yang, B., Self-assembly of photonic crystals from polymer colloids. *Current Opinion in Colloid & Interface Science* **2009**, *14* (2), 103-114.
9. Werts, M. H. V.; Lambert, M.; Bourgoin, J.-P.; Brust, M., Nanometer Scale Patterning of Langmuir–Blodgett Films of Gold Nanoparticles by Electron Beam Lithography. *Nano Letters* **2002**, *2* (1), 43-47.
10. Park, S. Y.; Lytton-Jean, A. K. R.; Lee, B.; Weigand, S.; Schatz, G. C.; Mirkin, C. A., DNA-programmable nanoparticle crystallization. *Nature* **2008**, *451* (7178), 553-556.
11. Macfarlane, R. J.; Lee, B.; Jones, M. R.; Harris, N.; Schatz, G. C.; Mirkin, C. A., Nanoparticle Superlattice Engineering with DNA. *Science* **2011**, *334* (6053), 204-208.
12. Rothmund, P. W. K., Folding DNA to create nanoscale shapes and patterns. *Nature* **2006**, *440* (7082), 297-302.
13. Zhang, Y.; Seeman, N. C., Construction of a DNA-Truncated Octahedron. *Journal of the American Chemical Society* **1994**, *116* (5), 1661-1669.
14. Ke, Y.; Sharma, J.; Liu, M.; Jahn, K.; Liu, Y.; Yan, H., Scaffolded DNA Origami of a DNA Tetrahedron Molecular Container. *Nano Letters* **2009**, *9* (6), 2445-2447.
15. Ke, Y.; Ong, L. L.; Shih, W. M.; Yin, P., Three-Dimensional Structures Self-Assembled from DNA Bricks. *Science* **2012**, *338* (6111), 1177-1183.
16. Liu, W.; Halverson, J.; Tian, Y.; Tkachenko, A. V.; Gang, O., Self-organized architectures from assorted DNA-framed nanoparticles. *Nature Chemistry* **2016**, *8* (9), 867-873.
17. Romano, F.; Russo, J.; Kroc, L.; Šulc, P., Designing Patchy Interactions to Self-Assemble Arbitrary Structures. *Phys Rev Lett* **2020**, *125* (11), 118003.
18. Liu, X.; Zhang, F.; Jing, X.; Pan, M.; Liu, P.; Li, W.; Zhu, B.; Li, J.; Chen, H.; Wang, L.; Lin, J.; Liu, Y.; Zhao, D.; Yan, H.; Fan, C., Complex silica composite nanomaterials templated with DNA origami. *Nature* **2018**, *559* (7715), 593-598.
19. Hong, F.; Jiang, S.; Lan, X.; Narayanan, R. P.; Šulc, P.; Zhang, F.; Liu, Y.; Yan, H., Layered-Crossover Tiles with Precisely Tunable Angles for 2D and 3D DNA Crystal Engineering. *Journal of the American Chemical Society* **2018**, *140* (44), 14670-14676.

20. Zheng, J.; Birktoft, J. J.; Chen, Y.; Wang, T.; Sha, R.; Constantinou, P. E.; Ginell, S. L.; Mao, C.; Seeman, N. C., From molecular to macroscopic via the rational design of a self-assembled 3D DNA crystal. *Nature* **2009**, *461* (7260), 74-77.
21. Ji, M.; Liu, J.; Dai, L.; Wang, L.; Tian, Y., Programmable Cocrystallization of DNA Origami Shapes. *Journal of the American Chemical Society* **2020**, *142* (51), 21336-21343.
22. Zhang, F.; Jiang, S.; Wu, S.; Li, Y.; Mao, C.; Liu, Y.; Yan, H., Complex wireframe DNA origami nanostructures with multi-arm junction vertices. *Nature Nanotechnology* **2015**, *10* (9), 779-784.
23. Qi, X.; Zhang, F.; Su, Z.; Jiang, S.; Han, D.; Ding, B.; Liu, Y.; Chiu, W.; Yin, P.; Yan, H., Programming molecular topologies from single-stranded nucleic acids. *Nature Communications* **2018**, *9* (1), 4579.
24. Shani, L.; Michelson, A. N.; Minevich, B.; Fleger, Y.; Stern, M.; Shaulov, A.; Yeshurun, Y.; Gang, O., DNA-assembled superconducting 3D nanoscale architectures. *Nature Communications* **2020**, *11* (1), 5697.

CHAPTER 6

CONCLUSIONS AND FUTURE DIRECTIONS

6.1 Conclusions

DNA nanotechnology over the course of nearly four decades has grown from a tool for structural assembly tool to the construction of complex nano-robots that could someday be used as vaccines. The work covered in my thesis explores various directions in trying to advance the field of DNA nanotechnology. One continuing roadblock in effective utilization of these nanostructures in living systems is their fundamental functional limitation. Towards this end, we probed two novel self-assembling building blocks: small molecule host-guest interactions and protein-DNA conjugates.

For the first direction in chapter 2, I utilized the small molecule adamantane-cucurbituril[7] (Ad/CB[7]) host-guest binding interactions as the alternative self-assembling building block. For this purpose, we made conjugates of these small molecules with DNA and checked their binding capabilities. We then demonstrated the capability of these interactions to assemble 1D origami nanofibers and finally utilized these interactions for closing and opening of a DNA nanostructure using a functional peptide. The work done in this project demonstrates the capability of these orthogonal interactions to be utilized in parallel with DNA hybridization for the construction of smart-nano-vehicles for the effective delivery of drugs.

In chapter 3, I looked at an origami DNA tetrahedral cage with 4 cavities to bind a trimeric KDPG aldolase protein with a DNA handle per each monomer. My collaborators and I then elucidated an electron density map of this hybrid DNA nanostructure by cryo-

EM single particle reconstruction. We thereafter simulated various models with varying number of proteins bound to the tetrahedral cage, and fit the previously elucidated electron density map. Through this study we believe that the methodology developed using our simulation and fitting tools could be applied to fit low resolution electron density maps of future protein-DNA hybrid nanostructures. This study is the first such example demonstrating the structural understanding of protein-DNA hybrid nanostructure that incorporates a conjugate as a structural building block. The work also incorporates into it various features like small molecule linker modelling and a protein simulation model that could be used with oxDNA, making the approach of studying such nanostructures more universal.

In chapter 4, my coworkers and I developed an automation design software for the development of curved DNA origami structures. The developments shown in this work hold particular promise for two reasons: first, the development of such a software makes the capability of designing DNA nanostructures readily available to the larger scientific community; and second, because this is the first such demonstration of automation of completely enclosed 3D origami curved structures. I believe that through this study, we are one more step closer to complete automation of all DNA origami structures.

In chapter 5, I explored the direction of assembly of higher-order self-assembled nanostructures with predictable lattice arrangements. We have successfully demonstrated the capability of modelling the lattice arrangements of a tetrastack geometry using DNA nanostructures. I have further been able to experimentally demonstrate the ability to make the individual components and assemble them into 1D fibers. I have also been able to

replicate the 3D assembly of a published lattice arrangements using a DNA octahedron. Although we have not been able to demonstrate the formation of a tetrastack using DNA origami icosahedrons yet, the directions pursued holds much promise to their possible realization and thereby its application to be used as an optical metamaterial.

Thus, the work covered in my thesis explores various directions in trying to advance DNA nanotechnology. I believe that the projects demonstrated through my work covered here paves the path for future scientists to explore various directions such as biomimicry, DNA based metamaterial constructions, scaffolds for cryo-electron microscopy, tools for cellular modulation etc.

6.2 Future directions

Growing advances in DNA nanotechnology have brought much attention to this field. Scientists across various disciplines have now started to increasingly use this technology for various applications. This brings me to discuss a few directions that I envision the field to undertake in the foreseeable future.

6.2.1 Functional biomimicry

Over the span of last decade, construction of diverse higher ordered self-assembled DNA architectures¹⁻⁴ has seen an increasing rise especially after the birth of DNA origami⁵ and DNA bricks¹. However, very few of these complex architectures have been shown to be used for functional purpose. A large part of the vision of making these architectures has been to mimic biological assemblies and thereafter function. I personally believe construction of functional DNA based nanostructures could be the next big jump within the field. A few such directions include: an artificial organelle based of a DNA-lipid

conjugates, a simple functional DNA based functional protein like GFP, or a DNA-gated ion channel having selective transport capabilities for a particular protein.

6.2.2 Improvements in protein-DNA nanotechnology

The next increasing focus within the field of DNA nanotechnology has been to improve the functionality of the self-assembled DNA nanostructures. One approach that is growing in prominence is to bring proteins into the fold of DNA nanotechnology. There have been two such examples: one was to use DNA binding proteins⁶ to self-assemble and build protein-DNA hybrid nanostructures and the other was to use DNA-protein conjugates⁷ as a self-assembling building block for the same. However, the field is yet to demonstrate the building of hybrid nanostructures using rationally designed proteins. There are multiple reasons inhibiting this transition as of now. One is the lack of a design software capable of handling both these technologies. The other reason is that the design rules of protein-DNA hybrid systems have yet to be figured out. Although we have made a small effort to bridge this gap in my thesis here, there is a lot more work to be done in this regard.

After the synthesis of these hybrid nanostructures, using them would be the next task. A few examples of selective functional proteins have been adhered to DNA nanostructures, and they have shown promise to be used as candidates for therapeutic applications⁸⁻⁹. But much needs to be done in understanding the exact internalization mechanisms and pathways in a living system. Alternate routes of internalization other than

the traditionally-known endocytosis need to be explored for effective usage of these nanostructures as drug delivery vehicles.

6.2.3 Automation of DNA nanotechnology

For the broader applicability of DNA nanotechnology by scientists, there is an increasing need for more access to this technology. This could be done by automation software designs that take the desired shape as input and then give the required DNA sequences for self-assembly as output. There has been progress to this end by a select few groups¹⁰⁻¹². However, the software designed to date explore select DNA design technologies, some limited to only 2D structures, others to 3D. The field is yet to come up with one uniform software reaching across all of DNA nanotechnology and all possible shapes.

6.2.4 Structural DNA nanotechnology

DNA nanotechnology has still much to achieve in terms of some of the foundational goals, like utilizing DNA scaffolds for programmable orientation of proteins and thereafter elucidating their structure using X-ray crystallography. Although the field of structural elucidation has evolved by itself with the growing prominence in the technique of cryo-EM¹³, the foundational goal still remains relevant. Efforts in this direction have been made by groups both the directions of X-ray crystallography and cryo-EM. Some efforts have gone in the direction of expanding cavity sizes in self-assembled DNA crystals,¹⁴ whereas others have tried to position and orient proteins on DNA origami scaffolds¹⁵⁻¹⁶ to solve their structure by cryo-EM. The field has yet to demonstrate the capability to solve the structure of an unknown protein by either technique. Efforts in

multiple directions need to be done to realize this dream. One foundational problem in this is the technique needed to anchor proteins on the DNA scaffolds. The present strategies use DNA binding sequences or conjugation techniques to DNA followed by anchoring them on the scaffold. These strategies are often not realizable by protein biochemists, so there is a dire need come up with a really simple and elegant technique to do the same. The other direction that needs to be explored by scientists is the construction of rationally desired 3D lattice structures of a designed geometrical packing. This is still a distant dream as the design rules of construction of such lattice structures are yet to be figured out. These architectures when made could have huge potential in the realization of electrical and optical metamaterials.

Biomimetic reconfigurable structures such as artificial ion channels¹⁷ and GPCR proteins are yet another direction that DNA nanotechnology has huge potential to grow into. Functionally relevant DNA nanostructures mimicking the action of proteins is a direction of much interest in the scientific world. These scientific achievements would have huge potential in applying these materials in a cell free world and towards real world applications.

6.3. References

1. Ducrot, É.; Gales, J.; Yi, G.-R.; Pine, D. J., Pyrochlore lattice, self-assembly and photonic band gap optimizations. *Opt. Express* **2018**, *26* (23), 30052-30060.
2. Hynninen, A.-P.; Thijssen, J. H. J.; Vermolen, E. C. M.; Dijkstra, M.; van Blaaderen, A., Self-assembly route for photonic crystals with a bandgap in the visible region. *Nature Materials* **2007**, *6* (3), 202-205.
3. Ngo, T. T.; Liddell, C. M.; Ghebrehbran, M.; Joannopoulos, J. D., Tetrastack: Colloidal diamond-inspired structure with omnidirectional photonic band gap for low refractive index contrast. *Applied Physics Letters* **2006**, *88* (24), 241920.

4. Edagawa, K.; Kanoko, S.; Notomi, M., Photonic amorphous diamond structure with a 3D photonic band gap. *Phys Rev Lett* **2008**, *100* (1), 013901.
5. Garcia-Adeva, A., Band gap atlas for photonic crystals having the symmetry of the kagomé and pyrochlore lattices. *New Journal of Physics* **2006**, *8* (6), 86-86.
6. Holland, B. T.; Blanford, C. F.; Stein, A., Synthesis of Macroporous Minerals with Highly Ordered Three-Dimensional Arrays of Spheroidal Voids. *Science* **1998**, *281* (5376), 538-540.
7. Maldovan, M.; Thomas, E. L., Diamond-structured photonic crystals. *Nature Materials* **2004**, *3* (9), 593-600.
8. Zhang, J.; Sun, Z.; Yang, B., Self-assembly of photonic crystals from polymer colloids. *Current Opinion in Colloid & Interface Science* **2009**, *14* (2), 103-114.
9. Werts, M. H. V.; Lambert, M.; Bourgoin, J.-P.; Brust, M., Nanometer Scale Patterning of Langmuir–Blodgett Films of Gold Nanoparticles by Electron Beam Lithography. *Nano Letters* **2002**, *2* (1), 43-47.
10. Park, S. Y.; Lytton-Jean, A. K. R.; Lee, B.; Weigand, S.; Schatz, G. C.; Mirkin, C. A., DNA-programmable nanoparticle crystallization. *Nature* **2008**, *451* (7178), 553-556.
11. Macfarlane, R. J.; Lee, B.; Jones, M. R.; Harris, N.; Schatz, G. C.; Mirkin, C. A., Nanoparticle Superlattice Engineering with DNA. *Science* **2011**, *334* (6053), 204-208.
12. Rothemund, P. W. K., Folding DNA to create nanoscale shapes and patterns. *Nature* **2006**, *440* (7082), 297-302.
13. Zhang, Y.; Seeman, N. C., Construction of a DNA-Truncated Octahedron. *Journal of the American Chemical Society* **1994**, *116* (5), 1661-1669.
14. Ke, Y.; Sharma, J.; Liu, M.; Jahn, K.; Liu, Y.; Yan, H., Scaffolded DNA Origami of a DNA Tetrahedron Molecular Container. *Nano Letters* **2009**, *9* (6), 2445-2447.
15. Ke, Y.; Ong, L. L.; Shih, W. M.; Yin, P., Three-Dimensional Structures Self-Assembled from DNA Bricks. *Science* **2012**, *338* (6111), 1177-1183.
16. Liu, W.; Halverson, J.; Tian, Y.; Tkachenko, A. V.; Gang, O., Self-organized architectures from assorted DNA-framed nanoparticles. *Nature Chemistry* **2016**, *8* (9), 867-873.
17. Romano, F.; Russo, J.; Kroc, L.; Šulc, P., Designing Patchy Interactions to Self-Assemble Arbitrary Structures. *Phys Rev Lett* **2020**, *125* (11), 118003.

18. Liu, X.; Zhang, F.; Jing, X.; Pan, M.; Liu, P.; Li, W.; Zhu, B.; Li, J.; Chen, H.; Wang, L.; Lin, J.; Liu, Y.; Zhao, D.; Yan, H.; Fan, C., Complex silica composite nanomaterials templated with DNA origami. *Nature* **2018**, *559* (7715), 593-598.
19. Zhang, F.; Jiang, S.; Wu, S.; Li, Y.; Mao, C.; Liu, Y.; Yan, H., Complex wireframe DNA origami nanostructures with multi-arm junction vertices. *Nature Nanotechnology* **2015**, *10* (9), 779-784.
20. Qi, X.; Zhang, F.; Su, Z.; Jiang, S.; Han, D.; Ding, B.; Liu, Y.; Chiu, W.; Yin, P.; Yan, H., Programming molecular topologies from single-stranded nucleic acids. *Nature Communications* **2018**, *9* (1), 4579.
21. Shani, L.; Michelson, A. N.; Minevich, B.; Fleger, Y.; Stern, M.; Shaulov, A.; Yeshurun, Y.; Gang, O., DNA-assembled superconducting 3D nanoscale architectures. *Nature Communications* **2020**, *11* (1), 5697.

REFERENCES

CHAPTER 1

1. He, Y.; Ye, T.; Su, M.; Zhang, C.; Ribbe, A. E.; Jiang, W.; Mao, C., Hierarchical self-assembly of DNA into symmetric supramolecular polyhedra. *Nature* **2008**, *452* (7184), 198-201.
2. Watson, J. D.; Crick, F. H. C., Molecular Structure of Nucleic Acids: A Structure for Deoxyribose Nucleic Acid. *Nature* **1953**, *171* (4356), 737-738.
3. Bai, X.-c.; Martin, T. G.; Scheres, S. H. W.; Dietz, H., Cryo-EM structure of a 3D DNA-origami object. *Proceedings of the National Academy of Sciences* **2012**, *109* (49), 20012-20017.
4. Martin, T. G.; Bharat, T. A. M.; Joerger, A. C.; Bai, X.-c.; Praetorius, F.; Fersht, A. R.; Dietz, H.; Scheres, S. H. W., Design of a molecular support for cryo-EM structure determination. *Proceedings of the National Academy of Sciences* **2016**, *113* (47), E7456-E7463.
5. Seeman, N. C., Nucleic acid junctions and lattices. *Journal of Theoretical Biology* **1982**, *99* (2), 237-247.
6. Dong, Y.; Chen, S.; Zhang, S.; Sodroski, J.; Yang, Z.; Liu, D.; Mao, Y., Folding DNA into a Lipid-Conjugated Nanobarrel for Controlled Reconstitution of Membrane Proteins. *Angewandte Chemie International Edition* **2018**, *57* (8), 2072-2076.
7. Minchin, S.; Lodge, J., Understanding biochemistry: structure and function of nucleic acids. *Essays Biochem* **2019**, *63* (4), 433-456.
8. Aksel, T.; Yu, Z.; Cheng, Y.; Douglas, S. M., Molecular goniometers for single-particle cryo-electron microscopy of DNA-binding proteins. *Nature biotechnology* **2021**, *39* (3), 378-386.
9. Fu, T. J.; Seeman, N. C., DNA double-crossover molecules. *Biochemistry* **1993**, *32* (13), 3211-3220.
10. LaBean, T. H.; Yan, H.; Kopatsch, J.; Liu, F.; Winfree, E.; Reif, J. H.; Seeman, N. C., Construction, Analysis, Ligation, and Self-Assembly of DNA Triple Crossover Complexes. *Journal of the American Chemical Society* **2000**, *122* (9), 1848-1860.
11. Wang, X.; Chandrasekaran, A. R.; Shen, Z.; Ohayon, Y. P.; Wang, T.; Kizer, M. E.; Sha, R.; Mao, C.; Yan, H.; Zhang, X.; Liao, S.; Ding, B.; Chakraborty, B.; Jonoska, N.; Niu, D.; Gu, H.; Chao, J.; Gao, X.; Li, Y.; Ciengshin, T.; Seeman, N. C., Paranemic Crossover DNA: There and Back Again. *Chemical Reviews* **2019**, *119* (10), 6273-6289.

12. Winfree, E.; Liu, F.; Wenzler, L. A.; Seeman, N. C., Design and self-assembly of two-dimensional DNA crystals. *Nature* **1998**, *394* (6693), 539-544.
13. Roh, Y. H.; Ruiz, R. C. H.; Peng, S.; Lee, J. B.; Luo, D., Engineering DNA-based functional materials. *Chemical Society Reviews* **2011**, *40* (12), 5730-5744.
14. Liu, L.; Li, Z.; Li, Y.; Mao, C., Rational Design and Self-Assembly of Two-Dimensional, Dodecagonal DNA Quasicrystals. *Journal of the American Chemical Society* **2019**, *141* (10), 4248-4251.
15. Yan, H.; Park, S. H.; Finkelstein, G.; Reif, J. H.; LaBean, T. H., DNA-Templated Self-Assembly of Protein Arrays and Highly Conductive Nanowires. *Science* **2003**, *301* (5641), 1882-1884.
16. Yan, H.; Zhang, X.; Shen, Z.; Seeman, N. C., A robust DNA mechanical device controlled by hybridization topology. *Nature* **2002**, *415* (6867), 62-65.
17. Zheng, J.; Birktoft, J. J.; Chen, Y.; Wang, T.; Sha, R.; Constantinou, P. E.; Ginell, S. L.; Mao, C.; Seeman, N. C., From molecular to macroscopic via the rational design of a self-assembled 3D DNA crystal. *Nature* **2009**, *461* (7260), 74-77.
18. Dey, S.; Fan, C.; Gothelf, K. V.; Li, J.; Lin, C.; Liu, L.; Liu, N.; Nijenhuis, M. A. D.; Saccà, B.; Simmel, F. C.; Yan, H.; Zhan, P., DNA origami. *Nature Reviews Methods Primers* **2021**, *1* (1), 13.
19. Rothemund, P. W. K., Folding DNA to create nanoscale shapes and patterns. *Nature* **2006**, *440* (7082), 297-302.
20. Wagenbauer, K. F.; Sigl, C.; Dietz, H., Gigadalton-scale shape-programmable DNA assemblies. *Nature* **2017**, *552* (7683), 78-83.
21. Tikhomirov, G.; Petersen, P.; Qian, L., Fractal assembly of micrometre-scale DNA origami arrays with arbitrary patterns. *Nature* **2017**, *552* (7683), 67-71.
22. Ong, L. L.; Hanikel, N.; Yaghi, O. K.; Grun, C.; Strauss, M. T.; Bron, P.; Lai-Kee-Him, J.; Schueder, F.; Wang, B.; Wang, P.; Kishi, J. Y.; Myhrvold, C.; Zhu, A.; Jungmann, R.; Bellot, G.; Ke, Y.; Yin, P., Programmable self-assembly of three-dimensional nanostructures from 10,000 unique components. *Nature* **2017**, *552* (7683), 72-77.
23. Yao, G.; Zhang, F.; Wang, F.; Peng, T.; Liu, H.; Poppleton, E.; Šulc, P.; Jiang, S.; Liu, L.; Gong, C.; Jing, X.; Liu, X.; Wang, L.; Liu, Y.; Fan, C.; Yan, H., Meta-DNA structures. *Nature Chemistry* **2020**, *12* (11), 1067-1075.

24. Han, D.; Qi, X.; Myhrvold, C.; Wang, B.; Dai, M.; Jiang, S.; Bates, M.; Liu, Y.; An, B.; Zhang, F.; Yan, H.; Yin, P., Single-stranded DNA and RNA origami. *Science* **2017**, *358* (6369), eaao2648.
25. Hu, Y.; Niemeyer, C. M., From DNA Nanotechnology to Material Systems Engineering. *Advanced Materials* **2019**, *31* (26), 1806294.
26. Simmons, C. R.; Zhang, F.; Birktoft, J. J.; Qi, X.; Han, D.; Liu, Y.; Sha, R.; Abdallah, H. O.; Hernandez, C.; Ohayon, Y. P.; Seeman, N. C.; Yan, H., Construction and Structure Determination of a Three-Dimensional DNA Crystal. *Journal of the American Chemical Society* **2016**, *138* (31), 10047-10054.
27. Hong, F.; Jiang, S.; Lan, X.; Narayanan, R. P.; Šulc, P.; Zhang, F.; Liu, Y.; Yan, H., Layered-Crossover Tiles with Precisely Tunable Angles for 2D and 3D DNA Crystal Engineering. *Journal of the American Chemical Society* **2018**, *140* (44), 14670-14676.
28. Zhang, T.; Hartl, C.; Frank, K.; Heuer-Jungemann, A.; Fischer, S.; Nickels, P. C.; Nickel, B.; Liedl, T., 3D DNA Origami Crystals. *Advanced Materials* **2018**, *30* (28), 1800273.
29. Tian, Y.; Zhang, Y.; Wang, T.; Xin, H. L.; Li, H.; Gang, O., Lattice engineering through nanoparticle-DNA frameworks. *Nature materials* **2016**, *15* (6), 654-661.
30. Liu, W.; Tagawa, M.; Xin, H. L.; Wang, T.; Emamy, H.; Li, H.; Yager, K. G.; Starr, F. W.; Tkachenko, A. V.; Gang, O., Diamond family of nanoparticle superlattices. *Science (New York, N.Y.)* **2016**, *351* (6273), 582-586.
31. Tian, Y.; Lhermitte, J. R.; Bai, L.; Vo, T.; Xin, H. L.; Li, H.; Li, R.; Fukuto, M.; Yager, K. G.; Kahn, J. S.; Xiong, Y.; Minevich, B.; Kumar, S. K.; Gang, O., Ordered three-dimensional nanomaterials using DNA-prescribed and valence-controlled material voxels. *Nature Materials* **2020**, *19* (7), 789-796.
32. Shani, L.; Michelson, A. N.; Minevich, B.; Fleger, Y.; Stern, M.; Shaulov, A.; Yeshurun, Y.; Gang, O., DNA-assembled superconducting 3D nanoscale architectures. *Nature Communications* **2020**, *11* (1), 5697.
33. Majewski, P. W.; Michelson, A.; Cordeiro, M. A. L.; Tian, C.; Ma, C.; Kisslinger, K.; Tian, Y.; Liu, W.; Stach, E. A.; Yager, K. G.; Gang, O., Resilient three-dimensional ordered architectures assembled from nanoparticles by DNA. *Science Advances* **2021**, *7* (12), eabf0617.
34. Madsen, M.; Gothelf, K. V., Chemistries for DNA Nanotechnology. *Chemical Reviews* **2019**, *119* (10), 6384-6458.

35. Perrault, S. D.; Shih, W. M., Virus-Inspired Membrane Encapsulation of DNA Nanostructures To Achieve In Vivo Stability. *ACS Nano* **2014**, *8* (5), 5132-5140.
36. Yang, Y.; Wang, J.; Shigematsu, H.; Xu, W.; Shih, W. M.; Rothman, J. E.; Lin, C., Self-assembly of size-controlled liposomes on DNA nanotemplates. *Nature chemistry* **2016**, *8* (5), 476-483.
37. Zhang, Z.; Yang, Y.; Pincet, F.; Llaguno, M. C.; Lin, C., Placing and shaping liposomes with reconfigurable DNA nanocages. *Nature Chemistry* **2017**, *9* (7), 653-659.
38. Grome, M. W.; Zhang, Z.; Pincet, F.; Lin, C., Vesicle Tubulation with Self-Assembling DNA Nanosprings. *Angewandte Chemie International Edition* **2018**, *57* (19), 5330-5334.
39. Zhang, C.; Tian, C.; Guo, F.; Liu, Z.; Jiang, W.; Mao, C., DNA-Directed Three-Dimensional Protein Organization. *Angewandte Chemie International Edition* **2012**, *51* (14), 3382-3385.
40. Praetorius, F.; Dietz, H., Self-assembly of genetically encoded DNA-protein hybrid nanoscale shapes. *Science* **2017**, *355* (6331), eaam5488.
41. Xu, Y.; Jiang, S.; Simmons, C. R.; Narayanan, R. P.; Zhang, F.; Aziz, A.-M.; Yan, H.; Stephanopoulos, N., Tunable Nanoscale Cages from Self-Assembling DNA and Protein Building Blocks. *ACS Nano* **2019**, *13* (3), 3545-3554.
42. Jin, J.; Baker, E. G.; Wood, C. W.; Bath, J.; Woolfson, D. N.; Turberfield, A. J., Peptide Assembly Directed and Quantified Using Megadalton DNA Nanostructures. *ACS Nano* **2019**, *13* (9), 9927-9935.
43. Buchberger, A.; Simmons, C. R.; Fahmi, N. E.; Freeman, R.; Stephanopoulos, N., Hierarchical Assembly of Nucleic Acid/Coiled-Coil Peptide Nanostructures. *Journal of the American Chemical Society* **2020**, *142* (3), 1406-1416.
44. Jiang, T.; Meyer, T. A.; Modlin, C.; Zuo, X.; Conticello, V. P.; Ke, Y., Structurally Ordered Nanowire Formation from Co-Assembly of DNA Origami and Collagen-Mimetic Peptides. *Journal of the American Chemical Society* **2017**, *139* (40), 14025-14028.
45. Trinh, T.; Liao, C.; Toader, V.; Barłóg, M.; Bazzi, H. S.; Li, J.; Sleiman, H. F., DNA-imprinted polymer nanoparticles with monodispersity and prescribed DNA-strand patterns. *Nature Chemistry* **2018**, *10* (2), 184-192.
46. Deptuch, G.; Besson, A.; Rehak, P.; Szelezniak, M.; Wall, J.; Winter, M.; Zhu, Y., Direct electron imaging in electron microscopy with monolithic active pixel sensors. *Ultramicroscopy* **2007**, *107* (8), 674-84.

47. Williams, S.; Lund, K.; Lin, C.; Wonka, P.; Lindsay, S.; Yan, H., *Tiamat: A Three-Dimensional Editing Tool for Complex DNA Structures*. 2008; Vol. 5347, p 90-101.
48. Douglas, S. M.; Marblestone, A. H.; Teerapittayanon, S.; Vazquez, A.; Church, G. M.; Shih, W. M., Rapid prototyping of 3D DNA-origami shapes with caDNAno. *Nucleic Acids Research* **2009**, *37* (15), 5001-5006.
49. Jun, H.; Wang, X.; Bricker, W. P.; Bathe, M., Automated sequence design of 2D wireframe DNA origami with honeycomb edges. *Nature Communications* **2019**, *10* (1), 5419.
50. Jun, H.; Shepherd, T. R.; Zhang, K.; Bricker, W. P.; Li, S.; Chiu, W.; Bathe, M., Automated Sequence Design of 3D Polyhedral Wireframe DNA Origami with Honeycomb Edges. *ACS Nano* **2019**, *13* (2), 2083-2093.
51. Veneziano, R.; Ratanalert, S.; Zhang, K.; Zhang, F.; Yan, H.; Chiu, W.; Bathe, M., Designer nanoscale DNA assemblies programmed from the top down. *Science* **2016**, *352* (6293), 1534-1534.
52. Benson, E.; Mohammed, A.; Gardell, J.; Masich, S.; Czeizler, E.; Orponen, P.; Högberg, B., DNA rendering of polyhedral meshes at the nanoscale. *Nature* **2015**, *523* (7561), 441-444.
53. Benson, E.; Mohammed, A.; Bosco, A.; Teixeira, A. I.; Orponen, P.; Högberg, B., Computer-Aided Production of Scaffolded DNA Nanostructures from Flat Sheet Meshes. *Angewandte Chemie International Edition* **2016**, *55* (31), 8869-8872.
54. Jun, H.; Zhang, F.; Shepherd, T.; Ratanalert, S.; Qi, X.; Yan, H.; Bathe, M., Autonomously designed free-form 2D DNA origami. *Science Advances* **2019**, *5* (1), eaav0655.

CHAPTER 2

1. Winfree, E.; Liu, F.; Wenzler, L. A.; Seeman, N. C., Design and self-assembly of two-dimensional DNA crystals. *Nature* **1998**, *394* (6693), 539-544.
2. Yan, H.; Park, S. H.; Finkelstein, G.; Reif, J. H.; LaBean, T. H., DNA-Templated Self-Assembly of Protein Arrays and Highly Conductive Nanowires. *Science* **2003**, *301* (5641), 1882-1884.
3. Rothemund, P. W. K., Folding DNA to create nanoscale shapes and patterns. *Nature* **2006**, *440* (7082), 297-302.
4. Douglas, S. M.; Dietz, H.; Liedl, T.; Högberg, B.; Graf, F.; Shih, W. M., Self-assembly of DNA into nanoscale three-dimensional shapes. *Nature* **2009**, *459* (7245), 414-418.
5. Ke, Y.; Ong, L. L.; Shih, W. M.; Yin, P., Three-Dimensional Structures Self-Assembled from DNA Bricks. *Science* **2012**, *338* (6111), 1177-1183.
6. Hong, F.; Zhang, F.; Liu, Y.; Yan, H., DNA Origami: Scaffolds for Creating Higher Order Structures. *Chemical Reviews* **2017**, *117* (20), 12584-12640.
7. Zheng, J.; Birktoft, J. J.; Chen, Y.; Wang, T.; Sha, R.; Constantinou, P. E.; Ginell, S. L.; Mao, C.; Seeman, N. C., From molecular to macroscopic via the rational design of a self-assembled 3D DNA crystal. *Nature* **2009**, *461* (7260), 74-77.
8. Jin, J.; Baker, E. G.; Wood, C. W.; Bath, J.; Woolfson, D. N.; Turberfield, A. J., Peptide Assembly Directed and Quantified Using Megadalton DNA Nanostructures. *ACS Nano* **2019**, *13* (9), 9927-9935.
9. Buchberger, A.; Simmons, C. R.; Fahmi, N. E.; Freeman, R.; Stephanopoulos, N., Hierarchical Assembly of Nucleic Acid/Coiled-Coil Peptide Nanostructures. *Journal of the American Chemical Society* **2020**, *142* (3), 1406-1416.
10. Freeman, R.; Han, M.; Álvarez, Z.; Lewis, J. A.; Wester, J. R.; Stephanopoulos, N.; McClendon, M. T.; Lynsky, C.; Godbe, J. M.; Sangji, H.; Luijten, E.; Stupp, S. I., Reversible self-assembly of superstructured networks. *Science* **2018**, *362* (6416), 808-813.
11. Daly, M. L.; Gao, Y.; Freeman, R., Encoding Reversible Hierarchical Structures with Supramolecular Peptide–DNA Materials. *Bioconjugate Chemistry* **2019**, *30* (7), 1864-1869.
12. Jiang, T.; Meyer, T. A.; Modlin, C.; Zuo, X.; Conticello, V. P.; Ke, Y., Structurally Ordered Nanowire Formation from Co-Assembly of DNA Origami and Collagen-Mimetic Peptides. *Journal of the American Chemical Society* **2017**, *139* (40), 14025-14028.

13. Xu, Y.; Jiang, S.; Simmons, C. R.; Narayanan, R. P.; Zhang, F.; Aziz, A.-M.; Yan, H.; Stephanopoulos, N., Tunable Nanoscale Cages from Self-Assembling DNA and Protein Building Blocks. *ACS Nano* **2019**, *13* (3), 3545-3554.
14. Praetorius, F.; Dietz, H., Self-assembly of genetically encoded DNA-protein hybrid nanoscale shapes. *Science* **2017**, *355* (6331), eaam5488.
15. Kashiwagi, D.; Sim, S.; Niwa, T.; Taguchi, H.; Aida, T., Protein Nanotube Selectively Cleavable with DNA: Supramolecular Polymerization of “DNA-Appended Molecular Chaperones”. *Journal of the American Chemical Society* **2018**, *140* (1), 26-29.
16. McMillan, J. R.; Mirkin, C. A., DNA-Functionalized, Bivalent Proteins. *Journal of the American Chemical Society* **2018**, *140* (22), 6776-6779.
17. Goetzfried, M. A.; Vogele, K.; Mückl, A.; Kaiser, M.; Holland, N. B.; Simmel, F. C.; Pirzer, T., Periodic Operation of a Dynamic DNA Origami Structure Utilizing the Hydrophilic–Hydrophobic Phase-Transition of Stimulus-Sensitive Polypeptides. *Small* **2019**, *15* (45), 1903541.
18. Wilks, T. R.; Bath, J.; de Vries, J. W.; Raymond, J. E.; Herrmann, A.; Turberfield, A. J.; O’Reilly, R. K., “Giant Surfactants” Created by the Fast and Efficient Functionalization of a DNA Tetrahedron with a Temperature-Responsive Polymer. *ACS Nano* **2013**, *7* (10), 8561-8572.
19. Serpell, C. J.; Edwardson, T. G. W.; Chidchob, P.; Carneiro, K. M. M.; Sleiman, H. F., Precision Polymers and 3D DNA Nanostructures: Emergent Assemblies from New Parameter Space. *Journal of the American Chemical Society* **2014**, *136* (44), 15767-15774.
20. Woo, S.; Rothmund, P. W. K., Programmable molecular recognition based on the geometry of DNA nanostructures. *Nature Chemistry* **2011**, *3* (8), 620-627.
21. Gerling, T.; Wagenbauer, K. F.; Neuner, A. M.; Dietz, H., Dynamic DNA devices and assemblies formed by shape-complementary, non–base pairing 3D components. *Science* **2015**, *347* (6229), 1446-1452.
22. Loescher, S.; Walther, A., Supracolloidal Self-Assembly of Divalent Janus 3D DNA Origami via Programmable Multivalent Host/Guest Interactions. *Angewandte Chemie International Edition* **2020**, *59* (14), 5515-5520.
23. Kim, J.; Jung, I.-S.; Kim, S.-Y.; Lee, E.; Kang, J.-K.; Sakamoto, S.; Yamaguchi, K.; Kim, K., New Cucurbituril Homologues: Syntheses, Isolation, Characterization, and X-ray Crystal Structures of Cucurbit[n]uril (n = 5, 7, and 8). *Journal of the American Chemical Society* **2000**, *122* (3), 540-541.

24. Barrow, S. J.; Kasera, S.; Rowland, M. J.; del Barrio, J.; Scherman, O. A., Cucurbituril-Based Molecular Recognition. *Chemical Reviews* **2015**, *115* (22), 12320-12406.
25. Cao, L.; Šekutor, M.; Zavalij, P. Y.; Mlinarić-Majerski, K.; Glaser, R.; Isaacs, L., Cucurbit[7]uril-Guest Pair with an Attomolar Dissociation Constant. *Angewandte Chemie International Edition* **2014**, *53* (4), 988-993.
26. Eftink, M. R.; Andy, M. L.; Bystrom, K.; Perlmutter, H. D.; Kristol, D. S., Cyclodextrin inclusion complexes: studies of the variation in the size of alicyclic guests. *Journal of the American Chemical Society* **1989**, *111* (17), 6765-6772.
27. Webber, M. J.; Langer, R., Drug delivery by supramolecular design. *Chemical Society Reviews* **2017**, *46* (21), 6600-6620.
28. Vinciguerra, B.; Cao, L.; Cannon, J. R.; Zavalij, P. Y.; Fenselau, C.; Isaacs, L., Synthesis and Self-Assembly Processes of Monofunctionalized Cucurbit[7]uril. *Journal of the American Chemical Society* **2012**, *134* (31), 13133-13140.
29. Ghosh, S. K.; Dhamija, A.; Ko, Y. H.; An, J.; Hur, M. Y.; Boraste, D. R.; Seo, J.; Lee, E.; Park, K. M.; Kim, K., Superacid-Mediated Functionalization of Hydroxylated Cucurbit[n]urils. *Journal of the American Chemical Society* **2019**, *141* (44), 17503-17506.
30. Tigges, T.; Heuser, T.; Tiwari, R.; Walther, A., 3D DNA Origami Cuboids as Monodisperse Patchy Nanoparticles for Switchable Hierarchical Self-Assembly. *Nano Letters* **2016**, *16* (12), 7870-7874.
31. Moghaddam, S.; Yang, C.; Rekharsky, M.; Ko, Y. H.; Kim, K.; Inoue, Y.; Gilson, M. K., New Ultrahigh Affinity Host-Guest Complexes of Cucurbit[7]uril with Bicyclo[2.2.2]octane and Adamantane Guests: Thermodynamic Analysis and Evaluation of M2 Affinity Calculations. *Journal of the American Chemical Society* **2011**, *133* (10), 3570-3581.
32. Zou, L.; Braegelman, A. S.; Webber, M. J., Spatially Defined Drug Targeting by in Situ Host-Guest Chemistry in a Living Animal. *ACS Central Science* **2019**, *5* (6), 1035-1043.
33. Braegelman, A. S.; Webber, M. J., Integrating Stimuli-Responsive Properties in Host-Guest Supramolecular Drug Delivery Systems. *Theranostics* **2019**, *9* (11), 3017-3040.
34. Juurikka, K.; Butler, G. S.; Salo, T.; Nyberg, P.; Åström, P., The Role of MMP8 in Cancer: A Systematic Review. *Int J Mol Sci* **2019**, *20* (18), 4506.

35. Patterson, J.; Hubbell, J. A., Enhanced proteolytic degradation of molecularly engineered PEG hydrogels in response to MMP-1 and MMP-2. *Biomaterials* **2010**, *31* (30), 7836-7845.

CHAPTER 3

1. Krishnan, Y.; Seeman, N. C., Introduction: Nucleic Acid Nanotechnology. *Chemical Reviews* **2019**, *119* (10), 6271-6272.
2. Hong, F.; Zhang, F.; Liu, Y.; Yan, H., DNA Origami: Scaffolds for Creating Higher Order Structures. *Chemical Reviews* **2017**, *117* (20), 12584-12640.
3. Watson, J. D.; Crick, F. H. C., Molecular Structure of Nucleic Acids: A Structure for Deoxyribose Nucleic Acid. *Nature* **1953**, *171* (4356), 737-738.
4. Chen, K.; Kong, J.; Zhu, J.; Ermann, N.; Predki, P.; Keyser, U. F., Digital Data Storage Using DNA Nanostructures and Solid-State Nanopores. *Nano Letters* **2019**, *19* (2), 1210-1215.
5. Chen, K.; Zhu, J.; Bošković, F.; Keyser, U. F., Nanopore-Based DNA Hard Drives for Rewritable and Secure Data Storage. *Nano Letters* **2020**, *20* (5), 3754-3760.
6. Song, T.; Eshra, A.; Shah, S.; Bui, H.; Fu, D.; Yang, M.; Mokhtar, R.; Reif, J., Fast and compact DNA logic circuits based on single-stranded gates using strand-displacing polymerase. *Nature Nanotechnology* **2019**, *14* (11), 1075-1081.
7. Qian, L.; Winfree, E., Scaling Up Digital Circuit Computation with DNA Strand Displacement Cascades. *Science* **2011**, *332* (6034), 1196-1201.
8. Seelig, G.; Soloveichik, D.; Zhang, D. Y.; Winfree, E., Enzyme-Free Nucleic Acid Logic Circuits. *Science* **2006**, *314* (5805), 1585-1588.
9. Thubagere, A. J.; Thachuk, C.; Berleant, J.; Johnson, R. F.; Ardelean, D. A.; Cherry, K. M.; Qian, L., Compiler-aided systematic construction of large-scale DNA strand displacement circuits using unpurified components. *Nature Communications* **2017**, *8* (1), 14373.
10. Li, S.; Jiang, Q.; Liu, S.; Zhang, Y.; Tian, Y.; Song, C.; Wang, J.; Zou, Y.; Anderson, G. J.; Han, J.-Y.; Chang, Y.; Liu, Y.; Zhang, C.; Chen, L.; Zhou, G.; Nie, G.; Yan, H.; Ding, B.; Zhao, Y., A DNA nanorobot functions as a cancer therapeutic in response to a molecular trigger in vivo. *Nature Biotechnology* **2018**, *36* (3), 258-264.
11. Jiang, Q.; Song, C.; Nangreave, J.; Liu, X.; Lin, L.; Qiu, D.; Wang, Z.-G.; Zou, G.; Liang, X.; Yan, H.; Ding, B., DNA Origami as a Carrier for Circumvention of Drug Resistance. *Journal of the American Chemical Society* **2012**, *134* (32), 13396-13403.
12. Hu, Q.; Li, H.; Wang, L.; Gu, H.; Fan, C., DNA Nanotechnology-Enabled Drug Delivery Systems. *Chemical Reviews* **2019**, *119* (10), 6459-6506.

13. Douglas, S. M.; Bachelet, I.; Church, G. M., A Logic-Gated Nanorobot for Targeted Transport of Molecular Payloads. *Science* **2012**, *335* (6070), 831-834.
14. Das, R.; Baker, D., Macromolecular Modeling with Rosetta. *Annual Review of Biochemistry* **2008**, *77* (1), 363-382.
15. Praetorius, F.; Dietz, H., Self-assembly of genetically encoded DNA-protein hybrid nanoscale shapes. *Science* **2017**, *355* (6331), eaam5488.
16. Xu, Y.; Jiang, S.; Simmons, C. R.; Narayanan, R. P.; Zhang, F.; Aziz, A.-M.; Yan, H.; Stephanopoulos, N., Tunable Nanoscale Cages from Self-Assembling DNA and Protein Building Blocks. *ACS Nano* **2019**, *13* (3), 3545-3554.
17. Douglas, S. M.; Marblestone, A. H.; Teerapittayanon, S.; Vazquez, A.; Church, G. M.; Shih, W. M., Rapid prototyping of 3D DNA-origami shapes with caDNAno. *Nucleic Acids Research* **2009**, *37* (15), 5001-5006.
18. Lyumkis, D., Challenges and opportunities in cryo-EM single-particle analysis. *J Biol Chem* **2019**, *294* (13), 5181-5197.
19. Procyk, J.; Poppleton, E.; Sulc, P., *Coarse-Grained Nucleic Acid-Protein Model for Hybrid Nanotechnology*. 2020.
20. Suma, A.; Poppleton, E.; Matthies, M.; Šulc, P.; Romano, F.; Louis, A. A.; Doye, J. P. K.; Micheletti, C.; Rovigatti, L., TacoxDNA: A user-friendly web server for simulations of complex DNA structures, from single strands to origami. *Journal of Computational Chemistry* **2019**, *40* (29), 2586-2595.
21. Poppleton, E.; Bohlin, J.; Matthies, M.; Sharma, S.; Zhang, F.; Šulc, P., Design, optimization and analysis of large DNA and RNA nanostructures through interactive visualization, editing and molecular simulation. *Nucleic Acids Research* **2020**, *48* (12), e72-e72.
22. Snodin, B. E.; Randisi, F.; Mosayebi, M.; Šulc, P.; Schreck, J. S.; Romano, F.; Ouldridge, T. E.; Tsukanov, R.; Nir, E.; Louis, A. A.; Doye, J. P., Introducing improved structural properties and salt dependence into a coarse-grained model of DNA. *The Journal of chemical physics* **2015**, *142* (23), 234901.
23. Pettersen, E. F.; Goddard, T. D.; Huang, C. C.; Couch, G. S.; Greenblatt, D. M.; Meng, E. C.; Ferrin, T. E., UCSF Chimera--a visualization system for exploratory research and analysis. *J Comput Chem* **2004**, *25* (13), 1605-12.

CHAPTER 4

1. Gao, D.; Lin, X. P.; Zhang, Z. P.; Li, W.; Men, D.; Zhang, X. E.; Cui, Z. Q., Intracellular cargo delivery by virus capsid protein-based vehicles: From nano to micro. *Nanomedicine : nanotechnology, biology, and medicine* **2016**, *12* (2), 365-76.
2. Somiya, M.; Liu, Q.; Kuroda, S. i., Current Progress of Virus-mimicking Nanocarriers for Drug Delivery. *Nanotheranostics* **2017**, *1* (4), 415-429.
3. Sercombe, L.; Veerati, T.; Moheimani, F.; Wu, S. Y.; Sood, A. K.; Hua, S., Advances and Challenges of Liposome Assisted Drug Delivery. *Frontiers in Pharmacology* **2015**, *6* (286).
4. Tanner, P.; Baumann, P.; Enea, R.; Onaca, O.; Palivan, C.; Meier, W., Polymeric Vesicles: From Drug Carriers to Nanoreactors and Artificial Organelles. *Accounts of Chemical Research* **2011**, *44* (10), 1039-1049.
5. Bhaskar, S.; Lim, S., Engineering protein nanocages as carriers for biomedical applications. *NPG Asia Materials* **2017**, *9* (4), e371-e371.
6. Chandrasekaran, A. R.; Levchenko, O., DNA Nanocages. *Chemistry of Materials* **2016**, *28* (16), 5569-5581.
7. Rothemund, P. W. K., Folding DNA to create nanoscale shapes and patterns. *Nature* **2006**, *440* (7082), 297-302.
8. Douglas, S. M.; Dietz, H.; Liedl, T.; Högberg, B.; Graf, F.; Shih, W. M., Self-assembly of DNA into nanoscale three-dimensional shapes. *Nature* **2009**, *459* (7245), 414-418.
9. Zhang, F.; Jiang, S.; Wu, S.; Li, Y.; Mao, C.; Liu, Y.; Yan, H., Complex wireframe DNA origami nanostructures with multi-arm junction vertices. *Nature Nanotechnology* **2015**, *10* (9), 779-784.
10. Jun, H.; Zhang, F.; Shepherd, T.; Ratanalert, S.; Qi, X.; Yan, H.; Bathe, M., Autonomously designed free-form 2D DNA origami. *Science Advances* **2019**, *5* (1), eaav0655.
11. Veneziano, R.; Ratanalert, S.; Zhang, K.; Zhang, F.; Yan, H.; Chiu, W.; Bathe, M., Designer nanoscale DNA assemblies programmed from the top down. *Science* **2016**, *352* (6293), 1534-1534.
12. Jun, H.; Shepherd, T. R.; Zhang, K.; Bricker, W. P.; Li, S.; Chiu, W.; Bathe, M., Automated Sequence Design of 3D Polyhedral Wireframe DNA Origami with Honeycomb Edges. *ACS Nano* **2019**, *13* (2), 2083-2093.

13. Benson, E.; Mohammed, A.; Gardell, J.; Masich, S.; Czeizler, E.; Orponen, P.; Högberg, B., DNA rendering of polyhedral meshes at the nanoscale. *Nature* **2015**, *523* (7561), 441-444.
14. Dietz, H.; Douglas, S. M.; Shih, W. M., Folding DNA into Twisted and Curved Nanoscale Shapes. *Science* **2009**, *325* (5941), 725-730.
15. Han, D.; Pal, S.; Nangreave, J.; Deng, Z.; Liu, Y.; Yan, H., DNA Origami with Complex Curvatures in Three-Dimensional Space. *Science* **2011**, *332* (6027), 342-346.
16. Ke, Y.; Ong, L. L.; Shih, W. M.; Yin, P., Three-Dimensional Structures Self-Assembled from DNA Bricks. *Science* **2012**, *338* (6111), 1177-1183.
17. Ong, L. L.; Hanikel, N.; Yaghi, O. K.; Grun, C.; Strauss, M. T.; Bron, P.; Lai-Kee-Him, J.; Schueder, F.; Wang, B.; Wang, P.; Kishi, J. Y.; Myhrvold, C.; Zhu, A.; Jungmann, R.; Bellot, G.; Ke, Y.; Yin, P., Programmable self-assembly of three-dimensional nanostructures from 10,000 unique components. *Nature* **2017**, *552* (7683), 72-77.
18. Douglas, S. M.; Marblestone, A. H.; Teerapittayanon, S.; Vazquez, A.; Church, G. M.; Shih, W. M., Rapid prototyping of 3D DNA-origami shapes with caDNANO. *Nucleic Acids Research* **2009**, *37* (15), 5001-5006.
19. Williams, S.; Lund, K.; Lin, C.; Wonka, P.; Lindsay, S.; Yan, H. In *Tiamat: A Three-Dimensional Editing Tool for Complex DNA Structures*, Berlin, Heidelberg, Springer Berlin Heidelberg: Berlin, Heidelberg, 2009; pp 90-101.
20. Sun, W.; Boulais, E.; Hakobyan, Y.; Wang, W. L.; Guan, A.; Bathe, M.; Yin, P., Casting inorganic structures with DNA molds. *Science* **2014**, *346* (6210), 1258361.
21. Helmi, S.; Ziegler, C.; Kauert, D. J.; Seidel, R., Shape-Controlled Synthesis of Gold Nanostructures Using DNA Origami Molds. *Nano Letters* **2014**, *14* (11), 6693-6698.
22. Zhang, Z.; Yang, Y.; Pincet, F.; Llaguno, M. C.; Lin, C., Placing and shaping liposomes with reconfigurable DNA nanocages. *Nature Chemistry* **2017**, *9* (7), 653-659.
23. Grossi, G.; Dalgaard Ebbesen Jepsen, M.; Kjems, J.; Andersen, E. S., Control of enzyme reactions by a reconfigurable DNA nanovault. *Nature Communications* **2017**, *8* (1), 992.
24. Linko, V.; Eerikäinen, M.; Kostianen, M. A., A modular DNA origami-based enzyme cascade nanoreactor. *Chemical Communications* **2015**, *51* (25), 5351-5354.
25. Douglas, S. M.; Bachelet, I.; Church, G. M., A Logic-Gated Nanorobot for Targeted Transport of Molecular Payloads. *Science* **2012**, *335* (6070), 831-834.

26. Li, S.; Jiang, Q.; Liu, S.; Zhang, Y.; Tian, Y.; Song, C.; Wang, J.; Zou, Y.; Anderson, G. J.; Han, J.-Y.; Chang, Y.; Liu, Y.; Zhang, C.; Chen, L.; Zhou, G.; Nie, G.; Yan, H.; Ding, B.; Zhao, Y., A DNA nanorobot functions as a cancer therapeutic in response to a molecular trigger in vivo. *Nature Biotechnology* **2018**, *36* (3), 258-264.
27. Snodin, B. E. K.; Romano, F.; Rovigatti, L.; Ouldridge, T. E.; Louis, A. A.; Doye, J. P. K., Direct Simulation of the Self-Assembly of a Small DNA Origami. *ACS Nano* **2016**, *10* (2), 1724-1737.
28. Snodin, B. E.; Randisi, F.; Mosayebi, M.; Šulc, P.; Schreck, J. S.; Romano, F.; Ouldridge, T. E.; Tsukanov, R.; Nir, E.; Louis, A. A.; Doye, J. P., Introducing improved structural properties and salt dependence into a coarse-grained model of DNA. *The Journal of chemical physics* **2015**, *142* (23), 234901.
29. Kim, D.-N.; Kilchherr, F.; Dietz, H.; Bathe, M., Quantitative prediction of 3D solution shape and flexibility of nucleic acid nanostructures. *Nucleic Acids Research* **2011**, *40* (7), 2862-2868.

CHAPTER 5

1. Ducrot, É.; Gales, J.; Yi, G.-R.; Pine, D. J., Pyrochlore lattice, self-assembly and photonic band gap optimizations. *Opt. Express* **2018**, *26* (23), 30052-30060.
2. Hynninen, A.-P.; Thijssen, J. H. J.; Vermolen, E. C. M.; Dijkstra, M.; van Blaaderen, A., Self-assembly route for photonic crystals with a bandgap in the visible region. *Nature Materials* **2007**, *6* (3), 202-205.
3. Ngo, T. T.; Liddell, C. M.; Ghebrebrihan, M.; Joannopoulos, J. D., Tetrastack: Colloidal diamond-inspired structure with omnidirectional photonic band gap for low refractive index contrast. *Applied Physics Letters* **2006**, *88* (24), 241920.
4. Edagawa, K.; Kanoko, S.; Notomi, M., Photonic amorphous diamond structure with a 3D photonic band gap. *Phys Rev Lett* **2008**, *100* (1), 013901.
5. Garcia-Adeva, A., Band gap atlas for photonic crystals having the symmetry of the kagomé and pyrochlore lattices. *New Journal of Physics* **2006**, *8* (6), 86-86.
6. Holland, B. T.; Blanford, C. F.; Stein, A., Synthesis of Macroporous Minerals with Highly Ordered Three-Dimensional Arrays of Spheroidal Voids. *Science* **1998**, *281* (5376), 538-540.
7. Maldovan, M.; Thomas, E. L., Diamond-structured photonic crystals. *Nature Materials* **2004**, *3* (9), 593-600.
8. Zhang, J.; Sun, Z.; Yang, B., Self-assembly of photonic crystals from polymer colloids. *Current Opinion in Colloid & Interface Science* **2009**, *14* (2), 103-114.
9. Werts, M. H. V.; Lambert, M.; Bourgoïn, J.-P.; Brust, M., Nanometer Scale Patterning of Langmuir-Blodgett Films of Gold Nanoparticles by Electron Beam Lithography. *Nano Letters* **2002**, *2* (1), 43-47.
10. Park, S. Y.; Lytton-Jean, A. K. R.; Lee, B.; Weigand, S.; Schatz, G. C.; Mirkin, C. A., DNA-programmable nanoparticle crystallization. *Nature* **2008**, *451* (7178), 553-556.
11. Macfarlane, R. J.; Lee, B.; Jones, M. R.; Harris, N.; Schatz, G. C.; Mirkin, C. A., Nanoparticle Superlattice Engineering with DNA. *Science* **2011**, *334* (6053), 204-208.
12. Rothemund, P. W. K., Folding DNA to create nanoscale shapes and patterns. *Nature* **2006**, *440* (7082), 297-302.
13. Zhang, Y.; Seeman, N. C., Construction of a DNA-Truncated Octahedron. *Journal of the American Chemical Society* **1994**, *116* (5), 1661-1669.

14. Ke, Y.; Sharma, J.; Liu, M.; Jahn, K.; Liu, Y.; Yan, H., Scaffolded DNA Origami of a DNA Tetrahedron Molecular Container. *Nano Letters* **2009**, *9* (6), 2445-2447.
15. Ke, Y.; Ong, L. L.; Shih, W. M.; Yin, P., Three-Dimensional Structures Self-Assembled from DNA Bricks. *Science* **2012**, *338* (6111), 1177-1183.
16. Liu, W.; Halverson, J.; Tian, Y.; Tkachenko, A. V.; Gang, O., Self-organized architectures from assorted DNA-framed nanoparticles. *Nature Chemistry* **2016**, *8* (9), 867-873.
17. Romano, F.; Russo, J.; Kroc, L.; Šulc, P., Designing Patchy Interactions to Self-Assemble Arbitrary Structures. *Phys Rev Lett* **2020**, *125* (11), 118003.
18. Liu, X.; Zhang, F.; Jing, X.; Pan, M.; Liu, P.; Li, W.; Zhu, B.; Li, J.; Chen, H.; Wang, L.; Lin, J.; Liu, Y.; Zhao, D.; Yan, H.; Fan, C., Complex silica composite nanomaterials templated with DNA origami. *Nature* **2018**, *559* (7715), 593-598.
19. Zhang, F.; Jiang, S.; Wu, S.; Li, Y.; Mao, C.; Liu, Y.; Yan, H., Complex wireframe DNA origami nanostructures with multi-arm junction vertices. *Nature Nanotechnology* **2015**, *10* (9), 779-784.
20. Qi, X.; Zhang, F.; Su, Z.; Jiang, S.; Han, D.; Ding, B.; Liu, Y.; Chiu, W.; Yin, P.; Yan, H., Programming molecular topologies from single-stranded nucleic acids. *Nature Communications* **2018**, *9* (1), 4579.
21. Shani, L.; Michelson, A. N.; Minevich, B.; Fleger, Y.; Stern, M.; Shaulov, A.; Yeshurun, Y.; Gang, O., DNA-assembled superconducting 3D nanoscale architectures. *Nature Communications* **2020**, *11* (1), 5697.

CHAPTER 6

1. Ong, L. L.; Hanikel, N.; Yaghi, O. K.; Grun, C.; Strauss, M. T.; Bron, P.; Lai-Kee-Him, J.; Schueder, F.; Wang, B.; Wang, P.; Kishi, J. Y.; Myhrvold, C.; Zhu, A.; Jungmann, R.; Bellot, G.; Ke, Y.; Yin, P., Programmable self-assembly of three-dimensional nanostructures from 10,000 unique components. *Nature* **2017**, *552* (7683), 72-77.
2. Tikhomirov, G.; Petersen, P.; Qian, L., Fractal assembly of micrometre-scale DNA origami arrays with arbitrary patterns. *Nature* **2017**, *552* (7683), 67-71.
3. Wagenbauer, K. F.; Sigl, C.; Dietz, H., Gigadalton-scale shape-programmable DNA assemblies. *Nature* **2017**, *552* (7683), 78-83.
4. Praetorius, F.; Kick, B.; Behler, K. L.; Honemann, M. N.; Weuster-Botz, D.; Dietz, H., Biotechnological mass production of DNA origami. *Nature* **2017**, *552* (7683), 84-87.
5. Rothemund, P. W. K., Folding DNA to create nanoscale shapes and patterns. *Nature* **2006**, *440* (7082), 297-302.
6. Praetorius, F.; Dietz, H., Self-assembly of genetically encoded DNA-protein hybrid nanoscale shapes. *Science* **2017**, *355* (6331), eaam5488.
7. Xu, Y.; Jiang, S.; Simmons, C. R.; Narayanan, R. P.; Zhang, F.; Aziz, A. M.; Yan, H.; Stephanopoulos, N., Tunable Nanoscale Cages from Self-Assembling DNA and Protein Building Blocks. *ACS nano* **2019**, *13* (3), 3545-3554.
8. Hu, Q.; Li, H.; Wang, L.; Gu, H.; Fan, C., DNA Nanotechnology-Enabled Drug Delivery Systems. *Chemical Reviews* **2019**, *119* (10), 6459-6506.
9. Li, S.; Jiang, Q.; Liu, S.; Zhang, Y.; Tian, Y.; Song, C.; Wang, J.; Zou, Y.; Anderson, G. J.; Han, J.-Y.; Chang, Y.; Liu, Y.; Zhang, C.; Chen, L.; Zhou, G.; Nie, G.; Yan, H.; Ding, B.; Zhao, Y., A DNA nanorobot functions as a cancer therapeutic in response to a molecular trigger in vivo. *Nature Biotechnology* **2018**, *36* (3), 258-264.
10. Jun, H.; Shepherd, T. R.; Zhang, K.; Bricker, W. P.; Li, S.; Chiu, W.; Bathe, M., Automated Sequence Design of 3D Polyhedral Wireframe DNA Origami with Honeycomb Edges. *ACS nano* **2019**, *13* (2), 2083-2093.
11. Veneziano, R.; Ratanalert, S.; Zhang, K.; Zhang, F.; Yan, H.; Chiu, W.; Bathe, M., Designer nanoscale DNA assemblies programmed from the top down. *Science* **2016**, *352* (6293), 1534-1534.

12. Jun, H.; Zhang, F.; Shepherd, T.; Ratanalert, S.; Qi, X.; Yan, H.; Bathe, M., Autonomously designed free-form 2D DNA origami. *Science Advances* **2019**, *5* (1), eaav0655.
13. Bai, X. C.; McMullan, G.; Scheres, S. H., How cryo-EM is revolutionizing structural biology. *Trends in biochemical sciences* **2015**, *40* (1), 49-57.
14. Simmons, C. R.; MacCulloch, T.; Zhang, F.; Liu, Y.; Stephanopoulos, N.; Yan, H., A Self-Assembled Rhombohedral DNA Crystal Scaffold with Tunable Cavity Sizes and High-Resolution Structural Detail. *Angewandte Chemie International Edition* **2020**, *59* (42), 18619-18626.
15. Aksel, T.; Yu, Z.; Cheng, Y.; Douglas, S. M., Molecular goniometers for single-particle cryo-electron microscopy of DNA-binding proteins. *Nat Biotechnol* **2021**, *39* (3), 378-386.
16. Martin, T. G.; Bharat, T. A. M.; Joerger, A. C.; Bai, X.-c.; Praetorius, F.; Fersht, A. R.; Dietz, H.; Scheres, S. H. W., Design of a molecular support for cryo-EM structure determination. *Proceedings of the National Academy of Sciences* **2016**, *113* (47), E7456-E7463.
17. Langecker, M.; Arnaut, V.; Martin, T. G.; List, J.; Renner, S.; Mayer, M.; Dietz, H.; Simmel, F. C., Synthetic lipid membrane channels formed by designed DNA nanostructures. *Science (New York, N.Y.)* **2012**, *338* (6109), 932-936.

APPENDIX A

SUPPLEMENTAL MATERIAL FOR CHAPTER 2

Stimulus responsive DNA nanostructures *via* high-affinity host–guest interactions
Raghu Pradeep Narayanan,^{1,2} Alex Buchberger,^{1,2} Lei Zou,³ Tara MacCulloch, Nour
Eddine Fahmi,² Hao Yan,^{1,2} Fei Zhang,^{1,2,4} Matthew J. Webber,^{3*} Nicholas
Stephanopoulos^{1,2*}

(* mwebber@nd.edu, nstephal@asu.edu)

1. School of Molecular Sciences, Arizona State University, Tempe AZ
2. Center for Molecular Design and Biomimetics, The Biodesign Institute, Arizona State University, Tempe AZ
3. Chemical & Biomolecular Engineering, University of Notre Dame, Notre Dame IN
4. Department of Chemistry, Rutgers University-Newark, Newark NJ

Supporting Information

- S1. Materials and supplies
- S2. General protocols
- S3. Synthesis of small molecules
- S4. Synthesis and characterization of small molecule-DNA conjugates
- S5. DNA sequences used
- S6. Experimental protocols for DNA conjugates and origami
- S7. Supplementary Figures
- S8. Sequence of DNA cuboid origami staples and handles
- S9. Sequence of DNA nano-box origami staples and handles
- S10. References

S1. Materials and supplies.

All DNA sequences were purchased from Integrated DNA technologies (IDT). Triethylammonium acetate buffer, methanol, 1-hydroxyadamantane, and dimethyl sulfoxide (DMSO) were purchased from Sigma Aldrich. The DBCO-sulfo-NHS linker was purchased from Glen Research (Fisher Scientific). Adamantane-maleimide, β CD-azide and CB[7]-azide were synthesized as described in Section S3. The M13 scaffold strand was amplified and purified in-house.

S2. General protocols.

Purification by RP-HPLC. Following reaction, DNA conjugates were purified using a C-18 column on an Agilent 1220 Infinity LC HPLC. The mixtures were purified using a linear gradient method, with Buffer-A (water with 50 mM triethylammonium acetate (TEAA)) and Buffer-B (methanol). A linear gradient was run from 10% to 100% Buffer B over 60 minutes. Conjugates were monitored and collected based on 260 nm (for DNA) and 309 nm (for DBCO) absorbances. Peaks were tested for purity and identified by MALDI-TOF mass spectrometry.

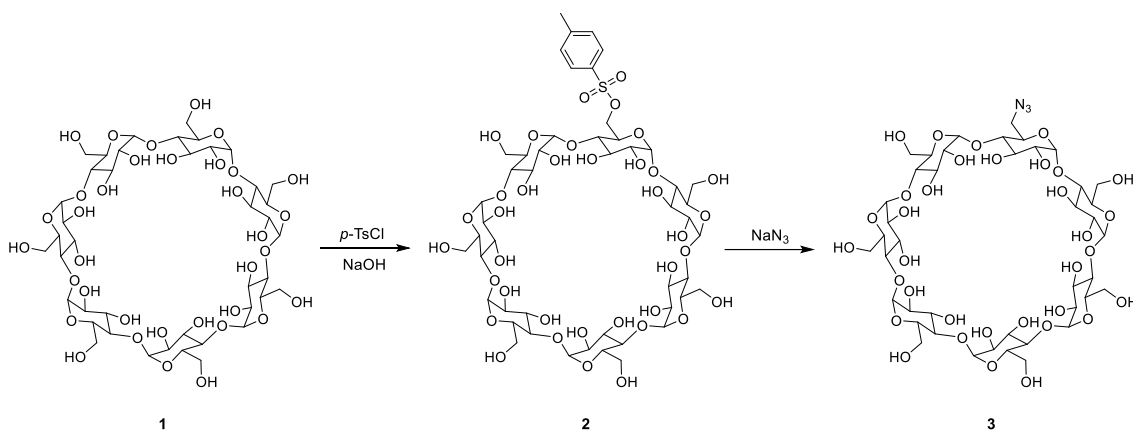
Mass characterization by MALDI-TOF MS. All purified products were characterized on an AB SCIEX 4800 MALDI TOF/TOF in the positive ion mode, with 3-Hydroxyphenylacetic acid (HPA) as the matrix. Samples were spotted onto a MALDI plate using a sandwich technique (sample-matrix-sample).

PAGE analysis of conjugates. Small molecule-DNA conjugates were analyzed using 20% native PAGE. To each lane was added 20 μ l of a 1 μ M sample, and the gel was

electrophoresed using at constant voltage (200 V) for 3 h at 4°C, then stained with ethidium bromide and imaged with a Bio-Rad Molecular Imager GelDOC XR+ imaging system.

S3. Synthesis of small molecules.

General methods. Except as noted otherwise, all non-aqueous reactions were carried out in oven-dried glassware under a balloon pressure of argon or nitrogen. Reagents were commercially available and used as received; anhydrous solvents were purchased as the highest grade from Sigma-Aldrich. Reactions were monitored by thin layer chromatography using 0.25 mm Silicycle silica gel 60 F₂₅₄ plates. Flash column chromatography was performed using Silicycle 40-60 mesh silica gel. Yields are reported as isolated yields of spectroscopically pure compounds. ¹H and ¹³C NMR spectra were obtained using 400 and 500 MHz Varian spectrometers. Chemical shifts are reported in parts per million (ppm, □) referenced to the residual ¹H resonance of the solvent (CDCl₃, 7.26 ppm and DMSO-*d*₆, 2.49 ppm). ¹³C spectra are referenced to the residual ¹³C resonance of the solvent (CDCl₃, 77.16 ppm and DMSO-*d*₆, 39.52 ppm). Splitting patterns are designated as follows: s, singlet; br, broad; d, doublet; dd, doublet of doublets; t, triplet; q, quartet; m, multiplet.

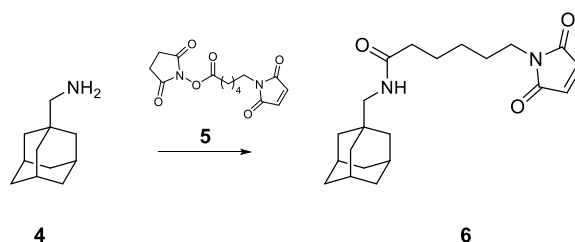


Scheme S1: Synthesis of β CD-azide (3).

6-Mono-*O*-(*p*-toluenesulfonyl)- β -cyclodextrin (2). To a cooled (0-5 °C) suspension containing β -cyclodextrin (1) (20.0 g, 17.6 mmol) in 0.4 M aq. NaOH (250 mL) was added 13.4 g of *p*-toluenesulfonyl chloride (70.3 mmol, 4.0 eq.) in small portions over a 15 min. period. The mixture was stirred at 0-5 °C for 45 min. and the insoluble solid was filtered. The pH of the filtrate was adjusted to \sim 8.0 by addition of conc. HCl and the mixture was stirred for 1 h at r.t. and at 5 °C overnight. The precipitated solid was filtered, washed with three 15-mL portions of water and three 15-mL portions of acetone. After drying at 60 °C under vacuum for 24 h, 6-mono-*O*-(*p*-toluenesulfonyl)- β -cyclodextrin (2) was obtained as a white solid: yield 7.92 g (35%); ¹H NMR (DMSO-*d*₆) \square 2.43 (s, 3H), 3.10-3.45 (m, 14H), 3.45-3.66 (m, 28H), 4.10-4.60 (m, 6H), 4.76 (brs, 2H), 4.83 (brs, 5H), 5.50-5.91 (m, 14H), 7.41 (d, 2H, *J* = 8.2 Hz) and 7.73 (d, 2H, *J* = 8.2 Hz); mass spectrum (MALDI), *m/z* 1310.47 [M-H+Na] (theoretical *m/z* 1310.36).

6-Monodeoxy-6-monoazido- β -cyclodextrin (3). 6-Mono-*O*-(*p*-toluenesulfonyl)- β -cyclodextrin (2) (4.0 g, 3.10 mmol) was suspended in *dd* H₂O (50 mL) and subsequently

heated to 80 °C. Sodium azide (1.0 g, 15.5 mmol, 3.0 eq.) was added and the mixture was stirred at 80 °C for 20 h. The mixture was filtered while still hot, the filtrate cooled to r.t. and added dropwise to 400 mL of acetone under vigorous stirring. The resulting precipitate was filtered and washed with two 10-mL portions of acetone. The dried solid was again dissolved in 25 mL of water with gentle heating, cooled to r.t. and dripped into 300 mL of acetone. The precipitated solid was filtered, washed with two 10-mL portions of acetone and dried under vacuum at 50 °C. 6-Monodeoxy-6-monoazido- β -cyclodextrin (3) was obtained as a white solid: yield 3.14 g (87%); $^1\text{H NMR}$ (DMSO- d_6) δ 3.40-3.21 (m, 14H), 3.49-3.82 (m, 28H), 4.40-4.57 (m, 6H), 4.76-4.90 (m, 7H), 5.85-5.57 (m, 14H); mass spectrum (MALDI), m/z 1181.83 [M-H+Na] (theoretical m/z 1181.36); FTIR (KBr) $\nu=2104\text{ cm}^{-1}$ (N_3).



Scheme S2: Synthesis of Ad-maleimide (6).

Adamantane-maleimide (6). To a solution containing adamantane methylamine (4) (38 mg, 0.23 mmol, 1.5 eq.) in anhydrous THF (1.5 mL) was added triethylamine (63 μL , 45 mg, 0.45 mmol, 3.0 eq.) followed by 4-maleimidobutyric acid *N*-succinimidyl ester (5) (46 mg, 0.15 mmol). The mixture was stirred at r.t. for 20 h. The mixture was quenched by addition of satd. aq. NaHCO_3 (5 mL) and extracted with EtOAc (2 x 5 mL). The organic

layer was washed with 0.5 N HCl (5 mL), water (2 mL) and evaporated under diminished pressure. The residue was purified on a silica gel column (1.5 x 10 cm), eluting with 20:1 CH₂Cl₂-MeOH (visualization with iodine). The product was obtained a colorless syrup: yield 41 mg (82%); ¹H NMR (CDCl₃) □ 6.72 (s, 2H), 3.59 (t, *J* = 6.0 Hz, 2H), 2.96 (d, *J* = 6.2 Hz, 2H), 2.17 (t, *J* = 7.1 Hz, 2H), 2.01-1.91 (m, 5H), 1.76-1.57 (m, 6H) and 1.50 (d, *J* = 2.8 Hz, 6H); ¹³C NMR (CDCl₃) □ 171.9, 171.1, 169.0, 134.2, 51.1, 40.2, 37.2, 36.9, 33.9, 28.2, 25.6 and 25.1; mass spectrum (MALDI), *m/z* 358.99 [M⁺] (theoretical *m/z* 358.23)

Cucurbit[7]uril-azide. The CB[7]-N₃ molecule (as depicted in Figure S2.1B) was synthesized according to previously reported methods.¹

S4. Synthesis and characterization of small molecule-DNA conjugates.

Synthesis of Adamantane-DNA conjugates. Conjugates were synthesized by Maleimide-thiol chemistry (Figure S2.1A). Thiol-DNA was obtained by cleavage of disulfide-modified DNA (in 100 mM 1xPBS) with 50 equivalents of TCEP•HCl (Figure S2.2A). The solution was agitated at room temperature for 25 minutes and maintained at pH of 7.5; we note that TCEP•HCl is acidic and adding a large excess can dramatically reduce the pH and potentially degrade the DNA. Following reaction, the mixture was passed through a NAP-5 column to remove the excess TCEP•HCl, and the product was characterized by MALDI-TOF MS. The thiolated DNA was conjugated to adamantane by exposure to 5 equivalents of adamantane-maleimide (as a solution in DMSO) in 1xPBS (pH7.5). The reaction mixture was agitated and maintained at 37 °C overnight. After

reaction, the desired conjugate was purified through RP-HPLC and characterized by MALDI-TOF MS (Figure S2.3).

Synthesis of CB[7]-DNA and β CD-DNA conjugates. Conjugates were synthesized using strain promoted alkyne azide cycloaddition (SPAAC) chemistry (Figure S2.1B,C), similar to previous reports². Briefly, DBCO-DNA was synthesized by adding 5 molar equivalents of DBCO-sulfo-NHS ester (in DMSO) into a 1mM solution of amine modified DNA strand in 1xPBS buffer (pH 8.0). Two aliquots were added, at 6-hour intervals. Care was taken to maintain a slightly basic pH; in the event that the pH turned acidic, some 10xPBS (pH 8.0) was added. Following linker addition, the reaction was agitated and maintained overnight at 37 °C. Following incubation, the reaction mixture was passed through a NAP-5 column to remove excess linker, and purified via reverse phase HPLC (RP-HPLC). The purified products were characterized by MALDI-TOF MS (Figure S2.2B). To these DNA-DBCO conjugates (in 1xPBS, pH 8.0) was added 2 molar equivalents of CB[7]-azide or β CD-azide, as a solution in DMSO. The reaction mixture was agitated and maintained at 37 °C overnight. Following reaction, the mixture was purified using RP-HPLC and the conjugate peaks verified using MALDI-TOF MS (Figure S2.3).

S5. DNA sequences used.

All DNA strands for DBCO coupling were obtained from IDT with a 5'-C6-amine modification. All DNA strands for adamantane coupling were obtained from IDT with a

5'- C6-thiol modification. Stars below indicate complementary sequences. All sequences are written 5'→3'.

DNA1 (10 nt): GGCTGGCTGG

DNA2 (21 nt): TGAGTTCCGTCAGGTCTGCTC

DNA1* (10 nt): CCAGCCAGCC

DNA2* (21 nt): GAGCAGACCTGACGGAACTCA

S6. Experimental protocols for DNA conjugates and origami.

Competition study. Ad-DNA1 and either CB[7]-DNA1 or β CD-DNA1 were combined in an equimolar ratio, to a final of concentration 1 μ M for each conjugate (Figure 2.2B, S2.6D). To study the K_{eq} , the inhibitor small molecule 1-hydroxyadamantane (Ad-OH) was added in ratios ranging from 1 to 10 equivalents (final concentration of 1-10 μ M). All solutions were made to a final volume of 20 μ L, and annealed in a PCR machine using the annealing protocol described below. The signal attributable to the fused complex of Ad-DNA1 and CB[7]-DNA1 was plotted as a function of the concentration of Ad-OH inhibitor and fit to a 3-parameter least-squares regression model to determine IC_{50} (GraphPad Prism 8.0). Then, the ratio of concentrations for Ad-OH to Ad-DNA1 at this value were multiplied by the known affinity for Ad-OH to determine $K_{eq,rel}$ (Figure 2.2C,D).

Annealing protocol for individual conjugates. Samples were heated to 90°C for 5 min, and then cooled according to the following ramp: hold at 86°C for 5min; decrease by 1 °C/5 min to 71°C; hold at 70°C for 15min; decrease by 1 °C/15 min to 40°C; hold at 39 °C

for 10min; decrease by 1 °C/10 min to 26°C; hold at 25 °C for 30min; hold at 20°C for 15min; hold at 15 °C for 5min; hold at 10°C.

Cuboid annealing protocol. To form cuboids, samples were held at 65 °C for 15 min, followed by a gradient from 60-40 °C at a rate of 0.5 °C/hour and then quick cooling to, and storage at, 4 °C. This protocol was used for the “one pot” annealing of fibers, as well as formation of individual cuboids for the hierarchical assembly experiments in Figures 2.3, 2.4, S2.6A-C.

Nano-Box Annealing protocol. To form boxes, samples were held at 90 °C for 5 min, followed by a gradient from 86-71 °C at a rate of 1 °C/5 min, followed by a gradient from 70-40 °C at a rate of 1°C/15min, followed by another gradient from 39-20 °C at the rate of 1°C/10min, and then quickly cooled and storage at, 10 °C.

DNA origami cuboid design. The 3D cuboid “monomer” was based on the design of Walther and coworkers.³ Between 1 and 8 of the staples at the edges of the cuboid were extended with either DNA1* or DNA2* ssDNA handles (see Section S8 for complete list of staples). The staple locations were chosen to give the widest possible interaction interface between the cuboids, and are enumerated in Figure S5.

DNA origami nano-box Design. The nano-box was designed to have two halves (Figure S2.12) with dimensions: 6 duplex lengths for the sides, amounting to 12 nm height per half, and 12 duplex lengths for the bottom and the lid, amounting to a length of 24 nm. The width was calculated to be around 34 nm. ((88 bases *0.34nm) + 2nm front + 2nm back). The top and the bottom half were connected by staples having a poly thymidine linkers of

5 bases between them as well. The handle positions on both the halves were chosen such that when they closed they would symmetrically align themselves.

Origami formation. All origami solutions were made to 100 μ L volumes with 20 nM of the M13 scaffold and 10 equivalents of staples (200 nM) in 1XTAE-18.5mM MgCl₂ buffer. Staples bearing handles were also added at 10x excess. The samples were heated and slowly cooled in a PCR machine using the cuboid/box annealing protocol described above.

For the one pot assembly (Figure 2.3B), the origami solutions were made with the conjugates in 10x excess compared to the handles e.g. for 8 handles these strands were added at 80x excess (1.6 μ M) with two possible permutations: Ad-DNA1 & CB[7]-DNA2 (lane7) or Ad-DNA2 & CB[7]-DNA1/ β CD-DNA1 (lane 4 and7/ lane5) with respective complementary handles (S8).

For the control one pot assembly (Figure 2.3B, lanes 8 and 9), the origami solutions were made in the same way as above except that the respective handles were replaced with poly(T) handles (DNA1* control and DNA2* control, S8).

For alternating co-polymer assembly (Figure 2.4A), the origami solutions were made with the same conjugates on both sides of the origami, with all four possible permutations: Ad-DNA1, CB[7]-DNA1, Ad-DNA2, or CB[7]-DNA2 (corresponding to lanes 1-4 in Figure 2.4B). To avoid potential scrambling of handles, we probed two combinations of origami: (1) cuboids with Ad-DNA1 + cuboids with CB[7]-DNA2; and (2) cuboids with Ad-DNA2 + cuboids with CB[7]-DNA1 (lanes 5 and 6, respectively in Figure 2.4B). We

found that sample (2) gave a longer distribution of fibers by AGE, though sample (1) also clearly yielded fiber assemblies.

For the hierarchical assembly with purified cuboids (Figure 2.4E), the origami structures with handles (DNA1* and DNA2*, S8) were annealed first without the conjugates. The structures were purified by spin filtration as described below, the conjugates were added in two-fold excess, and the mixture was annealed from 45°C to 40°C at 0.5 °C/hr followed by rapid cooling to 4°C.

For all the different versions of the Box (Figure 2.5B), the origami structures were annealed with 10x excess of staple and handle sequences (handles (DNA2*)). For the stimulus responsive demonstration experiments, the nanostructures were incubated with 120x excess of CB[7]-DNA2 (10 x 12 handles). For the closing experiment, the box was incubated with 120x excess of Ad-Peptide-Ad. For the opening back experiment using MMP-8 protein, the protein was added in to preformed closed box nanostructures in 1200x excess (10X to the Ad-Peptide-Ad) and incubated at 37°C. In all cases except the opening back experiment, the nanostructures were formed in a one-pot assembly.

Purification of folded origami structures. The origami reaction mixtures were purified using 100 kDa molecular weight cutoff filters (Amicon). A fresh Amicon filter was first equilibrated with 1xTAE buffer with 12.5 mM Mg²⁺ at 8000 RCF for 20 minutes. Next, 0.5 mL of origami solution was added and spun at low centrifugation speeds of 1550 RCF for 20 minutes. This process was repeated 5 times with fresh buffer. All spins were carried out at room temperature in an Eppendorf centrifuge 5424.

Transmission electron microscopy (TEM) characterization. 5 μL of sample was adsorbed on a formvar stabilized carbon type-B, 400mesh copper grid (Ted Pella, part number 01814-F) that had been glow-discharged for 1 minute. The sample was stained using 5 μL of a 2 wt% aqueous uranyl formate solution containing 25 mM sodium hydroxide. The grids were left to sit idle for 5 minutes before the samples applied onto it to avoid breakage due to excess charge from the glow discharge process. Samples were incubated for 5 minutes. Grids were allowed to float on a drop of the required sample or stain before wicking excess liquid using a Whatman filter paper.

Characterization of Folded structures. Samples were run on 1.2% Agarose gels made in 1xTAE with 20 mM MgCl_2 buffer, and pre-stained with ethidium bromide. The running buffer was 1xTAE with 12.5 mM MgCl_2 . To 10 μL of the annealed sample from the PCR reaction was added 1 μL of 10x loading dye. The gels were electrophoresed for 1-1.5 hours at a constant voltage of 90 V at 4°C.

Quantification of array length distributions. TEM images were assessed to determine the frequency of different array lengths, with between 2600-6400 origami cuboids counted for each of the four experimental conditions shown. The resulting frequency distribution, on the basis of mass fraction, as well as the cumulative mass fraction were plotted with step-wise increase in length of one origami. Both curves were fit to standard lognormal function (GraphPad Prism 8.0) to determine the population mean length, with $R^2 > 0.98$ for all fits.

S7. Supplementary Figures

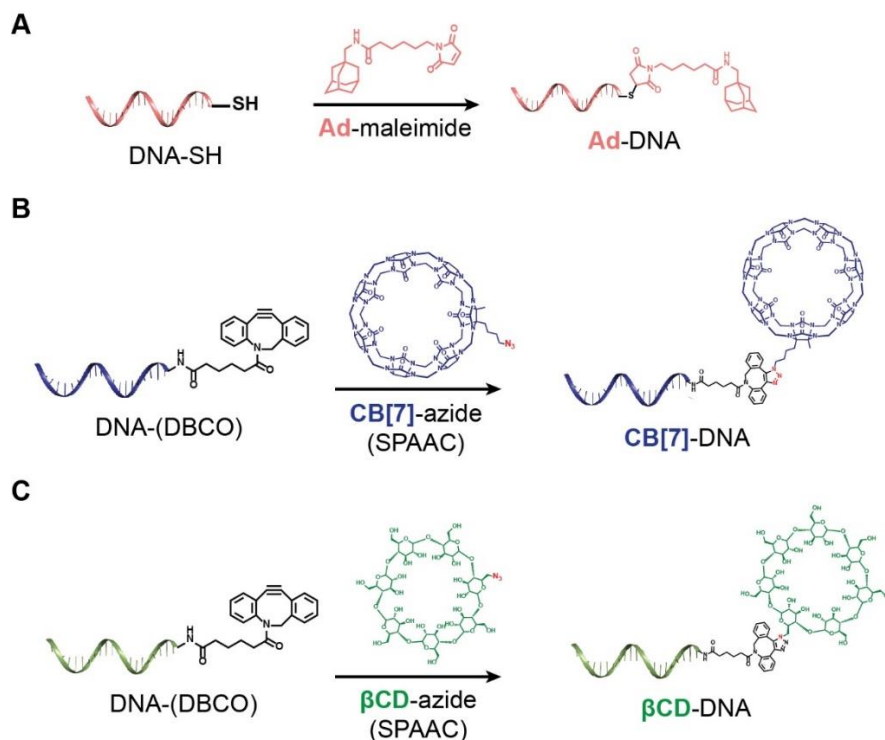


Figure S2.1: Synthesis of small molecule-DNA conjugates. A) Synthesis of Ad-DNA through the Michael addition of 5'-thiolated DNA to an Ad-maleimide linker. B,C) Synthesis of CB[7]-DNA and β CD-DNA, respectively, via strain-promoted azide-alkyne cycloaddition (SPAAC) between DNA-dibenzocyclooctyne (DBCO) and the corresponding azide.

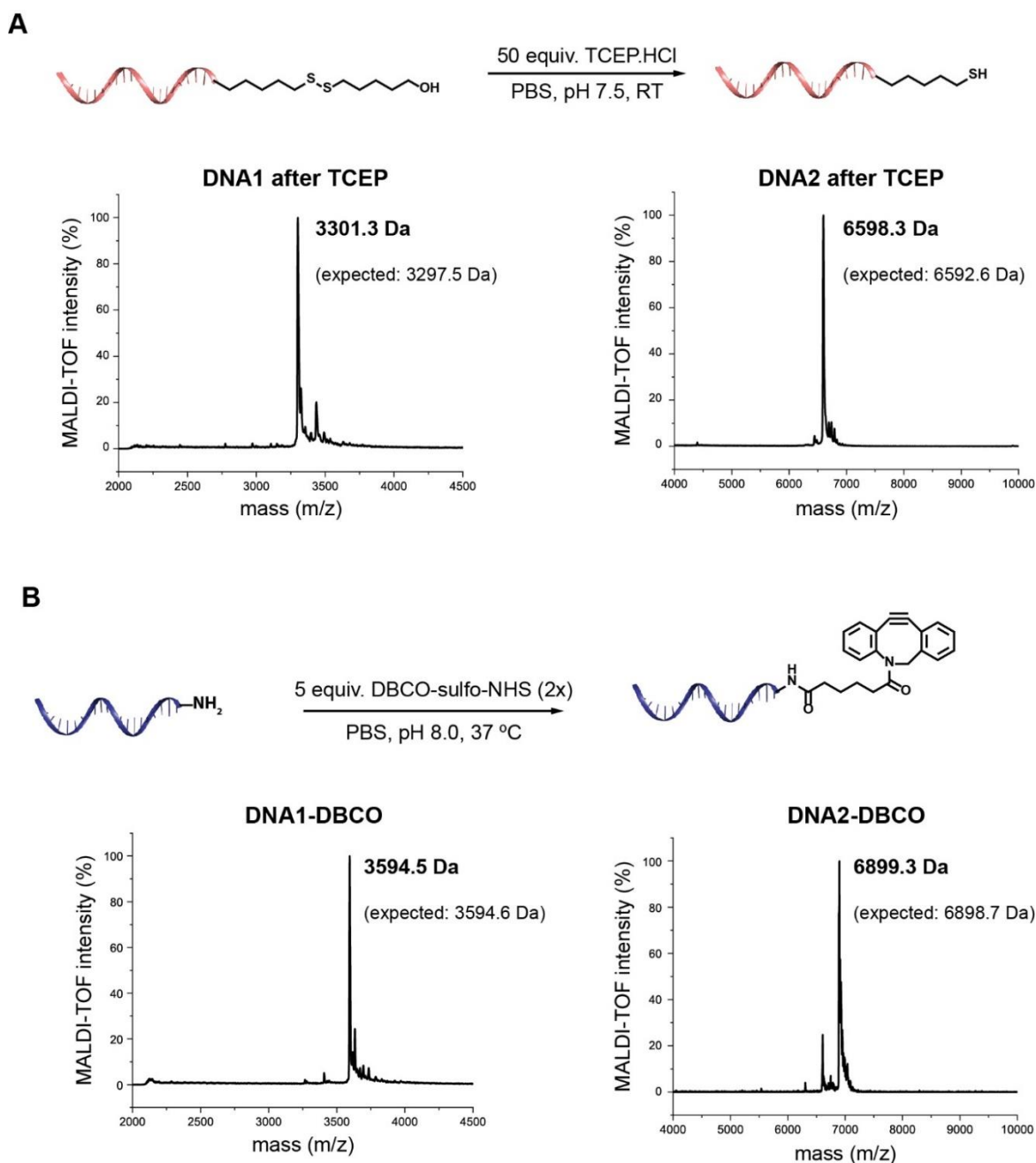


Figure S2.2: Synthesis of thiol-DNA and DNA-DBCO. A) TCEP cleavage to yield thiolated-DNA, along with MALDI-TOF MS spectra of purified DNA1-thiol and DNA2-thiol. B) Synthesis of DNA-DBCO from the corresponding DNA-amine and DBCO-sulfo-NHS, along with MALDI-TOF MS spectra of purified DNA1-DBCO and DNA2-DBCO.

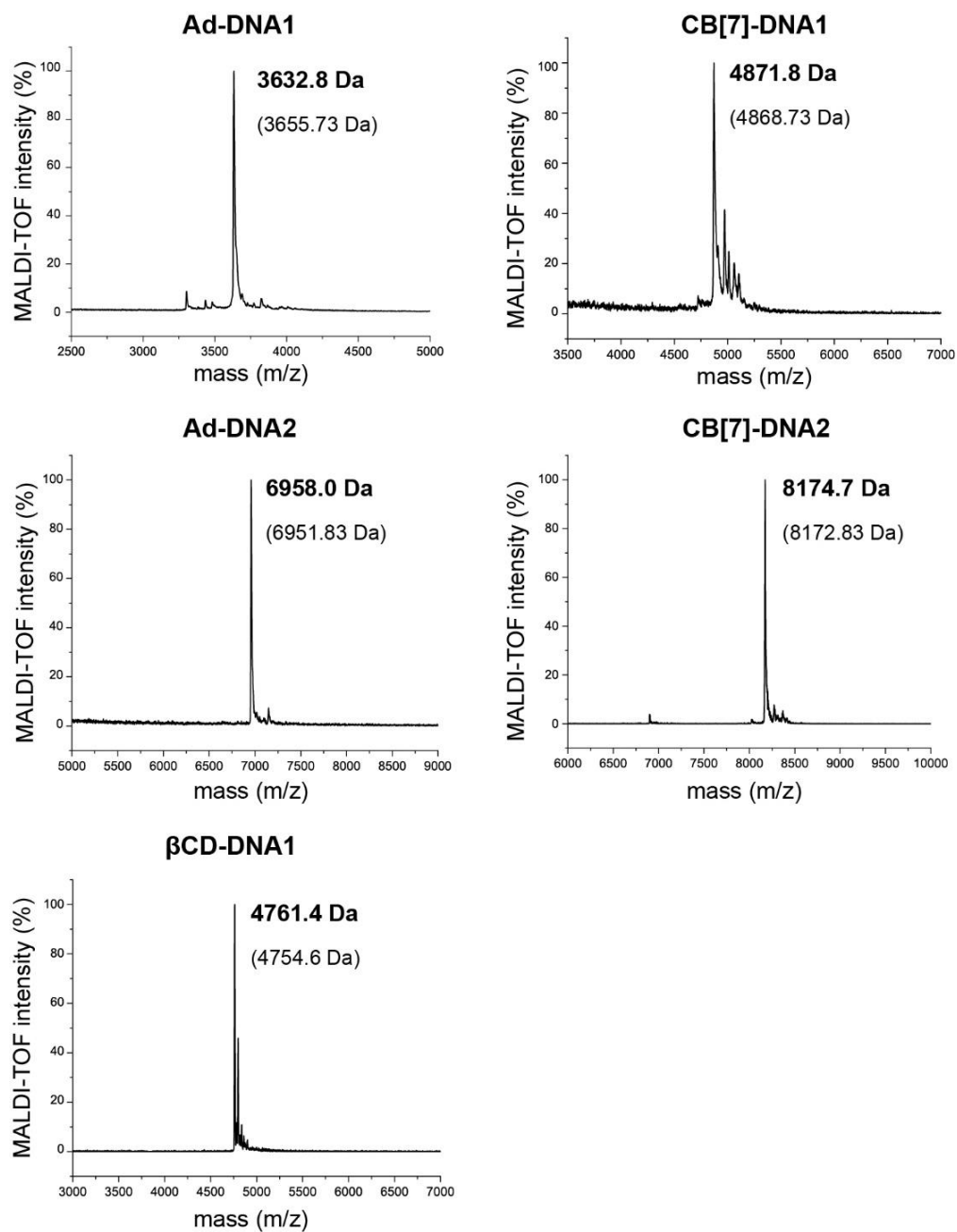


Figure S2.3: MALDI-TOF MS of indicated purified DNA conjugates.

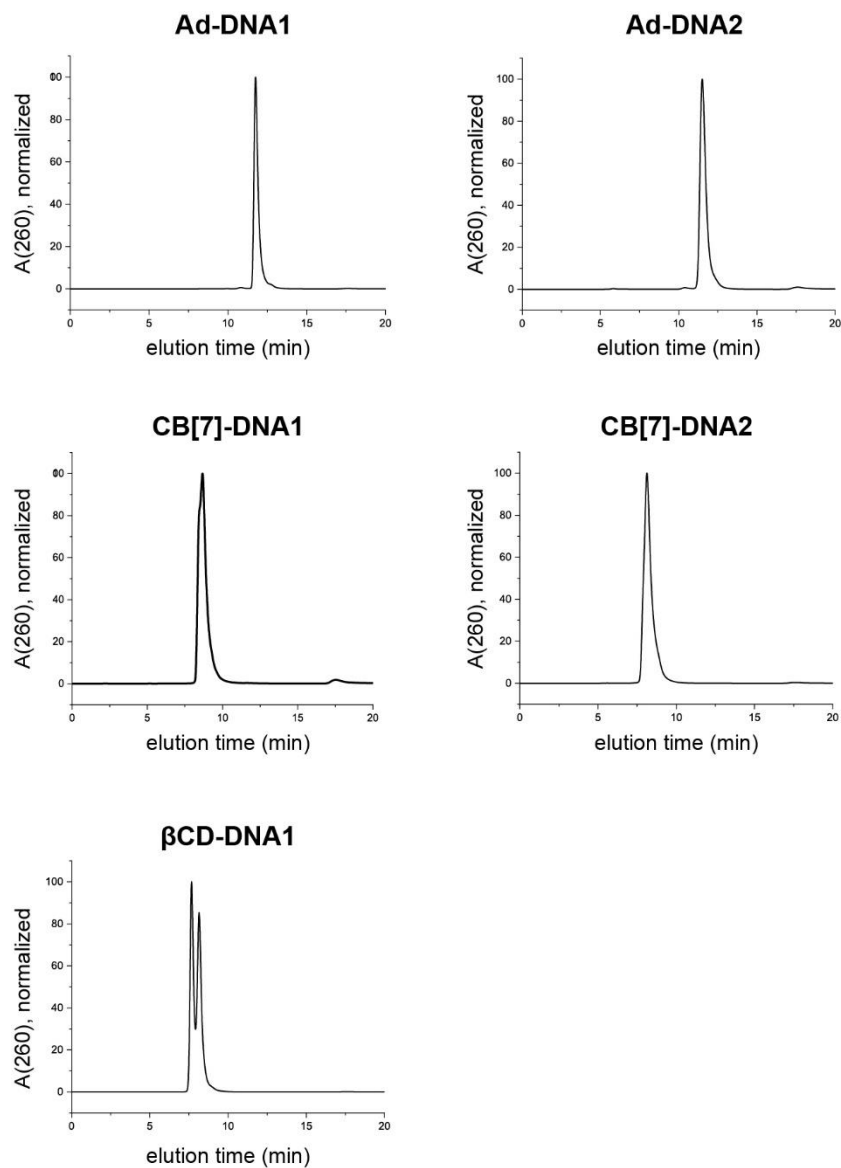
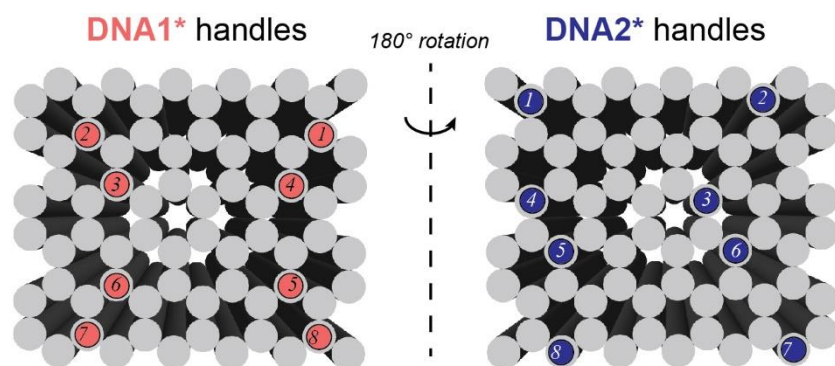


Figure S2.4: Analytical HPLC traces of indicated purified DNA conjugates. The double peak seen in the β CD-DNA conjugate is most likely due to the HPLC resolution of the two regioisomers for the triazole product of SPAAC, as both peaks have identical mass spectra.



| # Handles | Handle Locations |
|-----------|------------------------|
| 1 | 3 |
| 2 | 3, 6 |
| 3 | 3, 6, 5 |
| 4 | 3, 6, 5, 4 |
| 5 | 3, 6, 5, 4, 7 |
| 6 | 3, 6, 5, 4, 7, 1 |
| 7 | 3, 6, 5, 4, 7, 1, 2 |
| 8 | 3, 6, 5, 4, 7, 1, 2, 8 |

Figure S2.5: Location of handles on origami. For each # of handles, the locations indicate which spots on the diagram were extended with handles for Ad (pink) and CB[7] or β CD (blue) DNA conjugates.

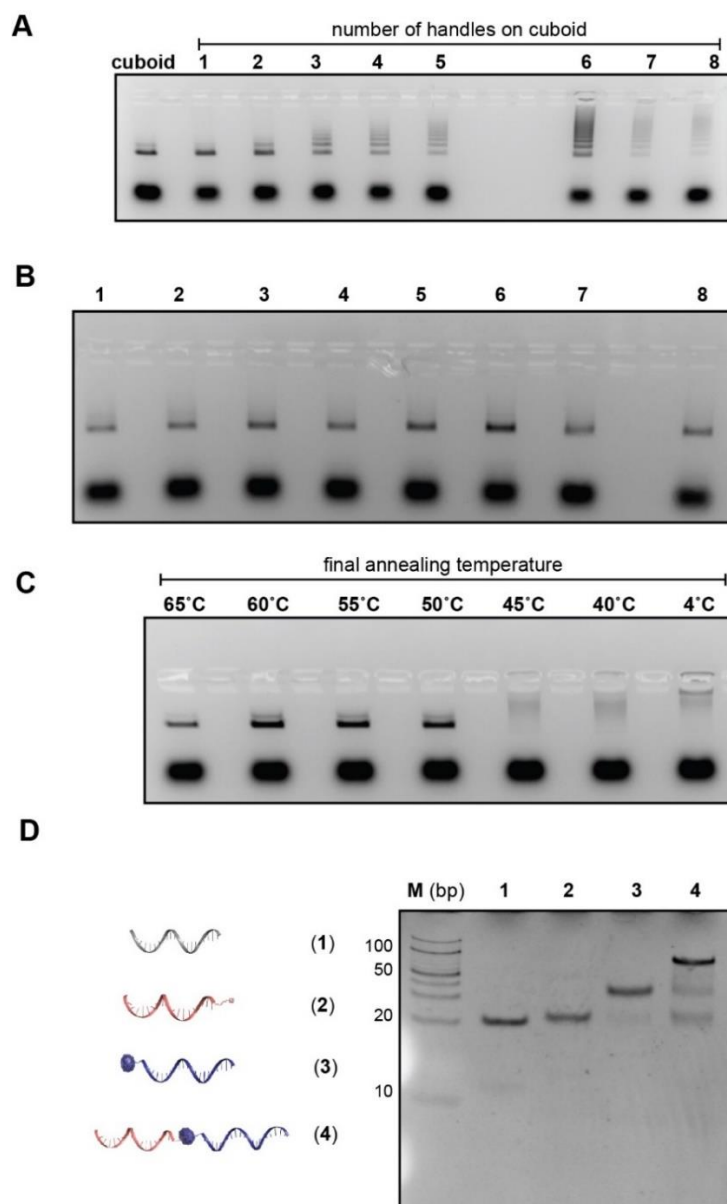


Figure S2.6: Additional gel characterization of assembly. A) AGE of cuboid one-pot assembly with indicated number of handles for CB[7]-DNA1 and Ad-DNA2 conjugates. The sample with eight handles yields the highest molecular-weight bands. B) AGE of one-pot assembly of samples with indicated number of handles, and with 50,000 equivalents of Ad-OH added as a competitor. No higher molecular weight bands are seen, demonstrating that assembly is mediated by the host-guest interaction. C) Dependence of final annealing temperature (i.e. end-point of thermal ramp) on fiber assembly. Only at 45 °C and below are assemblies seen; higher temperatures yield primarily monomers. D) Native-PAGE of host-guest assembly with DNA2 conjugates (compared with Figure 2B, which used DNA1 conjugates). Lane M: dsDNA ladder (bp); 1: DNA2; 2: Ad-DNA2; 3: CB[7]-DNA2; 8: Ad-DNA2 + CB[7]-DNA2.

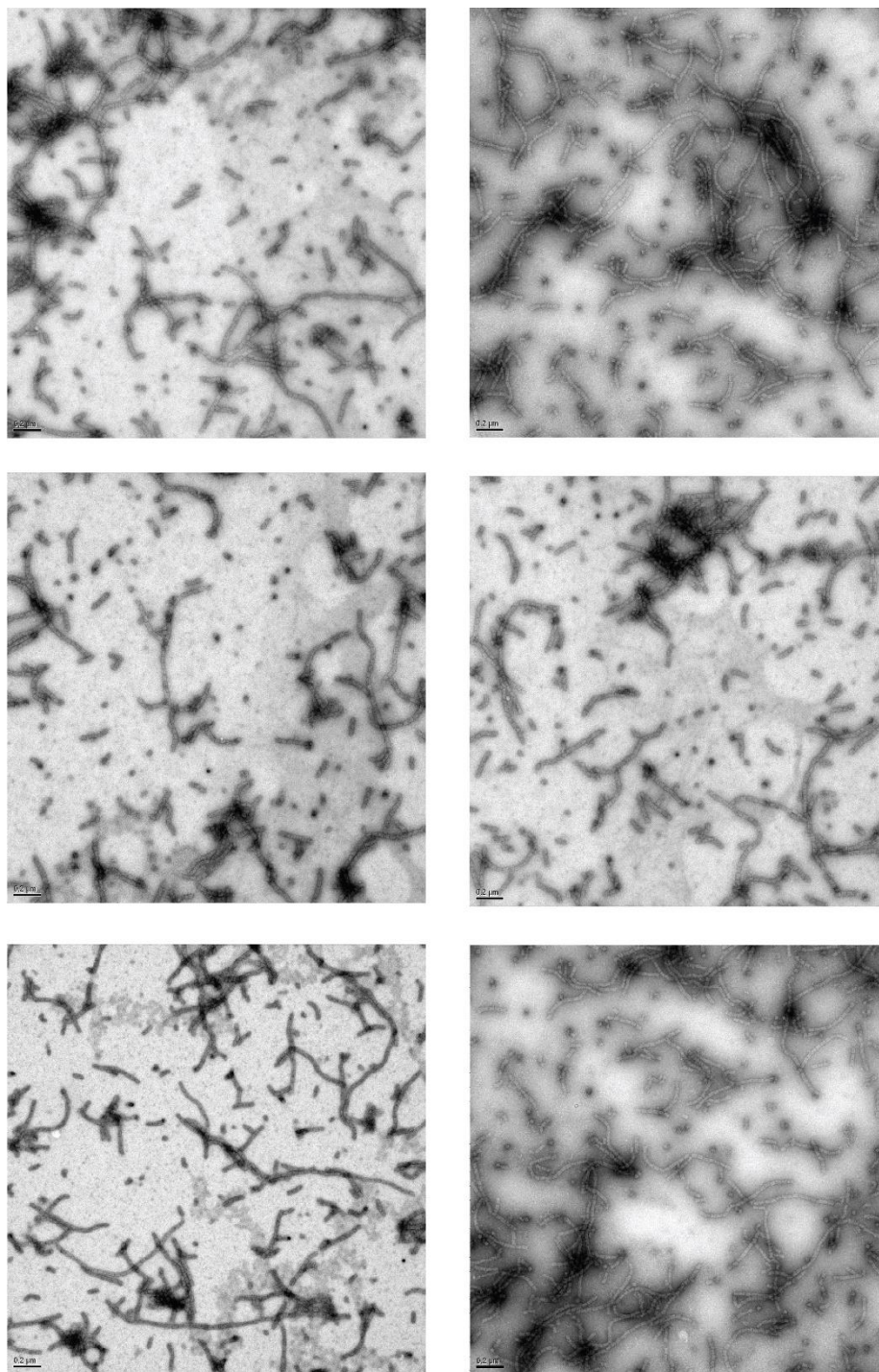


Figure S2.7: Additional TEM images of one-pot assembly of cuboids with Ad-DNA2 + CB[7]-DNA1.

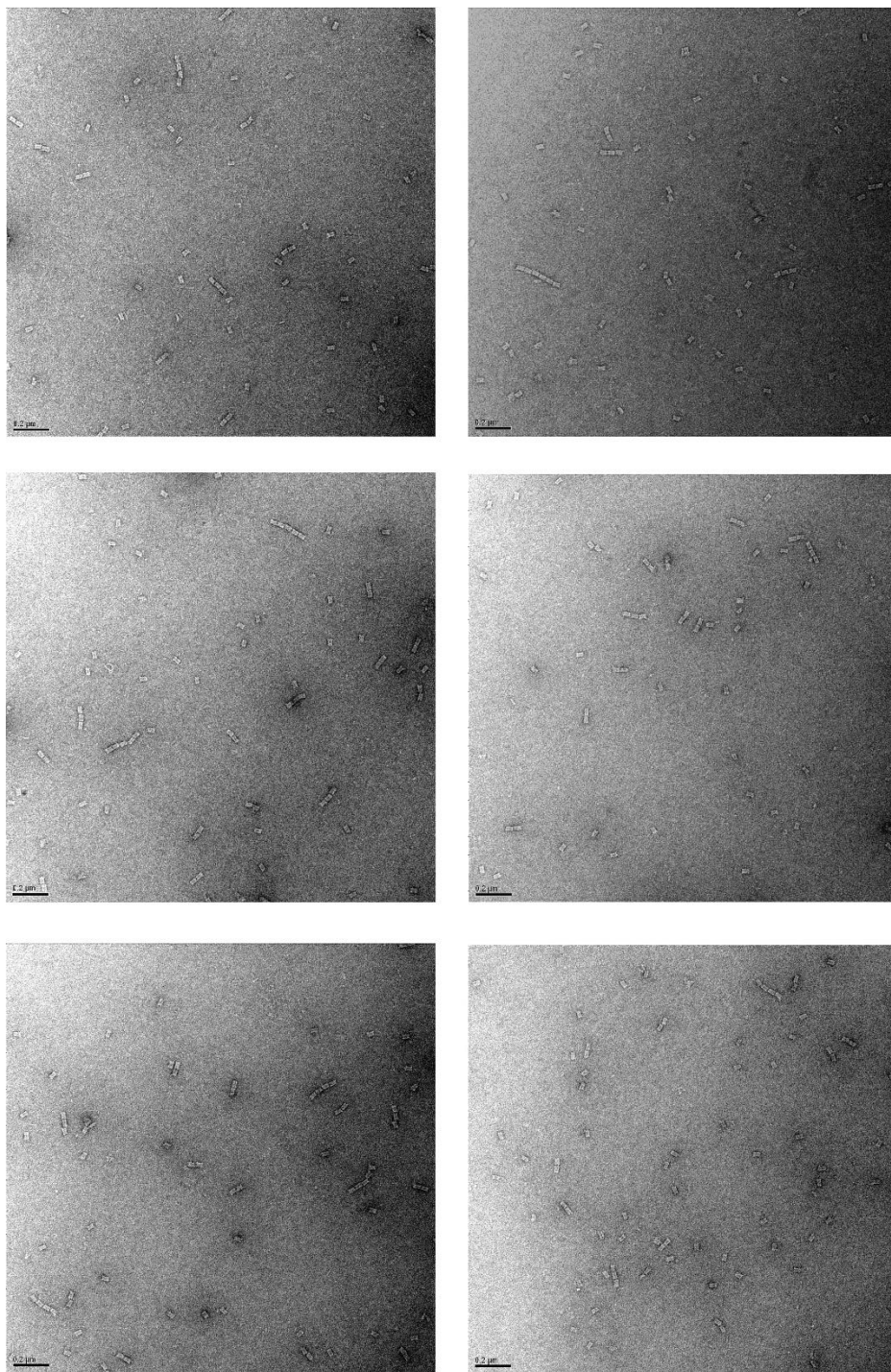


Figure S2.8: Additional TEM images of one-pot assembly of cuboids with Ad-DNA2 + β CD-DNA1.

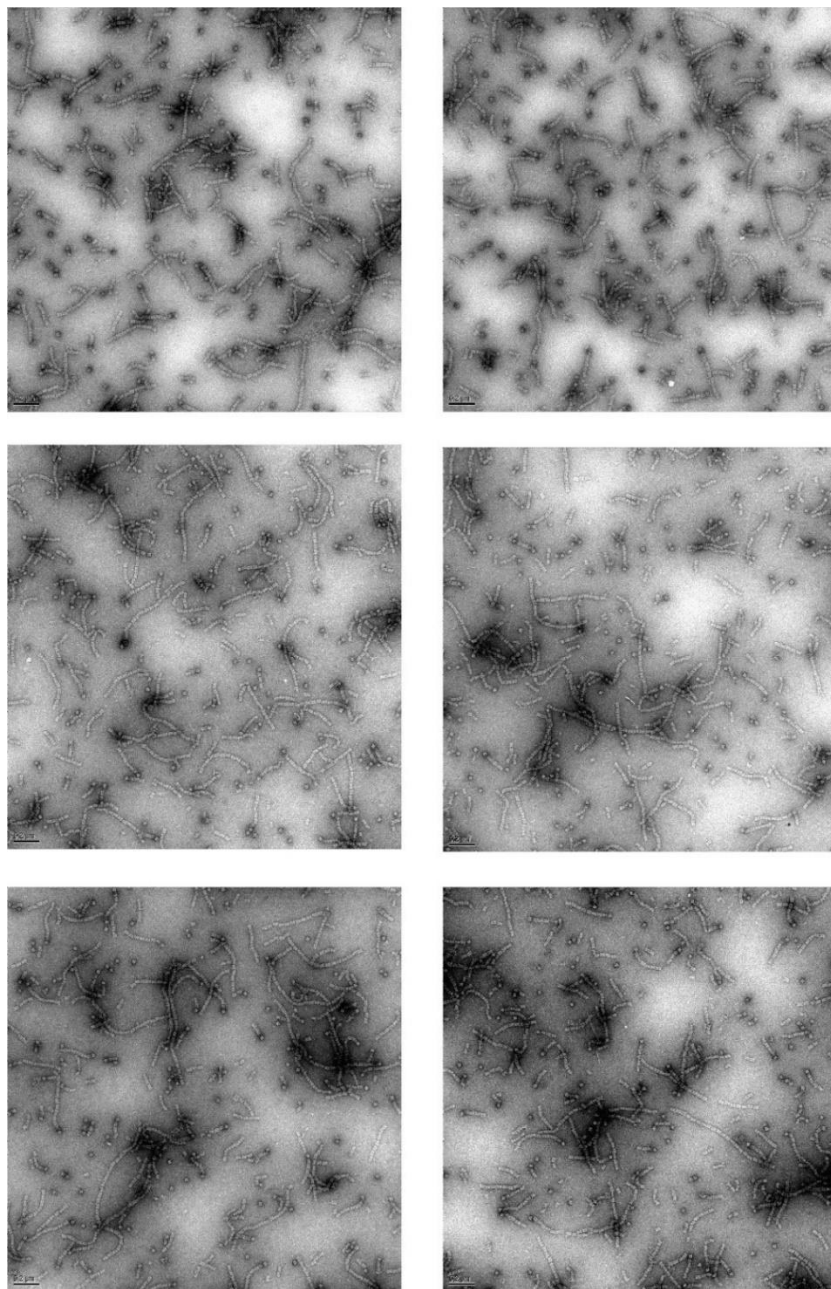


Figure S2.9: Additional TEM images of alternating copolymer assembly. This sample corresponds to assembly of cuboids modified with Ad-DNA1 on both sides with cuboids with CB[7]-DNA2 on both sides (the sample quantified in Figure 4D).

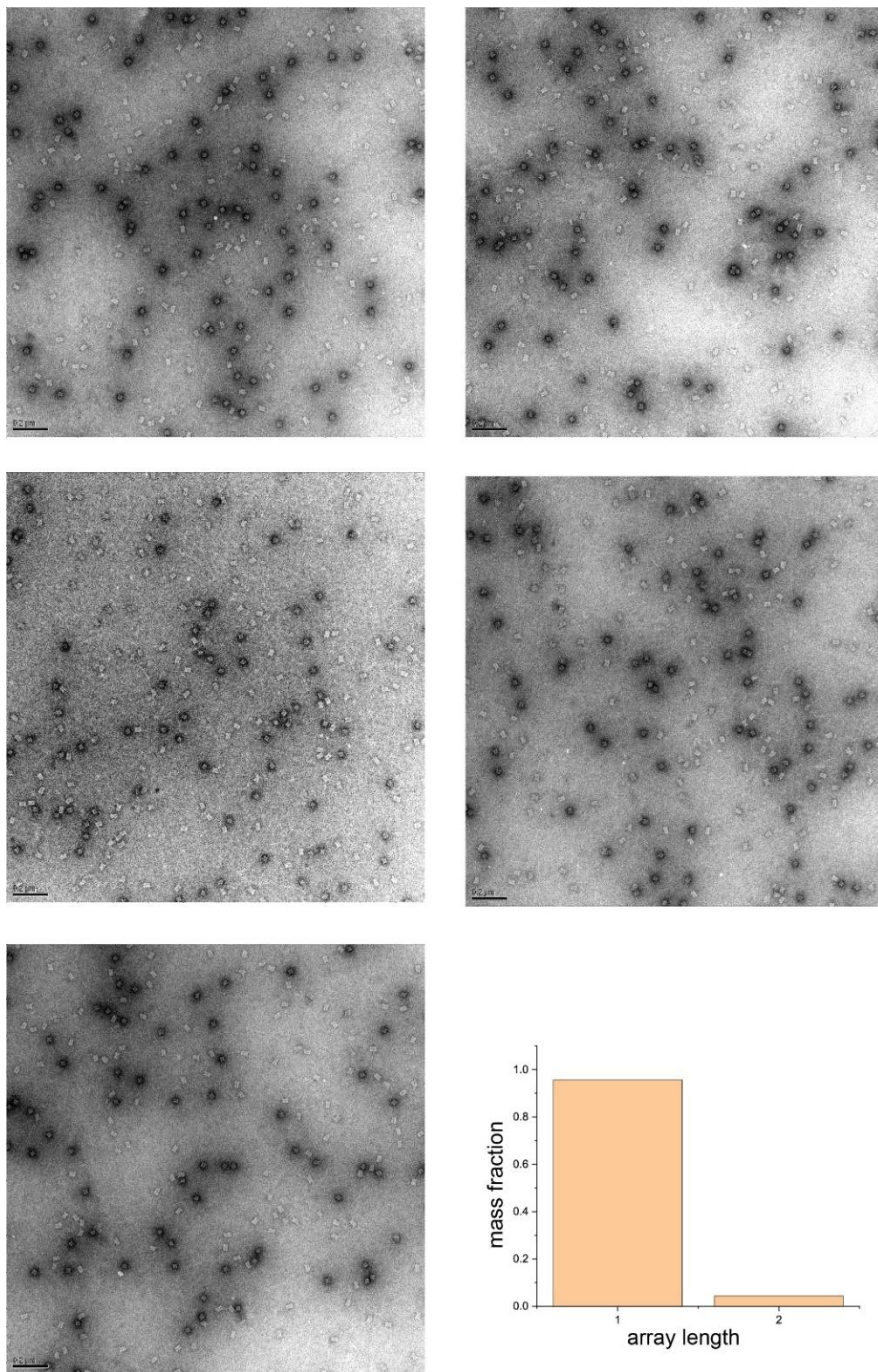


Figure S2.10: TEM images and length distribution of cuboids with CB[7]-DNA2 on both sides. No arrays are seen, confirming that the hydrophilic host alone does not drive self-assembly.

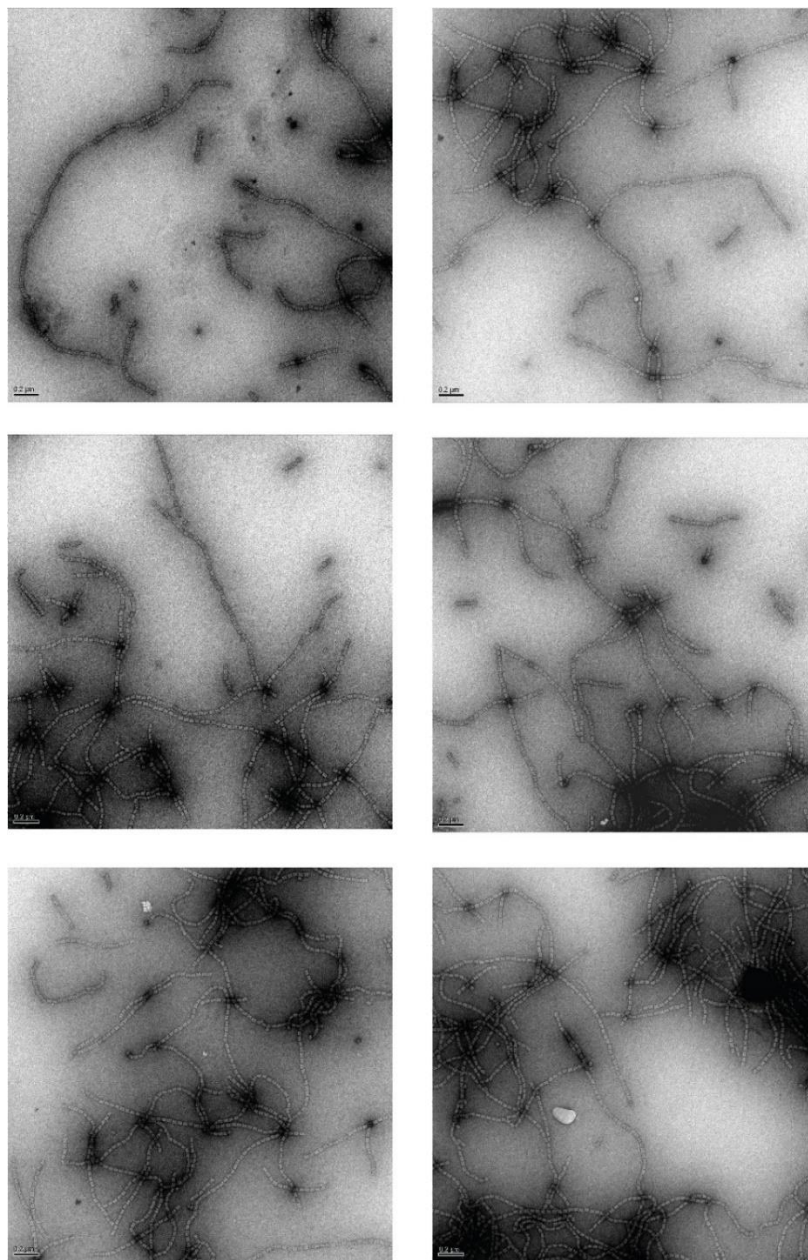


Figure S2.11: Additional TEM images of hierarchical assembly of purified cuboids with pre-formed DNA1-Ad/CB[7]-DNA2 complex. This sample corresponds to Pathway (2) in Figure 4E, and the length distribution in Figure 4H.

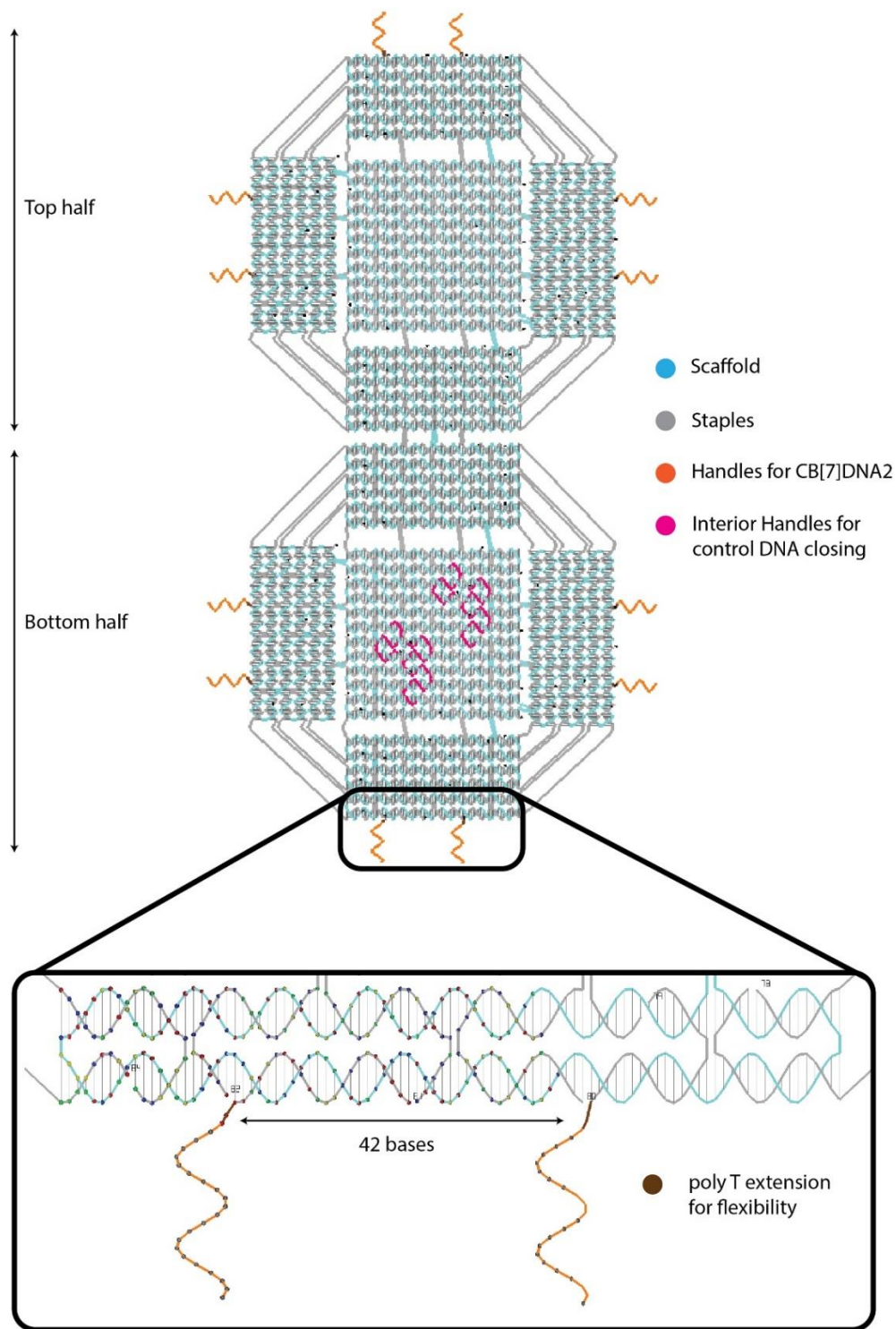


Figure S2.12: Design details of DNA nano-box.

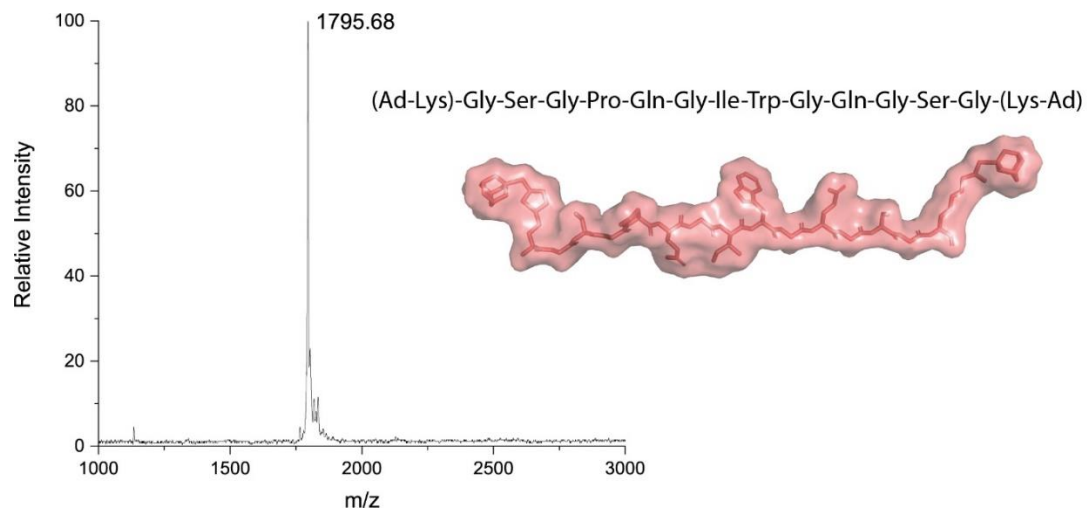


Figure S2.13: Characterization of Ad-peptide-Ad

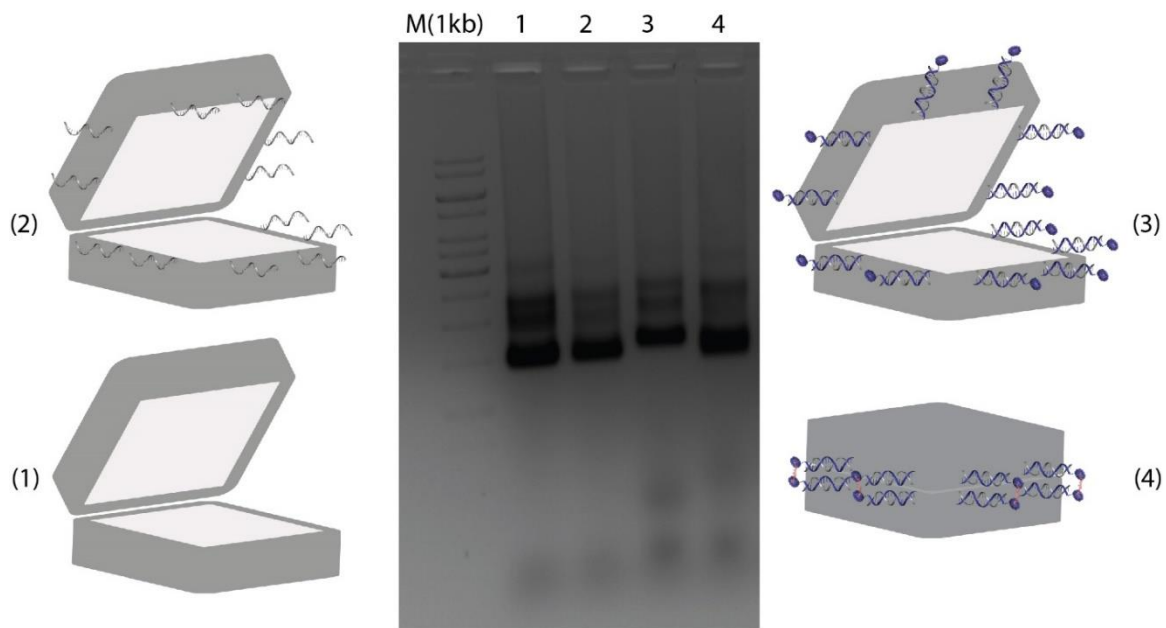


Figure S2.14: AGE of DNA nano-box. Lane M(1kb)= dsDNA ladder, Lane1: All staple nano-box, Lane2: nano-box with 12 handles, Lane3: nanobox with CB[7]-DNA2 attached, Lane4: Closed nano-box with Ad-peptide-Ad attached.

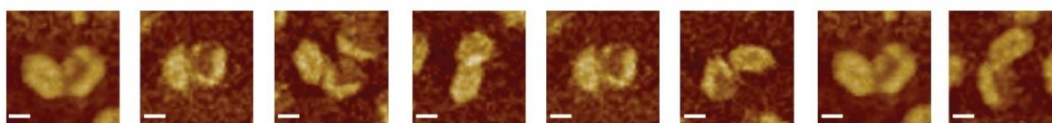
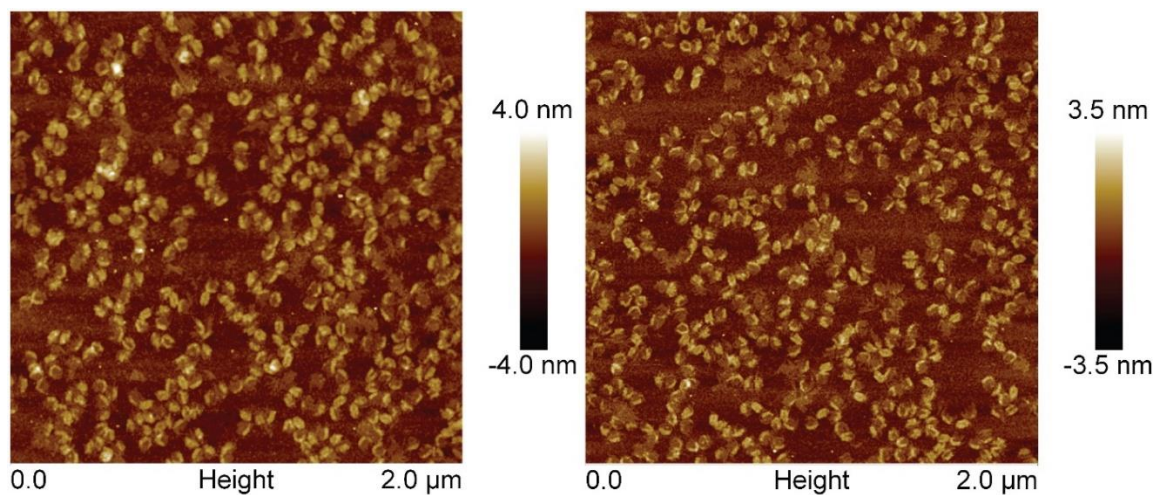


Figure S2.15: Additional AFM images of the DNA nano-box in its open state, with CB[7]-DNA2 attached to it. Insets have a scale bar of 30nm.

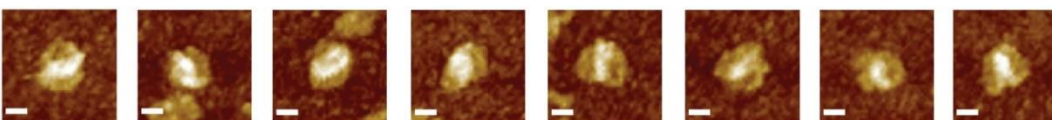
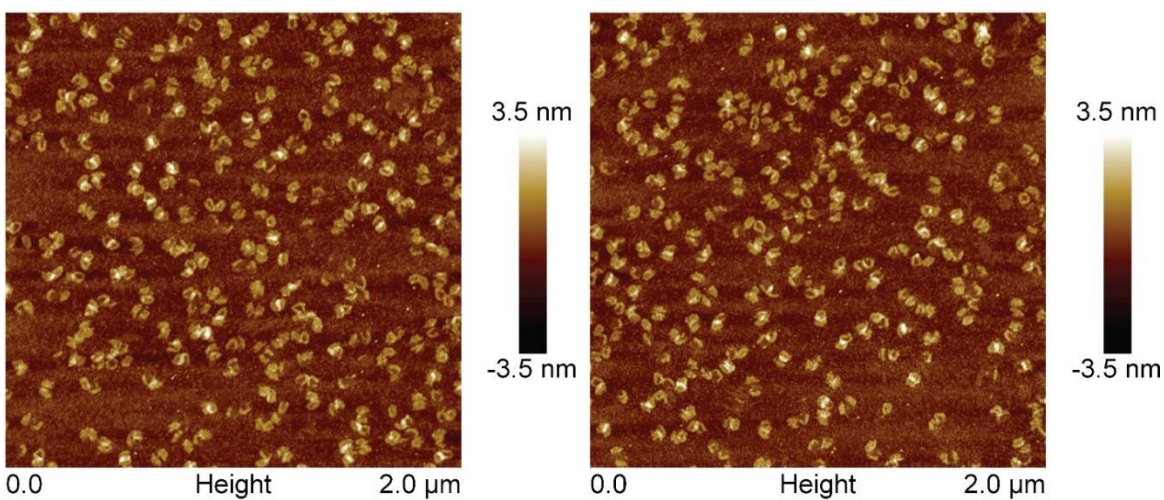


Figure S2.16: Additional AFM images of the DNA nano-box in its closed state, with CB[7]-DNA2 after the addition of Ad-aptide-Ad. Insets have a scale bar of 30nm.

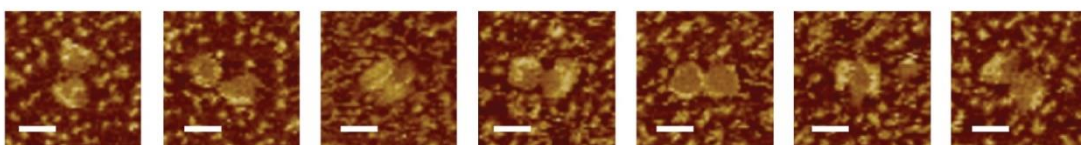
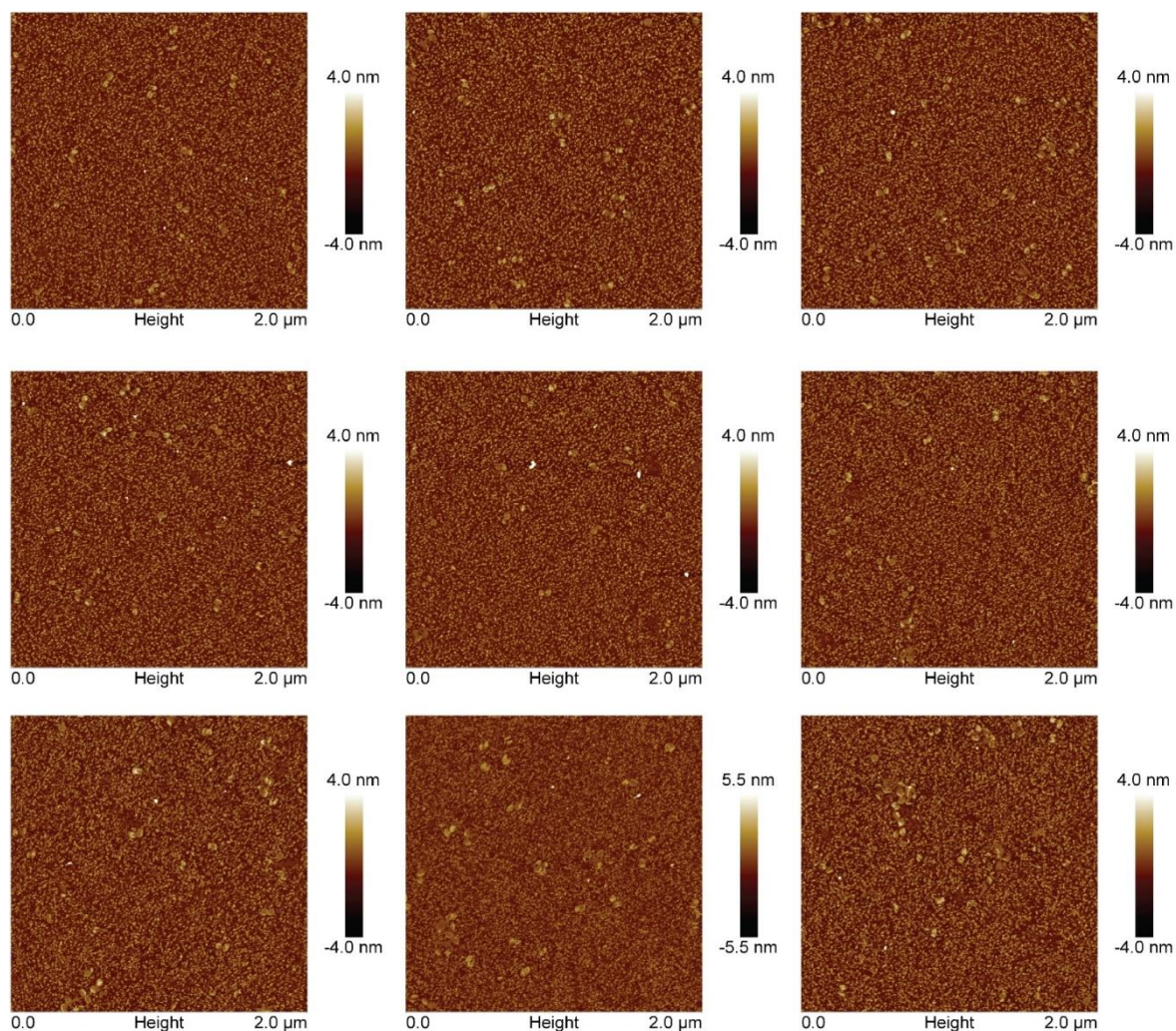


Figure S2.17: AFM images of the opened DNA nano-box after the addition of MMP8 protein to the closed nano-box using Ad-peptide-Ad. Insets have a scale bar of 50nm.

S8. Sequence of DNA Cuboid origami staples and handles.

| Core staples |
|---|
| TTA AAG ATA AAC CCT AAA AGA ACC CAG TCA CAG AT |
| ATT TAG CAA ATA AAC GGC GTA GAT GAG GGT TGT GG |
| AGA AGA ATT AGA AAA CTG AAA TAC TTT TAC ACA GA |
| CAG GCG TAA CCA ACT CCG TGG GAA CAT TTA AAG AT |
| ATC TTA TAC CAG ATT TAA AAG GTG TGT TTA TCA AC |
| TTA GCG TTT GCA AGC CTT AAG GCT TTC AGC TAA AT |
| TTT TTC ATT TTT TTA AAT GAA AAT TTT TAG ATT AA |
| TTA ATT TGC CAT CGA TAT GGG AAG GAT TAT ACC AA |
| TGT ATC GGT TTC GTC TTC GCA AAG ACA CCG GAA AT |
| TGC TCG GGA CGA CGA CAA AAC TAG AAA AGC CCA TA |
| TGA AAG TTT GAG CAT CAA ATC AAC AGT TGA AGA TT |
| TGG TGA ACA AAG AGG CAA AGA ATT AGC AAA AAC AT |
| ATT AGA GGC ATT TTC AAT ACC AGT TAC TAG ACA AT |
| AAG CAG AAC CTC AGA TGA TGA ACG CGC GGG GAC TT |
| AGT GAG GCG GAT GTG CTG CAA GAT ACC ATA TAA AT |
| CCA GAA AAA TAT GCA GAT CGA GCC AGT AAT ATT CC |
| TGG TAA TAA CCA TCA CTT GCC TGA GTA GAA GAA CT |
| CGC GAG CTG AGT TTG ACT TCC ATA AAG AAT ATA AT |
| GGT TTC AAT CAA CCA GAC CGG AAA AAG AGA GAA AG |
| TCA ATT GTT ATG GTC ATA GCT GTT TTG CCC GAA CG |
| GGC GGG GTT TAG GGT TGC TCA GAA AGG GAT ACT GA |
| TAA TCG TAA GAG TGG TTC CGA AAA GAT TCA CCT TCT GAC TTC AGG TAA G |
| ATT CAT TGA ATC CCC GTA AAG AAA TCC AGA CTA AC |
| TTA ACC GGA AAA TAA GAC GAG CGT AGT AGC GTT TC |
| AGA GCC GTC TGT GTG AAG TTG GCA CCT TGC TAA TG |
| GCG CTT TTA TTC TTT CCT TAT CAT TAT TTA CGA AT |
| ACA CCA ACG TAG TCC ACT ATT AAA CCG AGA TGG CG |
| CAT AAG ATC GAA TCG ATC AAA GGC AGC TTA ATT GC |
| AAA TCG TCA TGT AAT AGA TGA CAA CAA CCT GTA TC |
| GGG ACG CCA GTT TCC CAT CAA AAG TCA TAT AGG GG |
| TCA CAG AGC CAT CAG ATC ATC GAG CGG GTA TTA AA |
| AAA TTA TTC ATT AAC ATA CAA TCC ATC ATA ATA TA |
| GGT GAT TAG CTG AGA CTC CTC AAG GTT AAT GAC CC |
| GAA CGG AAT AGC CAC CCA AAC AGC ATC GGA ACG AG |
| AAT GCA AAA TGA ATT ATT GAG GGA TAT GGT TCT AA |
| GCA CGA GAA ACA AAT AAC ATC CCC AGA ACG AGT AG |
| CTA TTT ATC CAA GCA AAC TCC AAC AGC AAC ATA GC |
| GCT ATC AGT TAT AAA ACC ACT CAT GTA TCA TCG CC |
| ACG CTG AGA AGG CCC TTT AAA TAG CAA TAG CTA TA |
| ACA ACT TTA ATT TCT GTA GAC AGC CCT CAT ACA TG |
| AGG TCA CCA GTC GCC ACC ATA TAA GTA TAG CCG GA |

| |
|--|
| TAC TAA ATA TTG ACG ATT CAC AAT ACA TAT AAG AA |
| ACT ACC CGT CGG ATT AAA ATT CGC GTC TGG CCA GC |
| CTA CGA AGG CAC TAA AAG AAC TAA GCG ATT TTA CA |
| ATC CAA ATC CTT CCA ATA GAT AAT ACA TTT GAC GA |
| TAT GAT TAG AGA GCT TCT GAA AGC GGA TTG CTG CC |
| AAG AAT GAA TGG TGG CAC AAT AGA TAA TAT CCA GG |
| GAG CTA TGT AAA TAT ATT GCG CAT TGA GAG AAT AA |
| CTT CTG ACC TAA CGG ATG TAG ATT CTG AAA GGC GC |
| GAT CTA AAG TTC ACC CTC TCG TTT TAG TAA GAG GT |
| AAA ATA CCA CAA GAT TCG TAG CTC GTC TGG ACT AG |
| TCA AAA CGT TAT AGT CAG AAG CAG AAA CAG TTC AG |
| CGC AAA TTC AGG GAA GGC GTA ACA GCA AGC CCA AT |
| GTT ATT CCA CAT GGG ATC CAA AAA AAA GGC TCC AA |
| AAG TAG TAC CGG TGT ATC ACC GTA CCC CAG CAA AA |
| ACG GTA ACA GAG AGC CAC CAC CAT TGG CTC ATA CG |
| GTT TTT TTC AAA TGC TGA CCG AGG ATT AAG AAA AG |
| TTT AAC TAA CAA CTA ATA AGG AAT TAA TGA AAG TA |
| GTG CCT AAT GCA CAC AAG CCT TTA TTA ATT CGT AA |
| ATT AAA TTC TAT CAC CAT GAT TCC CAA TTA TGA GC |
| ACT AAA AAG AAC TGA TTG GCT CGG CAA AAT CCC AG |
| AAT TGG CTT AGT ATC AGG CTA TTT TTG CGC AAC GC |
| GTA GCC TCT TCT GTT GGT GCC GGA GCC AGC TCG TT |
| AGC TTG CTT TCG AGG TGG CCG ACA TAA AAT GGA AG |
| GTT TTT TAA CCT CCG GCC ATC AAG GTG CAT CAT CA |
| CTC CCT ATT AAT TTT AAT TGC GAT TAA GTT GGA GA |
| GTA AAA TAC CAA GCA ACG GGG ATC GTT ATC GCC CA |
| TTA GAA CCA ATG AAA CCA GTT ACA TAA CAG TTC AA |
| CAG TAT CCT CAT TAA AGC CCA CCA CGA ACC GCA CA |
| ACA GGA AAA ATA CAT TGC TTT GAA AAA CAA TAA AT |
| CGC ATA ACC GAA AGG CCG AAA ACC AGC CAA AAT TT |
| CCA TAT AAA CTA TCG GCC AAT TAC AAA ACA AAT TA |
| GAC GGA CGG AAT AAG TTC AAG AAT AAA GCG ATA TG |
| AAT CGG CCA GGC GGT CAA ATC TAA AGT AAC ATC GT |
| AGC ATT AGC AAA CCT CAA ATG CTT TTT AAG CCG AG |
| TAA CTC TGA ATT TAC CGT ACA GGA CCT ATT TAA GA |
| AAA GCA TTG ACC CTC AGT CAT AAT TCG GCA TAC AG |
| TGA GTT ACT TTT TCA ACA AAA ATT GGG CTT GGT AA |
| GAA CTG ATA GAC AGA GGT GGC AAT CAT CAT AAG AG |
| TAT TTG GTT TTT TTC CAG TCG GGA AAG CTA ACC AG |
| TTT ATC AAA ATC GCG TTA GAA AAG ACA AGA GCA CT |
| ACA AGT GAA TTT GCC ATC AAA AAT CAA AAT TTT GC |
| TTA GCA TAG CCC CCT TGT GCA GCA CTT ACC ATC TG |

| |
|--|
| TAG ATT CTA ATG CGG GAA TTT TGC ACG CTA AAA CG |
| CAG ACG CGC CGC ATC AAA GTA GTA ACC AGA ACA TG |
| GTT AGT TTC ACA TTA GAT AAG AAC GGT TTA AAG CC |
| AAA AGT TTT AAT AAA CAA GCG CGA AAC AAA GTA CA |
| GCA AAG GGG GTT TGC GTG TGC CAG CTG CAT TGA AC |
| AAG AAC TGC GAA CGA GTA GTC AGG CAC CCT CTG CC |
| CTG TAA AGA TGT CAC GAA TGC CTG TCA CAT TTG GG |
| TGA CAA TAA TTA ACC CAT ATT TTG CAT AAC CCA GC |
| ACG TTC GGG AGT ACC AAG TCA ATT ATC CCT TAA AG |
| TTT GCC CCA GCC GCC TGG CAA AGC GCC ATT TAC CT |
| AAA CAT AAA GTC ATG TAA CAA CAG TAA TAA ACA TG |
| AGA TAA GTC CGT ACC GAG CTC GTC ACT CTA GCC AG |
| TCT ACG GTG TAC AGA CCT TGC GCA GAC GGT CAA TC |
| AAT ACA TAC ACA GTA TGA GAA ACA ATG AAC GTG AG |
| GGT GGA GGT TGC CGG AAA CGT CGA CGA GGC AAC CA |
| CAA CTT ATC ATG AAT TAT TCA TCA AAT AAT GGT TA |
| TAT AAG GCC GGG TAA CGA GGA TCC AAA TAT CAA AC |
| CTT TAG CCG CCC CCC CTG GTG TAC TGG TAA TAG CG |
| AAT CTT AAT TCG AGT ACC GGA ATT ATT TAG GAC GG |
| GAA TTA GTT AAT TTC TGG GGT TAT ATT CAT AGG TC |
| CGC CTT ATA ATG CCA GTT TGA GGC GAT GAT GTT TA |
| CGT ACG GGG TCA GTG CCA GGC GCA TAG GCG AAT GG |
| AGC GAA AGC CGT TAG CGG TTA GTA GAG CCT TTA AT |
| CCT TAT TAC GTA CAA CAG TTT CAG CGG AGT GTG AT |
| CGG AAA CAG TAC ATA AAA TTT ACC TTT TTT ATG CA |
| GGA ACG AGG AGA GAT TTC TTT GAC CTG TAA TGC CA |
| GCT GAC CTT CAT CAA GAA GCT CAG AGC CGC CGC AT |
| AAA AAT CCT GTT TGA TGA TAC GTG AAT AAA GCA AA |
| AGG TCA GAA CAG CAC CAC GTA ATC CTT TCC ACA AG |
| AAC TTA CCG AAA GTC AAT ATT TCA TTT GAA TTC CT |
| TAA AAC GGA AAA GGA AAT GCA AAT ATT CAT TTT AC |
| AAT AAC ATG TAT CCG GTC AAG CAA GCC GCC ACA AA |
| ATT CAT CCT ACC AAG AAA ACA AGC AAG CCG TCC AA |
| AAC AGG CGA AGA ATA GCG ATC CAG AAC AAT ATT AC |
| TTT CTT ACC AAC CCA GCA CGC CAA ACC GAC AAG GA |
| TTG AGA ATA CAC CAA CCA AGT TTC GAG GAC TGG AG |
| GAC TGA ACG CGC GAC GAC AGC ATG TAA CAA TTG GA |
| GGT TCA ACG CTT TTA GGC AGT TGC TGG TTT TGC AT |
| CAG AAA CAG CTG TTT AGT ATC ATA GAA CGG TCC CG |
| TCA TCC GCT CAC AAT TCA GCT CAA TCA ATA TCT GG |
| ACC GGT GAG AGA TAT TCT CTA TGC GTT ATA CAT TT |
| GGT CTG GCG ACG CGC CAT TCA GGC TGA GAG AAA CC |

| |
|---|
| GTC TAG CAG CTT TTG TTA AAT AAG AGG GCT TCT TC |
| CTG ACC TGT CAT TGG GCT CTT TTT GAA TGG CTA TT |
| AAT GTA CGG TAA CAT GTT GCG GAT GCT CCT TTC AA |
| ACT ACC TTT GTT TTT TTA ACC AAT AGG AAC ATC AA |
| TAA ATC ATA CAG GCA TAC CGC ACT ATC TAA TTT CT |
| TAC AAT CGT AGT ATC GGA AAC AGA GCA CAG ACA AT |
| AGA GAC GAT ACT TTT GCG CTA CAG AGG CTT TCA TT |
| CCA AAC CAG GCC CTG AGC AGC TGA TTG CCC TGC CA |
| ATT CTT TAC AAG ACG GGG GGT AAT CAA TAA TGA CT |
| GGT GGA TTG AGT GAG CGT AGC CAG CTT TCA TCA TTT TTT TTT |
| ATA AGA TTA ATT ACC CTT GAC CAT AAA TCA AAA TTT TTT TTT |

PolyT edge staples

| |
|--|
| TTT TTT TTT CGA AAG ACT TTG ATA AGA TTT TTT TTT |
| TTT TTT TTT GGC TTG CAG AAA GAC TTT TTT TTT TTT |
| TTT TTT TTT TGA GAC GGG CAA AGA GTT GCA GCA TTT TTT TTT |
| TTT TTT TTT CGC TTC TGG GAA GGG CGA TTT TTT TTT |
| TTT TTT TTT GAT AGG TCA TTC CGG CAC TTT TTT TTT |
| TTT TTT TTT CCT GTA ATA CTT TTG CCC AAA AAA GCT TGC CGT T |
| TTT TTT TTT AGT CTG GAG CAA CCC CAA AAA CAG TTT TTT TTT |
| TTT TTT TTT AGC TAA ATC GGT TGC AAT GCC TGA TTT TTT TTT |
| TTT TTT TTT ATT ACA GGT AGA ATT CAA CTA ATG TTT TTT TTT |
| ATA CAG ATG ATG ACA AGA ACC GGA TAT TCT TTT TTT TT |
| TTA TAT ATT CTA GTT GCA ATT TCT TAA ACA GCT TTT TTT TTT |
| TTT TTT TTT TCG GTG CGG AAA CGA CGG TTT TTT TTT |
| TTT TTT TTT AAC CGT CTA TCA TTG ATT AGT AAT AAG TGG |
| GTC GAA CGC AAG GAT ATA GGG AGA ACA TAC GAG CCG GAA GCA TAT TTT TTT TT |
| TTT TTT TTT GCT TTT GCA AAA TTT AGA CTG GAT TTT TTT TTT |
| TTT TTT TTT ACA TTA AAT CCG TAA TGG TTT TTT TTT |
| TTT TTT TTT CAT TAA ATT TTT GTT AAA TCT TCC TGA GTA |
| TTT TTT TTT GAA TTA CCT TAT CGG AAC AAC ATT TTT TTT TTT |
| TGC GCC CTG AAT AAA GCC TCA GAG CAT AAT TTT TTT TT |
| TTT TTT TTT CCA GTG CCA CAT TAT GAC TTT TTT TTT |
| TTT TTT TTT CAA CTT TGA AAG AGG AAG GGA ACG CTC CAT TAA A |
| TTT TTT TTT CGG AGA GGG TAG TCA TTG CCT GAG TTT TTT TTT |
| TTT TTT TTT GGT CAT TTT TTT AAA TAT TTT TTT TTT |
| TTT TTT TTT AGC GTC CAA TAC TGC GGA AAC GAG AAG ACT ATT AAT |
| TTT TTT TTT AGC GGT CCA CGC AGT GTT GTT CCA TTT TTT TTT |
| TTT TTT TTT AGA GGC AAA TGT CGA AAT TTT TTT TTT |
| TTT TTT TTT CTC ACT GCC CGC TCT TTT CAC CAG TTT TTT TTT |
| TTT TTT TTT TTC ATG AGG TAA AAC GAA TTT TTT TTT |
| TTT TTT TTT CCT GTT TAG GCT GCT CAT TTT TTT TTT |

| |
|--|
| TTT TTT TTT CAG ATA CAT AAC AAA TAG CGA GAG TTT TTT TTT |
| TTT TTT TTT TCA GTG AAT AAG GCT TTA ACA AAC TAT ATT CGC A |
| TTT TTT TTT ATT ACC CAA ATC TTT AAT CAT TGT TTT TTT TTT |
| TTT TTT TTT CCA TAT TTA ACA TAC AAT TTT TTT TTT TTT |
| TTT TTT TTT AAA TGA AAA ACC GAC TTG AGC TTT TTT TTT |
| GCG TTT GCG GAG CAG CAG AGG AAG GTT ATC TAA AAT TTT TTT TTT |
| TTT TTT TTT GAA CTG GCA AGA ATA GAA AGG TTT TTT TTT |
| TTT TTT TTT ATC CTG AAT GCC TTT AGC GTC TTT TTT TTT |
| TTT TTT TTT CAC CAC CCT CAT TTT CCC GCC ACA GAG CCA CAA G |
| TTT TTT TTT GAT AAG TGC CGT CGA GTG CTC AGG TTT TCA CAA AAT CCC C |
| TTT TTT TTT ATA ATC GGC TGT TTC ATC GTA TTT TTT TTT |
| TTT TTT TTT ATC TTT AGG AGC GAA GTA TTA TTT TTT TTT |
| TTT TTT TTT CGC TCA ATC GTC ATC GCG CAG TTT TTT TTT |
| TTT TTT TTT CAA AGA ACG CGA ACT GAA CAC TTT TTT TTT |
| TTT TTT TTT GAC TTT ACA AGA AAC CAA TCA TTT TTT TTT |
| TTT TTT TTT CAA AGT TAC CAG TAC CCA AAA TTT TTT TTT |
| TTT TTT TTT TGG ATT ATA AAT TGA GAA TCG TTT TTT TTT |
| TGA CAG AGA TAC ATC GCC ATT AAA AAT ACT TTT TTT TT |
| TAA GTT AGA TTG AAT CCT GTC GCT AGG AAA TAC CTA CAT TTT GAT TTT TTT TT |
| TTT TTT TTT AGA CGA TTG GCC AAG CGT CAT TTT TTT TTT |
| TAT TCG CTC ATT TAA TTA TCA ATA TAT GTG AGT GAA TAA CCT TGT TTT TTT TT |
| TTT TTT TTT CTA CAA CGC CTG TAG CTC GTC ACA ACC GAT CAC C |
| TTT TTT TTT GAA ACA TGA AAG TAT TCG GAA CCA CCG CCT CAG GAG GAC C |
| TTT TTT TTT ACA TGG CTT TTG ATG ATT CCA GTT TGA TAT TCA C |
| TTT TTT TTT CAT TTG GGA ATT CCT CAG AGC TTT TTT TTT |
| TTT TTT TTT AAC AGT ACC CGA CCG TGT GAT TTT TTT TTT |
| TTT TTT TTT AAC AAC TAA AGG AAT TGT GTA CCA GCA GTC |
| TGA TAT AAT CCA GCA GAC ACC GCC TGC AAC AGT GCC TTT TTT TTT |
| AAA TGA AAT GCG ACC AGT AAT AAA AGG GAT TTT TTT TT |
| TTT TTT TTT AGA CTG TAG CGC TAC CAG GCG TTT TTT TTT |
| TTT TTT TTT CGA ACG AAC CAC CTG ATT GTT TTT TTT TTT |
| TTT TTT TTT CAT TCT GGC CAA ATA TAC AGT TTT TTT TTT |
| TTT TTT TTT GGA ATC ATT TTG AGG CAG GTC TTT TTT TTT |
| TTT TTT TTT AGC GAT AGC CAG ATA GCC GAA TTT TTT TTT |
| TTT TTT TTT AAA TAA GGC GTT TAA CGT CAA TTT TTT TTT |
| TTT TTT TTT ATT CTG TCC AGA AGG CGT TTT TTT TTT TTT |
| TTT TTT TTT AGG GCG ACA TTC CAG TAC AAA TTT TTT TTT |
| TTT TTT TTT TTC ACG TTG AAA ATC TTT CGA AT |

| handle location | DNA1* handles-right side |
|-----------------|--|
| 1 | TTT TTT TTT CTT CTG TAA ATC TGA AAA CAT TTT TTT TTT CCAGCCAGCC |
| 2 | TTT TTT TTT ACG CTG AGA GCC AAC AAA GAA TTT TTT TTT CCAGCCAGCC |
| 3 | ACC ACC AGA AAA GGT AAA GTA TTT TTT TTT CCAGCCAGCC |
| 4 | AGG CGA ATT CCA ATC GCA AGA TTT TTT TTT CCAGCCAGCC |
| 5 | TTT TTT TTT CCT GAA CAA GCC AAA GAC AAA TTT TTT TTT CCAGCCAGCC |
| 6 | TTT TTT TTT AGC GAA CCT ACC GGA ACC AGA TTT TTT TTT CCAGCCAGCC |
| 7 | GCC ACC ACC GGA TAT TAT TCT TTT TTT TTT CCAGCCAGCC |
| 8 | AAT AAT TTT TTT TTT TTT CCAGCCAGCC |

| | DNA1* handles-left side |
|---|--|
| 1 | GTT TGG AAC AAG CAA AGG GCG AAA TTT TTT TTTCCAGCCAGCC |
| 2 | AAG TGT AAA GCC AAT TGC GTT GCG TTT TTT TTT CCAGCCAGCC |
| 3 | TTT TTT TTT GTA ATG TGT AGG ATA AAT TAA TGC TTT TTT TTT CCAGCCAGCC |
| 4 | TTT TTT TTT GAA GAT TGT ATA TGT TAA AAT TCG TTT TTT TTTCCAGCCAGCC |
| 5 | ATC AGG TCT GAG GAA GCC TTT TTT TTT CCAGCCAGCC |
| 6 | GCA ACT AAA GGT CAA TAA TTT TTT TTT CCAGCCAGCC |
| 7 | TTT TTT TTT CCG CGA CCT CGA ACT GAC TTT TTT TTT CCAGCCAGCC |
| 8 | TTT TTT TTT TGA TAC CGA GGT CGC TGA TTT TTT TTT CCAGCCAGCC |

| | DNA2* handles-right side |
|---|---|
| 1 | TTT TTT TTT CTT CTG TAA ATC TGA AAA CAT TTT TTT TTT GAGCAGACCTGACGGAACTCA |
| 2 | TTT TTT TTT ACG CTG AGA GCC AAC AAA GAA TTT TTT TTT GAGCAGACCTGACGGAACTCA |
| 3 | ACC ACC AGA AAA GGT AAA GTA TTT TTT TTT GAGCAGACCTGACGGAACTCA |
| 4 | AGG CGA ATT CCA ATC GCA AGA TTT TTT TTT GAGCAGACCTGACGGAACTCA |
| 5 | TTT TTT TTT CCT GAA CAA GCC AAA GAC AAA TTT TTT TTT GAGCAGACCTGACGGAACTCA |
| 6 | TTT TTT TTT AGC GAA CCT ACC GGA ACC AGA TTT TTT TTT GAGCAGACCTGACGGAACTCA |
| 7 | GCC ACC ACC GGA TAT TAT TCT TTT TTT TTT GAGCAGACCTGACGGAACTCA |
| 8 | AAT AAT TTT TTT TTT TTT GAGCAGACCTGACGGAACTCA |

| | DNA2* handles-left side |
|---|---|
| 1 | GTT TGG AAC AAG CAA AGG GCG AAA TTT TTT TTTGAGCAGACCTGACGGAACTCA |
| 2 | AAG TGT AAA GCC AAT TGC GTT GCG TTT TTT TTT GAGCAGACCTGACGGAACTCA |
| 3 | TTT TTT TTT GTA ATG TGT AGG ATA AAT TAA TGC TTT TTT TTT GAGCAGACCTGACGGAACTCA |
| 4 | TTT TTT TTT GAA GAT TGT ATA TGT TAA AAT TCG TTT TTT TTTGAGCAGACCTGACGGAACTCA |
| 5 | ATC AGG TCT GAG GAA GCC TTT TTT TTT GAGCAGACCTGACGGAACTCA |
| 6 | GCA ACT AAA GGT CAA TAA TTT TTT TTTGAGCAGACCTGACGGAACTCA |
| 7 | TTT TTT TTT CCG CGA CCT CGA ACT GAC TTT TTT TTTGAGCAGACCTGACGGAACTCA |
| 8 | TTT TTT TTT TGA TAC CGA GGT CGC TGA TTT TTT TTTGAGCAGACCTGACGGAACTCA |

| |
|--|
| DNA1*-right control sequences |
| TTT TTT TTT CCT GAA CAA GCC AAA GAC AAA TTT TTT TTT TTTTTTTTTT |
| TTT TTT TTT AGC GAA CCT ACC GGA ACC AGA TTT TTT TTT TTTTTTTTTT |
| AGG CGA ATT CCA ATC GCA AGA TTT TTT TTTTTTTTTTTTTT |
| GCC ACC ACC GGA TAT TAT TCT TTT TTT TTT TTTTTTTTTT |
| TTT TTT TTT CTT CTG TAA ATC TGA AAA CAT TTT TTT TTT TTTTTTTTTT |
| ACC ACC AGA AAA GGT AAA GTA TTT TTT TTT TTTTTTTTTT |
| TTT TTT TTT ACG CTG AGA GCC AAC AAA GAA TTT TTT TTT TTTTTTTTTT |
| AAT AAT TTT TTT TTT TTT TTTTTTTTTT |
| |
| DNA1*-left control sequences |
| TTT TTT TTT GTA ATG TGT AGG ATA AAT TAA TGC TTT TTT TTT TTTTTTTTTT |
| TTT TTT TTT CCG CGA CCT CGA ACT GAC TTT TTT TTT TTTTTTTTTT |
| TTT TTT TTT TGA TAC CGA GGT CGC TGA TTT TTT TTT TTTTTTTTTT |
| ATC AGG TCT GAG GAA GCC TTT TTT TTT TTTTTTTTTT |
| GTT TGG AAC AAG CAA AGG GCG AAA TTT TTT TTTTTTTTTTTTTT |
| TTT TTT TTT GAA GAT TGT ATA TGT TAA AAT TCG TTT TTT TTTTTTTTTTTTTT |
| AAG TGT AAA GCC AAT TGC GTT GCG TTT TTT TTT TTTTTTTTTT |
| GCA ACT AAA GGT CAA TAA TTT TTT TTT TTTTTTTTTT |
| |
| DNA2*-right control sequences |
| TTT TTT TTT CCT GAA CAA GCC AAA GAC AAA TTT TTT TTT TTTTTTTTTTTTTTTTTTTTTT |
| TTT TTT TTT AGC GAA CCT ACC GGA ACC AGA TTT TTT TTT TTTTTTTTTTTTTTTTTTTTTT |
| AGG CGA ATT CCA ATC GCA AGA TTT TTT TTT TTTTTTTTTTTTTTTTTTTTTT |
| GCC ACC ACC GGA TAT TAT TCT TTT TTT TTT TTTTTTTTTTTTTTTTTTTTTT |
| TTT TTT TTT CTT CTG TAA ATC TGA AAA CAT TTT TTT TTT TTTTTTTTTTTTTTTTTTTTTT |
| ACC ACC AGA AAA GGT AAA GTA TTT TTT TTT TTTTTTTTTTTTTTTTTTTTTT |
| TTT TTT TTT ACG CTG AGA GCC AAC AAA GAA TTT TTT TTT TTTTTTTTTTTTTTTTTTTTTT |
| AAT AAT TTT TTT TTT TTT TTTTTTTTTTTTTTTTTTTTTT |
| |
| DNA2*-left control sequences |
| TTT TTT TTT GTA ATG TGT AGG ATA AAT TAA TGC TTT TTT TTT TTTTTTTTTTTTTTTTTTTTTT |
| TTT TTT TTT CCG CGA CCT CGA ACT GAC TTT TTT TTT TTTTTTTTTTTTTTTTTTTTTT |
| TTT TTT TTT TGA TAC CGA GGT CGC TGA TTT TTT TTT TTTTTTTTTTTTTTTTTTTTTT |
| ATC AGG TCT GAG GAA GCC TTT TTT TTT TTTTTTTTTTTTTTTTTTTTTT |
| GTT TGG AAC AAG CAA AGG GCG AAA TTT TTT TTT TTTTTTTTTTTTTTTTTTTTTT |
| TTT TTT TTT GAA GAT TGT ATA TGT TAA AAT TCG TTT TTT TTT TTTTTTTTTTTTTTTTTTTTTT |
| AAG TGT AAA GCC AAT TGC GTT GCG TTT TTT TTT TTTTTTTTTTTTTTTTTTTTTT |
| GCA ACT AAA GGT CAA TAA TTT +A1:A43+A12:A43TTT TTTTTTTTTTTTTTTTTTTTTT |

S9. Sequence of DNA nano-box origami staples and handles.

| |
|--|
| TATCATTCCATTTTCCAGACGACGACAATATTTAACAAATTCATT |
| AACGCCAGAAACAACATGTTTCAGATAATCGGC |
| AAGCAAGCGCATGTAGAAACCAATCACTAATGCA |
| GAACGCGCGCTGCAAGGCGATTAAGACGTTGT |
| GGGGATGTCTGTTTATCAACAATAATCCTA |
| TGCCGAAACCAAGAAAATAATATCCCGATAAGTCCT |
| GAACAACGCTATTACGCCAGCTGCA |
| TCGGTGCGGGCCTCTTCTGTTGGGAAGGGCGA |
| GAGGCGAATTATTGGCCAGTGCCAAGCTTGGCGAAAG |
| AAGATGATGGTTTTCCAGTCACGTTGGGT |
| AAAACGACCATTTCAATTACCTGATTTACATC |
| TAAAGCCTACAGTAACAGTACCTGCAAAAG |
| AAACAAAATTAATTACGAAACAAACATCAAGATTCATAAATCAA |
| TGCCTGCAGGTCGCAAGTTACAAAATCGCTGA |
| CACACAACCAATAACGGATTGCGCCGA |
| CTATCAGGGAGATAGGGTTGAGTGTGTTGGGTACCGAGCTCGAAACTCTAGAGGATCCCC |
| CCATATCAAAATTGGGGTGCCTAATGAGTAAAGTG |
| GCCCTTCAACCAGAAGGAGCGGATA |
| GCTAACTCACATTTGGAAGGGTTAGAACCATT |
| GAAATAAAGAAATTGCATTTGCACGTAACATTCTTCTGTAA |
| AAAGTTTTAATGAAACAGTATAACGTCAGATGAATATGTAGATTTTCAGGTTT |
| GGGAGAAAATACGAGCCGGAAGCATGA |
| TTGCTTTGAATACGAAATTGTTATCCGCTCTGCCCGC |
| TAGCTGTTTCCTGTGTTTCGTAATCATGGTCATTGTTCCAGTT |
| CTGAATAAAATTGCGTTGCGCTCACACAATTC |
| TTTCCAGTATCCTGATTGTTTGGAGCAATTC |
| CTTTTACCTGATTATCAGATGATGTTATACTT |
| TCCATGCAAAATCCCTTATAAATTTCCAGCTGCATTAATGACGGGAAACCTGTGCTG |
| GAAAAGAGGAAGGTTATCTAAAACCTCGTATTAAA |
| AGCAAGCGACAAACAATTCGACAATATCTTTAGG |
| TCCTCCGCTGGCCCTGAGGCTGATT |
| AATTTTAAAAGTTTGATTGCCCGA |
| ACGTTATTTTTACAGTTGAAAGGAATTGTCAGTT |
| TAAGACGCTGTGAGTGAATAACCTTGTGCGGAACAAGAAACCGTAACATTATCATTTT |
| ATCATCATATTCCAGTGAGACGGGCAACAAGAGTTGC |
| ATCAATATATATTGGGCGCCAGGGTCCC |
| AGCAGGCGAAAATATACATTTGAGGATTTGAGCCGTCAA |
| GGAGAGGCGGTTTGCATCGGCCAACGCGCGGTTCAAAGAAT |
| CTTTGTCCACGCTGGTTTGCGGTTTTT |
| ATCCAGAATAACAATAATAGATTAAGAAGTATTAGA |
| CITCTTTGATTAGTAACCTGTTTGATGGTGGT |
| CATCTTCTGATTTAAGAACGCGAGGCGTTGCTTAT |
| TCTCCGTGTAGCGAACCTCCCGATTTTTTGTCTA |
| ATTTGCCACTTAAATCAAGATTAGTTTTTCTTGCGG |
| GAGGTTTTGAGCGAGTAACAACCCTTGACCGT |

| |
|---|
| TTAAATGTTTTGTAAATCAGCTC TTTT GTAAAA |
| ATTTATCCTAAACGTTAATATTTT TTTT ATTTTTA |
| ACCAATAGTCCTGTAGCCAGCTTTGATGGGCG |
| AATCGGAACCCCTTAATTCGCGTCTGGCCTGAACGC |
| CATCAAAAATTTTAAAGGGAGCCCCGACACTA |
| CTCCAGCCAGGTCACGTTGGTGTACATCAACA |
| TCATTACCGGAACAAACGGCGGAGTCGGAT |
| CCGGTATTCTTTTCTAAATTTAATGGTTAATTT |
| AATGGGATCGTTTTATTTTCATCTCGAGAAC |
| TGTCCAAGTACCGCACTCAGTAGGAA |
| AGGGCTTAATTTAAATCAGATATAGAAGGCGCCCA |
| ATAGCAAGCTTTTGGAGAATCGCCATATCAACAGT |
| CATCGTAAAGTATCGGCCTCAGGATTCTGG |
| ATTTACGAAGCTTCCGGCACCGCAGATCGCA |
| TTTTTTGGGGTTTTTGAGGGGACGACGCCCGTGC |
| ATCTGCCAGTTTTTCGAGGTGCCGTAAAGATCAAG |
| CAAAAGGTAATTTAGAACGGGTATTTAACTTTCT |
| GTCCACTATTTTTCGCCATTCAGGCTGCGCAGGCA |
| AAGCGCCATTTTTAAAGAACGTGGACTCCACAAGA |
| AATTAACCGTTTTCTGAGTAGAAGAACTCATATAA |
| CATCACTTGCTTTTGTAGCAACGAAATCGCACGCA |
| TAGAAACTATCGGCCTTGTTATTTA |
| CTTGCTGAACGCTCATGGAAATACCATTGCAACAG |
| GGCAAATCATTTTTCCCTTAGAATCCTTCGCTATTAATTAATT |
| AGCACAAATATTACCGCCAGCCTACATTT |
| GCCAGCAGAATCGTCTGAAATGGACTGGTAAT |
| TGACGCTCCAAATGAAAAATCTAACACCAGCAGAAGATAACAATA |
| CATTGGCACCTGCAACAGTGCCATCAGTAT |
| AAAGGGATTTTGACCAGTAATAAAAGGGATTCA |
| CCAGTCACACTTTTTTAGACAGGAACGGTGGCCGATT |
| GCTAGGGCGCTTTGAGATAGAACCCTTCTGACAT |
| TCTGGCCAACATTTTGGCAAGGTAGCGGTGCGGGC |
| GAATACGTGGCACAGAAACAGAGGTGAGGCGGCGCTGAGA |
| TAATGAAAATACCGAACGAACAGCATCAC |
| GTTGGGTTATTTTAAACATCGCCATTACGCGAAC |
| TGATAGCCCTTTATAACTATATGTAAAGGCTTAG |
| CTGAGAGACTTTCCTCAATCAATATCTGACCTCAAA |
| TATCAAATTTTACCTTTTAACTCCCATAGGT |
| ATGCAAATCCAATCGCAAGAC |
| AAAGAAAATAAGAATAAACACTAGTATCA |
| TCAAATATATTTTAGTTGAAATACCGACCGTGGTATAAAG |

| |
|---|
| GGAAAGCCGGCGAACGTTAATGCGCCGCTACACGTATAAC |
| TTATAATCCTCGTTAGAATCAGAGACCACACCCGCCGCGCTGGCG |
| AAAGGACACGCTGCGCGTAACCCGGGAGCT |
| TCACCCAATTGCTTTGACGAGCAGGGCGCG |
| GTGCTTTCGCGATGGCCACTACGAAAACCGT |
| TGGAAACGTCAAAGGGCGATGAACCA |
| AAACAGGAACGCCAGAATCCTGAGAAAAGAGTCTG |
| AGCCAGTGAGGCCACCGAGTAAGTGTTT |
| GGGTTGATATTTTTACAACTACAACGCCTGAGTT |
| TCGTACCAGTTTCGGAATAGGTGTATCATAATCAGTAGCGACAG |
| ACACTGTAGCATTCCACAGTTTTGTC |
| TTATACCACCGTACTCAGGAGGTTGTACCGTA |
| CATAGTTAAAGCCCAATAGGAACCCATTAGTACC |
| CCACGCATGCGTAACGATCTAAAGACAGCCCT |
| GAAACATGATTTATTTTCTGTATGGGATAGACGTT |
| AGTAAATGATTTAAGTATTAAGAGGCTGTTATTCT |
| AAGCGCAGTCTTCAACAGTTTCAGCGGATTTGCT |
| AAACAACTTTTTTCTGAATTTACCGTTCAATGGA |
| AATAGAAAGGAACAACATAAG |
| GAATTTTTCTTAAACAGCTTGACCATCGC |
| TCACGTTGAAAATCTCGTATCGGTTTATCAGCCGCTGAGG |
| GCGGAATCGTCTTTAAAGGAGCCTTAATTCAAAAA |
| AAAGGCTCCATTTATAAATATTCATTGAAATACT |
| AACGAGGGAACCGATATATTCGGTTTGCTTTC |
| CTTGCAAGGCTCAGCAGCGAAAGACGGCTTTGAG |
| AAAATGTTTATTTTTCGCGGATCGTCACCGAGTTA |
| AAGGCCGCTTTTTGACTGGATAGCGTCCAAATAGT |
| TAGCTAGCAACGGCTACAGAAGCATCGG |
| CACTAAAACAGAACCGCCACCCTCTTTTCAGGGA |
| GACTAAAGTAGAGCCACCACCCTCAAGAACCGC |
| CAACACTATCTTTAGTTTCCATTAACGGGACTTT |
| TTCATGAGGATTTATAACCCTCGTTTACCTAAGAG |
| TACGAAGGCACCAACCAATACGTAATGCCAC |
| CACCCTCATAAAACGAAAGAGGCATGTGTGCA |
| AATCACCATCATCGCCTGATAAATAAAGAATA |
| GCCACCCTCACTCATCTTTGACCCACAACGGA |
| GCCGAAAAGCGCGAAACAAAGTCCAGCGA |
| GATTTGTAGTAGCACCATTACCATGACGGAAA |
| AATCCGCGCCATTTGGGAATTAGACCGTCA |
| GCGAGAGGACATAACGCCAAAAGGAATTTAGCCGGAACGAGGCACCTGCTCCATGTTAC |
| AAGGGAACCGAAGTACGAGACGGTCAATCTTTTTACGAGGC |
| CCGACTTGAGCCAACTTTGAAAGAGGGTAACAAA |

| |
|---|
| TATGCGTTTGAGAAGAGTCAATAGGCTTAGAT |
| ATCGGAAAACATAGCGATATGAATTT |
| CCAACGCTTTAACACGCCAACATATAAGAGAATAT |
| TATACATTTTCGAGCCAGTAGTAATTTA |
| AGTAATTC AATTACCTTACCGA |
| GCAAAGACCATTACCCAAATCAACACAGATGA |
| ACGGTGTATAAAGGTGAATTATCAGCCAGCAA |
| TTATTCATCAGACCAGGCGCATAGACAAGAAC |
| CACAATCATCAAGAGTAATCTTGGCTGGCT |
| GACCTCAGGGAAGGTAAATATTTAGCAAG |
| CGGATATTACCACGGAATAAGTTTGACTCCTT |
| GCTGCTCAAAGGTGGCAACATATAAGAAAA |
| TAAAGTATTTAGGAATACCACATTTTTGCCCTGACGAGAACTTCAGTGAATAAGGCT |
| TTAATTGGCTTAGAGCTTAATTGAATATGCAAC |
| AATTGGGCTTGAGATGACCAGAACGAGTAGTATTC AACTAATG |
| TACATACATAGTTTAATTTCAACTTTACGGAACA |
| TAGCTATCTTAATAAAACGAACTAAATCATTG |
| TGAATTACGTATGTTAGCAAACGTAAGAAAC |
| ATTACGCACTTATGCGATTTTAAGGGAAGAAA |
| AAGCACCAGTCAGGACGTTGAACTGGC |
| GCGAGCAGAGGGTAATTGAGCGCTAAGAAAAGT |
| TCATTATAAACTGGCATGATTAATTTTTGT |
| AATCTACGTTACCGAAGCCCTTTTAAATATCA |
| ACATTATTGAGCAAGAAACAATGATTAAGCC |
| TAACAGTTGATTCCCAACAGGTAGAAAGATTG |
| GCGAACGATTTTCATTCCACAGTTGAGACGGTG |
| TCTGGAAGTTTTGTAGATTTAGTTTGACTAAATCT |
| CAGATAGCTCAACATGTTTTACTGAATAT |
| ATAGAGACGACGATAAAAATTTGCCA |
| CAAACCTCCTTTTGAAAAGAAGTCCAAAATA |
| CTCAAATGCTTTAAACAGTTC |
| AGAAAAAGACTTCAAATATCGACCGGAAG |
| ATCAAAAATCAGGTCTGATTGCATCAAAAAGAAGTACC |
| AGATTGTATAATTTAGTCAGAAGCAAAGCGTTACCC |
| TGACTATTATTTGCAAATATTTAAATTGCAGGA |
| AATGCTGTAACAGGTCAGGATTAGTTAAGAGG |
| GTTGATAATCTTTGTCATTTTTGCGGATGCTCCTTTT |
| GATAAGAGTTTAGAAAAGCCCAAAAACCCCG |
| CAATAACATTAGATACATTTTCATGTCAA |
| TTGTTTAAGTAGCATTAACTAGCGCAAATGG |
| TCAATAACTAACCACAAGAATTGAGAATAGCAA |
| GAGAGACTGTTTAGCTATATTTAATTCTAC |
| TTACAGAGCTGAAAAGGTGGCATCTCATTTGGGGC |
| TAATAGTACGTCAAAAATGAAAATAGAGCCTA |
| TCATATGTCAATCCAAAATAAGAACCATATT |

| |
|--|
| TTGCGATTGTTACAAAATAAACAGACGATTTT |
| TTTTGCACCCTAACGAGCGTCTTTCCAGCAGCCT |
| GAGCCGCCGTTTTGAATCTTACCAACGCAGCTACA |
| ATTTTATCCTTTCCAGCATTGACAGGAGACCACCA |
| CACCCTCAGTTTAGGGAAGCGCATTAGAAGAATAAC |
| ATAAAAACTTTAGCCGCCACCAGAACCAGGCCAC |
| AACAAAGTTTTACACCCTGAACAAAGTCGGGAGA |
| ATTAAGTATTTAATCAAATCACCGGTTTGCCATCTTTCA |
| TACCAGAAGGAAACCGGATAGCCG |
| CCTCCCTCCGGCATTTCGGTCATAGTTACGGAATACCCAAAAGAGGAAACGCAATAATA |
| GTTTACCAGCGCCAAAATAGAAAATTCATATGTTCCCCCTTAT |
| GCCGGCCTTTAGCGTCAGACTGTTTCAACCGATTGAGGGAGACAAAAGGGCGACAT |
| GGAACCTAAGACTCCTCAAGAGAAAGCGGATAAGT |
| ATCGATAGCAGCACCGCGTCACCAATGAAACCTTTAGCGCGTTT |
| AAGTATAGTCAAGTTTTCGAGA |
| TCATGGTTTTGCTCAGTACCGGATTAGG |
| TAGCAACCAGAGCCACCACGAACCGC |
| CGTATAAAAGAGCCGCCACCCTCACGGAACCG |
| CACCCTCATCAGTGCCTTGAGTATAAGTTT |
| ACGATTGGCCTTGATAAGGAGTGTACTGGTAAACAGTGCC |
| ATTAGCGGCAGTTAATGCCCCCTGTGGCTTTTGATGATACTTCA |
| AGCCAGCAGTAAGCGTCATACACCTATTTT |
| Stapes without handle extensions |
| TAACACCGGACCTGAAAGCGTAA |
| TTTTTGAATGGCTATTAGTCTT |
| ATCAAATTAGAAAAGCCTGTTGGAATCATAATTACTGCTG |
| GGCAGAGGATACAAATCTTACCATGATAAATAAGGCGTTACGCGAGAAAACTTTT |
| AGAAAGGAAGGGAAGAAAGCG |
| GCTTTTCCCGACAATGACAACAATACCGATAGTTGCGGTGAG |
| GAGGTGAAGCGAATAATAATTTTT |
| TACTATGGTTTAGAGCTTGACGG |
| GAGGGGGTTTTCAAAGCGAACCGGTTTTAATTCGAGCTCCCC |
| AAGCCCGAACGAGAATGACCATAA |
| TAACGGGGGTTGAGGCAGGTGAG |
| AAACAAATAATCCTCATTAA |
| Stapes with handle extensions (handles) |
| TAACACCGGACCTGAAAGCGTAA TT GAGCAGACCTGACGGAACTCA |
| TTTTTGAATGGCTATTAGTCTT TT GAGCAGACCTGACGGAACTCA |
| ATCAAATTAGAAAAGCCTGTTGGAATCATAATTACTGCTG TT GAGCAGACCTGACGGAACTCA |
| GGCAGAGGATACAAATCTTACCATGATAAATAAGGCGTTACGCGAGAAAACTTTT TT GAGCAGACCTGACGGAACTCA |
| TACTATGGTTTAGAGCTTGACGG TT GAGCAGACCTGACGGAACTCA |
| AGAAAGGAAGGGAAGAAAGCG TT GAGCAGACCTGACGGAACTCA |
| GCTTTTCCCGACAATGACAACAATACCGATAGTTGCGGTGAGTT GAGCAGACCTGACGGAACTCA |
| GAGGTGAAGCGAATAATAATTTTT TT GAGCAGACCTGACGGAACTCA |
| GAGGGGGTTTTCAAAGCGAACCGGTTTTAATTCGAGCTCCCC TT GAGCAGACCTGACGGAACTCA |
| AAGCCCGAACGAGAATGACCATAA TT GAGCAGACCTGACGGAACTCA |
| TAACGGGGGTTGAGGCAGGTGAG TT GAGCAGACCTGACGGAACTCA |
| AAACAAATAATCCTCATTAA TT GAGCAGACCTGACGGAACTCA |

S10. References

1. Vinciguerra, B.; Cao, L.; Cannon, J. R.; Zavalij, P. Y.; Fenselau, C.; Isaacs, L., Synthesis and Self-Assembly Processes of Monofunctionalized Cucurbit[7]uril. *Journal of the American Chemical Society* **2012**, *134* (31), 13133-13140.
2. Buchberger, A.; Simmons, C. R.; Fahmi, N. E.; Freeman, R.; Stephanopoulos, N., Hierarchical Assembly of Nucleic Acid/Coiled-Coil Peptide Nanostructures. *Journal of the American Chemical Society* **2020**, *142* (3), 1406-1416.
3. Tigges, T.; Heuser, T.; Tiwari, R.; Walther, A., 3D DNA Origami Cuboids as Monodisperse Patchy Nanoparticles for Switchable Hierarchical Self-Assembly. *Nano Letters* **2016**, *16* (12), 7870-7874.

APPENDIX B

SUPPLEMENTAL MATERIAL FOR CHAPTER 3

Characterization of Protein-DNA hybrid nanostructures through experiment and simulation

Raghu Pradeep Narayanan^{‡, α, β} Jonah Procyk^{‡, α, β} Yang Xu,^β Erik Poppleton,^β Purbasha Nandi,^{α, γ} Dewight Williams,^Δ Fei Zhang,^δ Hao Yan,^{α, β} Po- Lin Chiu*,^{α, γ} Nicholas Stephanopoulos*,^{α, β} Petr Šulc*,^{β, Ψ}

(*plchiu@asu.edu, nstephal@asu.edu, psulc@asu.edu)

^α, School of Molecular Sciences, Arizona State University, Tempe, AZ-85281, USA

^β, Center for Molecular Design and Biomimetics, The Biodesign Institute, Arizona State University, Tempe, AZ-85281, USA

^γ, Center for Applied Structural Discovery, The Biodesign Institute, Arizona State University, Tempe, AZ-85281, USA

^Δ, Erying Materials Center, Office of Knowledge Enterprise Development, Arizona State University, Tempe, AZ, USA

^Δ, Department of Chemistry, Rutgers University-Newark, Newark NJ, USA

^Ψ, Center for Biocomputing, Security and Society, The Biodesign Institute, Arizona State University, Tempe, AZ-85281, USA

Supporting Information

S1. Materials and supplies

- S2. Synthesis and characterization of KDPG aldolase protein-DNA conjugate, tetrahedral origami
- S3. Experimental protocols for TEM and Cryo-TEM
- S4. Processing of Cryo-EM data
- S5. Experimental details of Fluorophore Assay
- S6. Anisotropic Network Model Fitting
- S7. Cryo-Fitting Data
- S8. Supplementary Figures
- S9. Sequence of DNA origami staples/handles
- S10. References

- S1. Materials and supplies.

All DNA sequences were purchased from Integrated DNA technologies (IDT). The M13 scaffold strand was amplified and purified in-house. The protein was expressed in-house.

S2. Synthesis and characterization of KDPG aldolase protein-DNA building block, tetrahedral origami, 4 turn tetrahedron.

Synthesis of KDPG aldolase protein-DNA building block (PDNA-bb). The protein was expressed, purified and conjugated as before¹.

Origami formation. All origami solutions were made to 100 μ L volumes with 20 nM of the M13 scaffold and 10 equivalents of staples (200 nM) in 1XTAE-18.5mM MgCl₂ buffer. Staples bearing handles were also added at 10x excess. The samples were heated

and slowly cooled in a PCR machine using the tetrahedral annealing protocol described below.

Origami Tetrahedron annealing protocol. Samples were held at 90 °C for 5 min, followed by a gradient from 86-71 °C at a rate of 1 °C/5 min, followed by a gradient from 70-40 °C at a rate of 1°C/15 min, followed by another gradient from 39-20 °C at the rate of 1°C/10 min, and then quickly cooled, and stored at, 10 °C.

Annealing protocol for PDNA-bb bound into the tetrahedral origami frame.

Samples were heated to 45°C for 15 min, and then cooled slowly by a gradient from 40-4°C for over 12 hours. Pure PDNA-bb was added in 40x excess (4 sites*10X excess) to the impure tetrahedron origami structures, following which the sample was gel purified as described below.

Characterization of Tetrahedral origami structures. Samples were run on 1.2% Agarose gels made in 1xTAE with 20 mM MgCl₂ buffer, and pre-stained with ethidium bromide. The running buffer was 1xTAE with 12.5 mM MgCl₂. To 10 µL of the annealed sample from the PCR reaction was added 1 µL of 10x loading dye. The gels were electrophoresed for 1.5 hours at a constant voltage of 90 V at 4 °C.

Purification of tetrahedron origami structures. 20 nM, 200µL samples were run on a pre-stained 1.2% Agarose gel as before for 1.5-2 hours. Following which the band of choice was excised and put into a freeze and squeeze tube and kept in -80 °C for 1 hour, then centrifuged in the cold room at low centrifuge speeds of 1600 rcf for 40 min and characterized by TEM for intactness.

S3. Experimental protocols for TEM, Cryo-TEM and AFM

Transmission electron microscopy (TEM) characterization. 5 μL of sample was adsorbed on a formvar stabilized carbon type-B, 400 mesh copper grid (Ted Pella, part number 01814-F) that had been glow-discharged for 1 minute. The sample was stained using 5 μL of a 2 wt% aqueous uranyl formate solution containing 25 mM sodium hydroxide. The grids were left to sit idle for 5 minutes before the samples applied onto it to avoid breakage due to excess charge from the glow discharge process. Samples were incubated for 5 minutes. Grids were allowed to float on a drop of the required sample or stain before wicking excess liquid using a Whatman filter paper.

Plunging conditions for Cryo-TEM. 5 μL of sample was absorbed on the carbon side of the ultrathin carbon film on lacey carbon support film, 400 mesh copper grid (Ted Pella, part number 08124) that had been glow discharged for 1 minute. The grids were left to sit idle for 5 minutes before the samples applied onto it to avoid breakage due to excess charge from the glow discharge process. Samples were incubated for 5 minutes. Thereafter, the grids were plunged using an in-house manual plunger after 5-6 seconds into liquid ethane and immediately transferred to grid boxes in liquid nitrogen. The grids were stored in these boxes until they were imaged using the microscope.

S4. Processing of Cryo-EM data

Data acquisition. All cryo-EM data collections were completed in the Eyring Materials Center (EMC) at Arizona State University (ASU). The grid specimen was imaged using a Thermo Fisher/FEI Titan Krios transmission electron microscope (TEM) (Thermo Fisher/FEI, Hillsborough, OR) at an accelerating voltage of 300 keV. The electron scattering was recorded by a Gatan Summit K2 direct electron detector (DED) camera in

super-resolution mode (Gatan, Pleasanton, CA). For the tetrahedron dataset, the nominal magnification was set to 30,487x, corresponding to a physical pixel size of 1.64 Å/pixel at the specimen level. The defocus was varied from -0.8 to -2.5 µm. The camera counted rate was calibrated to 3.24 e⁻/pixel/second. The exposure time was 8 seconds, accumulating to a total dosage of 46.1 e⁻/Å². The procedure of low-dose imaging was automated using SerialEM software (version 3.8)² with customized macros.

For the PDNA-bb-bound tetrahedron dataset, the nominal magnification was set to 37,879X, corresponding to a physical pixel size of 1.32 Å/pixel at the specimen level. The defocus was varied from -0.8 to -2.5 µm. The camera counted rate was calibrated to 4.33 e⁻/pixel/second. The exposure time was 8 seconds, accumulating to a total dosage of 39.5 e⁻/Å².

Image processing

Image processing was generally conducted using the Relion software (version 3.1-beta)³⁻⁴. For the tetrahedron dataset, 3,448 cryo-EM movies were unpacked and gain normalized using IMOD software package (version 4.9)⁵. The specimen movements between frames were registered and averaged using MotionCor2 (version 1.2.1)⁶, and the CTF (contrast transfer function) parameters of the frame average were estimated using CTFFIND4 (version 4.1.13)⁷. The frame averages were imported into Relion for subsequent processing. 25,949 particles were manually selected from the micrographs using a Gaussian blob with a diameter of 802 Å. Iterative reference-free two-dimensional (2D) classification was performed using Relion to remove false positives and incomplete views. 20,714 selected particle images were used to generate a three-dimensional (3D)

initial model using Relion^{3-4, 8}. The cryo-EM density was then refined against the experimental particle images by imposing a tetrahedral symmetry. The final resolution was determined as 26.1 Å using a gold-standard FSC method at the cutoff of 0.143⁹.

For the PDNA-bb-bound tetrahedron, 2,619 cryo-EM movies were unpacked and gain normalized using IMOD software package⁵. The specimen movements between frames were registered and averaged using MotionCor2⁶. The CTF parameters of the frame average were estimated using CTFFIND4⁷. The frame averages were imported into Relion for subsequent processing and 10,255 particles were selected from the micrographs. Iterative reference-free 2D classification was performed to remove any false positives and incomplete views. 7,676 particle images were selected to generate a 3D initial model using Relion^{3-4, 8}. The cryo-EM density was then refined against the experimental particle images by imposing a tetrahedral symmetry. The final resolution was determined as 27.6 Å using a gold-standard FSC method at the cutoff of 0.143⁹.

S5. Experimental details of Fluorophore Assay

Sample for both the calibration curves, i.e. Cy5 labelled strand and the FAM-DNA1 KDPG aldolase protein, were prepared by making double stranded versions of each. This was first done by annealing the corresponding sample with its complementary strand in defined ratios (1X for the Cy5 strand and 3X excess for Protein-conjugate (since there are 3 DNA per protein)). These double stranded versions were then annealed and measured in a Nanolog fluorimeter (Horiba Jobin Yvon) using a quartz cuvette of 3-mm path

length having a sample volume of 60 μL at 495 nm for FAM-DNA1 (KDPG aldolase protein) and at 647 nm for the Cy5 labeled strand.

The calibration curves were fit using the equation $y = mx + c$, where in m is the slope and c is the intercept, where the emission peak values were taken at 520 nm for the FAM sample and 664 nm for the Cy5 sample.

S6. Anisotropic Network Model Fitting

KDPG Aldolase was fit with an Anisotropic Network model at a cutoff value of 13 \AA and force constant of 40.815 $\text{pN}/\text{\AA}$ at 100K. The analytical B-factors are plotted against the experimental B-factors in supplementary figure S3.6. Both high temp and low temp conditions used the same network fitting.

S7. Cryo Fitting Data

Tables 1 & 2: The below tables, report the Chimera fitting values for all 10 mean simulation models while maximizing the fit for correlation. Fitting values are broken up into large boxes by the Cryo Map (bolded text) used to perform the fitting. Within each large box, the fitting values for both the low temp and high temp mean models are reported at two different levels of the resolution shown in parentheses in each sub box.

Table 1

| | | | | | | | |
|---|-------------|---------|-----------------|---|-------------|---------|-----------------|
| Map | | | | | | | |
| run_it014_half1_class001_Td_26.9A.mrc | | | | Symmeterized NO Protein | | | |
| Low Temp Low Salt (26.9 A Resolution) | | | | Low Temp Low Salt (20.0 A Resolution) | | | |
| Models | corr | overlap | corr about mean | Models | corr | overlap | corr about mean |
| ext | 0.765 | 61.56 | 0.1763 | ext | 0.741 | 151.9 | 0.1071 |
| 1p | 0.7701 | 61.92 | 0.1766 | 1p | 0.7454 | 152.7 | 0.1042 |
| 2p | 0.7856 | 63.83 | 0.1937 | 2p | 0.7613 | 157.5 | 0.1206 |
| 3p | 0.7775 | 63.08 | 0.192 | 3p | 0.7531 | 155.8 | 0.1166 |
| 4p | 0.774 | 62.92 | 0.1847 | 4p | 0.7486 | 155.4 | 0.1847 |
| High Temp High Salt (26.9 A Resolution) | | | | High Temp High Salt (20.0 A Resolution) | | | |
| Models | corr | overlap | corr about mean | Models | corr | overlap | corr about mean |
| ext | 0.8026 | 66.71 | 0.2044 | ext | 0.7763 | 164.6 | 0.1201 |
| 1p | 0.7969 | 65.59 | 0.1959 | 1p | 0.7712 | 161.9 | 0.1205 |
| 2p | 0.816 | 68.71 | 0.2297 | 2p | 0.7895 | 170 | 0.1406 |
| 3p | 0.7793 | 66.67 | 0.194 | 3p | 0.7746 | 164.6 | 0.1146 |
| 4p | 0.7929 | 65.51 | 0.1974 | 4p | 0.768 | 161.8 | 0.1145 |
| Map | | | | | | | |
| run_it021_half1_class001_c1_29.8A.mrc | | | | Unsymmeterized NO Protein | | | |
| Low Temp Low Salt (30 A Resolution) | | | | Low Temp Low Salt (20 A Resolution) | | | |
| Models | corr | overlap | corr about mean | Models | corr | overlap | corr about mean |
| ext | 0.7373 | 46.1 | 0.1758 | ext | 0.7044 | 158.5 | 0.08397 |
| 1p | 0.7376 | 45.73 | 0.1766 | 1p | 0.7038 | 157.2 | 0.08635 |
| 2p | 0.7413 | 46.18 | 0.1799 | 2p | 0.7082 | 159.1 | 0.08943 |
| 3p | 0.7272 | 44.94 | 0.1704 | 3p | 0.6944 | 154.9 | 0.08269 |
| 4p | 0.7159 | 43.99 | 0.1506 | 4p | 0.6851 | 150.9 | 0.06637 |
| High Temp High Salt UnSym (30 A Resolution) | | | | High Temp High Salt UnSym (20 A Resolution) | | | |
| Models | corr | overlap | corr about mean | Models | corr | overlap | corr about mean |
| ext | 0.7519 | 47.24 | 0.1641 | ext | 0.7218 | 161.9 | 0.07619 |
| 1p | 0.7423 | 46.09 | 0.1573 | 1p | 0.7098 | 159 | 0.07561 |
| 2p | 0.7407 | 46.37 | 0.1575 | 2p | 0.706 | 68.71 | 0.2297 |
| 3p | 0.7351 | 46.01 | 0.1422 | 3p | 0.706 | 157.2 | 0.06651 |
| 4p | 0.7265 | 44.44 | 0.1348 | 4p | 0.7006 | 151.9 | 0.06265 |

Table 2

| | | | | | | | |
|--|--------|---------|-----------------|--|--------|---------|-----------------|
| Map | | | | | | | |
| Pro Tet run_it018_half2_class001.mrc | | | | Unsymmeterized YES Protein | | | |
| Low Temp Low Salt (30 A Resolution) | | | | Low Temp Low Salt (20 A Resolution) | | | |
| Models | corr | overlap | corr about mean | Models | corr | overlap | corr about mean |
| ext | 0.7457 | 22.88 | 0.2282 | ext | 0.7107 | 79.04 | 0.1094 |
| 1p | 0.7356 | 22.39 | 0.2079 | 1p | 0.7038 | 76.89 | 0.09572 |
| 2p | 0.7353 | 22.44 | 0.21 | 2p | 0.704 | 77.17 | 0.1023 |
| 3p | 0.7229 | 21.83 | 0.1704 | 3p | 0.6901 | 154.9 | 0.08269 |
| 4p | 0.751 | 22.97 | 0.2299 | 4p | 0.7187 | 150.9 | 0.06637 |
| High Temp High Salt (30 A Resolution) | | | | High Temp High Salt (20 A Resolution) | | | |
| Models | corr | overlap | corr about mean | Models | corr | overlap | corr about mean |
| ext | 0.7536 | 23.59 | 0.2211 | ext | 0.7216 | 81.46 | 0.1103 |
| 1p | 0.7362 | 22.86 | 0.1961 | 1p | 0.7052 | 78.7 | 0.09744 |
| 2p | 0.7629 | 24.02 | 0.2259 | 2p | 0.7307 | 82.95 | 0.1117 |
| 3p | 0.7661 | 24.09 | 0.233 | 3p | 0.7335 | 83.25 | 0.1114 |
| 4p | 0.7386 | 22.18 | 0.2 | 4p | 0.7043 | 76.6 | 0.08985 |
| Map | | | | | | | |
| run_it020_half2_class001.mrc | | | | Symmeterized YES Protein | | | |
| Low Temp Low Salt (26.9 A Resolution) | | | | Low Temp Low Salt (20 A Resolution) | | | |
| Models | corr | overlap | corr about mean | Models | corr | overlap | corr about mean |
| ext | 0.7554 | 29.69 | 0.2051 | ext | 0.7334 | 74.16 | 0.1252 |
| 1p | 0.767 | 30.41 | 0.2238 | 1p | 0.7404 | 75.36 | 0.1342 |
| 2p | 0.7956 | 31.97 | 0.2695 | 2p | 0.7684 | 79.5 | 0.1694 |
| 3p | 0.7812 | 31.23 | 0.2391 | 3p | 0.7562 | 77.46 | 0.1491 |
| 4p | 0.7876 | 31.57 | 0.2524 | 4p | 0.7601 | 78.34 | 0.152 |
| High Temp High Salt (26.9 A Resolution) | | | | High Temp High Salt (20 A Resolution) | | | |
| Models | corr | overlap | corr about mean | Models | corr | overlap | corr about mean |
| ext | 0.8168 | 33.79 | 0.2807 | ext | 0.7874 | 84.04 | 0.1688 |
| 1p | 0.8014 | 32.74 | 0.2424 | 1p | 0.7741 | 81.11 | 0.144 |
| 2p | 0.8306 | 34.72 | 0.298 | 2p | 0.8018 | 86.44 | 0.1817 |
| 3p | 0.8139 | 33.63 | 0.2571 | 3p | 0.7867 | 83.45 | 0.155 |
| 4p | 0.8054 | 32.9 | 0.2515 | 4p | 0.7784 | 81.66 | 0.1487 |

S8. Supplementary Figures

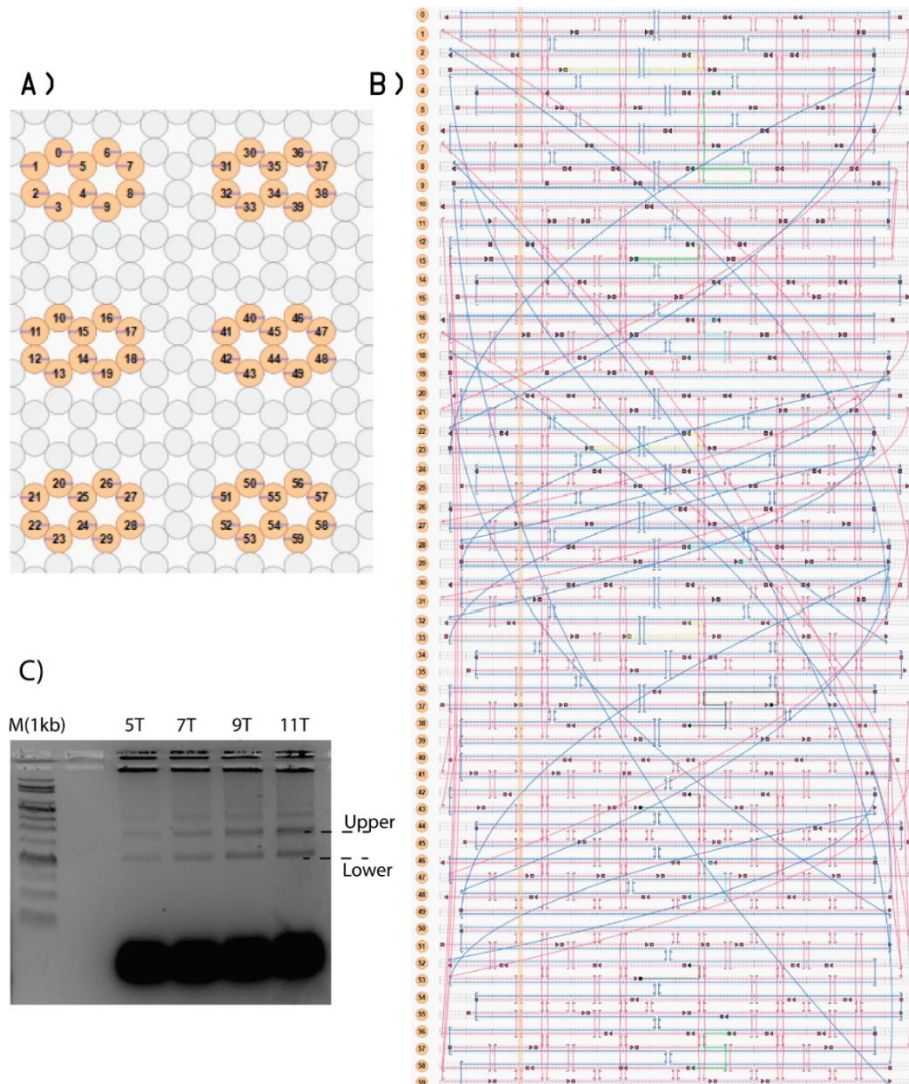


Figure S3.1. CADNANO design scheme of the tetrahedral origami cage. (A) Ten helix bundles used for each edge. (B) Design details of crossovers and connections. Light blue refers to the scaffold routing. Pick refers to the staple strands. Yellow, cyan, black and green represent the handle positions for each of the faces of the tetrahedron used for the incorporation of the PDNA-bb. (C) Agarose gel characterization of the tetrahedral frame with varying lengths of poly-thymidine linkers between arms. The bands shown as lower and upper were isolated and purified and characterized by negative stain TEM. Lane M(1kb)= 1kb ds ladder, Lanes 5T, 7T, 9T, 11T are origamis assembled with varying poly-thymidines ranging from 5 to 11 respectively.

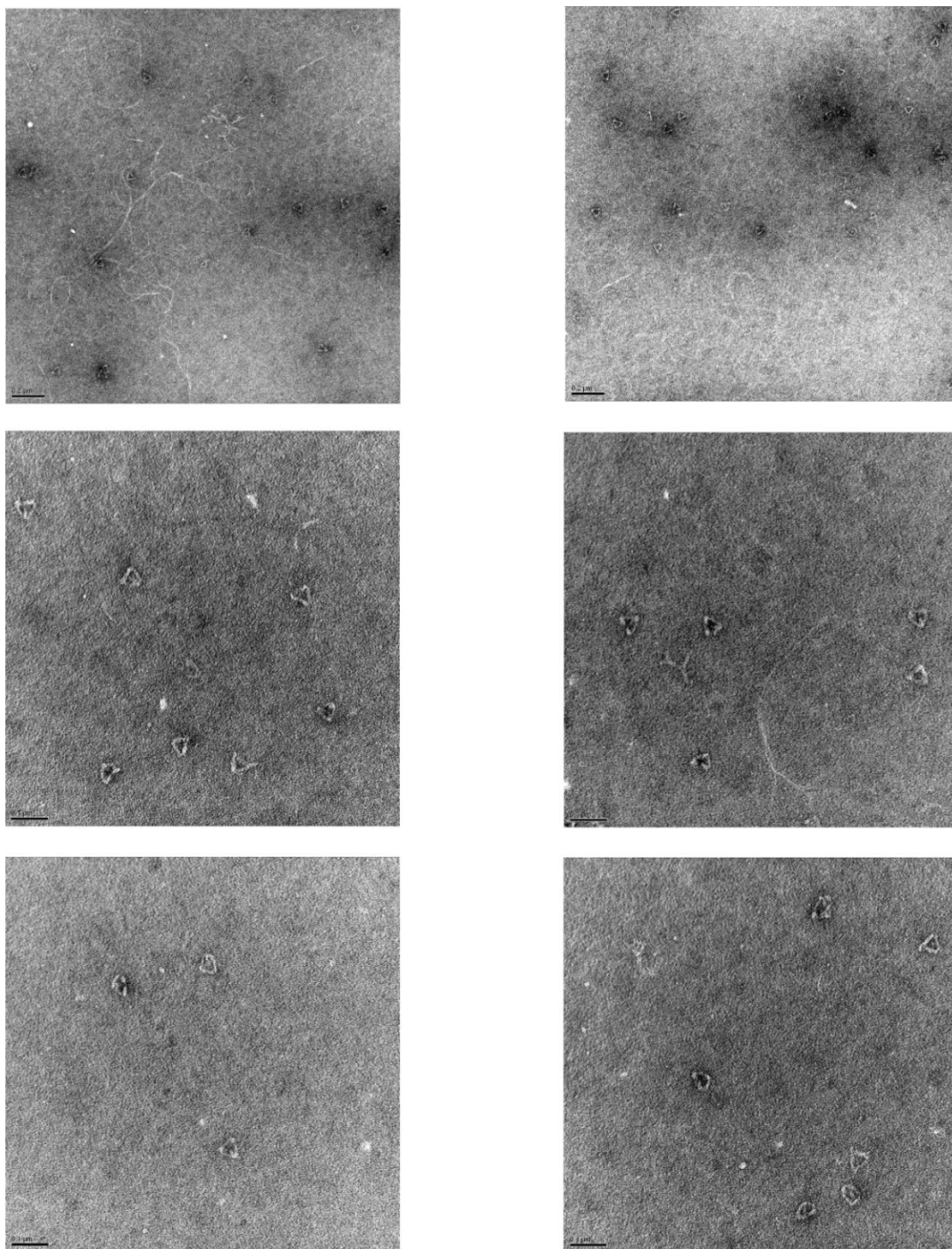


Figure S3.2. Negative stain images of the Lower-monomer band cut out and imaged

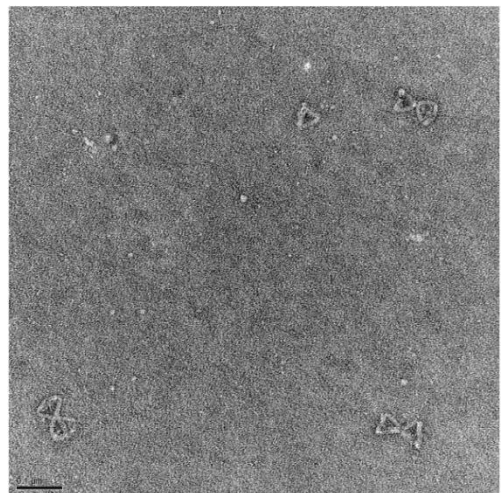
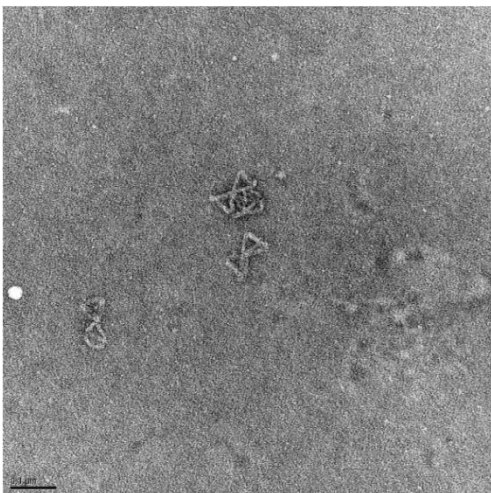
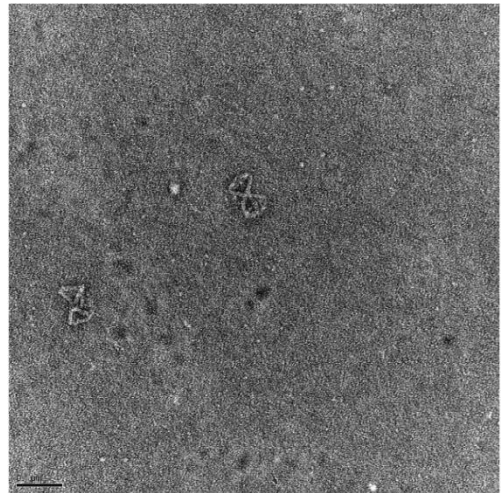
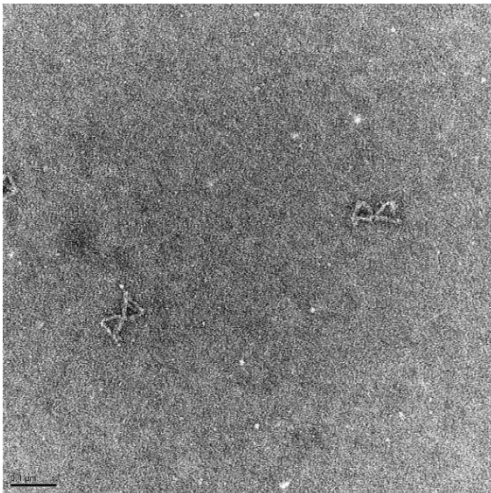
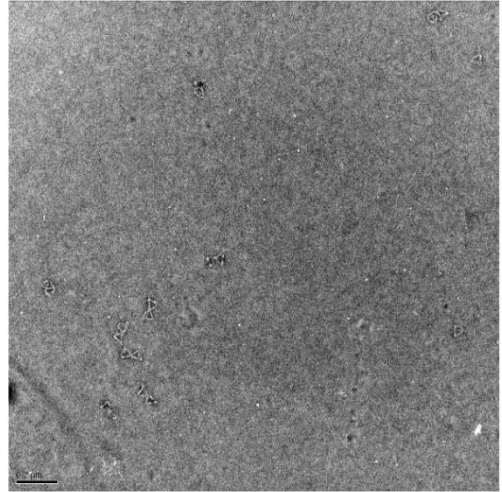
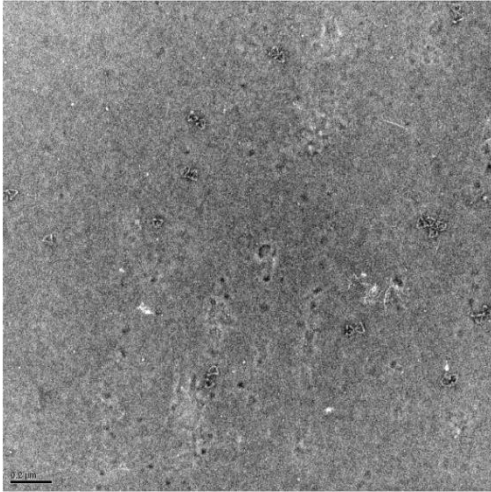


Figure S3.3. Negative stain images of the Upper-Dimer band cut out and imaged

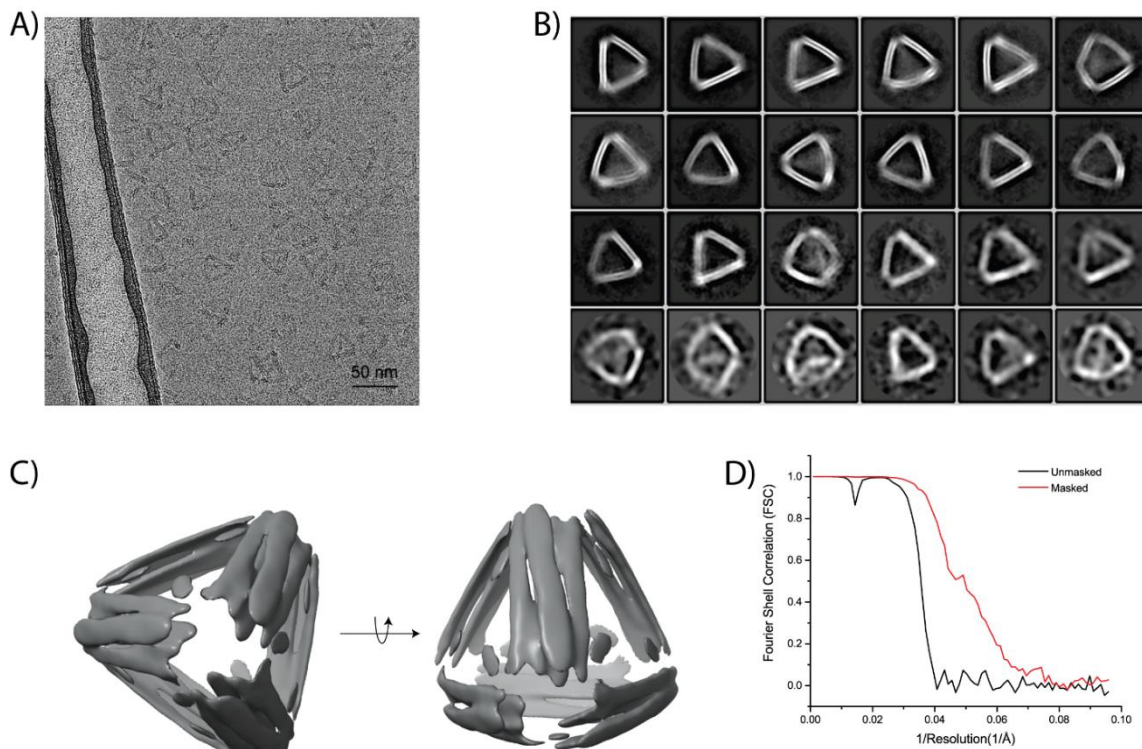


Figure S3.4. Cryo-EM analysis of the empty-cage tetrahedron. (A) Electron micrograph of the cryogenic tetrahedron. Black contrast represents the tetrahedrons and white stands for the background. Scale bar indicates 50 nm. (B) Representative 2D class averages. Box side lengths are 972 Å. (C) Two different views (edge and vertice) of the cryo-EM density map. (D) Fourier-shell correlation (FSC) plot of the 3D reconstruction.

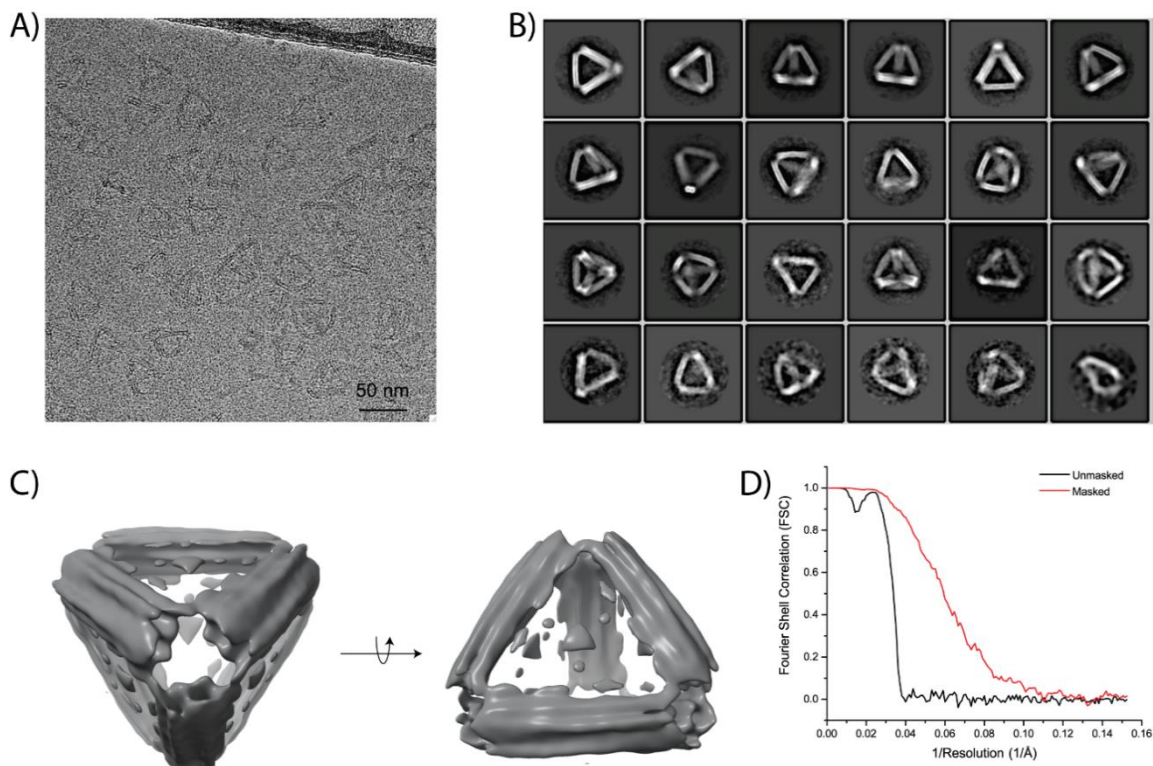


Figure S3.5. Cryo-EM analysis of the PDNA-bb incorporated tetrahedron. (A) Electron micrograph of the cryogenic PDNA-bb bound tetrahedron. Black contrast represents the protein-bound tetrahedrons and white stands for the background. Scale bar indicates 50 nm. (B) Representative 2D class averages. Box side lengths are 1024 Å. (C) Two different views (vertice and face) of the cryo-EM density map. (D) Fourier-shell correlation (FSC) plot of the 3D reconstruction.

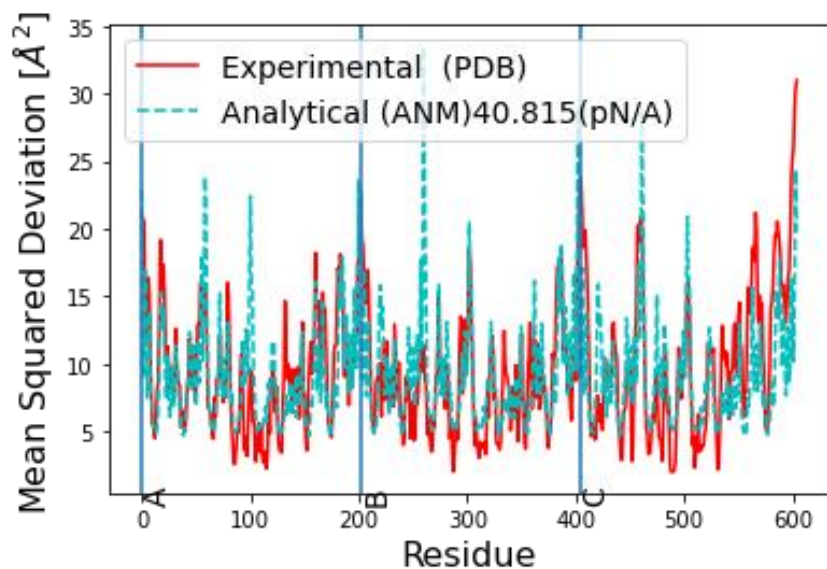


Figure S3.6. ANM fitting of KDPG Aldolase. Comparison of calculated and experimental B Factors of KDPG Aldolase from PDB file (1WAU).

S9. Sequences of DNA origami handles/staples

Staple sequences for empty tetrahedral origami cage and handle sequences for the incorporation of PDNA-bb into the different faces.

| | |
|----------------|--|
| Face1-1 staple | AGGCGCGCCACCCTCAGGCGA |
| Face1-2 staple | GAGTTGATTCATCAGTTGAGATTTAACGCCATATCATAACCC |
| Face1-3 staple | TTCCAGAAAAGCCCCAAAACC |
| Face2-1 staple | TTCATCACAAAGTTACCAAAT |
| Face2-2 staple | TTTACGAGCCAGTAATAAGCAACAACGCCAACATG |
| Face2-3 staple | GAAAAGGTAACGAGTATAACAGTTG |
| Face3-1 staple | GAGACAGTGCGGAGTGTACTG |
| Face3-2 staple | ATTACGTGAGGATTTAGAAGTA |
| Face3-3 staple | TGAATTAACGTATCCAATAAG |
| Face4-1 staple | TTTTAATGGAAACAAAGCATCACCTTGCTGGCAA |
| Face4-2 staple | TAATACCAAGCGCGAAACAAAACCGGAATCATAATTATTA |
| Face4-3 staple | CAGCAGAACTGGCTCATTATACCT |
| Face1-1-handle | AGGCGCGCCACCCTCAGGCGA GAGCAGACCTGACGGAECTCA |
| Face1-2-handle | GAGTTGATTCATCAGTTGAGATTTAACGCCATATCATAACCC GAGCAGACCTGACGGAECTCA |
| Face1-3-handle | TTCCAGAAAAGCCCCAAAACC GAGCAGACCTGACGGAECTCA |
| Face2-1-handle | TTCATCACAAAGTTACCAAAT GAGCAGACCTGACGGAECTCA |
| Face2-2-handle | TTTACGAGCCAGTAATAAGCAACAACGCCAACATG GAGCAGACCTGACGGAECTCA |
| Face2-3-handle | GAAAAGGTAACGAGTATAACAGTTG GAGCAGACCTGACGGAECTCA |
| Face3-1-handle | GAGACAGTGCGGAGTGTACTG GAGCAGACCTGACGGAECTCA |
| Face3-2-handle | ATTACGTGAGGATTTAGAAGTA GAGCAGACCTGACGGAECTCA |
| Face3-3-handle | TGAATTAACGTATCCAATAAG GAGCAGACCTGACGGAECTCA |
| Face4-1-handle | TTTTAATGGAAACAAAGCATCACCTTGCTGGCAA GAGCAGACCTGACGGAECTCA |
| Face4-2-handle | TAATACCAAGCGCGAAACAAAACCGGAATCATAATTATTA GAGCAGACCTGACGGAECTCA |
| Face4-3-handle | CAGCAGAACTGGCTCATTATACCT GAGCAGACCTGACGGAECTCA |

| |
|---|
| ACAGAGGCTTTGAGTAAACGGG |
| TGCCTTGAGTAAAGGATT |
| GCATAACCGAGGTGGCTCCAAAAGGAGCCAGC |
| TAAAACACGCGTTATACGACC |
| TATGCGATTTTACATTGCAACAGGAAAAACGCTCATATATATCCAG |
| AAAATCAGGTCTAGAGGGGGT TTTTTTTTTT TTTTGTTAAAATT |
| CCATATTTAGAACGCGCAATT |
| TTAAAACGACGAAGTATAGCCCGTT |
| AGAATCAAATCTTTTCATAA |
| AGGCGAAGAAAAATCTACTACAGGTAGAAATAGAG |
| GTATATTCCTCACCTCAGAACGTAATAGCGGGGTTTTTCC |
| GTAACGCCAGGCGGGCCGGATAGCAAGCCCACTCA |
| GCCTTCGGTCGCTGAGGCCCGGTTTATCAGC |
| GATTGCAGACTATTCAGAAAATCCCCCTCAAATGCGCTCCAATACTGCG |
| CTGACATTCTGGTCACACGACCAGTAATTTT |
| AAACACCGGATATTCATTAGAGTAACAAAGCG |
| CGACAAAAGGTAAAACCAAGATTACCGCGCCC |
| ATAAGAATAAACGTACAACGGAGATTTGTATCATCGACCGTTT |
| CTCAACCCTCAACCAGGCAGACTCCTCAA |
| AATAGAATTAATAACCCAGCGCCAAAAACGCAA |
| ACAAAGCT TTTTTTTTTT CCGAACTGACAGACCAGGCGC |
| AAACCAATTTTAGTCTATATGTAAATGCTTA |
| CAAATAAAAGAGACAAAAGGGCGATAATATCAA |
| CGCAAGAC TTTTTTTTTT AGACGCTGAGGTCTGAGAGAC |
| AATAGCACCGCTTCTGGAGCA |
| TTAGACTTAGTTACAAAATCGCGCATTGCTTCATTGA |
| GATGTGAGAATAGAAAGAAAAAGAATTTCTTAA |
| AAAGAAGAGCGGGAACAGGAAGGGTCACGCTGCGCGTAAC |
| TCAACAGCCAACCTAAAACGAAAGGTACCTTTACTATACGTAATG |
| TCTAAAATATCTTTAGGAAGA |
| CGATTGGCCATTTTTGTCAA |
| GCCGAATTGCGAATGAATCGGCCAACCAAGGGTTGG |
| CTCGAATTGCAGCTTGCGTACGGAATTATCATCAATAAGTTT |
| AGCTAATGAGAATAAGAACAAGCAAGGCCTG |
| CGGAGCTAACTCACATTGAAGCATTTCATGGTC |
| ATAAAAACCAAAATAGCGCAACACAAAGGAATTAC |
| AAAAATTTTTTAAACAGGAAGATTGATCATATGTACCCCGGA |
| TAATTGTATAATTCTGCGGGC |
| AATGTTTATTTGCCTTACCCTTCAAAAAGATTAAGA |
| GAACAAGAAAAATCTTTCCGAGAAAAATCCAAT |
| CCAAATATTGACGGAAGCCACCTATTAGC |
| ATTACGTGACATCAAGAAAACATTTTCCTTCTGTAAAT |
| ATATATCAATAACTCATCGTAAAGTACCGACAATAAACAATCAACAATA |

| |
|---|
| TGGCTATGAGAGCCAGCAAAC |
| CGATTAACGTCAGATGAAAAATAATTACAGAGAG |
| AGGGAGGCCTCAGAGCGTAATT |
| CCGGATGTGCTGCAAGGCCAGCTGAGCCACCACC |
| TTACCTGAGCAAAAGATTAGAGCCGTCATGCACT |
| AGAGAAGGCAAAAGAATGTTACTTTGTGCGAAATCCGCG |
| CCTACCATATCAAAAAAT |
| TCGTTTACATAATCAGTGAGGCCACCTGAGAACTCAAATTACCGC |
| TTATATATAAATAAGGCGCTA |
| CCGAGGTTTAAGAAGAGAGACTGAACACCC |
| TTTCCATTA AAAACCCCGATTTAGATT |
| TTTTGAACCTCCCGACTAGTTGCTATTTTGCACCC |
| TCCATGCGGAACTTTTCACTGCATTTTGCCTCAC |
| CAGTATTATTAATTA AAAA |
| TTTGCAACAGCTGATTGTTTGATGGTGGTTCCGATTT |
| GGCGCAAAGGCCCGTGGGTCTGGCCTTCTGAAA |
| TGTCCATCACGCAAATTAACCACTAATGCAGATACATAGGAATACCACA |
| TACGAGCACCAGTATAAATCG |
| GCAGCACCGTAA TTTTTTTTTT GCGCCGACA |
| GTTAAAGGCCGATTCCATAGATTTAGTTTGACTGG |
| TTTTCCAGAGGCATTTTGTAT |
| ATTTACCGTTCCAGTATGATTGTCACCGTAATAGGAACCCAT |
| TGCCTTCCACAGTGTGAAATTGTTATCTT |
| TTCAGTTGTAGCAATACTTCTCTACAGGGCTCGTC |
| CGTACCCTAAAGGTGCCGTAAAGCTACGTGAACCGTCT |
| GGAGAGAGGGCATGAAAGTATTA AAAATGCCCTACA |
| ACCAGCAAATCGGAGGCGAGATGCCCGAA |
| TCGCAAATGGTCA TTTTTTTTTT TTTGCGGATGGCCTCAACATGTT |
| ATACAATAGTGAGAATAACCTTGCCTTAGAA |
| AATAACATA TTTTTTTTTT AGCTACAATTTTTTCCAGAGC |
| AGTCAGAGGCGCCACCCTAGA |
| CAGCAACCATTAAAGTTCGTACCCCATTCGCCAT |
| ATTCCTTGCAGGGTTGATAATCACACTAATAG |
| GTTACGCATTAGACGGGAGCAGCCTACAGCCATA |
| TTTTGAGGGGACGGGCTGCGCAACT |
| GAGCGCCATTCAAAAAGGTGGCAACATCGTAGAAGAAGGAAA |
| TTTTGCAAACCTCAACCTTTTGATAAGAGGTCATTTT |
| GGTTTCATCGTAGGAATCTACCGCATCGG |
| TCAAAAAATCCTGCCCTTGTTCCTCAACATACGA |
| GGTGTACCAACTTGCAATCATAAGGGAATTTT |
| ATAGGCTGGCTGACCTTCATCAACCCAAAAGGCTTG |
| GGATTTGCTACGTTGGTACTCCAGCCAGCTT |

| |
|--|
| AACAATCTATCGGCGTTGATTAGTAATGGAT |
| CATGCTGCCGTCGGTTTAGCATCAATATAATCCAGCGTCACCTGCCTA |
| CCTGGTTGAGGCAGGTCCAGAACCCCGC |
| TGGCTTTTGAGGCAATTTACCGCCTTTTCAGTCTT |
| GTCAGGACGTTGGGAAGTCTT |
| TTGCCATGTCATATAAGCTGTAAATCAGCTCAAT |
| TAGGGGATCGTCACCCTAGTACGGTACATT |
| TTCGTATAACGTGCAGGAGGCCG TTTTTTTTTT GGGAAACCT |
| CGCTATTACGGATTAAGTCGACTCTAGAGGAGCTC |
| TACCATACAAACAATTCTTGG |
| TAGTTGACCGTACGCCATC |
| TCCATGACTAAACCCAGCGATTATTCGAGCTTC |
| GGAAGCCCGAAAGACTTCAACCAGACCGGAA |
| TTTGCTCATTAGACCATAAATCATT |
| ATCAGGGAATCCTTAATCAATCAATATCTTGAGGA |
| TTTGCTAGGGCGCTGGCAAGTGTAGCGTAAGAACCCTT |
| CTCGAAGGTAGCAAAATCACCAGTAGCACATCCGATTG |
| GAACTCTGAGTAGAAGAAGTG |
| AAGCCTGGGGTGGGTACCGAG |
| CGCATTTAGCCAGACCCGTCGGATTCTTATCAGGAAAC |
| GTA AAAATTGCGTAGATTTATCCACAAAAATGAA |
| TTTGGTCATAGTAGCGCCAAGGCCGAAACGAGAG |
| ACCATCGATAGACTTGATTAAAGGTGAATTATCTTTT |
| TTAATTACCAACAGTTGCGGT |
| TTATTTTCAGGTAGCCCTTAAACGCAAGTATGTTAG |
| ATATTTTCATTATTAGATGTCTGGAAGTTTCCTT |
| CTGTAATATCCCATCCTCTGTTTACATGTTT |
| TTAATTGATTGCTCAGGTCAGGCAGACGTGAAAGAGGCCTGAT |
| TTGAACGGGTATTAAGTAA |
| AGACACATTACGCATAATAACGGAATAAGCTATCTGA |
| TAAACAGTGTTGTTGAAGGAGTTGGGCGCGCG |
| CACAACGCTTTCCAGTCATTAAAGGGATTTTAGGCTAAACTTTCCTC |
| AAATTGAGCCGGAACGAGGCGATT |
| ACTTCTGAATAATGGAAGGTGAAAGCCGCCGCCA |
| TCCGGGAAATGGGATAGGTCAAACAACCTGACA |
| ATAACCTGTTTACTGAGAGAGTAACACTTTCATCAACATTAA |
| GAATACGTGGCACAGACAAGAACTGAACGAACC |
| TTTTTGGGGTCGAGGGAGCATACCGATAGCCC |
| ACATGGTTTGAATACCGACCGTGTGAATAATTTT |
| AGAGGGAAATACCTACTTACATT |
| AAGGGGCCTAATGAGTGGGAG |
| TCGCAACAAACGGCGGATAGCATTGAGATCTACGAGCT |

| |
|--|
| AATCAAGT TTTTTTTTTT AATCGGCAAAATAGAACGTGGTTTT |
| TAAAACATCG TTTTTTTTTT AAAAGGGACCTGAAAGCGTAATTT |
| ATCTTACTCAAGATTTGCGGGAAAC |
| CATCGGAACGAGGGTAGCGCTGTAGTTAGAGC |
| AATTTTTTCACGCCGATAGTT TTTTTTTTTT TCAGTAGCGAC |
| TAATACATTATGGCCACACA |
| TAAATTTACTGCTCCATACAC |
| ATAGAAGAGTGCGATAGCTTAGATTATT |
| ACTCCAACGTCAAAGGTAATTTAAGCCGAAAGGAGCGGGC |
| CGTTATGCGAAAAACCATCACCCA |
| TACCTTTTTAACCTCCGGCTGATGCACTTTTTCAA |
| ATCACTTGCAACGGAACATAA |
| TTCAGACGTTAGTATAAAGGAATTGCGAATAAT TTTTTTTTTT ACCGTCACC |
| AGGTTTAGAAGATAAGTCTTTA |
| AATCCCAAAGAAGT TTTTTTTTTT GTCCAGACGA |
| ACATACCATTACCATTAGGTT |
| GAACATATGGTTTACCACAAGAATTTAC |
| TATATTTTGACGCTCAATCGAGATGGTTAATTTT |
| AGTGAACCGGATTATCAGATGATTGATACACCGT |
| AATTAACGCTAACGAAACAATGAACGCGATAGAAGTTATCAAAATC |
| AAAGAAGGACTGGATAGCGATAGTAAGAGAG |
| TTTTAAACAGGGAAGAGCCCAAGAAAATTTAAGTTTATTTTGCA |
| GGACATTAAGCCAGAAGTTAGAAGTTTGCCGTTTGCCTGAA |
| TTAAATATGCAACTAACAGCAGCGAA |
| AAGAGAATCGATGAAAGACAG |
| TTCT TTTTTTTTTT GGCATGATTAAGACTCCTTCACG |
| CATATTCATCTTTGACCGACT |
| TCAACGACAGGTGCATCTGCCAGTTT |
| GCTTGACGGGGAAAAAGTTTG |
| GTCGTGCCAGCCAGTGAGACGG |
| ATGCGCTATTTTTAAGGGAAGAAAGCGCGAA |
| AAACAGACGTTGATATTCACAAACAAATATTA |
| GAAACAATGAAAGTAACAGTA |
| ATAAACAGTTGAGGCTGGGATAAGCTGCAGGTTGG |
| GAATAGGTGTATTTGGATTAT |
| AGGATGCGGTCCACTGGGGGTCAG |
| CGTCGCACACCGCCTGCAACAGTGCCACGCTTAAACAGA |
| AAAAATAAAGGCAGATAGCCGAGGCATTTTCGCACGTA |
| GACAATCATTGTGAATTACCA |
| CAAATATTTAACAATTTTGAA |
| TAGGGTGCTGGTTGAGAGAGTTCGTAAAAAGTGTA |
| GTTGGGAAGGGCGATCGGTGTTTTCCCAAGCTTG |

| |
|--|
| TTTTTCAGACGACGATAAAAC |
| ATTGGGCTTGCTGAAATAAC |
| GAAAACCGTTTTTATTTGGG |
| CTCAAATATCAAACCCGGAA |
| CGTTGT TTTTTTTTTT GTACCGTAACACTGAGTTTTTGTCGTCTTC |
| GGCAGATAATGCGCCCTTGCTCGGTACGCCAGAATCCGAGTA |
| CTAATTTGCCAGTTACATATACATAGC |
| ATCAATTCTCAACAGTTTCTT |
| TTCACCACACCCGCATGGTTGCTTTGACGAGCA TTTTTTTTTT CGCT |
| TTTTAAATATTTAAATTGAATCGTATCATTGCGCT |
| TTGCTTTCGATATACTCATAGCGCCTGTTGCCGA |
| TCCTTGAAGTTTTATTCTAAAACGGATTGCGCTGAGAGGCG |
| ATGAAAAATCTAGTACATAAATCAATATATGTGAGTATGCTTATCCGCTT |
| ATCTTCTAAATTCTTATGTAG |
| GGTGAGGAAAGGAATGGTCAGGACAACCTCGT |
| AACCAGGAGATCGCGTAGATGGGCGCATTTTCTGTAACGATCCGCCAC |
| AACTTTAAGAACCAGAACGAGTAGACATTATGTTA |
| CCTTTTACATCGGGAGAGCGTCTATCCTGA |
| ATATTCATTGAACGAGAATGTGAATATCAACGTA |
| ATGACAACCTTGATATTGAAAATCTC |
| TTTTTCAAATCACCGCTCAGAGCCGCCACCAGAATT |
| ATTATTCTGAAATTGATATGCCAGTGCCAGTCACGA |
| AATAGCAAGCAAATCAGATAGGCGTTTTAGC |
| CCACTACGAAGGCATAGGGCTTAATTGAGAAGCCAACGC |
| TTTAAAGAACGTTATCATTCAA |
| GGACAAAGCGAGTACAACTACAATTAGCGTATGG |
| GATAAGTCCT TTTTTTTTTT CAATCAATATAATAAGAGCAATT |
| GTTAGAAGCGTACTCGCGCTTTCACCAGCCAAC |
| CCCTGACAACAGTTATAGTCATTTTGCA |
| AACAACATAATAGAAGATGATGAAACAAAAGCCTTAAACATTCAATTC |
| CAAGAACAACAATGAATCGTAACCTATCGGCCTCA |
| TAAAGATATAATAACGGCTAAAGCGAAATATCGAGATGAAC |
| ATAGCTCACCGCGGTTTTTCAAAGAAACCACCAGTTTGCCCGAGA |
| GAATTCACCAATTTAGCGTCAGACTGCCC |
| CGGTTAAACGTTAATA TTTTTTTTTT AATAGTAA |
| AGTAACATTATCATTCTATTAACCCTTATAAA |
| TTTCGGAACCT TTTTTTTTTT CCACCACCAGAGCGCAGTCTCTGA |
| CCTACCGGAAGCCACCCTCAGAGCGACA |
| CCCTTGCCCCAGCAGGCGAAGAATAGGAACAAGAG |
| GAATCGTCATAA TTTTTTTTTT ATGTGAGCGTCTGGAGCAAAC |
| TAATTTAGGATGAGGAAGTT |
| GCATTCACCACCGAACCAGTTATTCAGCCATTTGG |

S10. References

1. Xu, Y.; Jiang, S.; Simmons, C. R.; Narayanan, R. P.; Zhang, F.; Aziz, A.-M.; Yan, H.; Stephanopoulos, N., Tunable Nanoscale Cages from Self-Assembling DNA and Protein Building Blocks. *ACS Nano* **2019**, *13* (3), 3545-3554.
2. Mastronarde, D. N., Automated electron microscope tomography using robust prediction of specimen movements. *Journal of structural biology* **2005**, *152* (1), 36-51.
3. Scheres, S. H. W., RELION: Implementation of a Bayesian approach to cryo-EM structure determination. *Journal of structural biology* **2012**, *180* (3), 519-530.
4. Zivanov, J.; Nakane, T.; Forsberg, B. O.; Kimanius, D.; Hagen, W. J.; Lindahl, E.; Scheres, S. H., New tools for automated high-resolution cryo-EM structure determination in RELION-3. *eLife* **2018**, *7*.
5. Kremer, J. R.; Mastronarde, D. N.; McIntosh, J. R., Computer visualization of three-dimensional image data using IMOD. *Journal of structural biology* **1996**, *116* (1), 71-6.
6. Zheng, S. Q.; Palovcak, E.; Armache, J.-P.; Verba, K. A.; Cheng, Y.; Agard, D. A., MotionCor2: anisotropic correction of beam-induced motion for improved cryo-electron microscopy. *Nature Methods* **2017**, *14* (4), 331-332.
7. Rohou, A.; Grigorieff, N., CTFFIND4: Fast and accurate defocus estimation from electron micrographs. *Journal of structural biology* **2015**, *192* (2), 216-221.
8. Punjani, A.; Rubinstein, J. L.; Fleet, D. J.; Brubaker, M. A., cryoSPARC: algorithms for rapid unsupervised cryo-EM structure determination. *Nature Methods* **2017**, *14* (3), 290-296.
9. Scheres, S. H. W.; Chen, S., Prevention of overfitting in cryo-EM structure determination. *Nature Methods* **2012**, *9* (9), 853-854.

APPENDIX C

SUPPLEMENTAL MATERIAL FOR CHAPTER 4

AUTONOMOUS DESIGN OF BIOMIMETIC 3D DNA ORIGAMI

CAPSULES

Daniel Fu^{‡, Ψ}, Raghu Pradeep Narayanan^{‡, α, β}, Fei Zhang,^δ Dewight Williams,^Δ John Schreck,^ϕ Hao Yan*,^{α, β} John Reif*^Ψ

(* *hao.yan@asu.edu, reif@cs.duke.edu*)

^α, School of Molecular Sciences, Arizona State University, Tempe, AZ-85281, USA

^β, Center for molecular design and biomimetics, The Biodesign Institute, Arizona State University, Tempe, AZ-85281, USA

^Δ, Erying Materials Center, Office of Knowledge Enterprise Development, Arizona State University, Tempe, AZ, USA

^δ, Department of Chemistry, Rutgers University-Newark, Newark NJ, USA

^Ψ, Department of Computer Science, Durham, NC 27708, USA

^ϕ, Department of Chemical Engineering, Columbia University, New York, NY 10027, USA

Table of contents

S1. Materials and supplies

S2. Protocols for formation, purification, TEM and cryo-TEM

S3. Design algorithm

S4. Molecular dynamic simulations

S5. Supplementary figures

S6. References

S1. Materials and supplies.

All DNA sequences were purchased from Integrated DNA technologies (IDT). The M13p18 and p3120 scaffold strands were amplified and purified in-house. All other scaffold strands were bought from New England Biosciences. All buffers were made in house and filtered to prior use.

S2. Protocols for formation, purification, TEM and cryo-TEM

Formation of DNA origami structures

The reaction mixtures contained 20nM of the scaffold strand along with 200nM of staple strands (10X molar excess in comparison to the scaffold strand) which were folded together in 1XTAE buffer containing 20mM MgCl₂ at pH 7.5. Thereafter the mixtures were thermally annealed in a PCR machine using different annealing protocols.

12 hour annealing protocol: Heat to 90°C for 5 min, jump to 86°C -5min and then decrease by 1°C/5min till 71°C, 70°C-15min and decrease by 1°C/15min to 40°C, 39°C-10min decrease by 1°C/10min to 26°C, 25°C-30min, jump to 20°C-15min, jump to 15°C-5min and jump to 10°C and maintained at that temperature.

24 hour annealing protocol: Heat to 90°C for 5 min, jump to 86°C-5min and then decrease by 1°C/5min till 76°C, 75°C-15min and decrease by 1°C/15min till 71°C, 70°C-20min decrease by 1°C/20min to 61°C, 60°C-30min decrease by 1°C/30min till 30°C, 29°C-20min decrease by 1°C/20min to 25°C, 24°C-15min decrease by 1°C/15min to 20°C, 19°C-10min decrease by 1°C/10min to 15°C, jump to 4°C and maintained at that temperature.

37 hour annealing protocol: Heat to 80°C for 4 min and then decrease by 1°C/4min till 61°C, 60.5°C-30min and decrease by 0.5°C/30min till 34.5°C, 34°C-60min decrease by 1°C/60min to 24°C, and maintained at that temperature.

48 hour annealing protocol: Heat to 90°C for 5 min, jump to 86°C-5min and then decrease by 1°C/5min till 81°C, 80°C-10min and decrease by 1°C/10min till 75°C, 74°C-30min decrease by 1°C/30min to 69°C, 68°C-40min decrease by 1°C/40min till 53°C, 52°C-60min decrease by 1°C/60min to 25°C, 24°C-80min decrease by 1°C/80min to 21°C, 20°C-30min, 19°C/10min decrease by 1°C/10min to 15°C, jump to 4°C and maintained at that temperature.

Gel electrophoresis of the DNA origami structures

Characterization of folded structures: Samples were run on a prestained-1.2% Agarose gel (with ethidium Bromide) made in 1XTAE -20mM MgCl₂ buffer. The running buffer was 1XTAE -12.5mM MgCl₂. 10µL of the annealed sample from the PCR along with 1µL of 10X loading dye was run in each of the wells of the agarose gel. The gels were run for 1-1.5 hours at a constant voltage of 90V at 4°C.

Purification of the folded structures: The fully annealed samples were run on a prestained-1.2% agarose gel (with ethidium Bromide) with 20µL (18µL of sample+2µL of loading dye) being loaded into each well and ran for 90 minutes at a constant voltage of 90V at 4°C. The running buffer was 1XTAE -12.5mM MgCl₂. Thereafter, the second lowest band, in some cases the band above that were cut out separately and put into a freeze and squeeze tube (the lowest band is the excess staples, so they were left out). Care was taken not to further chop up the bands cut out, which if done, was realized to the formation

of deformed structures, thus the rationale being to load into smaller wells and take the bands out as they appeared. The freeze and squeeze tubes were left in the -80°C freezer for over an hour/two (longer periods, did not affect the recovery yield of the structures). After which, the frozen tubes were spun down at 1600rcf in a table top centrifuge for 45-50min at room temperature (Lower centrifugation speeds ensures that the assembled structures do not fall apart and the longer times ensure that maximum recovery from the gel pieces). The recovered solution was concentrated using 100kDa amicon filters (pre-run with filtered 1XTAE-12.5mM MgCl_2 to make the membranes compatible) and spun at 1600rcf using a table top centrifuge.

Cryo-EM sample preparation: The above purified structures were dialyzed to remove the excess ethidium bromide in solution, using a 10kDa Float-a-lyser against 1XTAE-12.5mM MgCl_2 and concentrated as before.

Negative-stain TEM

5 μl of above prepared sample was adsorbed on a glow-discharged (1minute), commercially supplied formvar stabilized carbon type-B, 400mesh copper grids (Ted Pella, part number 01814-F) and stained using 5 μl of a 0.75% aqueous uranyl formate solution containing 25 mM sodium hydroxide. Samples were incubated for 15 to 300 s depending on the concentration of the sample. Excess liquid was wicked away with Whatmann filter paper and grids left to dry prior to imaging.

Cryo-EM: Preparation, acquisition, and processing of data

Structured DNA complexes were absorbed to a glow discharged ultrathin carbon film supported by a lacey carbon film on a 400-mesh grid (Protochips, Morrisville NC) for 1

minute with 8 repeated applications. Samples were applied to only one side of the carbon support with precaution to ensure that the grids were left a little wet between each application. Grids were directly plunge frozen into an ethane slurry at liquid nitrogen temperatures. Tilt series images of the samples were collected on a Titan Krios G2 (FEI/ThermoFisher) and K2 summit (Gatan, Pleasanton CA.) camera at 28,735 x magnification from -65 to $+65^\circ$ alpha with a 2° increment between images using batch methods in Serial EM (1, 2). The IMOD package (3) was used to reconstruction tomograms and visualize tilt series to determine the structures.

S3. Design Algorithm

Several sub-processes are automated to assist in the design of DNA capsules. Manual editing capabilities are also enabled in the user interface of CADAxisDNA at the output of each sub-process to enforce manual changes if a user chooses to do so.

Parsing of Input File

An input file is accepted in Stereolithography (.STL) format that describes a shape as a tessellation of triangular tiles. As a prerequisite, this shape must be axially symmetric, meaning it has radial symmetry with respect to a chosen axis. In order to convert the designated shape to helices, the shape must be able to be represented as a mesh of latitudinal rings. To create this mesh, CADAxisDNA first reads the vertices of the STL file which forms a point cloud surface. To fill any large tiles in the tessellation and create a more uniform distribution of points across the surface, tiles with large area are upsampled

using the barycentric method. Due to the geometry, the points can be projected to a 2D plane and the boundary of the shape can be obtained using an alpha-concave hull algorithm. Filtering for positive x -axis points effectively unrevolves the structure. The remaining line can then be split into equidistant points spaced according to an input interhelical distance (default = 2.6 nm). Each point is then revolved about the original axis to produce a mesh of the shape using latitudinal rings spaced at the interhelical distance.

Adjustment of Mesh Rings

Rings are then scaled to an appropriate circumference corresponding to expected helical geometries. These include the following and help in creating periodicity, symmetry, and stability for crossover placements.

Crossover factor – An integer value of which the number of crossovers on each ring is a multiple of. This value is consistent throughout the structure.

Crossover factor multiple – An integer value specific to each ring that describes its number of crossovers as a multiple of the crossover factor. The value is specific to each ring.

Base pair circumference – Calculated directly from the metric circumference using an axial rise of 0.332 nm.

Turns between crossovers – An integer value specific to each ring that describes the number of full helical turns between adjacent crossovers of a pair of nearest neighbor helical rings.

These adjustments contribute to the helical twist in base pairs per turn (bps/turn) and are iteratively found (described by the below pseudocode algorithm) until a ring satisfies a twist between 9 and 12 bps/turn.

1. assume ring is unstable // (not $9 < \text{bps/turn} < 12$)
2. while unstable
3. for Turns between crossovers from min to max // default 2 to 5
4. if $9 < \text{bps/turn} < 12$
5. stable
6. if unstable and $\text{bps/turn} > 12$
7. crossover factor multiple ++
8. else // increase the circumference by one interval of the number of crossovers
9. circumference += crossover factor * crossover factor multiple

Addition of Reinforcing Rings

Reinforcing rings can be optionally added. Current software capabilities only allow the one-to-one addition of a reinforcing ring to a base layer ring. Positions of the reinforcing rings are linearly extended at a selected angle from the base layer ring, and the circumference, height, and necessary helical geometry optimizations are calculated to do so. Some algorithmic assistance helps to then determine all pairs of nearest neighbor helices and the routing pathway of the scaffold strand, but for complex geometries it may

not be successful. A user may manually input the data. This step is typically trivial for a single layer design.

S4. Molecular Dynamics Simulations

We compare a wide range of structures to study the effects of reinforcement on both rigidity and formation yield improvement of local, high-resolution features. Reinforcement maintains the size and geometry of the structure but changes the routing of scaffold and staples to accommodate additional crossovers spanning between the inner layer and additional layers. Previous work has suggested that material and crossover density in DNA nanostructures contributes to both rigidity and resistance to degradation and thus should be an important design principle to thoroughly investigate, especially for applications of DNA capsules (4, 5, 6, 7). Molecular dynamics simulations are performed in oxDNA (8, 9). Structures are relaxed for at least 105 time steps with the DNA2 model at a salt concentration of 0.5 M, at room temperature ($T = 300\text{K}$), and a snapshot of the molecular conformation is saved every 103 time steps. We quantify the rigidity as a measurement of the RMSD with respect to the average structure per each molecule, and a mean RMSD (mRMSD) is also used to calculate an aggregate value across all molecules. In Figure 2, we show simulation results for cylinder and sphere shapes as fundamental examples of having in-plane curvature and both in-plane and out-of-plane curvature, respectively. We track changes in rigidity as additional reinforcing layers are added. In RMSD measurements per molecule, coloration shows a noticeable decrease in molecular movement after reinforcement. We also observe more fluctuation near the two endpoints of the structure due to less support in those areas where the structure terminates. In addition,

an aggregate score also shows a positive increase in rigidity associated with a decrease in the mRMS. Typically, we see that the overall rigidity improves upon reinforcement of one additional layer, but subsequent trends are less clear. It is important to note that in spite of decreases in rigidity with more than one reinforcing layer, all reinforced DNA capsules are still more rigid relative to the single layer variant of the shape. The process of reinforcement adds more nearest neighbor connections to each original helix, which most notably decreases the average continuous binding domain between each staple and the scaffold. There may be an inverse relationship between the crossover density and material density in curved DNA capsules, such that, counterintuitively, decreasing the crossover factor may help to offset loss of rigidity from shortened binding domains. Another option may be to design structures with a greater minimum crossover spacing. In lieu of a more thorough investigation of these properties in the current work, we suggest that the software now enables future studies to be performed on the mechanics of these complex nanostructures.

S5. Supplementary Figures

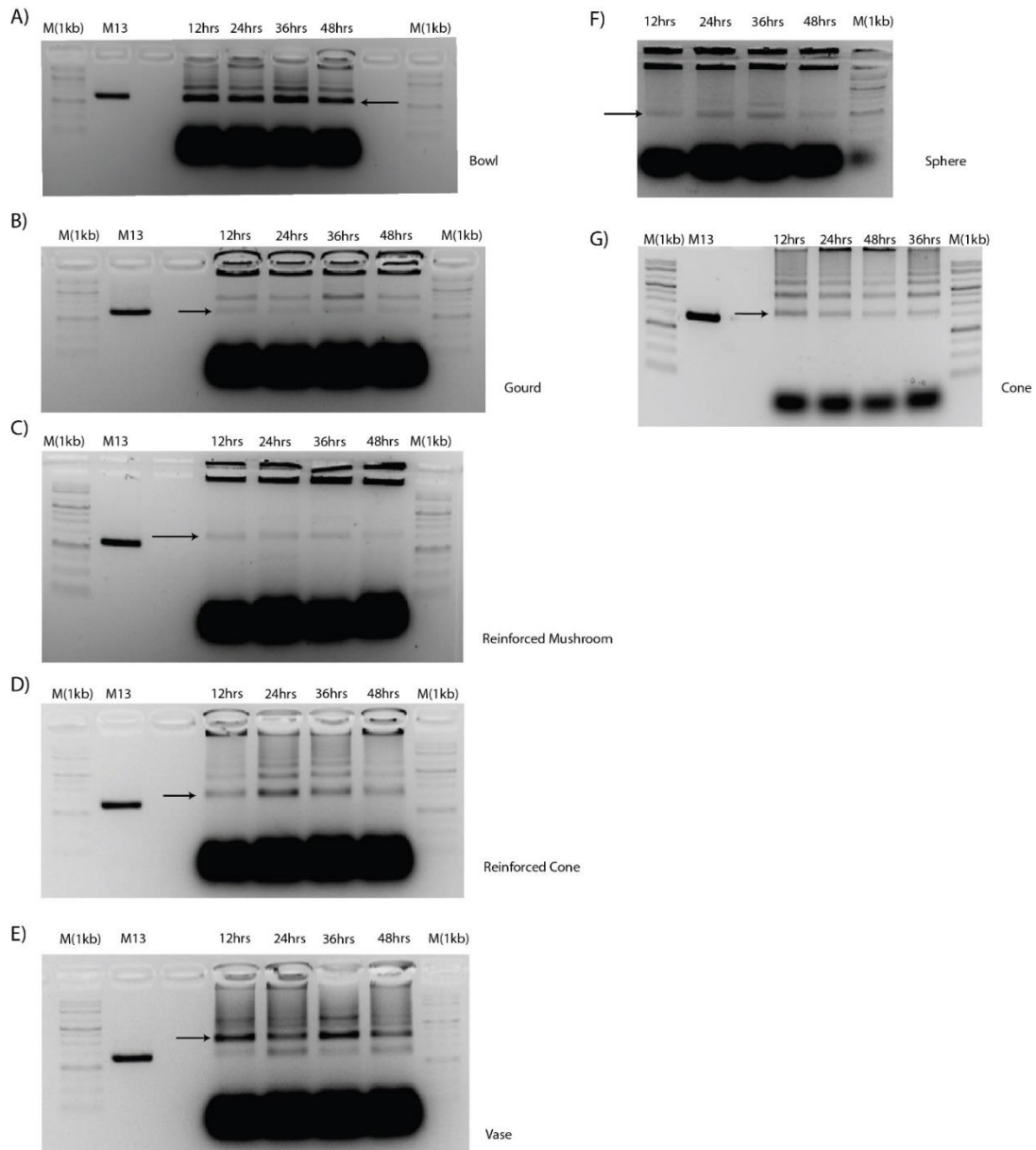


Figure S6. AGE of various structures tested across different annealing protocols. The arrows indicate the bands denoting the formation of the structures confirmed by negative stained TEM and Cryo-EM afterwards.

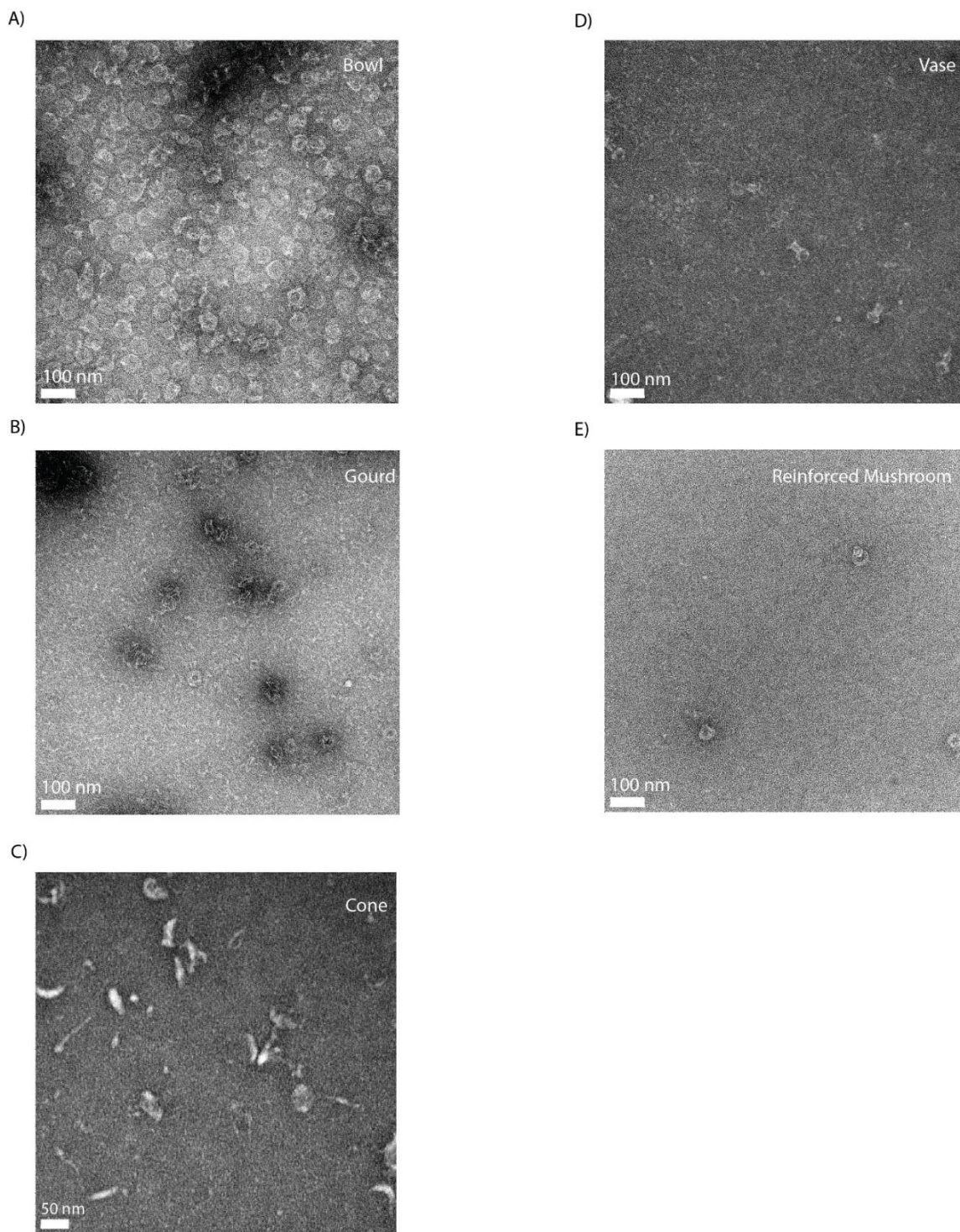


Figure S7. TEM visualization of formation of the various structures.

S6. References

- [1] Hagen, W. J., Wan, W., & Briggs, J. A. (2017). Implementation of a cryo-electron tomography tilt-scheme optimized for high resolution subtomogram averaging. *Journal of structural biology*, 197(2), 191-198.
- [2] Mastronarde, D. N. (2005). Automated electron microscope tomography using robust prediction of specimen movements. *Journal of structural biology*, 152(1), 36-51.
- [3] Kremer, J. R., Mastronarde, D. N., & McIntosh, J. R. (1996). Computer visualization of three-dimensional image data using IMOD. *Journal of structural biology*, 116(1), 71-76.
- [4] Y. Ke, G. Bellot, N. V. Voigt, E. Fradkov, W. M. Shih, *Chemical Science* 3, 2587 (2012).
- [5] Y. Ke, N. V. Voigt, K. V. Gothelf, W. M. Shih, *Journal of the American Chemical Society* 134, 1770–1774 (2012).
- [6] Y. Ke, et al., *Journal of the American Chemical Society* 131, 15903–15908 (2009).
- [7] T. G. Martin, H. Dietz, *Nature communications* 3, 1103 (2012).
- [8] B. E. K. Snodin, et al., *ACS Nano* 10, 1724–1737 (2016).
- [9] B. E. Snodin, et al., *The Journal of chemical physics* 142, 06B613 1 (2015).

APPENDIX D

SUPPLEMENTAL MATERIAL FOR CHAPTER 5

ASSEMBLING AN ORDERED 3D DNA TETRASTACK FROM MODELING TO EXPERIMENTS

Raghu Pradeep Narayanan^{‡,α,β} Michael Matthies,^{α,β} Dewight Williams,^Δ Hao Liu,^{α,β} Fei Zhang,^δ Nicholas Stephanopoulos,^{α,β} Hao Yan*,^{α,β} Petr Šulc*,^{β,Ψ}

(* hao.yan@asu.edu, psulc@asu.edu)

^α, School of Molecular Sciences, Arizona State University, Tempe, AZ-85281, USA

^β, Center for Molecular Design and Biomimetics, The Biodesign Institute, Arizona State University, Tempe, AZ-85281, USA

^Δ, Erying Materials Center, Office of Knowledge Enterprise Development, Arizona State University, Tempe, AZ, USA

^Δ, Department of Chemistry, Rutgers University-Newark, Newark NJ, USA

^Ψ, Center for Biocomputing, Security and Society, The Biodesign Institute, Arizona State University, Tempe, AZ-85281, USA

Table of contents

S1. Materials and supplies

S2. Protocols for making icosahedron origami, AuNP incorporation and formation of origami chains and lattices

S3. Experimental protocols for TEM

S4. Supplementary Figures

S5. Sequence of DNA origami staples

S1. Materials and supplies.

All DNA sequences were purchased from Integrated DNA technologies (IDT). The p3120 scaffold strand was amplified and purified in-house. All buffers were made in house and filtered to prior use.

DNA-Au sequence: /5ThioMC6-D/CTCACTACTACTACTACTCC

S2. Protocols for making icosahedron origami, AuNP incorporation and formation of origami chains and lattices.

Origami formation. All origami solutions were made to 100 μ L volumes with 20 nM of the p3120 scaffold and 5 equivalents of staples (100 nM) (unless otherwise mentioned) in 1XTAE-500 mM NaCl buffer. Staples bearing handles were added at 10x excess (200nM). The samples were heated and slowly cooled in a PCR machine using the 12 hour annealing protocol described below.

12 hour annealing protocol for the formation of Icosahedron. Samples were held at 90 °C for 5 min, followed by a gradient from 86-71 °C at a rate of 1 °C/5 min, followed by a gradient from 70-40 °C at a rate of 1°C/15min, followed by an another gradient from 39-20 °C at the rate of 1°C/10min, and then quickly cooled and storage at, 10 °C.

Characterization of origami structures. Samples were run on 1.2% Agarose gels made in 1xTAE with 12.5 mM MgCl₂ buffer, and pre-stained with ethidium bromide. The running buffer was 1xTAE with 12.5 mM MgCl₂. To 10 μ L of the annealed sample from

the PCR reaction was added 1 μ L of 10x loading dye. The gels were electrophoresed for 1.5 hours at a constant voltage of 90 V at 4°C.

Purification of origami structures by MWCO filters. 20 nM, 100 μ L samples were put in 100kDa 0.5 ml MWCO filters and filled with 1X TAE-500mM NaCl buffer to make it upto the 500 μ L mark. This tube was then spun at low centrifuge speeds of 1600 rcf for 20 min to remove the excess staples and handles. This process of washing was repeated 6 times after which the samples were characterized by TEM for intactness.

Purification using Freeze and Squeeze tubes. The bands excised from running the agarose gel was kept in these tubes following which they were run down immediately on a table top centrifuge at low speeds of 1600 rcf. The dry gel pieces were discarded away and the liquid below was characterized by negative stain TEM to check the formation of the required product.

AuNP DNA formation. 1ml of 5nm AuNP were used from the solution was pipetted into a 1.5ml Eppendorf tube. To this 5 μ L of 100mM Thiol activated DNA Au was added. This was vortexed nicely and frozen in -20°C freezer for 1 hour. Following this, the solution was thawed at room temperature and then spun down at maximum speed (16,000 rcf) at room temperature in a centrifuge. The AuNP became a red pellet at the bottom, care was take not to disturb the pellet while the clear supernatant was discarded. Then a fresh volume of 1ml of 1XPBS pH 7.5 buffer was added to this tube and vortexed again. This step was repeated 5X times to remove the excess unbound DNA to be washed off. Following this, AGE was performed in control with bare AuNPs, wherein the samples

moved into the gel and bare AuNPS did not, as they did not have DNA conjugated to it (Figure 5.2E lane 2 and 3).

Incorporation of AuNP into Icosahedrons. 20X excess of AuNP-DNA was taken in a tube to which purified Icosahedron monomers were added and annealed in a PCR tube from 50°C to 20°C over 12 hours. Following this, AGE was performed and the corresponding band was excised and purified using Freeze and squeeze method as described above.

Formation of Chains/lattices. The purified monomers by MWCO were mixed together in equal concentrations and annealed from 50°C to 20°C with a 0.2°C steps over a period of varying time scales ranging from 12 hours, 36 hours, 72 hours or 6 days depending on the choice of the protocol.

After optimization longer periods of anneal like 6 days proved better for forming larger/longer chains. This was the protocol used for the formation of lattice structures.

S3. Experimental protocols for TEM

Transmission electron microscopy (TEM) characterization. 5 μ L of sample was adsorbed on a formvar stabilized carbon type-B, 400mesh copper grid (Ted Pella, part number 01814-F) that had been glow-discharged for 1 minute. The sample was stained using 5 μ L of a 2 wt% aqueous uranyl formate solution containing 25 mM sodium hydroxide. The grids were left to sit idle for 5 minutes before the samples applied onto it to avoid breakage due to excess charge from the glow discharge process. Samples were incubated for 5 minutes. Grids were allowed to float on a drop of the required sample or stain before wicking excess liquid using a Whatman filter paper.

S4. Supplementary Figures

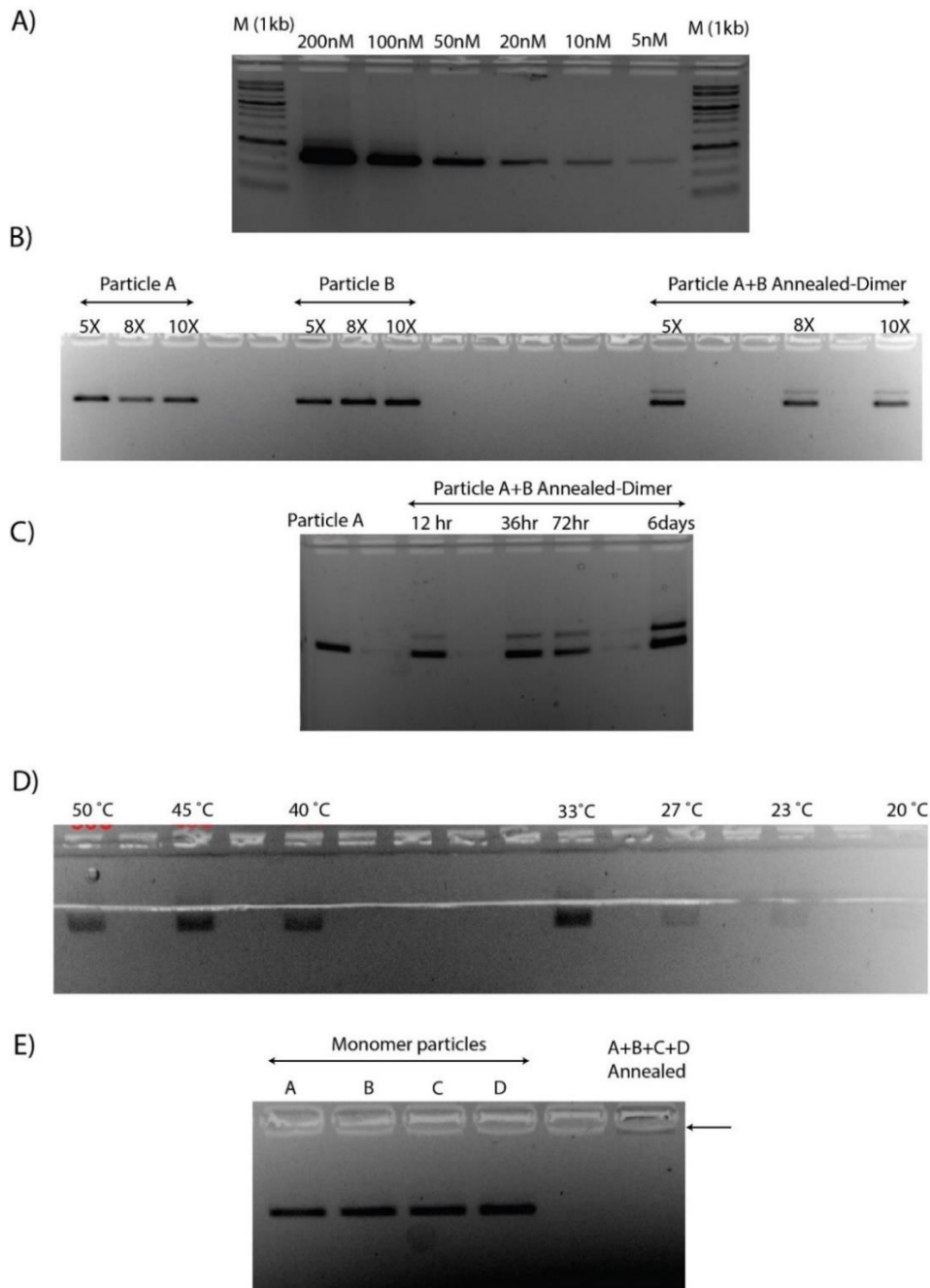


Figure S8. (A) Concentration screen of the homemade p3120 scaffold. (B) Optimization of dimer formation – staple excesses required. (C) Anneal protocol optimization of varying time scales ranging from 12 hours to 6 days. (D) Characterization of the temperature range wherein the formation of lattices takes place. (E) Characterization of lattice formation of 4 particle system, arrow indicates the lattice.

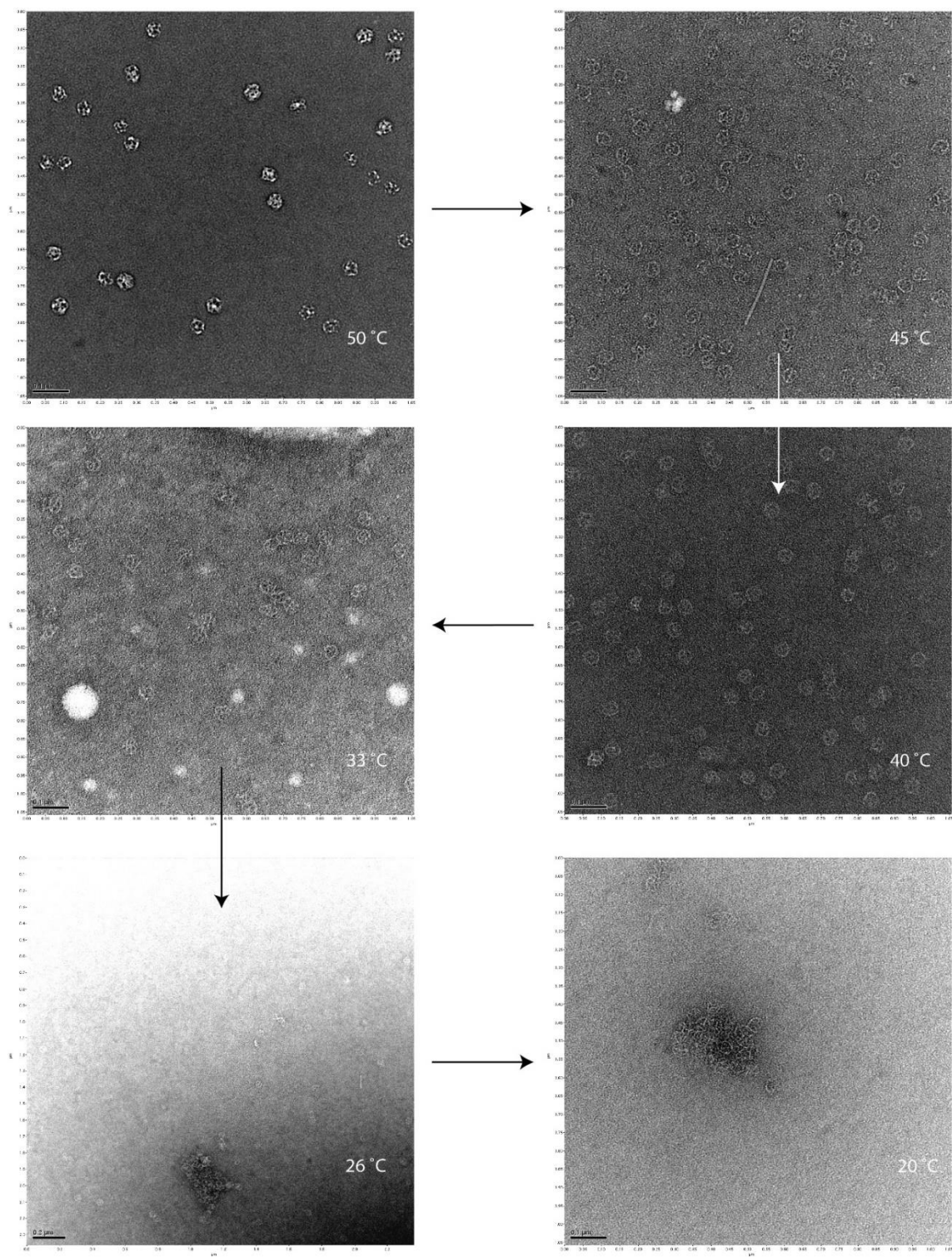


Figure S9. TEM visualization of formation of aggregates of the two particle system over various temperatures (from 50°C to 20°C).

S5. Sequences of DNA origami handles/staples

| | |
|------------------|--|
| Staple_strand_1 | GGGTTTTCCGCCATCGATA |
| Staple_strand_2 | GGTTAATCCAGCTTTTGTCCCTATGGCAG |
| Staple_strand_3 | TAGGGCGAATTTTTTTGGGTACCGGGCTTGATGCAATTTTTTGGGAGATTAACATGCTTCAATTTTTATTTTGCCT |
| Staple_strand_4 | AAGCCTGGTACGAGCCGGAAGCATCGGATAG |
| Staple_strand_5 | GCCAACGCCGTGCCAGCTGCATTAGACGGTA |
| Staple_strand_6 | CTGCGCAACGCGTCCCATTGCGCGTAATACG |
| Staple_strand_7 | CGTAGCGAGCTTTTTTCTGAATCAGGAGTCACGACGTTTTTTTGTAAAACGA |
| Staple_strand_8 | GGTAACGCCACCTCAGCGTATCGTGATCCATCGATTAAGTTG |
| Staple_strand_9 | CCGTAAGCAGCGGGCCTCT |
| Staple_strand_10 | ACTCACTACGCCAGTGAGCGCGCATTGAGG |
| Staple_strand_11 | GGCGAACGTGGCTTTTTGAGAAAGGAGGCGCTGGCAATTTTTGTGTAGCGGTGCTTAATGCGCCGTTTTTCTACAGGG |
| Staple_strand_12 | CTCACTGAATTGGGCGCTTCCCGCACCACA |
| Staple_strand_13 | GGCCCCAGACGATACGGGAGGGCTAGGAGCG |
| Staple_strand_14 | AAAGAACGTTTGAACAAGAGTCCTTGACGG |
| Staple_strand_15 | CTGTTGGGAAGTTTTTGCATCGGTCTAAATCGGAATTTTTCCCTAAAGGG |
| Staple_strand_16 | GGTCGAGGTGTCGCTATTACGCCAGCTGGCGAAGTTTTTTGG |
| Staple_strand_17 | TGTCTCATGATTTTTGCGGATACATAACGTGAACCATTTTTTACCCTAATC |
| Staple_strand_18 | AAACAAATAGGAAAAACCGT |
| Staple_strand_19 | GGAAAGCCAGCCCCGATTTAGAGCACTATT |
| Staple_strand_20 | TTTTGTTAAAATTTTTTTCGCGTTAAAATAGGCCGATTTTTAATCGGCAAAATAGGGTTGAGT |
| Staple_strand_21 | ATCAGCAACCCACGCTCACCGGCTAAGAATA |
| Staple_strand_22 | TGCACCCAATCCAGTTTCGATGTAAGCTCATT |
| Staple_strand_23 | AAATGTTGAAAGGAATAAGGGCATTGTAAG |
| Staple_strand_24 | GGGTTCCGCGCTTTTTACATTTCCCC |
| Staple_strand_25 | TTAGAAAAATCTATCAGGGCGATGGCCCACTTTTGAATGTAT |
| Staple_strand_26 | AGCCACTGGTTCAATATTAT |
| Staple_strand_27 | CGTTAATAGAAAAGTGCCACCTAAGACACGG |
| Staple_strand_28 | TGGTGGCCTAATTTTTTCTACGGCTACCAGCACTGCAT |
| Staple_strand_29 | GCTTTTCTGTCTTACCAG |
| Staple_strand_30 | TTTTAACCATTTTTGTTAAATCACCCACTCG |
| Staple_strand_31 | CTTTATCCCCGAGCGCAGAAGTGGGGGGCGCA |
| Staple_strand_32 | GAGTTGCTCTTTTTTGCCTGGCGTCAACTTTAAAAGTTTTTGTCTCATCAT |
| Staple_strand_33 | TGGTGTCTATTGTTGCCATTGCTACCGCGCCA |
| Staple_strand_34 | TCGGTCCCTTGCAAAAAAGCGGTGTGTATG |
| Staple_strand_35 | AAGGATCTTACTTTTTCGCTGTTGAGACTGATCTTCAATTTTTGCATCTTTTAGACTGGTGAGTTTTTACTCAACCAA |
| Staple_strand_36 | TCCGTAAGATCGTTTCTGGGTGAGCAAAAACCTGTCATGCCA |
| Staple_strand_37 | ATCTGCGCTCTTGCCCGCAG |
| Staple_strand_38 | CGGCGACCGTCATTCTGAGAATATAGCTCCT |
| Staple_strand_39 | CGCAGAAAAAATTTTTAGGATCTCAAGAGTTACATGATTTTTTCCCCATGT |
| Staple_strand_40 | ACGGGGTCTGTCTTACAGCT |
| Staple_strand_41 | CATAGCAGAATACGGGATAATACAGGCATCG |
| Staple_strand_42 | AAAAGGATCTTTTTTACCTAGATCCTAAAGTATATTTTTTATGAGTAAAC |
| Staple_strand_43 | AGCTAGAGTAAGTTACCAATGCTTAATCAGTTGTTGCCGGGA |
| Staple_strand_44 | AAACTCTCTGGAAAACGTTCTTCTCCTGCAA |
| Staple_strand_45 | GACCGAGATCCCTTATAAATCAACCAGATTT |
| Staple_strand_46 | CTCCCCGTCGTTTTTGTAGATAACTTGCTGCAATGATTTTTAACCAGGAGA |
| Staple_strand_47 | GGCGCTAGAGGGAAGAAAGCGAATACCATCT |
| Staple_strand_48 | CTCAAAGGCTGCGGCGAGCGGTATCCATAG |
| Staple_strand_49 | TAAACCAGCCATTTTTGCCGGAAGGGCCTCCATCCATTTTTGTCTATTAATGAGGCACCTATTTTTTCTCAGCGATC |

| | |
|------------------|--|
| Staple_strand_50 | AGTAGTTCGCTTGGTCTGAC |
| Staple_strand_51 | GAACATGTAATCAGGGGATAACGGAAGTTTT |
| Staple_strand_52 | CGACGCTCCCCTGACGAGCATCAGGTCATGA |
| Staple_strand_53 | CAGTTAATAGTTTTTTTTGCGCAACGCGCTCGTCGTT |
| Staple_strand_54 | GATCTTTTCTCCGGTCCCAACGATCAAGGCGAAGATCCTTT |
| Staple_strand_55 | GTTCCCGGACAGGACTATAAGAAAGCAGC |
| Staple_strand_56 | CCGATCGTTGTTTTTTCAGAAGTAAGTGCTGAAGCCATTTTTGTTACCTTCGCAAACCACCGCTTTTTTGGTAGCGGT |
| Staple_strand_57 | AGCTCACGGGGAAGCGTGGCGCTCTCTTGAT |
| Staple_strand_58 | AGTATTTGGTTGTTATCACTCATGGTTATGGACTAGAAGGAC |
| Staple_strand_59 | CTGTGTGCGTAGGTCGTTCCGCTCCACAGAGT |
| Staple_strand_60 | AATACTCATACTTTTTTCTTCTTTTAAACAGGATTAGTTTTTCAGAGCGAGG |
| Staple_strand_61 | CACTGGCAGCTGAAGCATTTATCAGGGTATCGACTTATCGC |
| Staple_strand_62 | AAAGGGGATGTTTTTAGCTGCAAGGGACTGAGACCG |
| Staple_strand_63 | GTTCTAGAGCACCGCTGCGC |
| Staple_strand_64 | CTGTAGGTATCTTTTTTTCAGTTCGGTACGAACCCCTTTTTGTTTCAGCCCG |
| Staple_strand_65 | TCTTGAAGTATGTAGGCGGTGCTAAGCTGGG |
| Staple_strand_66 | CCGGCAAAGAAAAGAGTTGGTAGTTCTCAT |
| Staple_strand_67 | GGCCGCCACCGTTTTTTCGGTGGAGCTGCGCGCTTGGCGTTTTTAAATCATGGCCTGTCCGCCTTTTTTCTCCCTTC |
| Staple_strand_68 | AATTGTTATCCTCCTGTTCC |
| Staple_strand_69 | AGATTACGGGTTTTTTTTGTTTGTACCAGGC |
| Staple_strand_70 | GATTATCACACGTTAAGGGATTTTCAAAAAT |
| Staple_strand_71 | GTTTTTCCATAGTTTTTGTCTCCGCC |
| Staple_strand_72 | AAGTCAGAGTTTTTTTGGCGAAAACCCCTGGAAGCTCCCTTTTTTTCGTGCGCTCGCTCACAAT |
| Staple_strand_73 | AAAAAGGCCGTTGCGTTGCGCTCACTGCCGCCAGGAACCGT |
| Staple_strand_74 | GAGCAAAGGCCTTTTTAGCAAAGG |
| Staple_strand_75 | AAATCAATCTTTAAATTAATAATCAGGAAA |
| Staple_strand_76 | TTGCCTGATGTCTATTTGCTTCATCAGCTCA |
| Staple_strand_77 | CCCGCCGCCACGCTGCGCGTAACCTTCTCTCG |
| Staple_strand_78 | CTTCCAGTCGGTTTTTGAACCTGTGCGGGGAGAGTTTTTTCGGTTTTCGTCTCGCTGCGCT |
| Staple_strand_79 | TCGATAAGCCCCCTCGAGGTCATGAATCG |
| Staple_strand_80 | CGTTGCTGGCCTCACATTA |
| Staple_strand_81 | GGAGGACTCCACTCTGTCCAGCTAAAGTGTA |
| Staple_strand_82 | TCCTGTGTGAGACCCCTGCCGCTTACCGGATATCATAGCTGTT |
| Staple_strand_83 | CTAAAACAAAGGGTTAGCAATCATTAGTGAG |
| Staple_strand_84 | GGATCCACTACTTATCCGGTAACTATCGTCTTGCAGCCCGGG |

APPENDIX E

PERMISSIONS TO USE COPYRIGHTED MATERIALS



Paranemic Crossover DNA: There and Back Again

Author: Xing Wang, Arun Richard Chandrasekaran, Zhiyong Shen, et al

Publication: Chemical Reviews

Publisher: American Chemical Society

Date: May 1, 2019

Copyright © 2019, American Chemical Society

PERMISSION/LICENSE IS GRANTED FOR YOUR ORDER AT NO CHARGE

This type of permission/license, instead of the standard Terms & Conditions, is sent to you because no fee is being charged for your order. Please note the following:

- Permission is granted for your request in both print and electronic formats, and translations.
 - If figures and/or tables were requested, they may be adapted or used in part.
 - Please print this page for your records and send a copy of it to your publisher/graduate school.
 - Appropriate credit for the requested material should be given as follows: "Reprinted (adapted) with permission from (COMPLETE REFERENCE CITATION). Copyright (YEAR) American Chemical Society." Insert appropriate information in place of the capitalized words.
 - One-time permission is granted only for the use specified in your request. No additional uses are granted (such as derivative works or other editions). For any other uses, please submit a new request.
- If credit is given to another source for the material you requested, permission must be obtained from that source.

BACK

CLOSE WINDOW

Wang, X.; Chandrasekaran, A. R.; Shen, Z.; Ohayon, Y. P.; Wang, T.; Kizer, M. E.; Sha, R.; Mao, C.; Yan, H.; Zhang, X.; Liao, S.; Ding, B.; Chakraborty, B.; Jonoska, N.; Niu, D.; Gu, H.; Chao, J.; Gao, X.; Li, Y.; Ciengshin, T.; Seeman, N. C., Paranemic Crossover DNA: There and Back Again. *Chemical Reviews* **2019**, *119* (10), 6273-6289. Copyright © 2019, American Chemical Society

Thank you for your order!

Dear Mr. raghu narayanan pradeep,

Thank you for placing your order through Copyright Clearance Center's RightsLink® service.

Order Summary

Licensee: Arizona State University
Order Date: Apr 4, 2021
Order Number: 5042060830029
Publication: Nature
Title: Design and self-assembly of two-dimensional DNA crystals
Type of Use: Thesis/Dissertation
Order Total: 0.00 USD

View or print complete [details](#) of your order and the publisher's terms and conditions.

Sincerely,

Copyright Clearance Center

Tel: +1-855-230-3415 / +1-978-846-2777
customercare@copyright.com
<https://myaccount.copyright.com>



RightsLink®

Winfree, E.; Liu, F.; Wenzler, L. A.; Seeman, N. C., Design and self-assembly of two-dimensional DNA crystals. *Nature* **1998**, *394* (6693), 539-544. Copyright © 1998, Macmillan Magazines Ltd.

Royal Society of Chemistry - License Terms and Conditions

This is a License Agreement between Raghu Narayanan Pradeep ("You") and Royal Society of Chemistry ("Publisher") provided by Copyright Clearance Center ("CCC"). The license consists of your order details, the terms and conditions provided by Royal Society of Chemistry, and the CCC terms and conditions.

All payments must be made in full to CCC.

| | | | |
|------------------|-------------|-------------|------------------------------------|
| Order Date | 04-Apr-2021 | Type of Use | Republish in a thesis/dissertation |
| Order license ID | 1109342-1 | Publisher | ROYAL SOCIETY OF CHEMISTRY |
| ISSN | 1460-4744 | Portion | Image/photo/illustration |

LICENSED CONTENT

| | | | |
|-------------------|--|------------------|--|
| Publication Title | Chemical Society reviews | Country | United Kingdom of Great Britain and Northern Ireland |
| Author/Editor | Royal Society of Chemistry (Great Britain) | Rightsholder | Royal Society of Chemistry |
| Date | 12/31/1971 | Publication Type | e-Journal |
| Language | English | URL | http://www.rsc.org/csr |

REQUEST DETAILS

| | | | |
|---|-----------------------------------|-----------------------------|----------------------------------|
| Portion Type | Image/photo/illustration | Distribution | Worldwide |
| Number of images / photos / illustrations | 1 | Translation | Original language of publication |
| Format (select all that apply) | Print, Electronic | Copies for the disabled? | Yes |
| Who will republish the content? | Academic institution | Minor editing privileges? | Yes |
| Duration of Use | Current edition and up to 5 years | Incidental promotional use? | No |
| Lifetime Unit Quantity | Up to 499 | Currency | USD |
| Rights Requested | Main product | | |

NEW WORK DETAILS

| | | | |
|-----------------|--|----------------------------|--------------------------|
| Title | Design and study of hybrid DNA nanostructures and complex 3D DNA materials | Institution name | Arizona State University |
| Instructor name | Hao Yan | Expected presentation date | 2021-04-14 |

ADDITIONAL DETAILS

| | | | |
|------------------------|-----|---|-------------------------|
| Order reference number | N/A | The requesting person / organization to appear on the license | Raghu Narayanan Pradeep |
|------------------------|-----|---|-------------------------|

REUSE CONTENT DETAILS

| | | | |
|---|--------|--|--|
| Title, description or numeric reference of the portion(s) | Fig 10 | Title of the article/chapter the portion is from | Engineering DNA-based functional materials |
| Editor of portion(s) | N/A | Author of portion(s) | Royal Society of Chemistry (Great Britain) |
| Volume of serial or monograph | N/A | Issue, if republishing an article from a serial | N/A |
| Page or page range of portion | 5739 | Publication date of portion | 2011-08-19 |

Roh, Y. H.; Ruiz, R. C. H.; Peng, S.; Lee, J. B.; Luo, D., Engineering DNA-based functional materials. *Chemical Society Reviews* **2011**, *40* (12), 5730-5744.

SPRINGER NATURE

Thank you for your order!

Dear Mr. raghu narayanan pradeep,

Thank you for placing your order through Copyright Clearance Center's RightsLink® service.

Order Summary

Licensee: Arizona State University
Order Date: Apr 4, 2021
Order Number: 5042131351665
Publication: Nature
Title: Fractal assembly of micrometre-scale DNA origami arrays with arbitrary patterns
Type of Use: Thesis/Dissertation
Order Total: 0.00 USD

View or print complete [details](#) of your order and the publisher's terms and conditions.

Sincerely,

Copyright Clearance Center

Tel: +1-855-239-3415 / +1-978-646-2777
customercare@copyright.com
<https://myaccount.copyright.com>



Copyright
Clearance
Center

RightsLink®

Tikhomirov, G.; Petersen, P.; Qian, L., Fractal assembly of micrometre-scale DNA origami arrays with arbitrary patterns. *Nature* **2017**, 552 (7683), 67-71. Copyright © 2017, Macmillan Publishers Limited, part of Springer Nature.

Thank you for your order!

Dear Mr. raghu narayanan pradeep,

Thank you for placing your order through Copyright Clearance Center's RightsLink® service.

Order Summary

Licensee: Arizona State University
Order Date: Apr 4, 2021
Order Number: 5042140033028
Publication: Nature
Title: Programmable self-assembly of three-dimensional nanostructures from 10,000 unique components
Type of Use: Thesis/Dissertation
Order Total: 0.00 USD

View or print complete [details](#) of your order and the publisher's terms and conditions.

Sincerely,

Copyright Clearance Center

Tel: +1-855-239-3415 / +1-978-646-2777
customercare@copyright.com
<https://myaccount.copyright.com>



RightsLink®

Ong, L. L.; Hanikel, N.; Yaghi, O. K.; Grun, C.; Strauss, M. T.; Bron, P.; Lai-Kee-Him, J.; Schueder, F.; Wang, B.; Wang, P.; Kishi, J. Y.; Myhrvold, C.; Zhu, A.; Jungmann, R.; Bellot, G.; Ke, Y.; Yin, P., Programmable self-assembly of three-dimensional nanostructures from 10,000 unique components. *Nature* **2017**, 552 (7683), 72-77.
Copyright © 2017, Macmillan Publishers Limited, part of Springer Nature.

Thank you for your order!

Dear Mr. raghu narayanan pradeep,

Thank you for placing your order through Copyright Clearance Center's RightsLink® service.

Order Summary

| | |
|---------------|--------------------------|
| Licensee: | Arizona State University |
| Order Date: | Apr 4, 2021 |
| Order Number: | 5042140157342 |
| Publication: | Nature Chemistry |
| Title: | Meta-DNA structures |
| Type of Use: | Thesis/Dissertation |
| Order Total: | 0.00 USD |

View or print complete [details](#) of your order and the publisher's terms and conditions.

Sincerely,

Copyright Clearance Center

Tel: +1-855-239-3415 / +1-978-646-2777
customercare@copyright.com
<https://myaccount.copyright.com>



Copyright
Clearance
Center

RightsLink®

Yao, G.; Zhang, F.; Wang, F.; Peng, T.; Liu, H.; Poppleton, E.; Šulc, P.; Jiang, S.; Liu, L.; Gong, C.; Jing, X.; Liu, X.; Wang, L.; Liu, Y.; Fan, C.; Yan, H., Meta-DNA structures. *Nature Chemistry* **2020**, *12* (11), 1067-1075. Copyright © 2020, The Author(s), under exclusive licence to Springer Nature Limited

Thank you for your order!

Dear Mr. raghu narayanan pradeep,

Thank you for placing your order through Copyright Clearance Center's RightsLink® service.

Order Summary

Licensee: Arizona State University
Order Date: Apr 4, 2021
Order Number: 5042140386584
Publication: Nature
Title: From molecular to macroscopic via the rational design of a self-assembled 3D DNA crystal
Type of Use: Thesis/Dissertation
Order Total: 0.00 USD

View or print complete [details](#) of your order and the publisher's terms and conditions.

Sincerely,


Copyright Clearance Center

Tel: +1-855-239-3415 / +1-978-646-2777
customercare@copyright.com
<https://myaccount.copyright.com>



RightsLink®

Zheng, J.; Birktoft, J. J.; Chen, Y.; Wang, T.; Sha, R.; Constantinou, P. E.; Ginell, S. L.; Mao, C.; Seeman, N. C., From molecular to macroscopic via the rational design of a self-assembled 3D DNA crystal. *Nature* **2009**, *461* (7260), 74-77. Copyright © 2009, Macmillan Publishers Limited.

 **Layered-Crossover Tiles with Precisely Tunable Angles for 2D and 3D DNA Crystal Engineering**
Author: Fan Hong, Shuoxing Jiang, Xiang Lan, et al
Publication: Journal of the American Chemical Society
Publisher: American Chemical Society
Date: Nov 1, 2018
Copyright © 2018, American Chemical Society

PERMISSION/LICENSE IS GRANTED FOR YOUR ORDER AT NO CHARGE


This type of permission/license, instead of the standard Terms & Conditions, is sent to you because no fee is being charged for your order. Please note the following:

- Permission is granted for your request in both print and electronic formats, and translations.
 - If figures and/or tables were requested, they may be adapted or used in part.
 - Please print this page for your records and send a copy of it to your publisher/graduate school.
 - Appropriate credit for the requested material should be given as follows: "Reprinted (adapted) with permission from (COMPLETE REFERENCE CITATION). Copyright (YEAR) American Chemical Society."
- Insert appropriate information in place of the capitalized words.
- One-time permission is granted only for the use specified in your request. No additional uses are granted (such as derivative works or other editions). For any other uses, please submit a new request. If credit is given to another source for the material you requested, permission must be obtained from that source.

BACK

CLOSE WINDOW

Hong, F.; Jiang, S.; Lan, X.; Narayanan, R. P.; Šulc, P.; Zhang, F.; Liu, Y.; Yan, H., Layered-Crossover Tiles with Precisely Tunable Angles for 2D and 3D DNA Crystal Engineering. *Journal of the American Chemical Society* **2018**, *140* (44), 14670-14676. Copyright © 2018, American Chemical Society

 **Construction and Structure Determination of a Three-Dimensional DNA Crystal**
Author: Chad R. Simmons, Fei Zhang, Jens J. Birktoft, et al
Publication: Journal of the American Chemical Society
Publisher: American Chemical Society
Date: Aug 1, 2016
Copyright © 2016, American Chemical Society

PERMISSION/LICENSE IS GRANTED FOR YOUR ORDER AT NO CHARGE

This type of permission/license, instead of the standard Terms & Conditions, is sent to you because no fee is being charged for your order. Please note the following:

- Permission is granted for your request in both print and electronic formats, and translations.
 - If figures and/or tables were requested, they may be adapted or used in part.
 - Please print this page for your records and send a copy of it to your publisher/graduate school.
 - Appropriate credit for the requested material should be given as follows: "Reprinted (adapted) with permission from (COMPLETE REFERENCE CITATION). Copyright (YEAR) American Chemical Society."
- Insert appropriate information in place of the capitalized words.
- One-time permission is granted only for the use specified in your request. No additional uses are granted (such as derivative works or other editions). For any other uses, please submit a new request. If credit is given to another source for the material you requested, permission must be obtained from that source.

BACK

CLOSE WINDOW

Simmons, C. R.; Zhang, F.; Birktoft, J. J.; Qi, X.; Han, D.; Liu, Y.; Sha, R.; Abdallah, H. O.; Hernandez, C.; Ohayon, Y. P.; Seeman, N. C.; Yan, H., Construction and Structure Determination of a Three-Dimensional DNA Crystal. *Journal of the American Chemical Society* **2016**, *138* (31), 10047-10054. Copyright © 2016, American Chemical Society

Marketplace™

Dear raghu narayanan pradeep,

Thank you for placing your order on [Marketplace™](#).

Order Summary:

Order date: 04 Apr 2021

Order number: 1109345

No. of items: 1

Order total: 0.00 USD

Billing Summary:

Payment method: Invoice

An invoice will be generated and emailed within 24 hours.

To view your order details, click the following link, sign in, and search for your order:

[Manage Account](#).

How was your experience? [Click here to give us feedback](#)

Please do not reply to this message.

To speak with a Customer Service Representative, call +1-855-239-3415 toll free or +1-978-646-2600 (24 hours a day), or email your questions and comments to support@copyright.com.

Sincerely,

The CCC Marketplace Team

Tel: 1-855-239-3415 / +1-978-646-2600

support@copyright.com

[Manage Account](#)



Zhang, T.; Hartl, C.; Frank, K.; Heuer-Jungemann, A.; Fischer, S.; Nickels, P. C.; Nickel, B.; Liedl, T., 3D DNA Origami Crystals. *Advanced Materials* **2018**, *30* (28), 1800273.

DNA-assembled superconducting 3D nanoscale architectures

SPRINGER NATURE

Author: Lior Shani et al
Publication: Nature Communications
Publisher: Springer Nature
Date: Nov 10, 2020

Copyright © 2020, The Author(s)

Creative Commons

This is an open access article distributed under the terms of the [Creative Commons CC BY](#) license, which permits unrestricted use, distribution, and reproduction in any medium, provided the original work is properly cited.

You are not required to obtain permission to reuse this article.

To request permission for a type of use not listed, please contact Springer Nature

Shani, L.; Michelson, A. N.; Minevich, B.; Fleger, Y.; Stern, M.; Shaulov, A.; Yeshurun, Y.; Gang, O., DNA-assembled superconducting 3D nanoscale architectures. *Nature Communications* **2020**, *11* (1), 5697. Copyright © 2020 Springer Nature Limited

SPRINGER NATURE

Thank you for your order!

Dear Mr. raghu narayanan pradeep,

Thank you for placing your order through Copyright Clearance Center's RightsLink® service.

Order Summary

Licensee: Arizona State University
Order Date: Apr 4, 2021
Order Number: 5042160596639
Publication: Nature Materials
Title: Ordered three-dimensional nanomaterials using DNA-prescribed and valence-controlled material voxels
Type of Use: Thesis/Dissertation
Order Total: 0.00 USD

View or print complete [details](#) of your order and the publisher's terms and conditions.

Sincerely,

Copyright Clearance Center

Tel: +1-855-239-3415 / +1-978-646-2777
customercare@copyright.com
<https://myaccount.copyright.com>



RightsLink®

Tian, Y.; Lhermitte, J. R.; Bai, L.; Vo, T.; Xin, H. L.; Li, H.; Li, R.; Fukuto, M.; Yager, K. G.; Kahn, J. S.; Xiong, Y.; Minevich, B.; Kumar, S. K.; Gang, O., Ordered three-dimensional nanomaterials using DNA-prescribed and valence-controlled material voxels. *Nature Materials* **2020**, *19* (7), 789-796. Copyright © 2020 Springer Nature Limited



Dear Raghu,

Your permission requested is granted and there is no fee for this reuse. In your planned reuse, you must cite the ACS article as the source, add this direct link <https://pubs.acs.org/doi/10.1021/nn5011914> and include a notice to readers that further permissions related to the material excerpted should be directed to the ACS.

If you need further assistance, please let me know.

Sincerely,

Simran Mehra

ACS Publications Support

Customer Services & Information

Website: <https://help.acs.org/>

Incident Information:

Incident #: 4258810

Date Created: 2021-04-05T04:40:39

Priority: 3

Customer: RAGHU PRADEEP

Title: Rights and permissions for thesis /dissertation

Description: Hello,

I would like to use the abstract figure from the article titled 'Virus-Inspired Membrane Encapsulation of DNA Nanostructures To Achieve In Vivo Stability' published in ACS Nano for my thesis titled 'Design and study of hybrid DNA nanostructures and complex 3D DNA materials'.

The link is <https://pubs.acs.org/doi/10.1021/nn5011914>

I kindly request you to provide me permission to do the same.

Thanks

Raghu Pradeep Narayanan

Perrault, S. D.; Shih, W. M., Virus-Inspired Membrane Encapsulation of DNA Nanostructures To Achieve In Vivo Stability. *ACS Nano* **2014**, 8 (5), 5132-5140.

Thank you for your order!

Dear Mr. raghu narayanan pradeep,

Thank you for placing your order through Copyright Clearance Center's RightsLink® service.

Order Summary

Licensee: Arizona State University
Order Date: Apr 4, 2021
Order Number: 5042170449739
Publication: Nature Chemistry
Title: Self-assembly of size-controlled liposomes on DNA nanotemplates
Type of Use: Thesis/Dissertation
Order Total: 0.00 USD

View or print complete [details](#) of your order and the publisher's terms and conditions.

Sincerely,

Copyright Clearance Center

Tel: +1-855-239-3415 / +1-978-646-2777
customercare@copyright.com
<https://myaccount.copyright.com>



Copyright
Clearance
Center

RightsLink®

Yang, Y.; Wang, J.; Shigematsu, H.; Xu, W.; Shih, W. M.; Rothman, J. E.; Lin, C., Self-assembly of size-controlled liposomes on DNA nanotemplates. *Nature chemistry* **2016**, 8 (5), 476-483. Copyright © 2016, Nature Publishing Group



Dear Mr. raghu narayanan pradeep,

Thank you for placing your request. A member of the publisher's permissions team will review your request and respond.

Upon approval of your request, you will receive an email quoting the royalty fee and terms set by American Association for the Advancement of Science. If American Association for the Advancement of Science denies your request, you will receive an email.

To complete the order, simply accept the fee and terms in that email and follow the link to complete the order. If you decline to place your order, simply ignore the email. Your order will not be filled and you will not be charged.

Request Summary:

Submit date: 04-Apr-2021

Request ID: 600039277

Publication: Science

Title: Self-assembly of genetically encoded DNA-protein hybrid nanoscale shapes.

Type of Use: Republish in a thesis/dissertation

Use this [link](#) to view your request details.

Please do not reply to this message.

To speak with a Customer Service Representative, call +1-855-239-3415 toll free or +1-978-646-2600 (24 hours a day), or email your questions and comments to support@copyright.com.

Sincerely,

Copyright Clearance Center

Praetorius, F.; Dietz, H., Self-assembly of genetically encoded DNA-protein hybrid nanoscale shapes. *Science* **2017**, *355* (6331), eaam5488.



Tunable Nanoscale Cages from Self-Assembling DNA and Protein Building Blocks

Author: Yang Xu, Shuoxing Jiang, Chad R. Simmons, et al

Publication: ACS Nano

Publisher: American Chemical Society

Date: Mar 1, 2019

Copyright © 2019, American Chemical Society

PERMISSION/LICENSE IS GRANTED FOR YOUR ORDER AT NO CHARGE

This type of permission/license, instead of the standard Terms & Conditions, is sent to you because no fee is being charged for your order. Please note the following:

- Permission is granted for your request in both print and electronic formats, and translations.
- If figures and/or tables were requested, they may be adapted or used in part.
- Please print this page for your records and send a copy of it to your publisher/graduate school.
- Appropriate credit for the requested material should be given as follows: "Reprinted (adapted) with permission from (COMPLETE REFERENCE CITATION). Copyright (YEAR) American Chemical Society." Insert appropriate information in place of the capitalized words.
- One-time permission is granted only for the use specified in your request. No additional uses are granted (such as derivative works or other editions). For any other uses, please submit a new request. If credit is given to another source for the material you requested, permission must be obtained from that source.

BACK

CLOSE WINDOW

Xu, Y.; Jiang, S.; Simmons, C. R.; Narayanan, R. P.; Zhang, F.; Aziz, A.-M.; Yan, H.; Stephanopoulos, N., Tunable Nanoscale Cages from Self-Assembling DNA and Protein Building Blocks. *ACS Nano* **2019**, *13* (3), 3545-3554. Copyright © 2019, American Chemical Society



Dear Raghu,

Your permission requested is granted and there is no fee for this reuse. In your planned reuse, you must cite the ACS article as the source, add this direct link <https://pubs.acs.org/doi/abs/10.1021/jacs.9b11158> and include a notice to readers that further permissions related to the material excerpted should be directed to the ACS.

If you need further assistance, please let me know.

Sincerely,

Simran Mehra

ACS Publications Support

Customer Services & Information

Website: <https://help.acs.org/>

Incident Information:

Incident #: 4258818

Date Created: 2021-04-05T05:02:26

Priority: 3

Customer: RAGHU PRADEEP

Title: Permission for thesis

Description: Hello,

I am graduate student at ASU submitting my thesis titled as 'Design and study of hybrid DNA nanostructures and complex 3D DNA materials' and would like to use the abstract figure from this paper titled 'Hierarchical Assembly of Nucleic Acid/Coiled-Coil Peptide Nanostructures' published in *Journal of the American Chemical Society* in my thesis.

The link to the article is <https://pubs.acs.org/doi/abs/10.1021/jacs.9b11158>

Please do provide m permission to use the same.

Thanks

Raghu Pradeep Narayanan

Buchberger, A.; Simmons, C. R.; Fahmi, N. E.; Freeman, R.; Stephanopoulos, N., Hierarchical Assembly of Nucleic Acid/Coiled-Coil Peptide Nanostructures. *Journal of the American Chemical Society* **2020**, *142* (3), 1406-1416.



Structurally Ordered Nanowire Formation from Co-Assembly of DNA Origami and Collagen-Mimetic Peptides

Author: Tao Jiang, Travis A. Meyer, Charles Modlin, et al

Publication: Journal of the American Chemical Society

Publisher: American Chemical Society

Date: Oct 1, 2017

Copyright © 2017, American Chemical Society

PERMISSION/LICENSE IS GRANTED FOR YOUR ORDER AT NO CHARGE

This type of permission/license, instead of the standard Terms & Conditions, is sent to you because no fee is being charged for your order. Please note the following:

- Permission is granted for your request in both print and electronic formats, and translations.
- If figures and/or tables were requested, they may be adapted or used in part.
- Please print this page for your records and send a copy of it to your publisher/graduate school.
- Appropriate credit for the requested material should be given as follows: "Reprinted (adapted) with permission from (COMPLETE REFERENCE CITATION). Copyright (YEAR) American Chemical Society." Insert appropriate information in place of the capitalized words.
- One-time permission is granted only for the use specified in your request. No additional uses are granted (such as derivative works or other editions). For any other uses, please submit a new request. If credit is given to another source for the material you requested, permission must be obtained from that source.

[BACK](#)

[CLOSE WINDOW](#)

Jiang, T.; Meyer, T. A.; Modlin, C.; Zuo, X.; Conticello, V. P.; Ke, Y., Structurally Ordered Nanowire Formation from Co-Assembly of DNA Origami and Collagen-Mimetic Peptides. *Journal of the American Chemical Society* **2017**, *139* (40), 14025-14028. Copyright © 2017, American Chemical Society

SPRINGER NATURE

Thank you for your order!

Dear Mr. raghu narayanan pradeep,

Thank you for placing your order through Copyright Clearance Center's RightsLink® service.

Order Summary

Licensee: Arizona State University
Order Date: Apr 4, 2021
Order Number: 5042180042829
Publication: Nature
Title: Hierarchical self-assembly of DNA into symmetric supramolecular polyhedra
Type of Use: Thesis/Dissertation
Order Total: 0.00 USD

View or print complete [details](#) of your order and the publisher's terms and conditions.

Sincerely,

Copyright Clearance Center

Tel: +1-855-239-3415 / +1-978-646-2777
customercare@copyright.com
<https://myaccount.copyright.com>



RightsLink®

He, Y.; Ye, T.; Su, M.; Zhang, C.; Ribbe, A. E.; Jiang, W.; Mao, C., Hierarchical self-assembly of DNA into symmetric supramolecular polyhedra. *Nature* **2008**, *452* (7184), 198-201. Copyright © 2008, Nature Publishing Group

Bai, X.-c.; Martin, T. G.; Scheres, S. H. W.; Dietz, H., Cryo-EM structure of a 3D DNA-origami object. *Proceedings of the National Academy of Sciences* **2012**, *109* (49), 20012-20017. Copyright (2012) National Academy of Sciences.

Martin, T. G.; Bharat, T. A. M.; Joerger, A. C.; Bai, X.-c.; Praetorius, F.; Fersht, A. R.; Dietz, H.; Scheres, S. H. W., Design of a molecular support for cryo-EM structure determination. *Proceedings of the National Academy of Sciences* **2016**, *113* (47), E7456-E7463. Copyright (2016) National Academy of Sciences.

Marketplace™

Dear raghu narayanan pradeep,

Thank you for placing your order on [Marketplace™](#).

Order Summary:

Order date: 04 Apr 2021

Order number: 1109348

No. of items: 1

Order total: 0.00 USD

Billing Summary:

Payment method: Invoice

An invoice will be generated and emailed within 24 hours.

To view your order details, click the following link, sign in, and search for your order:

[Manage Account](#).

How was your experience? [Click here to give us feedback](#)

Please do not reply to this message.

To speak with a Customer Service Representative, call +1-855-239-3415 toll free or +1-978-646-2600 (24 hours a day), or email your questions and comments to

support@copyright.com.

Sincerely,

The CCC Marketplace Team

Tel: 1-855-239-3415 / +1-978-646-2600

support@copyright.com

[Manage Account](#)



Dong, Y.; Chen, S.; Zhang, S.; Sodroski, J.; Yang, Z.; Liu, D.; Mao, Y., Folding DNA into a Lipid-Conjugated Nanobarrel for Controlled Reconstitution of Membrane Proteins. *Angewandte Chemie International Edition* **2018**, 57 (8), 2072-2076.

Thank you for your order!

Dear Mr. raghu narayanan pradeep,

Thank you for placing your order through Copyright Clearance Center's RightsLink® service.

Order Summary

Licensee: Arizona State University
Order Date: Apr 4, 2021
Order Number: 5042200568242
Publication: Nature Biotechnology
Title: Molecular goniometers for single-particle cryo-electron microscopy of DNA-binding proteins
Type of Use: Thesis/Dissertation
Order Total: 0.00 USD

View or print complete [details](#) of your order and the publisher's terms and conditions.

Sincerely,

Copyright Clearance Center

Tel: +1-855-230-3415 / +1-978-846-2777
customercare@copyright.com
<https://myaccount.copyright.com>



RightsLink®

Aksel, T.; Yu, Z.; Cheng, Y.; Douglas, S. M., Molecular goniometers for single-particle cryo-electron microscopy of DNA-binding proteins. *Nature biotechnology* **2021**, *39* (3), 378-386. Copyright © 2020, Springer Nature

OXFORD
UNIVERSITY PRESS

Thank you for your order!

Dear Mr. raghu narayanan pradeep,

Thank you for placing your order through Copyright Clearance Center's RightsLink® service.

Order Summary

Licensee: Arizona State University
Order Date: Apr 4, 2021
Order Number: 5042200796522
Publication: Nucleic Acids Research
Title: Rapid prototyping of 3D DNA-origami shapes with caDNAno
Type of Use: Thesis/Dissertation
Order Total: 0.00 USD

View or print complete [details](#) of your order and the publisher's terms and conditions.

Sincerely,

Copyright Clearance Center


Tel: +1-855-239-3415 / +1-978-646-2777
customercare@copyright.com
<https://myaccount.copyright.com>



RightsLink®

Douglas, S. M.; Marblestone, A. H.; Teerapittayanon, S.; Vazquez, A.; Church, G. M.; Shih, W. M., Rapid prototyping of 3D DNA-origami shapes with caDNAno. *Nucleic Acids Research* **2009**, 37 (15), 5001-5006. Copyright © 2009, Oxford University Press


Automated sequence design of 2D wireframe DNA origami with honeycomb edges
Author: Hyungmin Jun et al
Publication: Nature Communications
Publisher: Springer Nature
Date: Nov 28, 2019
Copyright © 2019, The Author(s)



Creative Commons
This is an open access article distributed under the terms of the [Creative Commons CC BY](#) license, which permits unrestricted use, distribution, and reproduction in any medium, provided the original work is properly cited.
You are not required to obtain permission to reuse this article.
To request permission for a type of use not listed, please contact [Springer Nature](#)

Jun, H.; Wang, X.; Bricker, W. P.; Bathe, M., Automated sequence design of 2D wireframe DNA origami with honeycomb edges. *Nature Communications* **2019**, *10* (1), 5419. Copyright © 2019

Automated Sequence Design of 3D Polyhedral Wireframe DNA Origami with Honeycomb Edges
Author: Hyungmin Jun, Tyson R. Shepherd, Kaiming Zhang, et al
Publication: ACS Nano
Publisher: American Chemical Society
Date: Feb 1, 2019
Copyright © 2019, American Chemical Society



PERMISSION/LICENSE IS GRANTED FOR YOUR ORDER AT NO CHARGE
This type of permission/license, instead of the standard Terms & Conditions, is sent to you because no fee is being charged for your order. Please note the following:

- Permission is granted for your request in both print and electronic formats, and translations.
- If figures and/or tables were requested, they may be adapted or used in part.
- Please print this page for your records and send a copy of it to your publisher/graduate school.
- Appropriate credit for the requested material should be given as follows: "Reprinted (adapted) with permission from (COMPLETE REFERENCE CITATION). Copyright (YEAR) American Chemical Society." Insert appropriate information in place of the capitalized words.
- One-time permission is granted only for the use specified in your request. No additional uses are granted (such as derivative works or other editions). For any other uses, please submit a new request. If credit is given to another source for the material you requested, permission must be obtained from that source.

[BACK](#) [CLOSE WINDOW](#)

Jun, H.; Shepherd, T. R.; Zhang, K.; Bricker, W. P.; Li, S.; Chiu, W.; Bathe, M., Automated Sequence Design of 3D Polyhedral Wireframe DNA Origami with Honeycomb Edges. *ACS Nano* **2019**, *13* (2), 2083-2093. Copyright © 2019, American Chemical Society

Veneziano, R.; Ratanalert, S.; Zhang, K.; Zhang, F.; Yan, H.; Chiu, W.; Bathe, M., Designer nanoscale DNA assemblies programmed from the top down. *Science* **2016**, *352* (6293), 1534-1534.



Programmable Cocrystallization of DNA Origami Shapes

Author: Min Ji, Jiliang Liu, Lizhi Dai, et al
Publication: Journal of the American Chemical Society
Publisher: American Chemical Society
Date: Dec 1, 2020

Copyright © 2020, American Chemical Society

PERMISSION/LICENSE IS GRANTED FOR YOUR ORDER AT NO CHARGE

This type of permission/license, instead of the standard Terms & Conditions, is sent to you because no fee is being charged for your order. Please note the following:

- Permission is granted for your request in both print and electronic formats, and translations.
- If figures and/or tables were requested, they may be adapted or used in part.
- Please print this page for your records and send a copy of it to your publisher/graduate school.
- Appropriate credit for the requested material should be given as follows: "Reprinted (adapted) with permission from (COMPLETE REFERENCE CITATION). Copyright (YEAR) American Chemical Society." Insert appropriate information in place of the capitalized words.
- One-time permission is granted only for the use specified in your request. No additional uses are granted (such as derivative works or other editions). For any other uses, please submit a new request. If credit is given to another source for the material you requested, permission must be obtained from that source.

BACK

CLOSE WINDOW

Ji, M.; Liu, J.; Dai, L.; Wang, L.; Tian, Y., Programmable Cocrystallization of DNA Origami Shapes. *Journal of the American Chemical Society* **2020**, *142* (51), 21336-21343. Copyright © 2020, American Chemical Society